Development of Monoclonal Antibodies for the Identification of Novel Invasion Associated Targets in Human Cancer

A thesis submitted for the degree of Ph.D.

by

Dermot O' Sullivan, B.Sc. Hons

Thesis research work described in this thesis was performed under the supervision of
Prof. Martin Clynes and Dr. Anne-Marie Larkin

National Institute for Cellular Biotechnology
Dublin City University

August 2011

I hereby certify that this material, which I now submit for assessment on the programme of study leading to the award of Ph D. is entirely my own work, that I have exercised reasonable care to ensure that the work is original, and does not to the best of my knowledge breach any law of copyright, and has not been taken from the work of others save and to the extent that such work has been cited and acknowledged within the text of my work.

Signed: _____ ID No.: 50586625

Date: _____

Acknowledgements

I would like to sincerely thank Dr. Anne Marie Larkin for all her help over these past few years. This thesis would not have been possible without her guidance, support and patience. This work is a testament to your help and kindness. Thank you! I would also like to thank Prof. Martin Clynes for welcoming me to the NICB and allowing me the opportunity to carry out this work. Working outside of the centre has shown me how lucky and priviliged I was to have worked under you.

My career here in the NICB has been helped along by so many people, and I would like to thank each and every one of them. Sharon, my first supervisor, led me through those early days with immense kindness, and made me feel at home. Laura, Naomi and Joanne, you were always there to answer my questions, to show me procedures, and to give me advice on all matters. Working in the lab was always a joy when you were there. I would also like to thank Aoife for all the good times we had since starting out on this Phd path together. To Alex, Sandra, Fiona, Erica, Kathy, Martina, Casper and Denis, I couldn't have worked with a crazier or funnier group of people. From nights out on the town, to 14 hour work days, you kept my spirits up when they were down, kept me smiling when feeling blue, and made my insanity that little less bit insane, by comparison. Thanks also to Paul and Mick for all their Proteomics and Mass Spec help. Couldn't have done this work without you. And thank you to Verena and Paula, for all your cell culturing help, and to Colin, and Niall, for you (much needed) expertise on all things statistical.

Special thanks must go to Carol and Yvonne. Coming in on those dark mornings was always made easier when seeing you in the office. Your tireless work, always carried out with a smile, has made this thesis, and many others, possible. You should both be made honorary Professors! Special thanks also to Joe, Ultan, Gillian and Mairead, for all their help.

Thanks to all my friends outside of the centre. Damo (yes, you are in the centre, I know!), Sue, Aoife Small, Conor and Vinnie, thanks for all the mad nights, the

laughs, the slaggings, and the 3am Mario Kart being played with one eye! Thank you to my family also, especially my mam and dad. Your kindness, support, understanding, and especially lunches and dinners, kept me going these past few years.

Finally, I would like to thank Vanesa, the greatest discovery of my Phd. You have always been my light at the end of the tunnel. You picked me up in my darkest moments, listened to my complaints, helped me through the tough times, and made the good times that much sweeter. Your help, both inside and outside the NICB, have been invaluable. I am looking forward to our time together in the sun now.

This thesis is dedicated to my loving parents,

Donal & Anne.

Abbreviations

Ab	-	Antibody
ABC/HRP	-	Streptavidin/biotin-Horseradish Peroxidase
ACN	-	Acetonitrile
ADAM	-	A Disintegrin and Metalloproteinase
ADAMTS	-	A Disintegrin and Metalloproteinase with Thrombospondin Motifs
ADC	-	Antibody Drug Conjugate
ADCC	-	Antibody-Dependent Cellular Cytotoxicity
ADEPT	-	Antibody-Directed Enzyme Prodrug Therapy
ADP	-	Adenosine diphosphate
Ag	-	Antigen
$AgNO_3$	-	Silver Nitrate
Anx	-	Annexin
AQP	-	Aquaporin
Arp	-	Actin Related Protein
ATCC	-	American Tissue Culture Collection
ATP	-	Adenosine triphosphate
BCR	-	B Cell Receptor
BFGF	-	Basic Fibroblast Growth Factors
BSA	-	Bovine Serum Albumin
BsAb	-	Bispecific antibody
Ca	-	Calcium
cAb	-	Chimeric Antibody
CAM	-	Cell Adhesion Molecules
CDC	-	Complement Dependent Cytotoxicity
CDR	-	Complementarity-Determining Region
CID	-	Collision Induced Dissociation
CHAPS	-	3 - ((3-Cholamidopropyl)dimethylammonio)-1-Propanesulfonic Acid
CME	-	Clathrin Mediated Endocytosis
CS	-	Chondroitin Sulfate
CSPG	-	Chondroitin Sulfate Proteoglycan

CT	-	Cancer/Testis
DAB	-	Diaminobenzidine
DC	-	Dendritic Cells
DMEM	-	Dulbeccos Modified Eagles Media
DMSO	-	Dimethyl Sulfoximide
DMSZ	-	Deutsche Sammlung von Mikroorganismen und Zellkulturen GmbH
DNA	-	Deoxyribonucleic acid
DS	-	Dermatan Sulfate
ECL	-	Enhanced Chemiluminescence
ECM	-	Extra Cellular Matrix
EGF	-	Epidermal Growth Factor
EGFR	-	Epidermal Growth Factor Receptor
EMA	-	European Medicines Agency
EMT	-	Epithelial-Mesenchymal Transition
EPCAM	-	Epithelial Cell Adhesion Molecule
ER	-	Estrogen Receptor
ES	-	Embryonic Stem (cells)
EtOH	-	Ethanol
F_{ab}	-	Antigen-binding fragment
FAK	-	Focal Adhesion Kinase
FAP	-	Fibroblast Activation Proteins
Fc	-	Fragment, Crystallisable
FCS	-	Foetal Calf Serum
FcR	-	Fc Receptors
FDA	-	Food and Drug Administration
FGF	-	Fibroblast Growth Factors
FITC	-	Fluoroscein-Isocyanate
Fv	-	Fragment, variable
GAG	-	Glycosaminoglycan
GAPDH	-	Glyceraldehyde-3-Phosphate Dehydrogenase
GAP	-	GTPase-Activating Protein
GPC	-	Glypican
GPI	-	Glycosylphosphatidylinositol

GS	-	Gamma Secretase
GTP	-	GuanosineTtriphosphate
HA	-	Hyaluronic Acid
HAMA	-	Human-Anti-Mouse Antibody
HAT	-	Hypoxanthine, Aminopterin, Thymidine
HcAb	-	Heavy chain antibodies
HCl	-	Hydrochloric Acid
Hep	-	Heparin
HEPES	-	4-(2-HydroxEthyl-)-Piperazine Ethane Sulphonic acid
HER2	-	Human Epidermal Growth Factor 2
HGF	-	Hepatocyte Growth Factor
HGFR	-	Hepatocyte Growth Factor Receptor
HLA	-	Human Leukocytes Antigen
HMG-CoA	-	3-hydroxy-3-methylglutaryl-coenzyme A
HS	-	Heparin Sulphate
HSP	-	Heat Shock Protein
HSPG	-	Heparan Sulphate Proteoglycan
HT	-	Hypoxanthine, Thymidine
ID	-	Identification
Ig	-	Immunoglobulin
IMS	-	Industrial Methylated Spirits
IP	-	Immunoprecipitation
ITAM	-	Immunoreceptor Tyrosine-based Activation Motifs
ITIM	-	Immunoreceptor Tyrosine-based Inhibitory Motifs
KAI	-	Kangai
kDa	-	Kilo Dalton
Kin	-	Kinesin
KLK	-	Kallikrein
KS	-	Keratan Sulfate
LC-MS	-	Liquid Chromatography – Mass Spectrometry
LTQ	-	Lysine Tyrosylquinone
mA	-	milliamps
MAb	-	Monoclonal Antibody
MAC	-	Membrane Attack Complex

MAPK	-	Mitogen-Activated Protein Kinase
MCSP	-	Melanoma Chondroitin Sulfate Proteoglycan
MeOH	-	Methanol
MHC	-	Major Histocompatibility Complex
MM	-	Multiple Myeloma
MMP	-	Matrix Metalloproteinase
MOPS	-	3-(N-morpholino)propanesulfonic acid
MS	-	Mass Spectrometry
MS/MS	-	Tandem Mass Spectrometry
MT	-	Membrane Type
MW	-	Molecular Weight
m/z	-	mass-to-charge ratio
NaOH	-	Sodium Hydroxide
Na_2CO_3	-	Sodium Carbonate
$Na_2S_2O_3$	-	Sodium Thiosulphate
NCI	-	National Cancer Institute
NH_4HCO_3	-	Ammonium Bicarbonate
NICB	-	National Institute for Cellular Biotechnology
NK	-	Natural Killer
NSCLC	-	Non Small Cell Lung Cancer
PAI	-	Physiological Inhibitor
PBS	-	Phosphate Buffered Saline
PcAb	-	Polyclonal Antibody
PEG	-	Polyethylene Glycol
PG	-	Proteoglycans
PIPS	-	Phosphoinosites
PNPP	-	P-Nitrophenyl Phosphate
Poly-HEMA	-	Poly-(-2-Hydroxyethyl Methacrylate)
PR	-	Progesterone Receptor
PVDF	-	Polyvinyl Difluoride
RAIT	-	Radioimmunotherapy
RECK	-	Reversion-inducing Cysteine Rich protein with Kazal Motifs)
RIPA	-	Radio Immunoprecipitation Assay

RNAi	-	Ribonucleic Acid interference
R.T.	-	Room Temperature
RTK	-	Receptor Tyrosine Kinase
ScFv	-	Single-Chain Fvs
SCR	-	Scrambled
SdAb	-	Single domain Antibodies
SDS-PAGE	-	Sodium Dodecyl Sulfate - Polyacrylamide Gel Electrophoresis
SF	-	Serum Free
SiRNA	-	Small Interfering Ribonucleic Acid
SLRP	-	Small Leucine-Rich Proteoglycan
SOP	-	Standard Operating Procedure
Src	-	Sarcoma
TBS	-	Tris Buffered Saline
TCF	-	T Cell Factor
TEM	-	Tetraspanin-Enriched-Micro-domains
TGF	-	Transforming Growth Factors
TLR	-	Toll Like Receptor
TM4SF	-	4 span Transmembrane Super Family
TNF	-	Tumour Necrosis Factor
Tris	-	Tris (hydroxymethyl) aminomethane
UHP	-	Ultra High Pure water
uPA	-	Urokinase
uPAR	-	Urokinase Receptor
VEGF	-	Vascular Endothelial Growth Factor
V_H	-	Variable Heavy chain
V_L	-	Variable Light chain
vol/vol	-	Volume to Volume ratio
WASF2	-	Wiscott-Aldrich Syndrome Protein Family member 2
WASP	-	Wiscott-Aldrich Syndrome Protein

Abstract

Monoclonal antibodies (MAbs) have emerged as an important therapeutic modality for the treatment of cancer, due to their high specificity, low toxicity, and the ability to activate components of the immune system. The research carried out in this thesis aims to identify novel antigens associated with cancer invasion, that could form the basis of anti-invasive therapeutic targets, through the generation of MAbs directed against the highly invasive MiaPaCa-2 clone 3 pancreatic cell line, and the MDA-MB-435-SF breast cancer cell line.

Two MAbs were identified that could successfully block cancer invasion *in vitro*. MAb 7B7 G5 (2) significantly reduced invasion in the MiaPaCa-2 clone 3 pancreatic cell line; the SKBR-3 and MDA-MB-231 breast cancer cell lines; the DLKP-M and H1299 lung cancer cell lines; the SNB-19 glioma cell line and the HCT-116 colon cancer cell line. Inhibition of invasion was also observed in the Lox IMVI melanoma cell line, but not significantly so. This MAb also significantly decreased cell motility in the MiaPaCa-2 clone 3 cell line. MAb 9E1 24 (6) significantly decreased cell invasion in the MiaPaCa-2 clone 3, MDA-MB-231, DLKP-I, DLKP-M, H1299, C/68 and Lox IMVI cell lines. Invasion was also inhibited in the SKBR-3 cell line, but not significantly so. Surprisingly, invasion was *increased* in the HCT-116 colon cancer cell line, following incubation with this MAb.

Other invasion-related processes were also decreased following incubation with the MAb 9E1 24 (6) and 7B7 G5 (2); MiaPaCa-2 clone 3 adhesion to fibronectin, and MMP-9 activity in the MDA-MB-231 breast cancer cell line. Immunohistochemical analysis of 9E1 24 (6) revealed that its target antigen is expressed to varying degrees in a wide range of tumour types (colon adenocarcinoma, pancreatic, breast, B-Cell lymphoma, Retinoblastoma and Glioma). Weaker staining was observed in normal colon, liver and prostate tissues.

MAb 9E1 24 (6) was shown to react with a 75kDa protein band on Western blot analysis. Immunoprecipitation studies, followed by LC-MS/MS analysis, revealed that its target antigen was Annexin A6, a 75kDa cellular calcium and phospholipid binding protein. This was further corroborated by decreased expression of the reactive 9E1 24 (6) band in Annexin A6-silenced cells. siRNA silencing of Annexin A6 significantly reduced invasion in the MiaPaCa-2 clone 3 and DLKP-M cell lines, suggesting a role for this protein in the invasion process.

A cross-linked immunoprecipitation approach with MAb 7B7 G5 (2) revealed two bands at approximately 70 and 80kDa. LC-MS/MS analysis identified these as Ku70 and Ku80 respectively, two subunits of the Ku heterodimer, which is involved in DNA double strand break repair. siRNA silencing of these two subunits in the MiaPaCa-2 clone 3 and DLKP-M cell lines significantly reduced levels of invasion *and* motility, indicating that they play a role in both processes. Immunofluorescence analysis on Ku70 and Ku80 silenced MiaPaCa-2 clone 3 cells revealed a significant decrease in MAb 7B7 G5 (2) reactivity on Ku80, but

not Ku70, silenced cells, suggesting that the Ku80 subunit is the main target antigen for MAb 7B7 G5 (2).

The research presented in this thesis is proof of principle of how MAbs can be successfully generated that specifically target invasion-related proteins, and can block cancer invasion *in vitro*. The identified proteins may have the potential to become useful therapeutic targets for the treatment of invasive cancers, and could lead to the development of new drugs that specifically target metastatic cancer cells.

Table of Contents

CHAPTER 1
INTRODUCTION

1.1 Cancer Metastasis

Metastatic disease – the spread of cells from the primary neoplasm to distant organs, and their relentless growth - is the primary cause of death for most cancer patients. The development of invasion, which initiates the metastatic cascade, is comprised of a series of biological processes that move tumour cells from the primary site to a distant location. Each of these processes can potentially be targeted by therapeutic agents; however, the molecular events of metastasis are highly complex, and not fully understood. This is reflected in the fact that there are currently no effective treatments available that target invading tumour cells. Understanding these molecular mechanisms, and the role of the numerous proteins involved, is of crucial importance in the development of novel therapies for use in the treatment and diagnosis of cancer.

1.1.1 Mechanisms of Invasion/Metastasis

The ability of cancer cells to acquire a metastatic phenotype represents one of the most dangerous aspects of tumour progression. Normal cells are anchorage dependent and are designed to commit "suicide" by apoptosis if detached from cells of their own kind. This is a measure that prevents cancer and other abnormal growths from arising in most cases. However, in tumour cells, this regulatory process is disrupted, through accumulation of genetic changes, allowing for the survival of the tumour cell. Metastasis is the spread of these malignant tumour cells from their primary site to a distant, secondary site. The process of metastasis occurs in a series of discrete steps, termed the “metastatic cascade”.

Firstly, the tumour cells undergo a transformation known as the epithelial-mesenchymal transition, or EMT, which is a typical feature of aggressive, invasive and metastatic cancer cells (de Wever *et al*., 2008). This is followed by invasion, which initiates the metastatic process. This consists of (1) changes in tumour cell adherence to cells and the extra cellular matrix (ECM), (2) proteolytic degradation of the surrounding tissue and (3) motility to physically

propel a tumour cell through tissue. These metastatic cells are then transported around the body, where they can then colonise distant organs and establish secondary tumour sites.

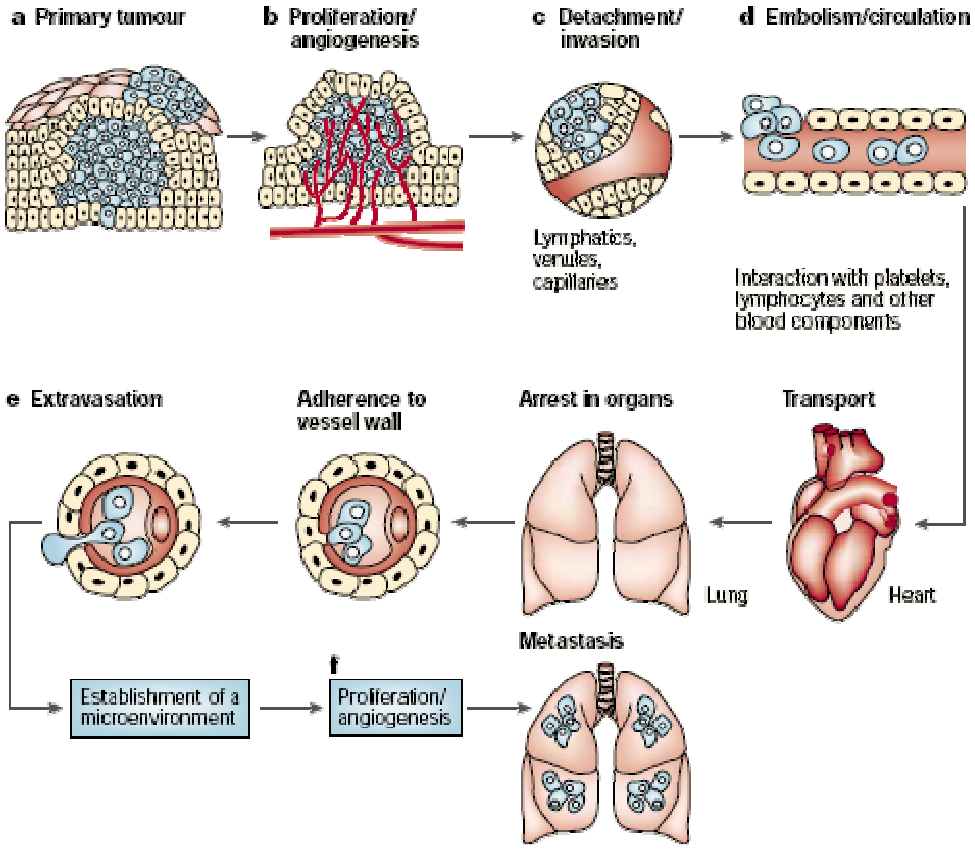

Figure 1.1: - The main steps involved in the formation of metastasis (Fidler, 2003)

EMT is a program of development of biological cells characterised by loss of cell adhesion, repression of E-cadherin expression, and increased cell mobility. It is normally observed in tissue morphogenesis during embryonic development and in fibrosing conditions succeeding tissue injury. During EMT, non-motile, polarised epithelial cells, embedded via cell-cell junctions in a cell collective, dissolve their cell-cell junctions and acquire characteristics similar to mesenchymal cells - non-polarised, motile and invasive (Yilmaz *et al*., 2009). Although the molecular basis of EMT are still not fully understood, several interconnected pathways and signalling molecules involved have been identified (growth factors, receptor tyrosine kinases, GTPases, β-catenin and integrins). Most of these pathways converge on the down regulation of the epithelial

molecule E-cadherin, an essential event in tumour invasion. (Guarino *et al*., 2007).

Once a cell undergoes EMT, it now has the ability to change its position within the tissue. Neoplastic cells are able to enter lymphatic and blood vessels through ECM invasion, allowing for the dissemination into the circulatory system, and finally, to undergo metastatic growth in distant sites. The process of tumour spreading within tissues uses migration mechanisms that are similar, if not identical, to those that occur in normal, non-neoplastic cells during physiological processes (Friedl *et al*., 2003).

In order for migration to occur, the cell body needs to alter its shape and stiffness, thus allowing it to interact with the surrounding tissue structures. Hereby, the ECM is the environment in which tumour cells proliferate and provides the substrate, along with a partial barrier towards the advancing cell body. Cell migration through the tissue results from a continuous cycle of interdependent steps:

(1) Polarisation and elongation of the cell body
(2) Formations of a pseudopod, through extension of the cell's leading edge
(3) Contraction of regions on the leading edge, or the entire cell body, thus generating traction force
(4) Cell body and trailing edge glides forward (Friedl *et al*., 2003).

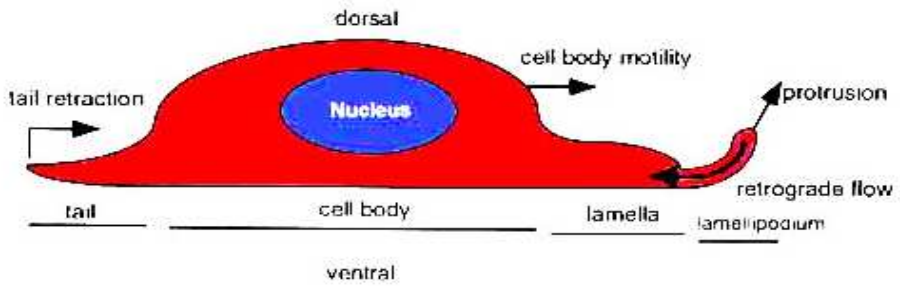

Figure 1.1.1: - Side view diagram of retrograde flow in lamillopodia in a motile/locomoting cell (Cramer, 1997)

Cell motility is also mediated by adhesion molecules. Cell adhesion molecules (CAMs) can be divided into 5 major families: the immunoglobulin superfamily, the integrins, selectins, cadherins and CD44 (Dowling *et al*., 2008).

Intravasation, or penetration of the basement membrane barrier by tumour cells, is achieved through the release a variety of proteases, glycosidases, and collagenases, thus allowing for the degradation of various components of the matrix and resulting in tumour cell invasion through tissue barriers, blood vessels, and lymph channel. Matrix metalloproteinases (MMPs) are a family of membrane-anchored proteolytic enzymes that can remodel the ECM by acting on a relatively broad range of targets including collagen, plasminogen, elastin, fibronectin and laminin (Dowling *et al*., 2008). Tumour cells may also release polypeptide factors that can modulate the type of proteoglycans produced by host mesenchymal cells (Kufe *et al*., 2003).

Once the tumour cell has detached from the primary site, and successfully invaded through the ECM, it then has several other phases to complete before it can colonise a second tumour site.

⇒ Survival & Arrest in the Bloodstream

Once the tumour cell invades through the ECM, it then enters the circulatory or lymphatic system, allowing it to travel to a new location. However, the bloodstream is a harsh environment for metastasising tumour cells because of velocity-induced shear forces and the presence of immune cells. Once the tumour cells have gained access to the blood system, they may be swept away to distant sites, which they can colonise. Within the bloodstream the tumour cells may interact with host components such as lymphocytes, monocytes and platelets through heterotypic adhesion. This may lead to larger clumps incorporating the tumour cells, lending them protection from mechanical stress and immune attack. Despite this, the chances of a cancer cell surviving circulation and establishing a new site is fewer than 10,000 to 1 (Zhao *et al*., 2010).

⇒ ***Lodgement at a Distant Site***

The circulation of the blood plays a significant role in determining where cancer cells travel. The cancer cells usually get trapped in the first set of capillaries, they encounter downstream from their point of entry. Frequently these are in the lungs, since returning deoxygenated blood leaving many organs is returned to the lungs for re-oxygenation. Once in a new site, the cells must again penetrate the basement membrane of the blood vessel and establish themselves in the new tissue.

⇒ ***Extravasation***

After tumour cells enter the systemic circulation, and in order for a metastatic tumour to develop, the cells must extravasate from the blood supply, invade local stroma, and develop their own microenvironment (Small *et al*., 2002). The formation of new blood vessels (angiogenesis) is stimulated, so that oxygen and vital nutrients can reach the growing tumour.

⇒ ***Growth***

Proliferation of the cancer cells at their new site is dependant on a number of factors including the nature of the environment it finds itself in and the nature of the tumour itself. These factors include resistance to host defence mechanisms of humoral and cellular nature and response to or requirement for specific growth factors. Failure in any one of these steps results in the death of the cancer cell, making this process highly inefficient. Millions of tumour cells can be shed into the circulatory system daily, with few secondary tumours forming (Kufe *et al*., 2003).

As has been shown, there are a multitude of factors involved in the metastatic process. Several key stages in the metastatic process have been shown to be controlled, directly or indirectly, through the cell surface, so the identification of these proteins that are preferentially expressed on the membrane of metastatic tumour cells is of fundamental importance in cancer research. The following sections will focus on various cell surface proteins, proteoglycans and

proteolipids that play a role in the metastatic process, including adhesion, ECM-degradation and cell motility.

1.1.2. Cell Surface Proteins in Invasion/Metastasis

Membrane proteins play a key role in cellular processes such as migration, adhesion, and cell survival. However, during transformation from a normal cell into a tumour cell, specific defects appear in these proteins, resulting in the loss of tumour suppressor genes, and alteration of cell cycle control. The cells become growth-factor independent, losing contact inhibition and features of differentiation (Chow, 2010). These transformed cells are a pre-requisite for metastasis, but they still need to acquire a wide range of molecular properties in order to complete the whole metastatic process, most of which are likely to be mediated by cell-surface proteins. Three different groups of molecules are essential for the metastatic cascade to occur:

1. ***Proteases***: - The proteolytic breakdown of proteins of the ECM is an essential step in the metastatic process. Several classes of proteases contribute to the breakdown and remodelling of the ECM, most of which are up-regulated in the course of metastatic cancer progression in different types of cancers. When invasive cells migrate through the ECM, proteases such as MMPs, serine proteases and cathepsins are utilised to proteolytically cleave and remove different ECM substrate types at cell-ECM interface. These proteases can originate from the cell surface, intracellularly or can be secreted (Friedl *et al*., 2008).

2. ***Cellular Adhesion Molecules (CAMs)***: - CAMs are glycoproteins expressed on the surface of cell membranes. In normal cells, they are involved in numerous cell processes such as cell proliferation, migration and differentiation. In tumourigenic cells, they have been reported to function as oncogenes or tumour suppressors, as well as regulators of tumour progression and metastasis. CAMs interact with other CAMs, as well as with multiple intracellular proteins and ECM components (Kerrigan *et al*., 1998).

The Cadherins, a type-1 transmembrane family of proteins, play an important role in cell adhesion, ensuring that cells within tissues are bound together. Loss of E-cadherin gene expression or of the E-cadherin protein, through EMT, is frequently found during tumour progression in most epithelial cancers (Vernon *et al*., 2004). Other membrane proteins involved in cellular adhesion include the immunoglobulin superfamily, selectins, and CD44. Integrins are also involved in adhesion, binding to a wide range of ECM molecules (Karmakar *et al*., 2003).

3. ***Cell surface and cytoskeletal proteins***: - mediate directional cell movement. This involves regulation of the actin cytoskeleton; an essential step for tumour cell migration, adhesion and invasion.

1.1.2.1 Cadherins

The cadherins are a family of homophilic, cell surface membrane glycoproteins capable of mediating cell-cell adhesion. Their extracellular regions consist of five tandemly repeated domains that require Ca^{2+} binding for their adhesiveness, rigidity and stability. The three most common cadherins are E-, N- and R-cadherins (based on the tissue from which they were first derived; epithelial, neural and retinal tissues respectively) (Baranwal *et al*., 2009).

E-cadherin, one of the most widely studied of the cadherins, is a single-span transmembrane glycoprotein of five repeats and cytoplasmic domain. It mediates homotypic adhesion in epithelial tissue, bonding epithelial cells together and relaying signals between the cells (Dowling *et al*., 2008). Down-regulation of E-cadherin reduces the cell-cell adhesion, facilitating detachment from the primary tumour and subsequent invasion into the surrounding tissue and environment. It has been suggested that loss of E-cadherin mediated cell-cell adhesion is a necessity for tumour cell invasion and metastasis formation (Heuberger *et al*., 2010).

Loss of E-cadherin function during tumour development can be caused by a variety of genetic or epigenetic mechanisms. Strathdee *et al.,* showed that in a

panel of cancer cell lines, E-cadherin expression is downregulated at the transcriptional level through the binding of proteins, such as Snail and Slug, to the E2 boxes in the promoter of the E-cadherin gene (Strathdee, 2002). It has also been shown that engagement of integrins α1β1 and α2β1 by collagen type I results in a loss of E-cadherin mediated cell-cell contacts, along with the activation of the β-catenin/TCF (T cell factor) pathway in pancreatic cancer cells (Yilmaz *et al.*, 2009). In adheren junctions, the intracellular domain of E-cadherin binds directly to β-catenin, that, in turn, associates with α-catenin, which links cadherin complexes to the actin cytoskeleton. There are a number of stimulations, such as growth factor stimulation, which results in E-cadherin-associated β-catenin tyrosine phosphorylation, and this phosphorylation destabilizes the E-cadherin complex and actin linkage. This causes loss of homophilic E-cadherin-dependent adhesion and induction of cell motility (Abe *et al*., 2008).

An important molecular event in cancer progression is the switching of the expression of E-cadherin to N-cadherin, a process that takes place through the EMT. N-cadherin expression has been shown to promote aggressive behaviour of tumour cells, ranging from interacting with receptor tyrosine kinases at the cell surface to encouraging the activation levels of Rho-GTPases in the cytosol. (Baranwal *et al.*, 2009). N-cadherin has also been implicated in promoting cell motility and migration – an opposite effect to that of E-cadherin. This switch in cadherins may provoke the tumour cell to migrate into different surroundings. E-cadherin is expressed by epithelial cells, whereas mesenchymal cadherins are found in stromal cells such as fibroblasts (Cavallaro *et al*., 2004).

1.1.2.2 Integrins

Integrins are a diverse family of glycoproteins that serve as the main link between a cell and the ECM, forming heterodimeric receptors for ECM molecules. Containing 18 α-subunits and 8 β-subunits, integrins are able to form at least 25 distinct pairings, each of which is specific for a unique set of ligands. Each integrin generally consists of a non-covalently linked α- and β- subunit, each of which consists of a large extracellular domain, a single membrane-

spanning domain, and a short, non-catalytic cytoplasmic tail (Gerger *et al*., 2009).

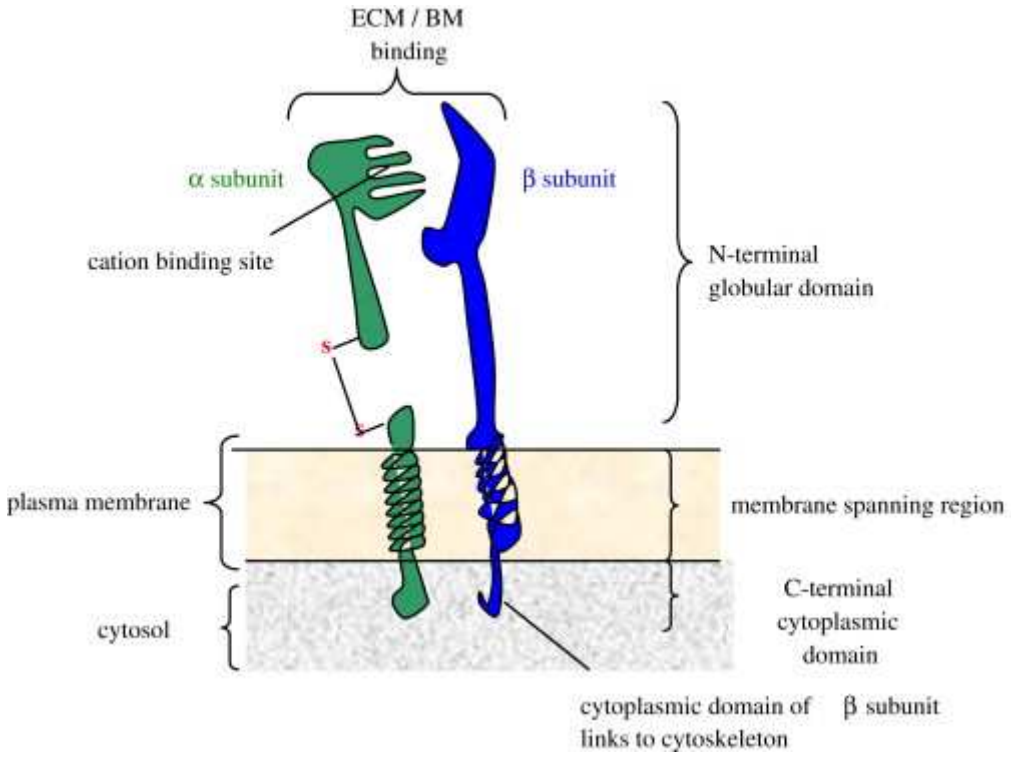

Figure 1.x: - Structure of integrin (Brooks *et al*., 2010)

Altered expression of integrins in tumour cells promotes metastasis through the following mechanisms:

(1). ***Integrin-mediated tumour cell de-adhesion to the surrounding ECM, thus enabling tumour cells to detach from the primary tumour:*** Integrins function as both mechanical adhesion and signalling molecules. For example, integrin αvβ3 binds a wide variety of ECM molecules, including fibronectin, fibrinogen, vitronectin and proteolysed forms of collagen and laminin (Brooks *et al*., 2010).

(2). ***Tumour cell migration into the ECM and surrounding stroma involving integrin-mediated adhesion/de-adhesion events:***

Integrins are vital for cell migration and invasion, not only because they directly mediate cell-ECM adhesion, but also because they regulate intracellular signalling pathways that control cytoskeletal organisation and force generation and survival. These pathways typically involve phosphorylation of focal

adhesion kinase (FAK), a cytoplasmic protein kinase that is localised at structures called focal adhesions (Brooks *et al*., 2010). FAK has been shown to promote cell migration through direct modulation of key proteins involved in the remodelling of the actin cytoskeleton, including the Rho subfamily of small GTPases (Hsia *et al*., 2003), N-WASP (Wu *et al*., 2004), and the Arp2/3 complex (Ichikawa *et al*., 1991).

(3). ***Release of proteolytic enzymes induced by integrin-mediated intracellular signalling events:***

The integrins not only mediate cell-ECM adhesion; ligand binding can also result in the activation of further intracellular signalling pathway, which then stimulates proteolysis. Degradation or disorganisation of the basement membrane is a key feature of a tumour's transition to a metastatic carcinoma (Egeblad *et al*., 2002). Cancer cells produce, activate and release several different types of proteases that specifically cleave ECM molecules. One family of proteases activated by up-stream stimulation of integrin receptors are the MMPs. There are a number of reports demonstrating that co-localisation of β1-integrin and MT1-MMP1 is a requirement for cancer cell invasion into a collagen matrix and that both MT1-MMP and β1-integrins have important roles in EMT (Cao *et al*., 2008). Work done by Brookes *et al*., have shown that MMP-2 can be localised in a proteolytically active form on the surface of invasive cells, through its direct binding of the $\alpha_v\beta_3$ integrin. This allows for facilitation of cell-mediated collagen degradation and directed cellular invasion (Brooks *et al*., 1996). Numerous other studies have also shown increased activation of MMPs during expression of integrins ($\alpha_v\beta_1$ and MMP-3; $\alpha_v\beta_6$ and MMP-9 in colon carcinoma cells (Werb *et al*., 1989)).

1.1.2.3 Regulation of the Actin Cytoskeleton

The formation of protrusive structures is a necessity for tumour cell movement and invasion. This is achieved through regulation of actin polymerisation. These protrusions, termed filopodia, lamellipodia and invadopodia, are driven by spatially and temporally-regulated actin polymerisation at the leading edge of the cell (Yamaguchi *et al*., 2007). Stabilisation of the protrusive structures is

achieved through integrin-mediated binding to the ECM of the actin cytoskeleton. This serves the additional role of co-ordinating signal transduction events that regulate cell movement (Kelley *et al*., 2008).

Lamellipodia are the major organelles involved in cell movement, building upon highly branched dendritic actin networks. They interact with their surrounding environment through N-cadherin, β1-1 integrin or the hyaluronan receptor CD44, (which is also important for the correct positioning of the membrane-bound MT1-MMP) (Yilmaz *et al*., 2009). Lamellipodia protrusion is initiated by localised polymerisation of actin, which in turn requires the generation of free barbed ends of actin filaments at the leading edge. There are three major mechanisms for generation of free barbed ends:

(1). ***de novo* nucleation by Arp2/3 complexes and formins**:

Actin polymerisation occurs by coupling to the actin-nucleating Arp2/3 complex, an activator of actin filament nucleation and branching (Yamaguchi *et al*., 2007), which in turn binds to a multifunctional adaptor protein, known as the Wiscott-Aldrich syndrome protein (WASP). This Arp2/3/WASP complex then connects to the inner leaflet of the plasma membrane via clustered phosphoinosites (PIPs) inserted therein. Arp2/3 can further interact laterally with established actin filaments to induce branching of pre-existing filaments to actin networks (Friedl *et al*., 2003).

(2). ***severing of pre-existing actin filaments by cofilin***:

The severing of existing actin filaments is carried out by cofilin in response to epidermal growth factors (EGF) and other growth factor stimuli. This severing activity has a dual effect on actin dynamics to promote cortical actin-based protrusions: the number of available barbed ends increase, thus allowing for rapid actin polymerisation at the cell cortex, independent of Arp2/3 complex activity. It also serves to boost F-actin depolymerisation, therefore utilising G-actin monomers in a further round of polymerisation (Kelley *et al*., 2008).

(3). ***uncapping of barbed ends on pre-existing actin filaments***:

At the trailing edge, focal contact disassembly occurs through several mechanisms. Actin binding and severing proteins (Cofilin) cap actin filaments and cause actin filament strand breakage, respectively, and focal contact components are cleaved through the cytoplasmic protease calpain (Friedl *et al*., 2003).

Cortactin is an adaptor protein that is present in lamellipodia and invadopodia that plays a role in stimulating actin nucleation and subsequent polymerisation by binding to F-actin and the Arp2/3 complex (Weed *et al*., 2001). In addition to regulating actin polymerisation within lamellipodia, cortactin also plays a role in the stabilisation of the actin networks formed by Arp2/3-driven polymerisation, a process congruent with the requirement for cortactin to maintain lamellipodia persistence. While not essential for lamellipodia formation, Cortactin is a crucial requisite for the creation of (matrix degrading) invadopodia. Invadopodia consist of an outer adhesive ring and a central actin-rich core. Cortactin, along with the non-receptor tyrosine kinase Src, and the membrane bound MT1-MMP plays an essential role in the formation and function of invadopodia. Integrins, such as αvβ3, in conjunction with their cytoplasmic interaction partners, are situated in the adhesive ring where they can mediate adhesion (Kelley *et al*., 2008).

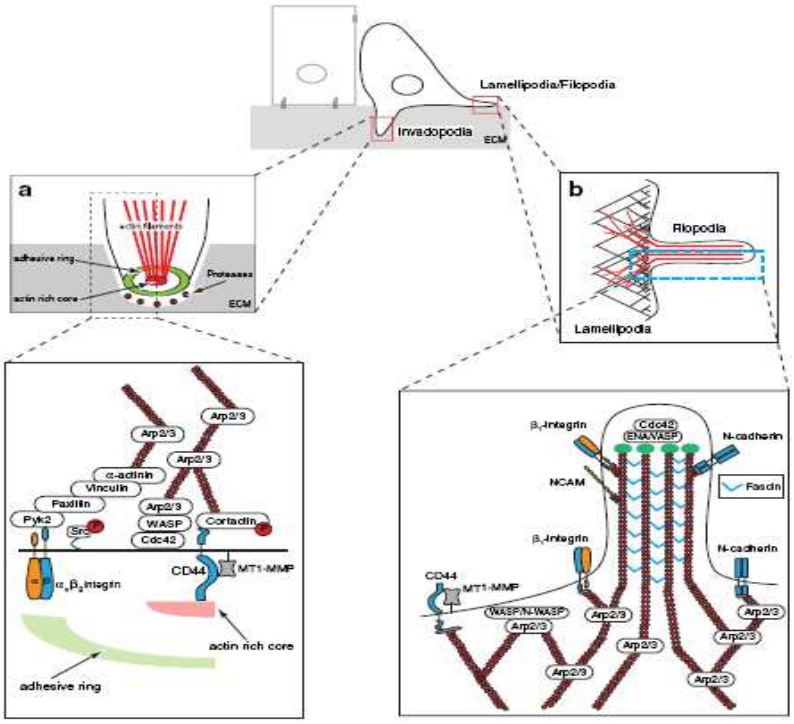

Figure 1.4: - Various proteins involved in lamillopodia/filopodia and invadopodia formation (Yilmaz *et al.*, 2009).

1.1.3 Proteoglycans

Proteoglycans (PGs) are ubiquitous biomolecules located in the ECM, on the cell surface and within cells that are heavily glycosylated. They consist of a core protein with one or more covalently attached glycosaminoglycan (GAG) chain(s) (Braga, 2008). These chains are long, linear carbohydrate polymers, and due to the occurrence of sulphate and uronic acid groups, they are negatively charged under physiological conditions.

Located at the cell-tissue-organ interface, PGs are thought to govern crucial regulatory roles in cellular control, including cell movement in various physiological and pathological contexts, such as:

- binding together ECM components such as hyaluronic acid, collagen, laminin and fibronectin.
- mediating cell-ECM adhesion.

- acting as a reservoir for growth factors.
- presentation of growth factors to growth factor receptors on cells; (Cattaruzza *et al*., 2006).

PGs also act as cell adhesion factors by encouraging the organisation of actin filaments in the cells cytoskeleton (Kufe *et al*., 2003). The complex nature of PGs on the tumour cell surface allows for modulation, directly or indirectly, of several facets of the tumour cell phenotype, including growth kinetics, invasiveness and metastatic potential (Rossi, 2009). There are a number of examples of PGs involved in the metastatic cascade.

1.1.3.1 Heparan Sulphate proteoglycans (HSPG): - Syndecan

HSPGs on the tumour cell surface have been shown to play an important role in many aspects of tumour phenotype and development, including cellular transformation, tumour growth, invasion and metastasis. Due to their negative charge, the heparin sulphate (HS) chains bind to a very wide variety of proteins, including the members of the fibroblast growth factor (FGF) family and their receptor tyrosine kinase, transforming growth factors (TGFs) (Rossi, 2009).

Over the past 30 years, substantial evidence has been gathered pointing to the role cell surface HSPGs play in inhibiting tumour invasion through the promotion of tight cell-cell and cell-ECM adhesion. There are numerous studies showing weak expression of heparin sulphate (HS) isolated from tumourigenic cells, when compared to normal cells. Alterations in HS have been shown to reduce the adhesive capacity of transformed cells. Low levels of cell surface HS also correlates with high metastatic activity of many tumours (Rossi, 2009). The most widely studied cell surface HSPG is the Syndecan family. Syndecans are a family of highly conserved type I transmembrane HSPGs and are expressed on virtually all cell types throughout development and adulthood. Syndecan-1 regulates cell behaviour by binding ECM molecules such as growth factors types I, III, and V collagen, fibronectin, thrombospondin, and tenascin, via its HS chains. It also binds to basic fibroblast growth factor (bFGF/FGF-2), a member

of the heparin-binding growth factor (Anttonen *et al*., 1999). In a range of epithelial tumours including colon (Levy *et al*., 1996), mesothelioma (Kumar-Singh *et al*., 1998), lung (Anttonen *et al*., 2001), hepatocellular carcinoma (Matsumoto *et al*., 1997), infiltrating ductal carcinoma of the breast (Stanley *et al*., 1999), and head and neck carcinoma (Anttonen *et al*., 1999), syndecan-1 expression on the tumour cell surface decreases with increasing metastatic potential. Thus, decreased expression of syndecan-1 on tumour cells parallels with a decrease in overall HS expression (Mennerich *et al*., 2004). This data suggests that HSPGs and syndecan-1 in particular, play an important role in helping to block metastasis.

Syndecan-1 has also been found to play an important role in supporting $\alpha_2\beta_1$ integrin-mediated adhesion. Work done by Vuoriluoto *et al.,* has shown, through overexpression and knock-down experiments, that syndecan-1 enhances binding of $\alpha_2\beta_1$ to collagen. Moreover, they showed that Syndecan-1 co-localises with $\alpha_2\beta_1$ integrin and contributed to proper organisation of the cortical actin. Crosstalk between syndecan-1 and $\alpha_2\beta_1$ integrin resulted in enhanced transcription of MMP-1 in response to collagen binding. These findings suggest that the $\alpha_2\beta_1$/syndecan-1 complex is important in regulating cell adhesion to collagen and in triggering integrin downstream signalling (Vuoriluoto *et al*., 2008).

Syndecan-2, also called fibroglycan, has been observed to participate in diverse biological processes, including matrix assembly, cell adhesion and signalling (Tkachenko *et al*., 2005). In work carried out by Choi *et al.,* overexpression of syndecan-2 was shown to enhance adhesion to collagen, cell migration and invasion in normal rat intestinal epithelial cells. Increased integrin $\alpha_2\beta_1$ expression levels were also observed. When $\alpha_2\beta_1$ integrin expression was knocked down in colon cancer cells, levels of syndecan-2 were also diminished, resulting in decreased adhesion and migration, suggesting a relationship between syndecan-2 and $\alpha_2\beta_1$ integrin in adhesion-mediated cell migration and invasion (Choi *et al*., 2009). Co-operation between syndecan-2 and the $\alpha_5\beta_1$ integrin has also been shown in adhesion of lung carcinoma cells to fibronectin substratum,

along with regulation of the actin cytoskeleton organisation (Kusano *et al*., 2004).

1.1.3.2 Melanoma Chondroitin Sulphate Proteoglycan

Melanoma chondroitin sulphate proteoglycan (MCSP) represents a unique glycoprotein–proteoglycan complex, with a 250 kDa core glycoprotein attached to a larger, 450 kDa proteoglycan component, via serine residues. It is a cell surface proteoglycan expressed relatively early in melanoma progression, and has been implicated in the malignant properties of advanced melanoma (Erfurt *et al*., 2009). Work done by Iida *et al*., have shown that MCSP interacts with a member of the MT-MMP family, allowing for the invasion of melanoma cells through type I collagen and degradation of type I gelatine (Iida *et al*., 2001).

MT3-MMP has been shown to be specifically localised with MCSP to ECM adhesion sites on the surface of melanoma cells. This interaction requires the expression of an intact chondroitin sulphate proteoglycan (CSPG). Work done by Iida *et al.*, suggests that the invasion of aggressive primary tumours within the dermis may be facilitated by MCSP enhancing the local concentration and/or activation of specific MMPs at contact sites between melanoma cells and the underlying ECM (Iida *et al*., 2001).

1.1.3.3 Versican

Versican is a CSPG consisting of a core protein with 12-15 chondroitin sulphate (CS) side chains covalently attached. It belongs to a family of extracellular proteoglycans (hyalectins) that bind to hyaluronan (HA) (Ricciardelli *et al*., 2007). Versican (which possesses four isoforms) regulates many diverse cellular processes, including adhesion, proliferation, apoptosis, migration and invasion through the highly negatively-charged chondroitin/ dermatan sulphate side chains. High levels of versican expression have been observed in a wide range of cancers, including; melanomas, osteosarcomas, lymphomas, breast, brain, prostate, colon, lung, pancreatic, endometrial, oral, and ovarian cancers (Ricciardelli *et al*., 2009), suggesting that it is important in promoting cancer cell

motility and invasion. Work carried out by Riccaedelli *et al.,* has shown that versican-treated cancer cells incorporate versican and hyaluronic acid into a prominent pericellular matrix that promotes their motility. Following versican treatment, a pericellular sheath of defined polarity is constructed by motile prostate cancer cells. The ability to construct this pericellular sheath correlated with the expression of the membranous HA receptor, CD44. All this suggests that tumour cells can form a polarised pericellular sheath through compartmentalised cell surface CD44 expression and ensuing assembly of HA/versican aggregates. The lack of a pericellular sheath at the leading edge of the cell may facilitate the attraction and binding to ECM components such as fibronectin, whilst at the trailing edge of the cell, the presence of a pericellular sheath inhibits cellular binding to ECM components, thus allowing for forward locomotion of the cell (Ricciardelli *et al*., 2007).

In work done by Kim *et al.,* (2009), the molecular pathways that link tumour cells, macrophages and metastasis was explored. Using the Lewis lung carcinoma cell line, components from the media, in which the cells were grown in, were purified, allowing for the identification of a factor that induced cytokine production by macrophages. This tumour-derived macrophage activator was ascertained as versican. It was also found that versican was recognized by TLR2 and TLR6, two receptor proteins that belong to a family of cellular sensors of microbially derived molecules and tissue damage. Using small interfering RNAs, they went on to silence versican in tumour cells, and used TNF and TLR-null mice. On the basis of the evidence obtained, it was proposed that in the Lewis lung carcinoma model, tumour-derived versican acts on macrophages through TLR2/TLR6, leading to the production of inflammatory cytokines which enhance metastasis (Kim *et al*., 2009; Mantovani *et al*., 2009).

1.1.3.4 HSPG: - Perlecan

Although HS acts as an inhibitor against the metastatic cascade, it may also play a role in promoting metastasis. HS present in the ECM is thought to be involved in this, although there is some evidence that cell surface HSPGs may also contribute to metastatic behaviour. HSPGs present in the ECM can originate

from cellular secretions (Perlecan) or from cell surface HSPGs, which are then proteolytically shed from the cell surface (Syndecans) (Reiland *et al*., 2004).

Perlecan is a major HSPG that is an important component of epithelial and endothelial basement membranes. Perlecan has recently been shown to support tumour progression and vascularisation in colon carcinoma (Sharma *et al*., 1998). Increased Perlecan levels have also been demonstrated in breast carcinomas (Iozzo *et* al., 1994) and in metastatic melanomas (Cohen et *al., 1994)* and correlated with a more aggressive phenotype (Savore *et al*., 2005)**.** One way in which Perlecan and other HSPGs in the ECM may promote metastasis is through the binding of chemokines or growth factors within close proximity to migrating tumour cells. Through this, haptotactic-gradients could be formed, providing specific stimuli for migrating cells. For example, hepatocyte growth factor (HGF) binds to HS, and this may be a means to create a reservoir of HGF within matrices adjacent to tumours. Date *et al*., have shown that when HGF activity is interrupted, carcinoma cell invasion is blocked, highlighting the relevance of this to metastasis (Date *et al*., 1998).

Along with its role in influencing cytokine activity, HSPG, when bound to the ECM, could also regulate cell migration, by providing an adhesive tract to facilitate movement. HS interactions with other molecules are usually of a weak affinity, thus allowing for cells to move along paths of HS. Additionally, HSPGs present in the ECM may bind to other molecules, thus masking them (e.g. collagen, fibronectin) resulting in a decrease in cell adhesion to the ECM. This possibility is supported by studies analysing tumour invasion through type I collagen gels. Non-invasive cells show substantial increases in invasion when heparin or heparan sulphates are added to the gels, and this is likely due to heparin binding to collagen and blocking adhesive interactions between the cell surface HSPGs and collagen (Savore *et al*., 2005). However, Perlecan may not always act to promote invasion, as it suppresses the growth and invasion of fibrosarcoma cells. This disparity in results suggest that Perlecan has a complex and wide ranging role in cell-ECM interaction; however, this may be due to the fact that Perlecan is part of the extracellular matrix in mesenchymal tissue, and

cells undergoing EMT may up-regulate Perlecan expression as part of their EMT programming (Date *et al*., 1998).

1.1.3.5 CD44-Related CSPG

Melanoma cells can express the CD44 core protein as a cell surface Chondroitin Sulphate Proteoglycan (CSPG) (Faassen *et al*., 1992). The CD44 proteoglycan forms a ubiquitously expressed family of cell surface adhesion molecules involved in cell-cell and cell-matrix interactions. CD44 proteins are composed of single chain molecules, containing an N-terminal extracellular domain, a membrane proximal region, a transmembrane domain, and a cytoplasmic tail. The primary ligand of CD44 is hyaluronic acid, a vital component of the extracellular matrix. Other CD44 ligands include osteopontin, serglycin, collagens, fibronectin, and laminin (Goodison *et al*., 1999).

Over expression of CD44 is conventionally believed to be detrimental for cancer patients because it may reflect the presence of more malignant metastatic tumours. Work done by Iida *et al.*, have shown that CD44, expressed as a CSPG, acts in unison with α2β1 integrin to support melanoma cell migration on type IV collagen and invasion for basement membranes. The integrin functions as the primary adhesion molecule for type IV collagen, while the CD44/CSPG mediates some aspect of melanoma cell migration that occurs as a post adhesion event (Iida *et al*., 1996).

Bourguignon *et al.,* have shown that CD44 plays a role in structuring the lamellopodial membrane extensions of the leading front of migrating cells. It was shown that the interaction of CD44 with Src kinases affected the cytoskeletal rearrangements at the filopodial-lamellopodial cell membrane protrusions by acting upon the underlying cortactin adaptor protein (Bourguignon *et al*., 2008).

1.1.4. Proteolipids

The term proteolipid is used to define all proteins containing covalently bound lipid moieties, including fatty acids, isoprenoids, cholesterol and

glycosylphosphatidylinositol. Examples of proteolipids include the tetraspanin family and GPI-anchors (lipidlibrary.aocs.org).

Human tetraspanin proteins are composed of 33 highly hydrophobic cell surface proteins that can form complexes in cholesterol-rich micro-domains, distinct from lipid rafts, on the cell surface in a dynamic reversible way. A core of several tetraspanin proteins form these complexes, which then organise other membrane proteins such as integrins, human leukocytes antigen (HLA) antigens and some growth factor receptors (Lazo, 2007). They consist of four conserved transmembrane domains, with characteristic extracellular loops, and short cytoplasmic domains. With a molecular weight range of 22–30 kDa, these relatively small proteins generally do not play the role of classical cell surface receptors. Instead, they function as molecular organisers of multi-protein membrane complexes, influencing a number of cellular functions, including proliferation, fusion, signalling, and migration (Stipp *et al*., 2003). As well as their role in cellular function, tetraspanins can form tetraspanin-enriched-micro-domains, or TEMs, through associations with each other, and other proteins, including integrins, immunoglobulin (Ig) superfamily members, proteoglycans, ligands, and growth factor receptors (Lafleur *et al*., 2009). The tendency of different tetraspanins to associate closely within TEMs probably underlies the ability of distinct tetraspanins to provide functional compensation for each other (Lazo, 2007).

1.1.4.1 Tetraspanins and Cell Adhesion: CD82 & CD151

The tetraspanin protein superfamily member CD82 (KAI-1, kangai, or CD33) is a member of the 4-span transmembrane super family (TM4SF) of type III membrane proteins, specifically of the tetraspanin subgroup. It is localized on the cell membrane and functions as a link between the actin cytoskeleton and membrane raft domains, inducing stable adhesion, spreading and development of membrane extensions (Lazo, 2007). KAI1/CD82 is a wide-spectrum tumour metastasis suppressor associated with proteins important for cell migration, such as cell adhesion molecules, growth factor receptors, and signalling molecules. Expression of CD82/KAI-1 in cancer patients correlates with a better prognosis,

while down-regulation of KAI-1/CD82 is commonly associated with clinically advanced cancers (Guo *et al*., 2009).

KAI-1/CD82 has been shown to stabilise E-cadherin– β -catenin complexes through inhibition of β-catenin tyrosine phosphorylation. This results in induction of homocellular adhesion and prevents cancer cell dissemination from primary cancer sites. A shift in Protein-Localisation of KAI-1/CD83 from the membrane in grade 1 ovarian tumours to the cytoplasm in grade 3 tumours may be a mechanism by which tumour cells lose their adhesive properties during malignant transformation (Houle *et al*., 2002).

Work done by Goa *et al*., suggested that synergism between wild-type p53 and JunB is involved in regulating the expression of KAI-1/CD83. When p53 dysfunction coincides with low expression of JunB, they may play an important role in down-regulating the expression of KAI-1 through synergism in human hepatocellular carcinoma (Guo *et al*., 2009). From all of this, it is apparent that KAI-1/CD82 is a pivotal molecule in the regulation of cancer cells behaviour and has important clinical and therapeutic implications in cancer.

CD151 is widely expressed on the surface of many cell types, where it associates strongly with laminin-binding integrins. Whereas other tetraspanins suppress tumour cell invasion and metastasis (Wright *et al*., 2004), CD151 promotes tumour malignancy (Testa *et al*., 1999), and its expression correlates with poor prognosis, enhanced metastasis, or increased motility in several cancer types (Yang *et al*., 2008). The best-known function of CD151 is its engagement of integrins in basal lateral cell surface complexes, such as α3β1 and α6β4, to facilitate cell-cell and cell-matrix adhesions (Chien *et al*., 2008). Lammerding *et al*., have shown that CD151 plays a key role as a regulator of α6β1 integrin adhesion strengthening. They proposed a “transmembrane linker” model in which (*i*) the integrin contacts laminin, (*ii*) CD151 forms an extracellular contact with the α subunit of laminin-binding integrins, and (*iii*) CD151 uses its short cytoplasmic tail to engage as yet unidentified membrane-proximal elements, thus strengthening integrin-mediated adhesion (Yang *et al*., 2008).

1.1.4.2 Tetraspanins and MMP Regulation

Work done by Penas *et al*., have shown that tetraspanins tend to localise into cellular lamillopodia and filopodia, thus their location at the cell surface allows them to orchestrate events such as pericellular proteolysis by membrane-anchored proteases (Penas *et al*., 2000). Along with β1- integrins and CD44, tetraspanin proteins such as CD63 and CD81 are associated with MT1-MMP (in human embryonic kidney cells, over-expression of CD63 correlates with a decrease in cell surface levels of MT1-MMP). MT1-MMP binds to the N-terminal region of CD63, leading to endocytosis and degradation of MT1-MMP in lysosomes. This suggests that CD63 seems to promote lysosomal degradation of MT1-MMP (Huang *et al*., 2006). Work carried out by Jang *et al*., showed that reduced CD63 expression contributes to the invasive and metastatic ability of human melanoma cells, and knockdown in MelJuso cells resulted in an increase in cell motility and activity of matrix-degrading enzymes such as MMP-2/-9 (Jang *et al*., 2003). CD63 has also been shown to associate with other tetraspanin proteins, (CD9 and CD81), and with β1 integrins in human melanoma cells (Iida *et al*., 2001).

CD151 has also been shown to associate with members of the MMP family. In human lung adenocarcinoma tissues, proMMP-7 is captured and activated on the cell membranes through interaction with CD151, while the activity was eliminated by their treatment with MMP inhibitors, anti-MMP-7 or anti-CD151 antibodies. This suggests that MMP-7, mediated by CD151, is involved in the pericellular activation mechanism, a crucial step in proteolysis on the tumour cell (Shiomi *et al*., 2005).

1.1.4.3 Tetraspanins and Cell Motility

Down regulation of the tetraspanin CD82 is a frequent occurrence in advanced stages of cancer, and has been strongly associated with a poor prognosis in patients with prostate, gastric, colon, cervical, ovarian, breast, skin, bladder, endometrial, lung, pancreatic, liver and thyroid cancer, melanoma and myeloma (Tonoli *et al*., 2005). It is known to inhibit migration and invasion by associating

directly, or through integrins, with a variety of different molecules. CD82, in conjunction with the α6 integrin chain and the epidermal growth factor receptor (EGFR), is accompanied by impaired laminin adhesion and migration, due to co-internalisation with CD82. Furthermore, the association of CD82 with EWI-2 strengthens the motility-inhibitory activity of EWI-2 on laminin and fibronectin. CD82 has also been shown to interfere with hepatocyte growth factor receptor (HGFR) signalling such that when bound by its ligand HGF, HGFR induces proliferation but is unable to stimulate lamellipodia formation and therefore, cell migration in a non-small-cell lung cancer line (Zoller, 2009).

CD151 has also been shown to play a role in cell motility. Overexpression of CD151 has been shown to result in increased motility, along with enhanced expression of MMP-9 and invasiveness (Hong *et al*., 2006). This has been shown to activate GTPase mediated pathways, which increases GTP binding to Cdc-42 and Rac, two proteins involved in the organisation of the cell cytoskeleton (Shigeta *et al*., 2003). As stated previously, CD151 forms complexes with the major laminin-5 receptors, α3β1 and α6β4 integrins, in lateral cell surface membranes. Its dissociation from laminin-binding integrins permits the migration of epithelial cells (Chometon *et al*., 2006).

CD9 is a 21-24 kDa surface molecule, and its down regulation is associated with tumour progression in numerous cancer types. In ovarian carcinoma cells, there is a correlation between expression levels of CD9 and β1, α2, α3, α5 and α6 integrin chains, and down-regulation of CD9 is associated with weaker matrix adhesion and diminished growth *in vivo* (Furuya *et al*., 2005). Work carried out by Huang *et al*., have shown that expression of CD9 is accompanied by the transcriptional down-regulation of WASF2, a member of the WASP family of proteins (Huang *et al*., 2006). WASF2 serves as a scaffold that links upstream signals to the activation of the Arp2/3 complex, which in turn mediates actin polymerisation. WASF2 is also crucial for the formation of filopodia and lamellipodia (Takenawa *et al*., 2007).

1.1.4.4 GPI-Anchored Proteins

Glycosylphosphatidylinositol (GPI-anchor) is a proteolipid that can be attached to the C-terminus of a protein during posttranslational modification. It is composed of a phosphatidylinositol group linked through a carbohydrate containing linker to the C-terminal amino acid of a mature protein. Many cell surface proteins are attached to the cell membrane through GPI-anchorage (Mayor *et al*., 2004). The presence of a GPI-anchor serves the following four functional roles: (1) the apical targeting of proteins in polarised cells, (2) GPI-anchors mediate the cell surface organisation of attached proteins through association with specialised cholesterol and sphingolipid-rich micro-domains, commonly known as "lipid rafts", (3) endocytosis of GPI-anchor proteins, leading to downstream signaling and, (4) cleavage of GPI-anchors by phospholipases to release soluble protein for signaling (for example, Cripto-1) (Lakhan *et al*., 2009).

GPI-anchored proteins usually lack a cytoplasmic domain, which results in the inhibition of direct intracellular protein signalling. In spite of this, many GPI-anchored proteins have been implicated in signalling (Ilangumaran *et al*., 2000) and different models for the underlying mechanism have been suggested (Simons *et al*., 2000).

GPI-APs are involved in a diverse range of functions, including cell migration and wound healing (uPAR) and protease regulation (RECK)

1.1.4.4.1 Urokinase – Type Plasminogen (uPA)

Urokinase (uPA) is a serine protease with a molecular weight of approximately 54 kDa. It is composed of two disulfide-linked chains, A and B, of molecular weights 18 kDa and 33 kDa, respectively.

The uPA system consists of:

- the plasminogen activator of the urokinase-type (also called “urokinase“ or “uPA“);

- its physiological inhibitor (PAI-1);
- and the uPA-receptor (uPAR), which is over-expressed on tumour cells (Gondi *et al*., 2009).

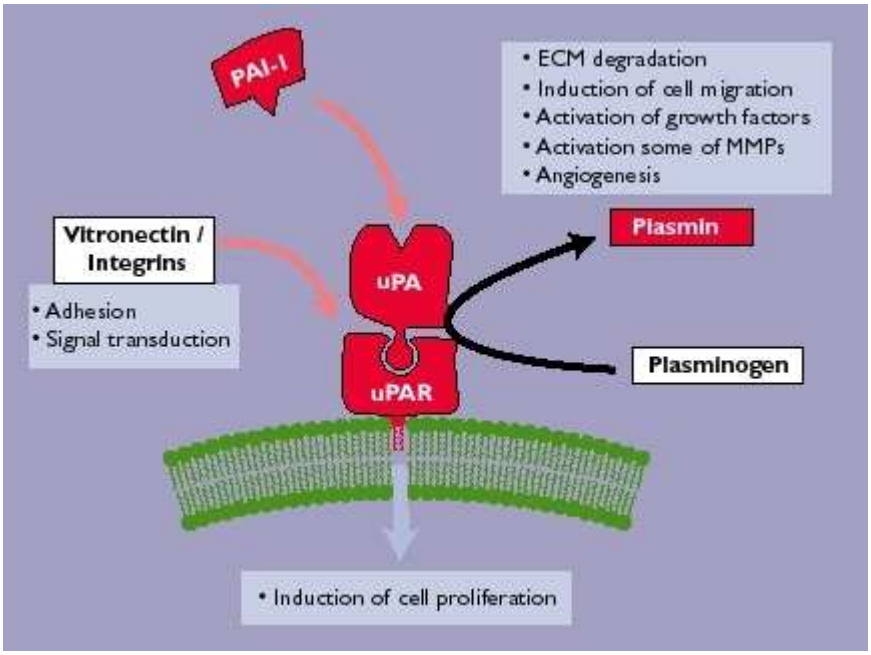

Figure 1.5: - The uPA system (www.wilex.com)

When uPA binds to its receptor, uPAR, a series of proteolytic processes occur, facilitating the conversion of plasminogen to plasmin (figure 1.5). This allows degradation of the ECM and activation of matrix metalloproteinases, which aids in tumour cell invasion into adjacent tissue, and eventually into the bloodstream (Aznavoorian, *et al*., 1993). uPAR also interacts functionally with matrix vitronectin, adhesion receptors of the integrin family, and G protein-coupled receptors. Its overexpression has also been reported in several types of human adenocarcinomas, including pancreatic cancer, gastric cancer, and colorectal cancer (Hildenbrand, *et al.*, 2010).

1.1.4.4.2 RECK

RECK (REversion-inducing Cysteine rich protein with Kazal motifs) is a GPI-anchored membrane bound protein involved in mediating tissue remodelling. Its primary role is in suppressing MMP-2, MMP-9 and MT1-MMP post-transcriptionally (Zambuzzi *et al*., 2009). RECKs inhibition of MMPs, secreted

by tumour cells, occurs through a glycosylation mechanism. In normal cells, four separate asparagine residues in the RECK protein sequence are N-glycosylated. In work carried out by Simizu *et al*., (2005) mutated RECK proteins were produced, where Asn residues were replaced with Glu in certain positions. The effect of absent glycosylation was then observed on MMP-2 and MMP-9 expression. It was found that glycosylation of the Asn297 was needed to inhibit MMP-9 secretion, while Asn352 glycosylation was required to inhibit MMP-2 activation. To confirm these observations, invasion assays were carried out on HT1080-RECK mutants (no glycosylation of Asn297 and Asn 352). This showed an increase in tumour cell invasion when compared to HT1080 cells expressing wild-type RECK (Clark *et al*., 2007).

1.1.4.4.3 Glypicans

Glypicans are a family of heparan sulfate proteoglycans that are linked to the exocytoplasmic surface of the plasma membrane by a GPI anchor. They are involved in cell growth, invasion and adhesion. Six members of the Glypican family have been identified in mammals, termed GPC1 to GPC6 (Nakato *et al*., 1995). Glypicans role in tumour progression involves its ability to regulate the activity of growth and survival factors. Work carried out by Kleef *et al*., showed that expression levels of GPC1 are significantly increased in a large number of pancreatic cancers (Kleeff *et al*., 1998). It was also shown that transfection of antisense GPC1 inhibited the mitogenic response of pancreatic cancer cells, *in vitro*, to FGF2 and heparin-binding EGF-like growth factor and decreased the tumorigenicity of the transfected cells (Kleeff *et al*., 1999).

GPC3 has also been observed in tumour progression. Work carried out by Lin *et al*., showed that GPC3 expression is downregulated in a majority of ovarian cancer cell lines. However, in all cases where GPC3 expression was lost, no mutations were found in the coding region of the gene; the promoter region of the GPC3 gene was hypermethylated. GPC3 expression was restored by treatment with a demethylating agent. In addition, the authors demonstrated that ectopic expression of GPC3 inhibits colony-forming activity in several ovarian cancer cell lines (Filmus *et al*., 2001).

1.1.5 Non-Cell Surface Proteins Involved in Invasion & Metastasis

1.1.5.1 Semaphorins

Semaphorins are a large family of conserved, secreted and transmembrane proteins that are involved in a variety of tumourigenic processes such as cell adhesion, migration and proliferation. Semaphorin receptors, the neurophilins and the plexins, are expressed by a wide variety of cell types, including endothelial and cancer cells. It is through these that semaphorins mediate crosstalk between tumour cells and multiple stromal cell types in the surrounding tumour microenvironment (Capparuccia *et al*., 2009). However, semaphorin-mediated signals have been shown to have both an anti-and pro-tumourigenic effect on cells. Work done by Barberis *et al*., have shown that following plexin activation by semaphorins, integrin-based focal-adhesive structures are rapidly disassembled, followed by actin depolymerisation and cytoskeletal remodelling, resulting in cellular collapse. Plexin activation can also inhibit the development of new adhesive complexes, and block the formation of lamellipodia, thus disrupting directional migration, by uncoupling cell-substrate adhesion from the cytoskeletal dynamics that are essential for cell migration (Barberis *et al*., 2004).

However, contrary to this, Swiercz *et al.*, have shown that the same receptor-ligand interaction can promote chemotaxis and maintain invasive growth, depending on whether plexin-B1 was associated with the oncogenic receptor tyrosine kinases (RTKs), Met and HER2 (Swiercz *et al*., 2008). This paradoxical effect is supported by expression levels in a range of tumour cells e.g. plexin-B1 over-expression correlates with increased invasiveness and metastatic progression in prostate cancer (Wong *et al*., 2007), whereas loss of plexin-B1 expression was found to correlate with poor prognosis in estrogen-receptor-positive breast cancer (Rody *et al*., 2007). This paradoxical effect is probably due to the multiple signalling cascades semaphorins stimulate in different tumour cells and in cells of the tumour microenvironment (Capparuccia *et al*., 2009).

1.1.5.2 Aquaporins

The aquaporins (AQPs) represent a ubiquitous family of small, integral-membrane proteins, which selectively transport water across cell plasma membranes (Andrews *et al*., 2008). A subset of AQPs, the aquaglyceroporins, also transport glycerol. AQPs are highly expressed in a variety of tumour cells, especially those with an aggressive phenotype. They have been proposed to play an important role in tumour biology, with recent observations showing them to be involved in cell proliferation and migration (Auguste *et al*., 2007; Hara-Chikuma *et al*., 2008). In tumour vascular endothelium cells, AQP1 is universally expressed. Work done using wild type and AQP1-null mice showed a tumour reduction in the AQP1-null mice, due to impaired endothelial cell migration. AQP-expressing cancer cells also show enhanced migration in vitro, along with greater local tumour invasion, cell extravasation, and metastases *in vivo*. This may be due to AQP-facilitated water influx into lamellipodia at the leading front of migrating cells (Hu *et al*., 2006). AQP3 is an aquaglyceroporin that is expressed in basal cells in human skin squamous cell carcinomas, which facilitates cell proliferation in different cell types. Mice without the AQP3 protein have been shown to be resistant to skin tumourigenesis, possibly due to reduced tumour cell glycerol metabolism and ATP generation. This data suggests that AQP expression in tumour cells facilitates cell growth and spread, and thus could be an important target for anti-tumour therapy (Verkman *et al*., 2008).

1.1.5.3 ADAMs

A disintegrin and metalloproteinases (ADAMs) are a family of proteins that share the metalloproteinase domain with matrix metalloproteinase's (MMPs). They can be divided into two structural groups: (1) membrane-anchored ADAMs and (2) ADAM with thrombospondin motifs (ADAMTS) (Takeda *et al*., 2006). Both groups of ADAMs are involved in diverse roles such as cell adhesion, cell migration, cell fusion, membrane protein shedding and proteolysis. Many tumourigenic cells have a high expression of ADAMs, which direct activities such as regulation of growth factor activities (EGF, Heparin Binding-EGF and TGF-α, and cytokines e.g. TNF-α) and integrin functions, leading to promotion

of cell growth and invasion (Mochizuki *et al*., 2007). Work done by Ishikawa *et al*., have shown that transfection of ADAM8 into lung cancer cells enhanced their invasive activity (Ishikawa *et al*., 2004), while Wildeboer *et al*., demonstrated that ADAM8 is highly regulated in human primary brain tumours such as astrocytomas, and the expression levels and activity are associated with invasiveness (Wildeboer *et al*., 2006).

One member of the ADAM family that has been proposed to play a role in the metastatic cascade is ADAM9, through its modulation of growth factor activity and integrin function. Secreted by activated stromal cells, ADAM9 is known to induce colon carcinoma cell invasion *in vitro* through binding to α6β4 and α2β1 integrins. It also improves cell adhesion and invasion of non-small cell lung carcinoma (NSCLC) cells via modulation of α3β1 integrin and sensitivity to growth factors, resulting in promotion of brain metastasis of the carcinoma cells (Mazzocca *et al*., 2005).

1.1.6 Therapeutic Targeting of Proteins

There are currently no clinically approved, anti-metastasis therapies available, therefore, the identification and validation of novel proteins involved in cancer metastasis is an essential first step in developing new and effective therapies against this process. Membrane and membrane-associated proteins show great promise as therapeutic targets because of their easy accessibility. Many of the new therapies being developed include antibody targeting of the protein of interest. Antibodies have the ability to recognise native proteins expressed on the tumour cell surface, allowing for receptor binding, and the blocking of ligand interaction. They can bind to proteins and recruit complement or immune effector cells, thus eliciting antibody-dependent cellular cytotoxicity (ADCC). They also have the ability to neutralise growth factors or cytokines by binding to them and forming immune complexes, allowing for there removal (Durrant *et al*., 2009). These factors make antibodies ideal agents for targeting cell surface proteins.

The $\alpha_v\beta_3$ integrin is an important receptor affecting tumour growth, local invasiveness, and metastatic potential. This integrin is expressed on various malignant tumours and mediates adhesion of tumour cells on a variety of extracellular matrix proteins, allowing these cells to migrate during invasion and extravasation (Felding-Habermann, 2003). Work carried out by Landon *et al*., have shown that etaracizumab, a fully humanised monoclonal antibody that targets the $\alpha_V\beta_3$ integrin, has been successful in decreasing ovarian cancer proliferation and invasion (Landen *et al*., 2008). The $\alpha_v\beta_1$ integrin is also being used for the development of targeted antibody therapy. Volociximab, a chimeric (82% human) antibody that specifically binds to $\alpha_V\beta_1$ integrin, blocks the integrins fibronectin binging site, leading to inhibited cell migration and the growth of new blood vessels. Testing is currently in the Phase I stage (Ricart *et al*., 2008).

The heparan sulfate proteoglycan syndecan-1 is highly expressed by myeloma cells and is shed into the myeloma microenvironment. Tests carried out in animal models have shown that high levels of shed syndecan-1 promote tumour growth and invasion, while in myeloma patients, high levels are associated with a poor prognosis. These findings suggest that syndecan-1 has the potential to be target for myeloma therapy (Yang *et al*., 2007).

There are numerous monoclonal antibodies (MAbs) available that specifically target the Syndecan-1 proteoglycan. Furthermore, antibody-drug conjugates (ADCs), cytotoxic drugs chemically linked to antibodies, can enhance the efficiency of chemotherapy drugs. An anti-CD138-maytansinoid conjugate has been shown to target the Syndecan-1 protein, inhibiting the growth of multiple myeloma (MM) tumour cells *in vitro* and *in vivo* (Ikeda *et al*., 2009).

As discussed, the tetraspanin transmembrane protein family have emerged as key players in the metastatic process, and as such, can be used as potential targets for cancer therapies. Several MAbs that target tetraspanins have an agonist effect. For example, an anti-CD151 antibody has been shown to stimulate cell adhesion, thereby preventing de-adhesion and immobilising tumour cells (Zijlstra *et al*.,

2008). In addition, anti-CD9 MAbs amplify the inherent tumour suppressor function of CD9 (Ovalle *et al*., 2007).

Cell surface proteins, proteoglycans and proteolipids play an integral part in the function of many cellular processes. Many of these proteins play a role in the different stages of tumour progression, carrying out a variety of complex functions. The interaction of these proteins with their environment and each other are varied, and to a large extent, still unknown. Some even seem to have a contradictory role in cancer progression. Understanding how these pathways contribute to the metastatic process, and what proteins play a critical role, is essential if we are to develop new cancer therapies.

The ability of MAbs to target these, and other, cell surface proteins involved in the invasion process makes them ideal candidates as therapeutic tools for the treatment of metastasis. They possess many clinically relevant properties, including high specificity, low toxicity, and the ability to activate components of the immune system. For these reasons, MAbs have become an integral part in studies to treat metastatic cancers.

1.2 Monoclonal Antibodies

Antibodies are proteins called immunoglobulins, produced by a biological host against the presence of a foreign molecule known as an "antigen". Antibodies occur in two forms: a soluble form secreted into the blood and tissue fluids, and a membrane-bound form attached to the surface of a B cell that is called the B cell receptor (BCR). The BCR allows a B cell to detect when a specific antigen is present in the body and triggers B cell activation. Activated B cells differentiate into either antibody generating factories called plasma cells that secrete soluble antibody, or into memory cells that survive in the body for years afterwards, allowing the immune system to remember an antigen and respond faster upon future exposures (www.chemprep.com). The antibodies produced recognise the antigen, and by cross reaction with other immune proteins, initiate an immunological response, thus destroying the invading presence.

In mammals, there are five antibody isotypes or classes, each designated by an "Ig" prefix (Immunoglobulin), known as IgA, IgD, IgE, IgG and IgM. These antibody classes differ in their biological properties, functional locations and their ability to deal with different antigens (Woof *et al*., 2004). The antibody isotype can undergo changes during development and upon activation of B cells. Immature, or naïve, B cells that have never been exposed to antigen only express cell surface bound IgM. These cells begin to express both IgM and IgD isotypes when reaching maturity – the co-expression of both these isotypes renders the B cell "mature" and ready to react to antigens. Once the cell bound antibody molecule engages with the antigens, the B cell is activated, leading to cell division and differentiation into an antibody-producing plasma cell. In this activated form, the B cell produces antibody in a secreted, rather than a membrane-bound, form. A proportion of daughter cells of the activated B cells undergo isotype switching, inducing production of the other antibody isotypes (IgE, IgA or, more commonly, IgG), that have defined roles in the immune system (www.immunoportal.com).

Antibodies are comprised of two antigen-binding fragments (F_{abs}), which are connected, via a flexible region (the hinge) to a constant, crystallisable fragment

(F_c). This structure is comprised of two pairs of polypeptide chains, each pair containing a heavy and light chain of dissimilar sizes (Chan *et al.*, 2009). Both heavy and light chains are folded into the immunoglobulin domains. The variable regions in the amino-terminal part of the molecule t recognise and bind antigens; the remaining part of the molecule consists of constant domains that vary among immunoglobulin classes. The F_c portion serves to bind a variety of effector molecules of the immune system, as well as molecules that establish the biodistribution of the antibody (Binyamin *et al.*, 2006).

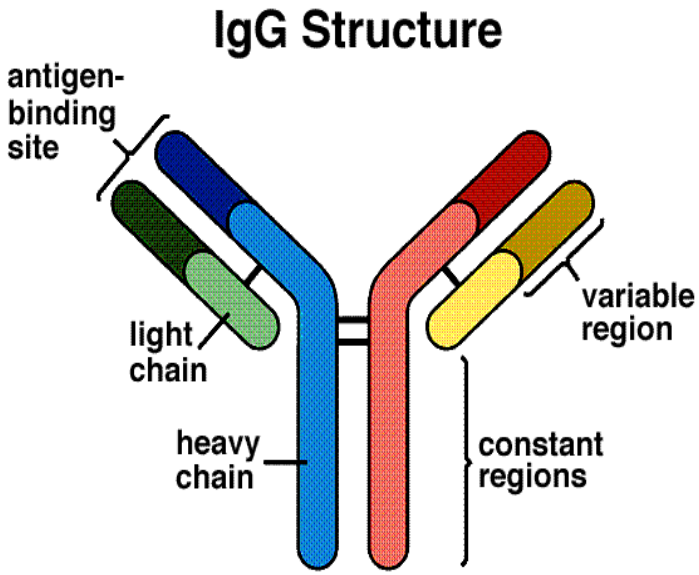

***Figure 1.2*: -** Antibody Structure. www.mhhe.com.

1.2.1 Hybridoma Technology

A major milestone in antibody production occurred in 1975 when Kohler and Milstein successfully fused an antibody-producing B cell with an immortalised myeloma cell line resulting in a hybridoma. These hybridoma cells could then be cloned and screened for large-scale production of monoclonal antibodies (MAbs). This work, which was reported in *Nature* and eventually earned the two scientists the Nobel prize in 1980, allowed for the production of virtually unlimited quantities of antibody molecules, in which all antibodies were identical and of the same precise specificity for a given epitope (Kohler & Milstein, 1975).

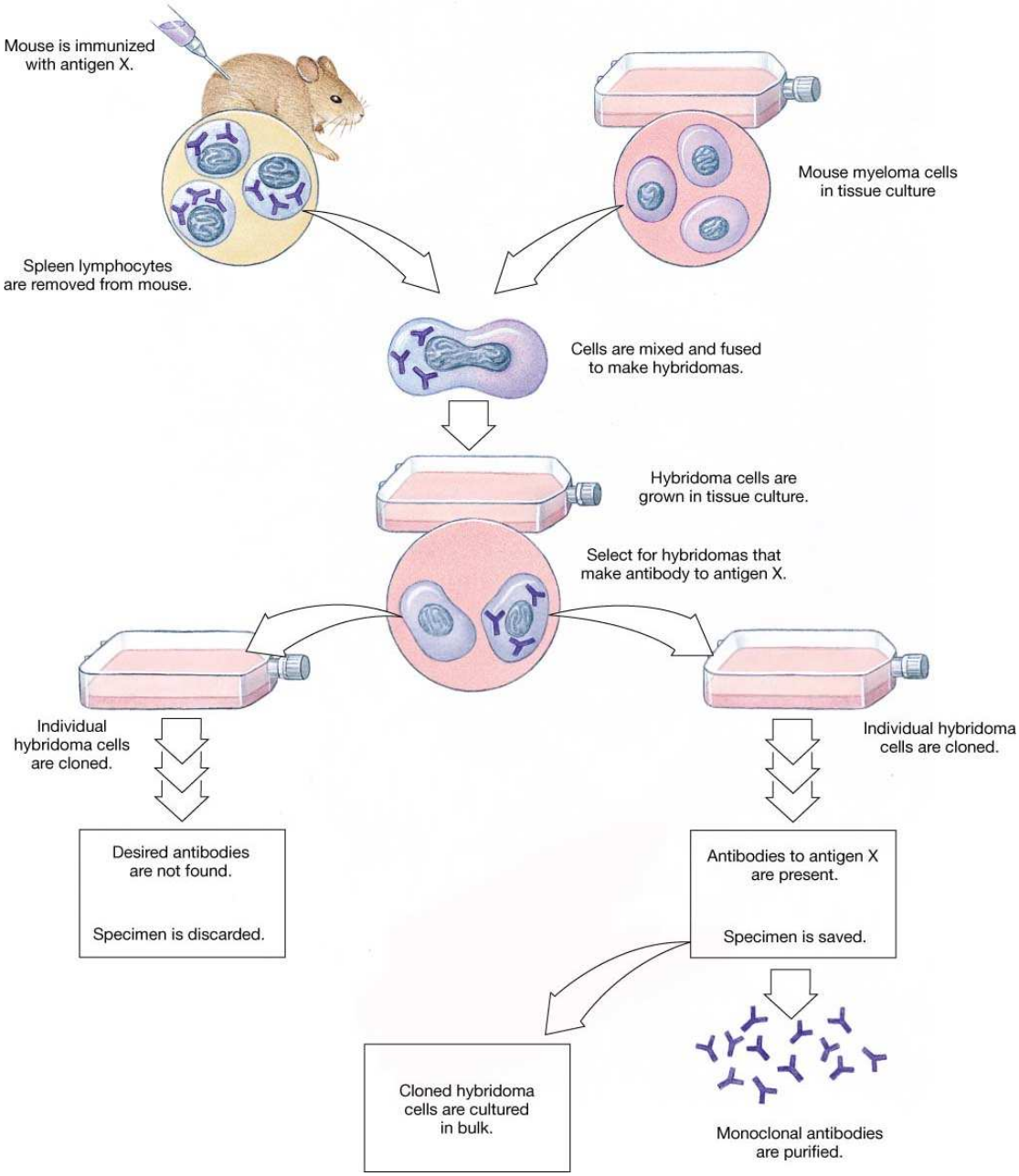

Figure 1.2.1: - Production of Monoclonal Antibodies. (www.uccs.edu)

1.2.2 Development of Therapeutic Antibodies

A major factor limiting the use of mouse MAbs in humans is the fact that the F_c region of the immunoglobulin structure is murine in origin. After intravenous administration of these MAbs patients developed human-antimouse antibodies (HAMAs) that were shown to complex with murine MAbs upon repeat administration. It has been demonstrated that HAMA responses were detected in approximately 50% of patients after a single injection of murine MAbs, and

greater than 90% of patients develop HAMA following two or three repeated injections (Sears *et al.*, 1984; Jaffers *et al.*, 1986). Therefore, it is desirable to convert the clinically interesting MAbs of murine origin into those that are physically or functionally more human Ig alike. Molecular engineering techniques have achieved this by grafting critical sequences in the human heavy-chain backbone onto the xenogeneic murine antibody structure, allowing for the retention of the Ag-binding specificities. This also imparts other attributes essential to enhanced clinical utility, such as decreased immunogenicity, longer serum half-life in humans, and the ability to recruit effector functions. Both chimerised and humanised MAb can be successfully administered to patients for prolonged treatment duration without inducing a clinically meaningful immune response (Binyamin *et al.*, 2006).

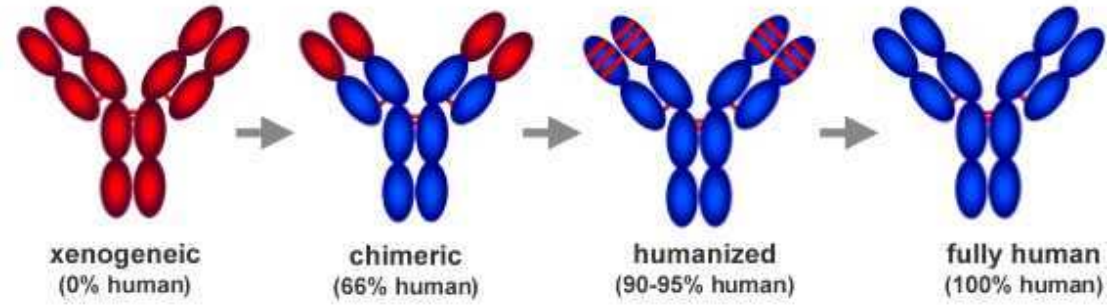

Figure 1.2.2: - Schematic representation of the development of therapeutic antibodies. www.4-antibodies.com

Chimeric Antibodies: - a chimeric antibody (cAb) is constructed by fusing the light and heavy chain variable regions (V_L and V_H respectively) of a murine MAb to the corresponding human constant regions. Approximately 70% of the structure of a cAb is of human origin (Qu *et al.*, 2005). The anti-CD20 MAb Rituximab, and the anti-EGFR Cetuximab are examples of a chimeric antibodies.

Humanised Antibodies: - in a humanised antibody, the V_L and V_H domains of the original murine MAb are further engineered so that only the complementarity-determining regions (CDRs), approximately 25% of the sequences, are grafted onto the scaffolds of corresponding human V region frameworks (termed CDR-grafting). A humanised MAb has less than 10% amino acid sequences of murine

origin (Qu *et al.,* 2005). Humanised antibodies are usually denoted by the addition of *–zumab* at the end of their name. Examples of humanised antibodies include the anti-HER2 Trastuzumab (Herceptin), and the anti-VEGF-A Bevacizumab (Avastin).

Fully Human Antibodies: - the derivation of fully human antibodies can be accomplished *in vitro* using the phage display technique. Amino acid sequences of heavy and light chain variable regions of the MAb must first be elucidated. This is accomplished by molecular cloning. Second, the humanised MAb is designed and the plasmid vector for mammalian expression of the humanised MAb is constructed. Third, the humanised MAb is expressed and produced in cell cultures. Fourth, the immunological and biochemical characteristics of the humanised MAb are examined and compared with those of the parent murine MAb (Qu *et al.,* 2005). The application of phage display technology has permitted the generation of human MAbs which encompass a wide range of specificities against hitherto refractory antigens.

A second method for producing fully human antibodies is through the use of xenomouse© technology. Xenomice are developed when heavy and light IgG chains are inactivated in mouse embryonic stem (ES) cells by gene-targeting technology. These cells are then used to generate mice with homozygous deletions, in which mouse antibody production is disrupted. Human heavy and light IgG chain loci are introduced into ES cells, which are used to generate mice containing human Ig loci, thus producing fully human antibodies in the presence of mouse antibodies. Breeding of these mice with immunoglobulin-inactivated mice generate xenoMice (Jakobovits *et al*., 2007).

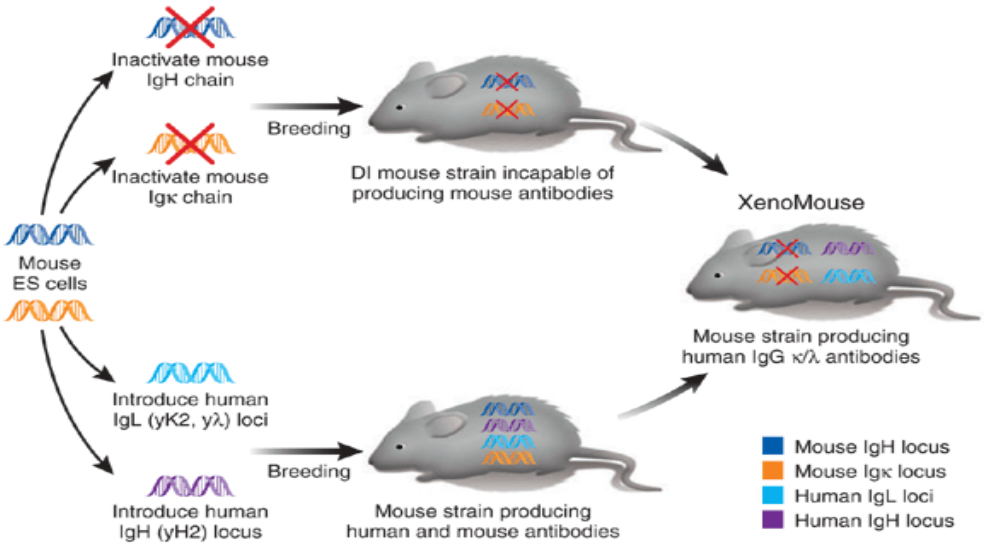

Figure 1.2.3: - Creation of Xenomouse strains (Jakobovits *et al*., 2007).

The Xenomouse platform has been used for the development of at least 18 human MAbs; Two (the anti-EGFR Panitumumab, and the anti-RANK Denosumab, used for the treatment of osteoporosis) are approved, nine are in clinical study (two at Phase II, five at Phase II and two at Phase III) and seven are discontinued (Nelson *et al*., 2010).

1.2.3 Monoclonal Antibodies as Cancer Therapeutics

The concept of using antibodies in cancer treatment was first proposed over a century ago by the German scientist Paul Ehrlich. He hypothesised that a "magic bullet" could be developed, based on an antibody, to selectively target disease; however, it was not until the advent of hybridoma technology that their use as a therapeutic agent became fully realised. A variety of mechanisms are thought to govern the anti-tumourigenic effects of MAbs. These include blocking of an activation signal that is necessary for continued cell growth, antibody-dependent cellular cytotoxicity (ADCC), complement dependent-cytotoxicity (CDC) and the ability of MAbs to alter the cytokine milieu or enhance development of an active anti-tumour immune response. Additionally, MAbs are also known to target the tumour microenvironment, which can result in inhibited tumour growth through restriction of pro-tumourigenic factors produced in the tumour stroma. (Weiner *et al.*, 2010).

1.2.3.1 ADCC

ADCC occurs when antibodies bind to antigens on tumour cells, resulting in the antibody Fc domain engaging with Fc receptors (FcR) present on the surface of immune effector cells (see figure 1.2.4). FcRs can activate downstream signalling through immunoreceptor tyrosine-based activation motifs (ITAMs) or deliver inhibitory signals through immunoreceptor tyrosine-based inhibitory motifs (ITIMs) (Ivashkiv *et al*., 2010). The main inhibitory FcR is the single chain CD32, whereas most Fc-dependent stimulatory signals are transduced by CD64 and CD16A. CD64 is a high-affinity receptor expressed by macrophages, dendritic cells (DCs), neutrophils and eosinophils (Weiner *et al*., 2010).

Trastuzumab (Herceptin) has been shown to activate an ADCC response in multiple breast cancer cell lines. Natural killer (NK) cells, a chief immune cell type involved in ADCC, express the Fc gamma receptor, to which the Fc domain of t binds, activating NK-mediated cell lysis. In mice bearing BT474 HER2 overexpressing xenografts, a tumour regression rate of 96% was observed following treatment with Herceptin. In contrast, mice lacking the Fc receptor lost much of the protective effect of Herceptin, with only 29% tumour growth inhibition observed (Clynes *et al.*, 2000)

After tumour cell lysis occurs, antigen-presenting cells can present tumour-derived peptides on MHC (major histocompatibility complex) class II molecules, thus promoting $CD4^+$ T-cell activation. Additionally, tumour-derived peptides can be presented on MHC class I molecules (cross-presentation), leading to $CD8^+$ cytotoxic T cell activation (Flynn *et al*., 2003).

Therefore, binding of MAbs to tumour cells enables the recognition of these targets by immune effector populations that express FcR receptors, such as NK cells, neutrophils, mononuclear phagocytes and dendritic cells (Weiner *et al*., 2010).

1.2.3.2 CDC: Blocking Ligand Binding & Signal Disruption

CDC is another method antibodies can us to direct cell kill (see figure 1.2.4). For example, the binding of two or more IgG molecules to the cell surface leads to

high-affinity binding of complement component 1q (C1q) to the Fc domain. This is followed by the activation of C1r enzymatic activity and subsequent activation of downstream complement proteins. The complement cascade results in the formation of pores by the membrane attack complex (MAC) on the tumour cell surface, leading to tumour cell lysis (Weiner, *et al.*, 2010). The anti-CD20 MAb Rituximab has been found to depend in part upon CDC, as well as ADCC, for its *in vivo* efficacy (Adams *et al*., 2005).

Many of the most commonly targeted tumour-associated antigens are growth factor receptors, which are frequently over-expressed in a number of solid tumours. Overexpression of these receptors has been linked to tumour cell growth and survival, through desensitising against chemotherapeutic agents. By blocking signalling through these receptors, MAbs have the capability to decrease growth rates and re-sensitise cells to cytotoxic agents. Members of the EGFR family are the target of many therapeutic antibodies, and are thus among the most potent inhibitors of signal transduction. Cetuximab and Panitumumab (anti-EGFR MAbs, FDA-approved in 2006 (Nelson *et al*., 2010)) function by blocking the interaction between the receptor and its activating ligand, and by sterically preventing the receptor from assuming the extended conformation required for dimerisation (Li *et al.*, 2005). Pertuzumab (anti-HER2, awaiting FDA approval) allows ligand binding to occur, but sterically inhibits the subsequent receptor heterodimerisation required for signal transduction (Franklin *et al*., 2004). (Pertuzumab binds to domain II of HER2, whereas Trastuzumab binds to domain IV (deVita *et al*., 2008)). Almost all unconjugated antibodies used as therapeutic agents disrupt the signals used by tumour cells for proliferation and survival (Weiner *et al.*, 2010).

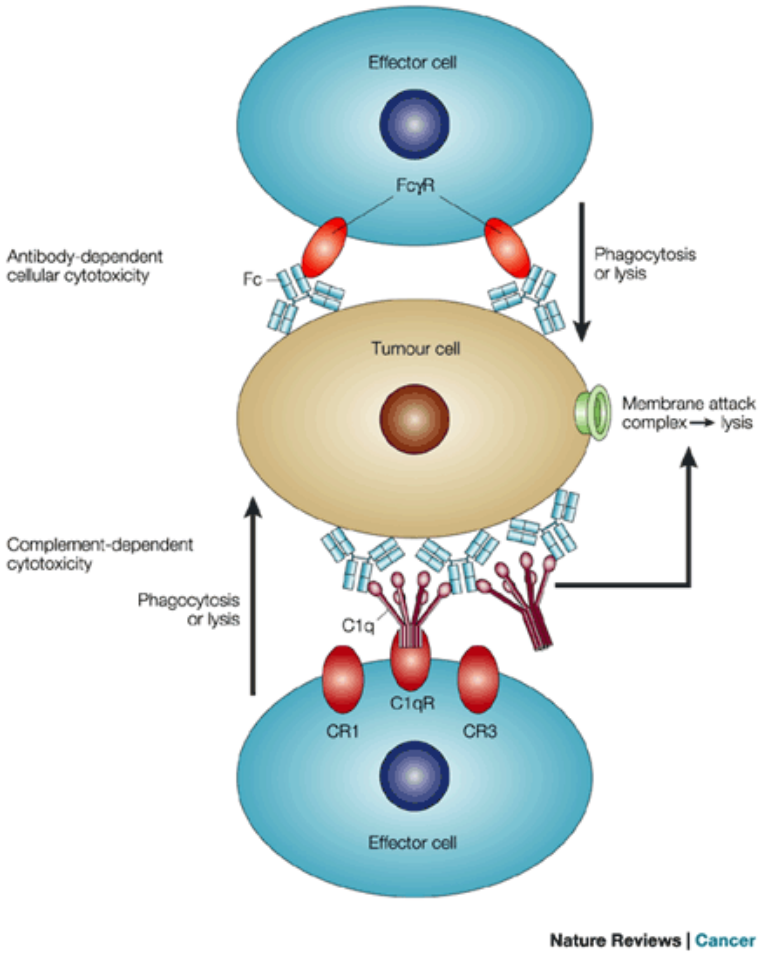

Figure 1.2.4: - MAb mediated ADCC and CDC (Carter, 2001)

1.2.3.3 Targeting the Tumour Microenvironment

The targeting of critical steps in the tumour microenvironment has shown therapeutic benefits in both preclinical and clinical settings. For example, many solid tumours express vascular endothelial growth factors (VEGFs), which bind to its receptor on the vascular endothelium, and thus stimulating angiogenesis. Bevacizumab, a VEGF-specific humanized MAb, blocks binding of VEGF to its receptor, resulting in hypoxia of the tumour. Cetuximab is also used as an anti-VEGF MAb (Weiner *et al.*, 2010).

The tumour stroma consists of numerous matrix proteins, along with blood vessels, and fibroblasts. These tumour-associated fibroblasts express FAP (fibroblast activation proteins), and are both functionally and phenotypically different from normal fibroblasts. FAP is thought to play a crucial role in tumour formation and metastasis, and is thus an attractive target for MAb therapy. Work

carried out by Scott *et al.*, have shown that an anti-FAP MAb (Sibrotuzumab) can successfully target this protein, with their study showing excellent tumour uptake and no localisation to normal tissue (Scott *et al.*, 2003). However, this MAb has undergone no further development, and no clinical trials involving its use are currently taking place.

Generic name (trade name; sponsoring companies)	Target	Antibody Format	Cancer Indication
Unconjugated antibodies			
Rituximab (Rituxan/Mabthera; Genentech/Roche/Biogen Idec)	CD20	Chimeric IgG1	Non-Hodgkin lymphoma
Trastuzumab (Herceptin; Genentech/ Roche)	HER2	Humanized IgG1	Breast cancer
Alemtuzumab (Campath/ MabCampath; Genzyme/Bayer)	CD52	Humanized IgG1	Chronic lymphocytic leukaemia
Cetuximab (Erbitux; ImClone Systems/Bristol–Myers Squibb)	EGFR	Chimeric IgG1	Colorectal cancer
Bevacizumab (Avastin; Genentech)	VEGFA	Humanized IgG1	Colorectal, breast and lung cancer
Panitumumab (Vectibix; Amgen)	EGFR	Human IgG2	Colorectal cancer
Ofatumumab (Arzerra; Genmab/ GlaxoSmithKline)	CD20	Human IgG1	Chronic lymphocytic leuakemia
Immunoconjugates			
Gemtuzumab ozogamicin (Mylotarg; Pfizer)	CD33	Humanized IgG4	Acute myelogenous leukaemia
^{90}Y-Ibritumomab tiuxetan (Zevalin; Biogen Idec)	CD20	Mouse	Lymphoma
Tositumomab and ^{131}I-tositumomab (Bexxar; GlaxoSmithKline)	CD20	Mouse	Lymphoma

Table 1: - Therapeutic monoclonal antibodies approved for use in oncology (Weiner *et al*., 2010)

1.2.4 Anti-Invasion/Metastasis MAbs

While current FDA-approved MAbs have greatly enhanced the field of cancer therapeutics, the majority of them are directed towards the treatment of primary and advanced cancers, and not metastatic disease. Metastatic cells pose the most dangerous threat to patient well-being; however, effective targeting of these cells remains an underdeveloped strategy when it comes to monoclonal antibody therapy. There are a number of studies taking place, in which MAbs are being generated against targets involved in the invasion process; however, none, as yet have received FDA approval for clinical use.

Gamma secretase (GS) is a unique multi-protein complex with activity as a cell surface protease that directly cleaves a variety of transmembrane proteins to

modify their function. Nicastrin is an essential component of the GS enzyme complex, required for its synthesis and recognition of substrates for proteolytic cleavage. (De Strooper, 2005). Work carried out by Filipović *et al*., (2010) revealed marked upregulation of nicastrin in human breast cancer compared to normal breast tissue. Nicastrin silencing in invasive breast MDA-MB-231 cells resulted in a marked reduction in both cell motility and invasion. A rabbit polyclonal antibody (PcAb) was then produced, raised against the extracellular domain of human nicastrin protein. This PcAb significantly reduced invasion levels in the MDA-MB-231 cell line by 70%. Mouse MAbs were also generated using the same method, and produced results similar to those seen with the PcAb. This proof of principle study suggests that developing MAbs against nicastrin could aid in future therapeutic treatments for invasive breast cancers.

A MAb generated against uPAR (Bauer *et al*., 2005), was shown to significantly decrease cell invasion and migration in the prostate cancer cell line, PC-3 *in vitro,* and caused a significant decrease in tumour volume *in vivo*. A humanised version of this MAb is expected to enter a Phase I clinical study shortly (Rabbani *et al*., 2010).

Axl is a member of a family of receptor tyrosine kinases that also includes Tyro3 and Mer (O'Bryan *et al.*, 1991; Lai and Lemke, 1991). Originally identified as a transforming gene in haematological malignancies (O'Bryan *et al.*, 1991; Janssen *et al.*, 1991), its dysregulation (or that of its ligand, Gas6) is implicated in the pathogenesis of a variety of human cancers. Its overexpression has been reported in a multitude of human cancers (Berclaz *et al.*, 2001; Sun *et al.*, 2004; Shieh *et al.*, 2005) and is associated with invasiveness and metastasis in lung (Shieh *et al.*, 2005), prostate (Sainaghi *et al.*, 2005), breast (Zhang *et al.*, 2008), gastric (Wu *et al.*, 2002) and pancreatic (Koorstra *et al.*, 2009) cancers, renal cell carcinoma (Chung *et al.*, 2003) as well as glioblastoma (Hutterer *et al.*, 2008). Generation of an anti-Axl MAb was achieved using phage-display antibody libraries (Li *et* al., 2009). Antibody YW327.6S2 recognizes both human and murine Axl. *In vivo* testing with this MAb reduced metastasis of MDA-MB-231 breast cancer cells to distant organs. In NSCLC models, YW327.6S2 also enhanced the efficacy of Erlotinib and chemotherapy in reducing tumour growth (Ye *et al*., 2010).

There are a number of clinical trials taking place involving MAbs that have shown show anti-invasive characteristics. Intetumumab, a fully human anti–αv integrin monoclonal antibody, has been shown to inhibit both migration and invasion of MDA-MB-231 breast cancer cells (Chen *et al*., 2008). It underwent Phase I clinical trials in combination with docetaxel in patients with metastatic, castration-resistant prostate cancer, and is now in Phase II clinical trials for the treatment of a variety of malignancies (Ning *et al*., 2010). A fully human, anti-HGF MAb, designated AMG-102, has shown anti-invasive effects in a leiomyosarcoma tumour-derived cell line, and is undergoing Phase I trials in combination with Bevacizumab/Motesanib in patients with advanced solid tumours (Rosen *et al*., 2010). In addition, the fully human monoclonal antibody AMG-102 was generated against HGF (Burgess *et al*., 2006). Subsequent testing of this MAb showed that it decreased invasion levels in SK-LMS-1 cells (a cell line derived from a leiomyosarcoma tumour). This MAb is undergoing Phase II clinical trials for patients with recurrent glioblastoma multiforme (Reardon *et al*., 2008), and Phase I trials in combination with Bevacizumab/Motesanib in patients with advanced solid tumors (Rosen *et al*., 2010).

There are also a number of MAb (and non-MAb therapeutic agents) in late stage clinical trials that are targeted against proteins involved in the invasion process:

Company	Target	Agent	Oncology indications	Development stage
Novartis	Hydroxyapatite of bone matrix	Zometa	Bone metastases in multiple myeloma and breast-to-bone metastasis	Marketed (February 2002)
Amgen	RANKL (RANK ligand)	Denosumab (humanized mAb)	Breast-to-bone metastasis and prostate-to-bone metastasis	Phase 3
	Angiopoietin 2	AMG-386 (Fc fragment linked to 20-residue peptide that binds angiopoietin-2)	Breast, ovarian and RCC	Phase 2
	IGF-1R	AMG-479 (a fully human mAb)	Advanced solid tumors	Phase 2
	c-MET	Rilotumumab (a fully human IgG2 mAb)	Metastatic colon cancer	Phase 2
Exelixis	pan-RTKs	XL-184 (small-molecule RTK inhibitor)	Thyroid cancer	Phase 3
	pan-RTKs	XL-184	Advanced solid tumors	Phase 2
OSI Pharmaceuticals	IGF-1R	OSI-906 (small-molecule RTK inhibitor)	Metastatic adrenocortical carcinoma	Phase 3
Adherex Technologies	N-cadherin	ADH-1 (a cyclic pentapeptide)	Melanoma	Phase 2
Antisense Pharmaceuticals	TGFβ	Trabedersen (a phosphorothioate oligodeoxynucleotide)	Glioblastoma	Phase 2
ArQule	c-MET	ARQ-197 (a small-molecule RTK inhibitor)	Various advanced solid tumors	Phase 2
Bristol-Myers Squibb	SRC-family protein-RTKs	Dasatinib (orally bioavailable small molecule)	Breast-to-bone metastasis, breast cancer (triple negative), colorectal cancer and liver	Phase 2
Centocor (Johnson & Johnson)	αvβ3/αvβ5 integrin	Intetumumab (fully human mAb)	Metastatic melanoma	Phase 2
Genentech	c-MET	MetMAb (a humanized monovalent 5D5 Fab mAb)	NSCLC	Phase 2
	SMO	GCD-0449 (small-molecule inhibitor)	Metastatic basal cell carcinoma, colorectal cancer and ovarian cancer	Phase 2
Global TransBiotech	Heparanase	PI-88 (phosphomannopentaose)	Malignant melanoma	Phase 2 (completed)
GlaxoSmithKline	c-MET, VEGF-R2, AXL RTKs	Foretinib (small-molecule RTK inhibitor)	Metastatic squamous cell carcinoma and gastric cancer	Phase 2
Facet Biotech	α5β1 integrin	Volociximab (a chimeric IgG4 mAb)	Various solid tumors	Phase 2
MethylGene	c-MET, VEGFR 1,2,3, Tie 2 and Ron RTKs	MGCD265 (small-molecule RTK inhibitor)	NSCLC	Phase 2
Merck	IGF-1	Dalotuzumab (MK-0646, a humanized mAb)	Metastatic colon cancer and others	Phase 2
	Cathepsin K	Odanacatib, a [2,2,2-trifluoro-1-(biphenyl-4-yl)ethyl]-4-fluoroleucine derivative of 4-fluoroleucine	Breast and bone metastases	Phase 2
Wilex	uPA	WX-UK1 (serine protease inhibitor)	Breast cancer and other solid tumors	Phase 2b
	uPA and other serine proteases	Mesupron (pro-drug of WX-UK-1)	Pancreatic, breast, and head and neck cancer	Phase 2

Table 2: - Select agents in late-stage development that target aggressive/metastatic cancers (Mack & Marshall, 2010)

1.2.5 Engineering MAbs

As stated previously, MAbs can be engineered in order to overcome immunogenicity problems associated with their murine origin (section 1.8.2). However, engineering techniques can also be employed to increase the efficacy of MAbs, through increased antigen binding, enhancement of its natural effector functions and increasing serum half life.

- **Bispecific Antibodies**

The ability of tumour cells to appropriate multiple mediators, which allow them to proliferate and spread, is one of the reasons why it is so difficult to treat. Therefore, simultaneous blocking of several targets would greatly enhance therapeutic efficacy. This is the reasoning behind bispecific antibodies (BsAb).

BsAb are antibody-based molecules that can simultaneously bind two separate and distinct antigens (or different epitopes of the same antigen). This is achieved through the presence of two distinct binding specificities, which are combined to an antibody by (1) chemically cross-linking two antibody molecules or antibody fragments, (2) fusion of two different cell lines to form a quadroma or trioma, or (3) recombinant DNA based approaches (Cao *et al*., 1998). BsAbs are mainly used to redirect cytotoxic immune effector cells, thus enhancing tumour cell kill through ADCC. One arm of the BsAb binds a tumour-associated antigen, while the other binds a determinant expressed on effector cells, e.g. CD3, which is expressed on T cell receptors (Willems *et al*., 2005). By facilitating this cross-linking, the BsAb triggers the activation of the effector cell, while bringing it into close proximity to the tumour cell, thus leading to effective tumour cell-killing (Shen *et al*., 2006). The first bsAb, Catumaxomab, which binds to both epithelial cell adhesion molecule (EPCAM) on tumour cells and CD3 on effector immune cells, received approval from the European Medicines Agency (EMA) in 2009 for the treatment of malignant ascites (Linke *et al*., 2010)

- **Single Chain Antibodies**

The conventional antibody (150 – 160kDa) is made up of two identical variable heavy chains (V_H) and two identical variable light chains (V_L) held together by interchain disulfide bonds. To improve the therapeutic value of antibodies, protein-engineering endeavours reduced the size of the antigen-binding moiety to a single-domain unit. Single chain antibodies, or single-chain Fvs (sFvs) are antibody fragments (25kDa) produced using phage display technology (Ohshima *et al*., 2010), that consist of only one V_L and one V_H domain, covalently connected to one another by a polypeptide linker. Their advantage over conventional antibodies lies in their ability to retain the specific, monovalent, antigen binding affinity of the parent Ab, while showing improved pharmacokinetics for tissue penetration (Harmsen *et al*., 2007).

- **Single Domain Antibodies/Nanobodies**

Single domain antibodies (sdAb), like sFvs, consist of antigen-binding fragments of the immunoglobulin, however, there are significantly smaller (11-15kDa).

Early work by Ward *et al*., (1988) showed that mouse sdAbs were able to function successfully, and it was proposed that, due to their smaller size, they could potentially penetrate tissues more effectively than conventional antibodies (Ward *et al.*, 1989). However, work on them was limited due to their poor solubility, their propensity to aggregate, and because they rarely retained the affinity of the parent. Interest in sdAbs was rekindled with the discovery of naturally occurring, single V-like domains in camelids (dromedary, camel, llama, and alpaca) (Hamers-Casterman *et al*., 1993). These peculiar heavy chain antibodies (hcAbs) lack light chains. Therefore, the antigen-binding site of hcAbs is formed only by a single domain that is linked directly via a hinge region to the Fc-domain. The variable domain is designated V_{HH} or nanobody) (Wesolowski *et al*., 2009). With this discovery, nanobodies specific for a given antigen could be generated though camelid immunisation, and subsequent cloning of its V_{HH} repertoire in phage display vectors (Arbabi Ghahroudi *et al*., 1997; Roodink *et al*., 2010)

Conventional antibodies have many advantageous features, such as their high affinity and selectivity for a target, their ease of discovery and production, and their low inherent toxicity. With nanobodies, not only are all this features present, they have other technological and biophysical advantages: they are highly stable to heat, retaining over 80% of their binding activity after 1 week of incubation at 37°C, thus indicating that they have a good shelf life; melting points of Nanobodies are in the range of 67- 78°C. They have also been shown to be stable in the presence of extremes of pH (Revets *et al*., 2005), allowing for their survival in harsh conditions such as the stomach. All these features make nanobodies as being potentially successful therapeutic agents for the treatment of cancer.

1.2.6 Conjugated MAbs

As described previously, MAbs attach to antigens on the cancer cell, inducing ADCC, CDC, or block ligands and signalling. These types of MAbs are known as “unconjugated” monoclonal antibodies. In addition to these mechanisms, increasing attention has turned to the possibilities of using antibodies as a delivery method for other, anti-cancer agents. By selectively targeting a drug to

the tumour site, an antibody can induce the desired biological effects with improved therapeutic index (McCarron *et al*., 2005). These drug-carrying antibodies are known as "conjugated" antibodies. To date, three antibody conjugate therapies have received FDA approval; the radioimmunoconjugates Ibritumomab tiuxetan (Zevalin) and [^{131}I]-tositumomab (Bexxar) for the treatment of lymphoma, and the drug conjugate Gemtuzumab ozogamicin (Mylotarg) for the treatment of acute myeloid leukaemia (FDA approval for this conjugate was withdrawn by the FDA in 2001, due to lack of data proving its efficacy. It is no longer available for use outside of a clinical trial (Ricart *et al*., 2007). Conjugation of a drug to an antibody makes it possible to achieve excellent localization of the drug at the desired site within the body (Senter *et al*., 2001). This increases the effective drug concentration within this target area, thereby optimizing the therapeutic effect of the agent.

Antibody Drug Conjugates (ADC): Standard cancer treatment regularly involves administering a regime of chemotherapeutic drugs that results in the death of actively dividing cells within the body, specifically cancer cells, but also healthy tissue. Selective targeting of these agents by conjugation to MAbs can improve efficacy and reduce side effects. Gemtuzumab ozogamicin was the first FDA-approved drug immunoconjugate targeting CD33 and carrying the highly toxic calicheamicin, a highly potent apoptotic antibiotic. Its use in patients with acute myeloid leukaemia resulted in a median of 6.8 months relapse-free survival and a 30% remission rate (Linenberger, 2005). However, this result could not be repeated, and FDA-approval was soon withdrawn. There are currently no FDA-approved ADCs on the market.

In July of this year, Genentech submitted a biologic license application to the US FDA for the ADC Trastuzumab–DM1 (T–DM1). This antibody conjugate combines the anti-HER2 Trastuzumab with the cytotoxic agent DM1. The application is based on the results of a Phase II trial that assessed the efficacy of T–DM1 in 110 women with HER2-positive advanced breast cancer whose disease had worsened after receiving at least two prior HER2-targeted treatments: Trastuzumab and lapatinib, as well as an anthracycline, a taxane and capecitabine (Hughes, 2010). (DM1 is a semi synthetic ansamacrolide, and

belongs to the maytansinoid class of anti-microtubular cytotoxic agents originally defined by the natural compound Maytansine (Cassady *et al*., 2004)).

Radioimmunotherapy (RAIT): involves the application of radioactive MAbs for targeted radiotherapy. ^{131}I-Tositumomab (Bexxar) and ^{90}Y-Ibritumomab tiuxetan (Zevalin) are the two FDA-approved radiolabeled anti-CD20 murine antibodies that have shown significant overall and complete response rates in patients with non-Hodgkin lymphoma, a disease that is quite radiosensitive as well as readily accessible to the antibody conjugates (Goldsmith, 2010).

Antibody-directed enzyme prodrug therapy (ADEPT): involves the application of antibody-enzyme conjugate, which then localises to its tumour-associated antigen. A suitable, non-toxic prodrug is then administered, which can be converted to its active cytotoxic form by the antibody-enzyme conjugate. The activated drug penetrates the tumour cells, destroying it in a localised manner. A Phase I clinical trial was carried out in 2006, with an antibody-enzyme conjugate on patients with nonresectable, locally recurrent, or metastatic histologically proven colorectal or other carcinoembryonic antigen-expressing cancer, however, there are no clinical trials currently taking place at time of writing.

1.2.7 MAb Therapy in Combination with Other Anti-Cancer Agents

Due to the highly complex nature of cancer, and the fact that a myriad of proteins are involved in its generation and progression, it is unlikely that any single agent will prove successful in treating it. For this reason, combination studies are carried out in order to investigate the potential of multi-drug therapies for the treatment of cancer. For example, in order to increase ADCC, Rituximab has been used in combination with cyclophosphamide, doxorubicin, vincristine, and prednisone in the treatment of patients with diffuse large B-cell lymphoma (Kim *et al*., 2006). Combination studies involving Trastuzumab with lapatinib (Blackwell *et al*., 2010), docetaxel (Sawaki *et al*., 2010), vinorelbine (Heinemann *et al*., 2010) and INCB7839, a potent and selective ADAM inhibitor (Newton *et al*,. 2010) are also taking place. Current clinically available drugs, which have shown some potential anti-tumourigenic properties are also being tested for any potential synergistic effect with standard cancer drugs.

1.2.7.1 Statins

The statins are a group of drugs commonly used for the treatment of lipid disorders, including hypercholesterolemia. They function by inhibiting 3-hydroxy-3-methylglutaryl-coenzyme A reductase (HMG-CoA reductase). HMG-CoA reductase catalyses the conversion of HMG-CoA into mevalonate in the mevalonate biosynthetic pathway (Graaf *et al*., 2004; Brown, 2007).

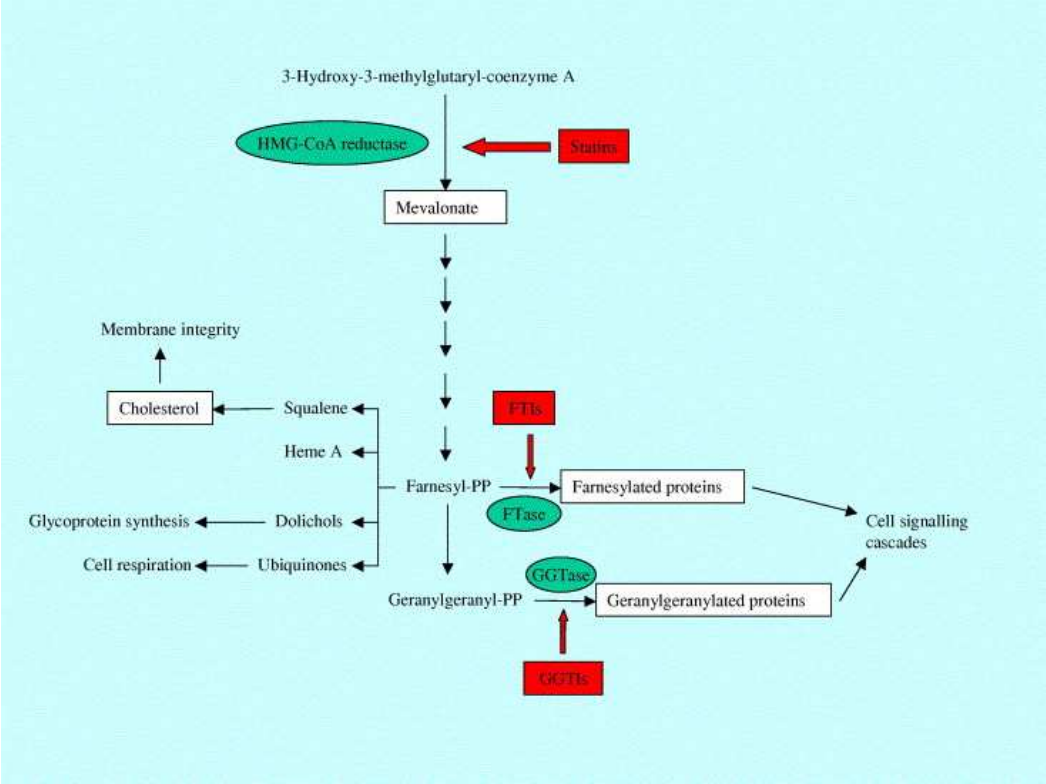

Figure 1.10: **-** Overview of the mevalonate pathway and targets for inhibition by statins, farnesyltransferase inhibitors and geranylgeranyltransferase inhibitors (Graaf *et al.*, 2004).

In addition to the cholesterol lowering effects of statins, a number of studies suggest that cancer incidences may be lower in patients receiving statins. Trials carried out by the Air Force/Texas Coronary Atherosclerosis Prevention Study (AFCAPS/TexCAPS) examining the use of Lovastatin for preventing coronary events, found the rates of new melanomas were significantly lower in the Lovastatin arm compared with the placebo arm. Furthermore, among the 41 participants who developed melanoma, there was a trend, although not statistically significant, toward earlier stage at diagnosis in the Lovastatin group

(Downs *et al*., 1998). A meta-analysis carried out described the incidence of melanoma in 12 qualifying randomised controlled statin trials, with 39,426 participants. They reported that 127 melanomas occurred, 59 among the 19,872 statin group participants and 68 among the 19,554 control group participants. The reported odds ratio for melanoma was in the direction of a protective effect, but did not reach significance. As the number of incident melanoma cases was low, a specific study to address the role of statins in preventing melanoma would need to be designed, with the required power to provide answers (Freeman *et al*., 2006).

Studies carried out by the Veterans affairs Health Care System showed that lung cancer incidences rates in statin users were also found to be significantly reduced (55% risk reduction) (Khurana *et al*., 2007). Several studies have also suggested that colorectal cancer rates are reduced amongst statin users, including the Molecular Epidemiology of Colorectal Cancer study (Poynter *et al*., 2005), and in the Rhine-Neckar-Odenwald population case-control study (Hoffmeister *et al*., 2007). Graaf *et al*., (2004) also reported that statin use was associated with a risk reduction of cancer of 20%. However, other studies have shown no benefit for statin use with respect to cancer prevention. Jacob *et al*., (2006) examined the association between use of cholesterol-lowering drugs and colorectal cancer incidence among 132,136 men and women in the Cancer Prevention Study II Nutrition Cohort. Current or 5 year use of cholesterol-lowering drugs was not associated with colorectal cancer incidence. A recent meta-analysis study including 6662 incident cancers and 2407 cancer deaths showed that statins did not reduce the incidence of cancer or cancer deaths and there was no reduction in any individual cancer type (Dale *et al*., 2006). These conflicting reports highlight the need for further studies on the effects of statins on cancer cells.

A number of studies have been carried out investigating the effects of statins on melanoma cells. Lovastatin was observed to induce apoptosis in A375 melanoma cells (Shellman *et al*., 2005), while enhancing responses to chemotherapy drugs in the B16 mouse model of melanoma (Feleszko *et al*., 1998, 2002). Atorvastatin was shown to inhibit invasion *in vitro* and metastasis *in vivo* in the A375M melanoma cells (Collisson *et al*., 2003); and work done by Depasquale and

Wheatley showed that Lovastatin reduced both melanoma cell growth and angiogenesis in an *in vitro* co-culture model angiogenesis system (Depasquale *et al*., 2006). These studies indicate that statins may play a role in melanoma prevention or treatment. However, the conflicting evidence from the chemoprevention studies suggests that further investigation is required to determine if standard cholesterol-lowering doses of statins will inhibit the growth of melanoma cells.

1.3 Aims of Thesis:

The aims of this thesis are as follows:

1. To generate monoclonal antibodies (MAbs) directed against the highly invasive MiaPaCa-2 clone 3 pancreatic cancer cell line, and the invasive MDA-MB-435-SF breast cancer cell line.

2. To develop a high throughput invasion assay system to screen resultant hybridomas *directly* for effects on invasion *in vitro*.

3. To identify MAbs that can significantly block cancer invasion *in vitro*, and to functionally characterise these MAbs in a range of invasive cancer models (pancreatic, breast, melanoma, lung, prostate, colon, and glioma). To investigate their effect on a number of related cellular processes, including motility, proliferation, MMP activity and adhesion *in vitro*.

4. To identify the antigens recognised by direct and cross-linked immunoprecipitation and proteomic analysis (mass spectrometry – LC-MS/MS).

5. To establish if the target proteins identified are involved in invasion by siRNA silencing of their respective genes.

6. To evaluate the expression of MAb targets in a range of human cancer cell lines, and normal and tumour tissues (breast, glioma, pancreatic, haematological malignancies).

7. To investigate the effect of Lovastatin, Mevastatin and Simvastatin on the invasion and motility levels in human melanoma cell lines, and to investigate any possible synergy between the developed MAbs and statins, in relation to inhibition of invasion in human cancers.

CHAPTER 2
MATERIALS & METHODS

2.1 Cell Culture

2.1.1 Cell Culture

Cell culture procedures were strictly adhered to as outlined in NICB SOP.

2.2. Cell Lines

Details of all cell lines used for the experiments detailed in this thesis are provided in Table 2.1. Cell lines were maintained in T25cm^3 (Costar 3056), T75cm^3 (Costar 3290) or T175cm^3 (Nunc, 156502) tissue culture flasks at 5% CO_2, 37°C and fed every 2-3 days. Cell lines were cultured through 7-10 passages before being discarded and replaced by new cultures grown from frozen stocks at an earlier passage.

Cell Line	Details-Histology	Invasion Status	Basal Medium, with Additions
BT20	Ductal Carcinoma of the breast	Invasive	DMEM; 10% FCS
BT474	Ductal Carcinoma of the breast	Non-Invasive	RPMI; 10% FCS, 1mM Na-pyruvate
BxPc-3	Pancreas, adenocarcinoma	Invasive	RPMI; 10% FCS
C/68 (Bright *et al*., 1998)	Prostate Cancer	Invasive	Keratinocyte; 25µg/ml BPE, 11 µg/ml EGF, 5% FCS *
DLKP	Poorly Differentiated Squamous Cell Lung Carcinoma	Low Invasion	ATCC; 5% FCS
DLKP-A (Clynes *et al*., 1992)	Adriamycin Resistant Variant of DLKP	Invasive	ATCC; 5% FCS
DLKP-I (McBride *et al.*, 1998)	Intermediate Sub-Population Cloned from DLKP	Highly Invasive	ATCC; 5% FCS
DLKP-M (McBride *et al.*, 1998)	Mesenchymal-Like Sub-Population Cloned from DLKP	Highly Invasive	ATCC; 5% FCS
DLKP-SQ (McBride *et al.*, 1998)	Squamous Sub-Population Cloned from DLKP	Low Invasion	ATCC; 5% FCS
DLKP-SQ-Mitox-6p (Joyce, H., unpublished)	Mitoxanthane Resistant Variant of DLKP-SQ after 6^{th} pulse of drug	Invasive	ATCC; 5% FCS
HCT-116	Colon Cancer	Highly Invasive	DMEM; 10% FCS
HT144	Human Melanoma	Invasive	McCoys 5A Media; 10% FCS
Lox IVMI	Human melanoma	Invasive	RPMI; 10% FCS
MCF-7	Breast carcinoma (ER +, PR +)	Non Invasive	RPMI; 10% FCS
MDA-MB-157	Triple Negative Breast carcinoma	Low Invasion	RPMI, 10% FCS
MDA-MB-231	Triple Negative Breast Adenocarcinoma	Highly Invasive	RPMI; 10% FCS
MDA-MB-361	HER2 positive Breast Adenocarcinoma	Invasive	RPMI; 10% FCS
MDA-MB-435-SF (Glynn *et al*., 2004)	Clonal subpopulation of human melanoma MDA-MB-435S (HER2 positive)	Invasive	RPMI; 10% FCS
MDA-MB-435-SF-Taxol-10p4p	Taxol Resistant varient of MDA-MB-435-SF	Invasive	RPMI; 10% FCS

(Glynn *et al*., 2004)	(HER2 positive)		
MDA-MB-453	HER2 positive Breast Carcinoma	Non-Invasive	RPMI; 10% FCS
MiaPaCa-2 clone 3 (Walsh *et al*., 2009)	Invasive clonal subpopulation of pancreatic cell line MiaPaCa-2	Invasive	DMEM; 5% FCS
MiaPaCa-2 clone 8 (Walsh *et al*., 2009)	Non-Invasive clonal subpopulation of pancreatic cell line MiaPaCa-2	Low Invasion	DMEM; 5% FCS
NCI-H1299	Large Cell Lung Carcinoma	Highly Invasive	RPMI, 1mM Na pyruvate, 5% FCS
SK-Mel-28	Human Melanoma	Invasive	RPMI; 10% FCS
SKBR-3	HER2 positive Breast Carcinoma	Low Invasion	RPMI; 10% FCS
SNB-19	Glioma	Highly Invasive	DMEM; 10% FCS

Table 2.2: - Cell lines used during the course of this thesis

ATCC: - American Tissue Culture Collection, Rockville, MD, USA.

- BT20, BT474, BxPc-3, HCT-116, MCF-7, MDA-MB-157, NCI-H1299

NICB: - National Institute for Cellular Biotechnology, D.C.U., Dublin, Ireland.

- DLKP, DLKP-A, DLKP-I, DLKP-M, DLKP-SQ, DLKP-SQ-Mitox-6p, MDA-MB-435-SF, MDA-MB-435-SF-Taxol-10p4p, MiaPaCa-2 clone 3, MiaPaCa-2 clone 8

NCI: - National Cancer Institute, Washington, D.C., USA

- SK-Mel-28

DSMZ: - Deutsche Sammlung von Mikroorganismen und Zellkulturen GmbH (German Collection of Microorganisms and Cell Cultures)

- SNB-19

MDA-MB-157, MDA-MB-361: - Berlex

Lox IMVI: - Radium Hospital, Norway.

2.3 Monoclonal Antibody Production

2.3.1 Immunogen for MAb Generation

The immunogen chosen for the generation of the 7B7 G5 (2) MAb was MiaPaCa-2 clone 3, an invasive clonal variant of the pancreatic cell line MiaPaCa-2. The immunogen chosen for the generation of the 9E1 24 (6) MAb was MDA-MB-435-SF, an invasive clonal variant of the melanoma cell line MDA-MB-435-S. Cells were detached from flasks using a non-enzymatic, cell dissociation solution (Sigma, C5914) to ensure that cell surface proteins remain undamaged.

2.3.2 Immunisation Regime

Using three BALB/c mice per immunisation, a primary immunisation with 2 X 10^6 cells (50µl volume), plus an equal volume of lipopeptide adjuvants, Pam3Cys-SKKKK (EMC microcollectors), Germany; L2000) was administered intraperitoneal; four booster immunisations were similarly administered at three weekly intervals. Polyclonal serum was obtained from tail bleeds of animals following the third and fourth booster injections; this was tested for reactivity against each respective target immunogen by immunofluorescence analysis. Serum from the tail bleed of a non-immunised mouse was used as a negative control.

- All experiments on animals were carried out under license and in compliance with the rules of The Cruelty to Animals Act, 1876, E.C. Directive 86/609EC

2.3.3 Fusion Procedure

The fusion procedure used for the production of monoclonal antibodies was a modification of the protocol outlined by Kohler and Milstein (1975). Prior to the removal of the spleen from the sacrificed mouse, SP/2/O-Ag 14myeloma cells (Shulman *et al.,* 1978) were prepared for cell fusion by harvesting 2 x 75cm^2 flasks and centrifuging at 1000 rpm for 5 minutes in HEPES Buffered Saline Solution-serum free medium (Lonza, CC-5022). This step was repeated twice. A cell count was then performed and the cells kept at 37°C.

A BALB/C mouse was then sacrificed by cervical dislocation. The animal was swabbed with 70% IMS and the spleen removed in a laminar flow cabinet with sterile instruments. Single cells were obtained by forcing the spleen through a sterile Falcon cell strainer (BD Falcon^{TM}, 352360) using the plunger from a sterile 10ml syringe into serum free DMEM (the DMEM referred to in this section is DMEM with Glutamax I (high glucose concentration – 4.5mg Gibco 61965-026)) containing pyridoxine and without sodium pyruvate or HEPES. This cell suspension was placed in a universal and the volume adjusted to 10mls. Large clumps of cells were allowed to pellet by standing at room temperature for 2-3 minutes. The supernatant was then transferred to a fresh centrifuge tube and centrifuged at 1000 rpm for 5 minutes. A cell count was performed as before.

Splenocyte and SP/2/O-Ag myeloma cells were mixed in a universal at a ratio of 10:1 (a minimum of 1 x 10^7 SP/2 are required for this procedure), centrifuged at 12,000 rpm for 5 minutes and resuspended in serum free medium. This step was repeated twice. Following the final washing step, 1ml of PEG (polyethylene glycol, Roche Diagnostics GmbH, Germany, 10783641001) (pre-warmed to 37°C) was added to the cell pellet with a Pasteur pipette using a gentle swirling and aspirating action for 30 seconds. After 30 seconds the aspiration was discontinued. 75 seconds after the start, 0.5ml of planting medium (DMEM with Glutamax I, 10% heat inactivated FCS (Gibco, 10108165), 5% Briclone (NICB Ltd., Ireland) and 1% HAT (Hypoxanthine, Aminopterin, Thymidine) (Gibco, 21060) was added slowly down the side of the universal while continuing to swirl gently. 5mls of planting medium was added over the next 5 minutes (at 1 minute intervals followed by the addition of 5mls). Following this step, the cell suspension was centrifuged at 500 rpm for 5 minutes. The supernatant was removed and the cells were resuspended in 10ml of plating medium and incubated at room temperature for 15 minutes.

Immunisation regimes and fusion procedures were kindly carried out by Dr. Anne-Marie Larkin.

2.3.4 Screening of Hybridomas

Generated hybridomas were screened directly for function on cell invasion against their parent immunogen. This was done using a 96-well invasion assay (see section 2.5.2). Hybridomas that produced an effect on cell invasion, either an increase or decrease, where chosen for further subculturing.

2.3.5 Subculture of Hybridomas

Positive clones were further sub-cultured to 6 well plates (Costar, 3335) and gradually transferred (fed 2x in HAT medium (Gibco, 21060-017), followed by a gradual change into HT (Hypoxanthine, Thymidine) medium (Gibco, 41065) – 50:50 HAT:HT. Eventually (within 2 weeks) hybridoma clones were weaned off HT (by decreasing HT gradually in feeds every three days) and fed with DMEM medium supplemented with 5% Briclone (NICB., Ireland) and 10% heat inactivated FCS (Invitrogen, BD Biosciences, 10082147).

2.3.6 Single Cell Cloning by Limiting Dilution

Using a multi-channel pipette (eppendorf), 100µl of DMEM growth medium was pipetted into each well of a sterile 96 well tissue plate. 100µl of cell suspension from the rapidly growing hybridomas at a concentration of 1 X 10^4 cells/ml was added to the top left hand well and mixed by pipetting. 1 in 2 doubling dilutions were performed down the left hand row of the plate (8 wells, 7 dilution steps) and mixed by pipetting, ensuring to change the pipette tip each time. 1 in 2 dilutions were also performed across the plate using a multi-channel pipette. Plates were then incubated for 7-10 days at 37°C, 5% CO_2. Wells with 1 or 2 cells were chosen. Hybridomas were cultured in T25cm^2 flasks and the procedure repeated. The selected clones were screened by Invasion assays (section 2.5.2) and immunofluorescence (section 2.9.2 & 2.9.2), and frozen stocks made of positive clones.

2.3.7 Isotype Analysis

Isotyping was carried out using The Isostrip Mouse Monoclonal Antibody Isotyping Kit (Roche Diagnostics GmbH, 1493027).

2.3.8 Purification of MAbs

Purified MAbs are required for cross linked immunoprecipitations (section 2.11.2), due to the presence of gelatin/carrier proteins in unpurified MAbs competing for coupling sites on the gel. Purification of MAbs was carried out using the Pierce NAb™ Spin Purification Kit (Pierce, 20530). 200µl of ImmunoPure® Immobilised Protein-L Plus gel slurry was dispensed into a Handee™ Spin Cup Column, along with 300µl of Binding Buffer, and centrifuged at 5000 x g for 1 minute (all subsequent centrifuges were at this speed and duration). Excess solution was discarded, leaving the gel in the spin cup. This was washed twice with 0.4ml of Binding Buffer, centrifuged and excess solution discarded. 250µl of antibody was dispensed into the spin cup, along with 250µl Binding Buffer, and incubated at 4°C overnight on a rocking platform. The following day, the solution was centrifuged, and the non-bound sample was retained, to analysis the efficiency and capacity of the binding. 0.4ml Binding Buffer was added to the spin cup, followed by centrifugation and discarding of the excess solution. This step was repeated twice. 0.4ml of IgM/IgG Elution Buffer was added to the solution, followed by 5 minute incubation at room temperature. This was repeated twice more, with each 0.4ml fraction being retained (the purified MAb should be eluted within the first 3 fractions). The high pH of the fractions were neutralised with the addition of 10µl of a Tris-HCl, pH 8.8, solution. The gel was then regenerated by washing in 0.4ml PBS, 3 times, centrifuging between every wash, and stored at 4°C in 0.5ml PBS. The immobilised protein can be re-used up to 10 times without significant loss in binding capacity.

2.3.9 Dialysis of MAbs

Dialysed MAbs are required for cross linked immunoprecipitations, due to the presence of amines in unpurified MAbs competing for coupling sites on the gel. Dialysis of MAbs was carried out using the Pierce Slide-A-Lyzer MINI Dialysis Units (Pierce, 69576). 100µl of MAb was dispensed into the Dialysis cup which, was placed in a floatation device, in PBS for a minimum of 15 minutes, allowing for buffer exchange to take place.

2.4 *In Vitro* Proliferation Assay

Cells were harvested at a concentration of 2 X 10^4 cells/ml in media. Volumes of 100µl/well of these cell suspensions were added to a 96 well plate (Costar, 3596) using a multichannel pipette. Plates were gently agitated to ensure an even dispersion of cells over a given plate. Cells were incubated at 37°C, 5% CO_2 overnight. Following this, 100µl of antibody was added to each well. Control wells were those with 100µl hybridoma media added to cell suspension. Plates were gently agitated, as above, and incubated at 37°C, 5% CO_2 for 6/7 days, until the control wells have reached 80-90% confluency. Assessment of cell survival in the presence of the antibodies was determined by the acid phosphatase assay.

2.4.1 Acid Phosphatase Assay

Following the incubation period of 6-7 days, media was removed from the plates. Each well on the plate was washed twice with 100µl PBS. This was then removed and 100µl of freshly prepared phosphatase substrate (10mM *p*-nitrophenol phosphate (Sigma 104-0) in 0.1M sodium acetate (Sigma, S8625), 0.1% triton X-100 (Sigma, X100), pH 5.5) was added to each well. The plates were then incubated in the dark at 37°C for 2 hours. Colour development was monitored during this time. The enzymatic reaction was stopped by the addition of 50µl of 1N NaOH. The plate was read in a dual beam plate reader at 405nm with a reference wavelength of 620nm

2.5 Extracellular Matrix Studies

2.5.1 Reconstitution of ECM proteins

Matrigel (Sigma, E-1270) was diluted to a working stock of 1 mg/ml in serum free DMEM. Fibronectin (Sigma, F-2006) was reconstituted in PBS to a stock concentration of 500 µg/ml. Aliquoted stocks were stored at -20°C.

2.5.2 Invasion Assays

This assay was set up using a Costar 24 well plate (Costar, 3524), containing 8.0µm pore sized inserts (BD Biosciences, 353097). For invasion (but not

motility) assays, a layer of Matrigel (BD Biosciences, 354234) was dispensed into the insert. Matrigel was diluted to 1mg/ml in serum-free DMEM medium. A volume of 100µl of this Matrigel was dispensed into each insert, and the plate was incubated overnight at 4°C. The following day, any excess Matrigel was removed from the inserts. Cells were harvested at a concentration of 1 X 10^6 cells/ml in media, and 100µl was added to each insert, along with 100µl of antibody/media (cells invading in the presence of hybridoma media were taken as 100%). A volume of 500µl media was added to each insert well. Cells were incubated at 37°C for 24 - 48hrs, depending on the cell line used.

Cell Line	Seeding Density	Incubation Time
MDA-MB-157	1 x 10^6	48hr
MDA-MD-231	1 x 10^6	24hrs
SKBR-3	1 x 10^6	48hrs
DLKP-I	1 x 10^6	48hrs
DLKP-M	1 x 10^6	24hrs
H1299	5 x 10^5	24hrs
MiaPaCa-2 clone 3	1 x 10^6	48hrs
BxPc-3	1 x 10^6	48hrs
Lox IMVI	1 x 10^6	24hrs
SNB-19	1 x 10^5	24hrs
C/68	1 x 10^6	48hrs
HCT-116	1 x 10^6	24hrs

Following this, the inner area of each insert was wiped with a cotton bud soaked in PBS, to remove any cells, while the outside of the insert was stained with 0.25% crystal violet. Staining of the inserts was sustained for a period of 10 minutes, followed by a gentle rinse, done in triplicate, in UHP and then allowed to dry. Quantification of the cells was achieved by doing a cell count per area per view at 20X magnification using a light microscope. 10 fields of view were counted per insert. A minimum of 2 inserts were used per sample tested.

For 96 well invasion assays, a Millipore 96 well invasion plate (Millipore, MAMIC8S10) was used. An identical procedure was followed, with the exceptions that 50µl Matrigel was dispensed into each insert, a cell suspension of 2.5 X 10^4 cells/ml was used, 50µl of antibody/media was added to each insert, and 150µl media was added to each insert well.

2.5.3 Motility Assays

Motility assays were carried out in an identical manner to invasion assays, as described in section 2.5.2, with the exception that the inserts were not coated in Matrigel.

2.5.4 Adhesion assay

Adhesion assays were performed using an adapted method of Torimura *et al.*, (1999). 250µl aliquots of ECM proteins were placed into wells of a 24-well plate. The plates were gently mixed to ensure the base of each well was completely covered with the solution. The plates were then incubated overnight at 4°C. The excess solution was then removed from the wells and washed twice with sterile PBS. To reduce nonspecific binding, 0.5 ml of sterile 0.1% BSA/PBS solution was dispensed into each well. The plates were incubated at 37°C for 20 minutes and then rinsed twice again with sterile PBS.

Cells were harvested and resuspended in media at a concentration of 2.5 X 10^4 cells/ml. 1ml of cells were plated onto 24 wells plates in triplicate and incubated for 60 minutes. Wells that had been coated with ECM proteins but contained no cells were used as blanks. Wells containing cells but not coated with ECM proteins were used as positive controls. After 60 minutes, the medium was removed from the wells and rinsed gently with sterile PBS. Cell number attached was assessed using the acid phosphatase assay (section 2.4.1).

2.5.5 Pre-incubation of cells with Matrigel coated flasks

Matrigel was coated onto flasks (1 ml/T25 cm^2) at a concentration of 1 mg/ml. Flasks were shaken gently to ensure complete coverage of the bottom of the flask. The coated flasks were then placed at 4°C overnight to allow the Matrigel

to settle. Before seeding flasks with cells, the flasks were placed into an incubator at 37°C for approximately 1 hours to allow the Matrigel polymerise. The excess media in the flasks was then removed and fresh complete media containing the cell suspension was added. Cells attached to the Matrigel on the bottom of the flask and after 70-90% confluency was achieved, were removed with 0.5ml/T25 cm^2 Dispase (BD Biosciences, 354235). Dispase is a bacillus derived neutral metalo protease that recovers cells cultured on Matrigel.

2.6 Anoikis assay

Poly- (2-hydroxyethyl methacrylate) (poly-HEMA, Sigma, P3932) was dissolved at 12 mg/ml in 95% ethanol. To coat 24-well plates, 100µl of poly-HEMA solution was added and allowed to dry in a laminar flow cabinet. After full evaporation, the coating step was repeated. Once evaporation was complete, wells were washed twice with sterile PBS. Cells (1 X 10^5cells/ml/well) were then plated onto standard 24-well tissue plates (adherent controls) or poly-HEMA-coated plates (non-adherent) and incubated for 24 hrs at 37°C in 5% CO2. After this time, 100µl of alamar blue vital dye (Serotec, BUF012B) was added to the 24-well plates to quantitatively measure cell survival. The plate was read in a dual beam plate reader at 570 nm with a reference wavelength of 600 nm. The level of anoikis was assessed as the percentage cell death relative to adherent controls over 24 hours.

2.7 Zymography Assay

2.7.1 Collection of Conditioned Media

Cells were cultured until 50-60% confluent. Cells were washed x3 in serum-free (SF) media. Cells were incubated in SF media (12 ml/T75 cm2 flask) for 60 min. After this time, cells were washed again x3 in SF media. 12mls of 1:1 SF media/MAb/Hybridoma media was added to the cells and incubated for 72 hrs. After such time, conditioned media was collected, centrifuged for 5 min at 1000 rpm, filtered through 0.22µm filter and stored at –80°C.

2.7.2 Zymography of Matrix Metalloproteinases

Conditioned media supernatants were prepared in a 4X non-reducing loading buffer (Invitrogen, NP0007) before being separated on a 10% zymogram (gelatin) gel (Invitrogen, EC61752BOX). This gel allows for the visualisation of MMP-2 and MMP-9. The gels were run at a constant voltage of 125V, 45mA for 90 minutes, or until the bromophenol blue dye front reached the end of the gel, in a 1X Tris-Glycine SDS running buffer (Biorad, 161-0732). After electrophoresis, the gel is incubated with a 1X Zymogram Renaturing Buffer (Invitrogen Developing buffer (LC2671) containing 2.5% Triton-X 100 (BDH, 30632), for 30 minutes at room temperature. The Renaturing Buffer is decanted, and 1X Zymogram Developing Buffer is added, followed by an addition 30 minute incubation at room temperature. Fresh Developing Buffer is added, and the gel is incubated at 37°C overnight. The gel is then stained with Brilliant blue G Colloidal Coomassie (Sigma, B2025).

2.8 Morphology Studies

Cells were grown to 70-80% confluency in a T75 cm^2, at which point a total volume of 12mls, 1:1 ratio fresh media:MAb is added. Cells are incubated for 24hrs at 37°C, and cell morphology is assessed visually.

2.9 Immunocytochemical Analysis

2.9.1 Immunofluorescence Studies on Live Cells

Viable MiaPaCa-2 clone 3 & clone 8 cells were tested for reactivity with antibodies by indirect immunofluorescence studies. When immunofluorescence studies are performed on viable cells only cell surface antigens are recognised (Schachner *et al.*, 1977). Cells were suspended to a concentration of 2 X 10^6 cells/ml in DMEM. 30µl of this cell suspension was added to a 10 well, 7mm microscope slide (Erie Scientific Company, 465-68X), and was incubated overnight at 37°C. After 24hrs, excess supernatant was tapped off, and the microscope slides were rinsed gently with warm PBS. Primary antibodies were added to each well (PBS was added to one well as a negative control), and were incubated overnight at 4°C. Primary antibodies were removed by washing in

PBS 3 times, at 3-minute intervals. 30µl of secondary antibody, fluorescein isothicyanate-linked (FITC) rabbit anti-mouse IgG (Dako, F0261), diluted 1/40, was added to each well, followed by a 30-minute incubation at room temperature. Secondary antibody was removed by PBS washing as mentioned above. Excess PBS was drained of with filter paper, and each slide was mounted using vectashield mounting medium (Vector, H-100) and coverslips, and sealed with nail varnish. Slides were viewed using a Nikon phase contrast microscope fitted with an FITC filter.

2.9.2 Immunofluorescence Studies on Fixed Cells

Cell suspension, volume added to slides and incubation is as described (2.9.1). After 24hrs, excess supernatant was tapped off, and the microscope slides were rinsed gently with PBS. Slides were then air dried overnight, wrapped in tin foil, and stored at -80°C. Slides are then removed from -80° C freezers, and left for 15 minutes prior to immunstaining. Cells were fixed in ice-cold acetone for 2-4 minutes.

2.10 Western Blot Analysis

2.10.1 Preparation of Whole Cell Lysates

Cells were grown to 80-90% confluency in culture flasks (T175cm^2 flask), media was removed, cells were trypsinised, pelleted and washed three times in ice cold PBS. Cells were resuspended in 1.5mls (per T175cm^2 flask) NP/40 lysis buffer (Appendix I, Table 1), RIPA lysis buffer (Sigma, R0278) or Lysis buffer C (Appendix I, Table 2) containing 1X protease inhibitor (Complete Mini^{TM}, 04693124001, Roche Diagnostics, GmbH). Cell suspensions were homogenised by passing through a 21 G syringe. Sample lysates were sonicated for 5 minutes and centrifuged at 14000 rpm for 10 minutes at 4°C. Supernatants containing extracted protein were transferred to fresh chilled eppendorf tubes in 250µl aliquots, and stored at -80°C. Protein concentration was quantified using the Bio-Rad or BCA assay as detailed in Section 2.10.2.

2.10.2 Protein Concentration Determination

Protein-Levels were determined using the Bio-Rad (for lysis buffer C cell lysates - Bio-Rad, 5000006) or BCA (for RIPA buffer cell lysates – Bio-Rad, 500-0001) protein assay kit.

2.10.3 Gel Electrophoresis

Proteins for Western blotting were separated by SDS-PAGE gel electrophoresis (Laemmli *et al.*, 1970), using 4-12% gradient gels (NP0335, NP0321). Approximately 15-30 μg of protein was applied to each well of the polyacrylamide gel. Pre-stained molecular weight markers (Invitrogen, LC5800) were also loaded onto the gel for the determination of the molecular weight of the unknown protein samples. Gels were run at 200 volts and 250 milliamps for 1-1.5 hours with 1X MOPS, Tris/ Glycine/ SDS running buffer (Invitrogen, NP0001). When the dye front of the molecular weight markers had reached the end of the gel, electrophoresis was stopped.

2.10.4 Western Blotting

Following separation on SDS gels, protein samples/immunoprecipitated sample were transferred to PVDF membranes (Roche Diagnostic GmbH, 03-010-040-001) using a semi-dry apparatus (Trans-Blot SD semi-Dry Transfer Cell, Bio-Rad, USA). Proteins were transferred at 15V, 34 milliamps, for 45 minutes

2.10.5 Development of Western Blots by Enhanced Chemiluminescence (ECL)

Following Western blotting, the filter paper was removed and the membrane blocked for non-specific binding by incubation for 1-4 hours on a rocking platform with Starting Block™ (TBS) Blocking Buffer (Pierce, 37542). After the blocking step was complete, the blot was rinsed once in TBS, and incubated with the primary antibody optimally diluted in TBS/0.1% (v/v) Tween 20 overnight at 4°C or 2 hours at R.T. on a rocking platform (MAbs generated in this study were used neat). The following day blots were washed 3 times within 90 minutes with TBS/0.5% (v/v) Tween 20. Blots were then incubated with an anti-mouse HRP-conjugated secondary antibody diluted in TBS/0.1% (v/v) Tween 20 for 1 hour at

room temperature on a rocking platform (See Appendix I, table 4, for full list of secondary Abs used and the dilutions). The blots were washed as before, laid on a glass plate covered in parafilm and incubated with ECL reagents (Amersham, RPN 2105) for 1 minute at room temperature. Following this, the solution was tapped off, the blot laid between two sheets of cling film, and exposed to Amersham Hyperfilm^{TM}, chemiluminescence film (GE Healthcare, 28906837) for various time periods and processed using standard x-ray developing procedures. Dried film was aligned with pre-stained molecular weight markers for molecular weight determination.

2.11 Immunoprecipitation Studies

2.11.1 Direct Immunoprecipitation

Protein was isolated from a number of cell lines, as described in section 2.10.1. 250µl test aliquots of supernatant were pre-cleared by incubation with protein-L (P3351, Sigma, UK), or Protein G (Pierce, 22852), 50µl of which was added to all test samples. All samples were incubated with two changes (2 x 2 hours) of protein-L/G agarose beads at 4°C on a rocking platform. Beads were removed by spinning at 2500rpm for 10 minutes at 4°C. Supernatants were removed to clean eppendorf tubes and 75µl of antibody (concentrated 5X supernatant, using Millipore Ultrafree-15 centrifuge filter units (Millipore, Z-36436-0) was added to 250µl lysate samples. 50µl of control mouse IgM (Chemicon, PP50) or control mouse IgG (Sigma, I5381) (used at a concentration of 22µg/ml) was added to 250µl negative control lysates. Antibody/lysate mixtures were incubated at 4°C overnight on a rocking platform. The following day, in order to precipitate the antibody-antigen complex, protein-L/G agarose was added to the antibody-antigen complex samples as before and incubated at 4°C for 4 hours on a rocking platform. Beads were removed by spinning at 2500rpm for 10 minutes at 4°C, and the supernatant discarded. The beads were then washed for 3 x 15 minute periods with buffers as described in Appendix III and pelleted at 2500rpm for 10 minutes. Following the final wash and spin, as much liquid as possible was removed from all samples. 75µl of 2X laemmili sample buffer was added to

original 250µl lysates and control sample beads. All samples were boiled for 10 minutes and stored at -80°C until required for SDS-PAGE/Western blot analysis.

2.11.2 Cross Linked Immunoprecipitation

Cross Linked I.P.s were carried out using the Seize ® Primary Immunoprecipitation Kit (Pierce, 45335). 200µl of AminoLink® gel slurry was added to a Handee™ Spin cup Column, and spun down at 5000 x g for 1 minute (all subsequent centrifuges were at this speed and duration). Excess slurry was discarded, leaving the gel in the spin cup. This was washed twice with 0.4ml of Coupling Buffer, centrifuged and excess solution discarded. 200µl of affinity-purified antibody (section 2.3.8, 2.3.9) was added to the gel, along with 200µl of Coupling Buffer. 4µl of Reducing Agent (Sodium Cyanoborohydride) was added to the mixture (1µl/100ul diluted antibody), which was then incubated over night at 4°C. This step is to facilitate cross-linking of the antibody to the gel. The gel was then centrifuged and washed with 0.4ml Coupling Buffer, followed by another centrifugation step. Excess solution was discarded. Following this, 0.4 ml of Quenching Buffer was added to the suspension, centrifuged, and excess solution discarded. 0.4ml of Quenching Buffer was then added to the gel/antibody complex, along with 4µl of Reducing Agent. This suspension was incubated with end-over-end mixing, for 30 minutes at room temperature, followed by centrifugation and discarding of any excess solution. The gel was then washed 6 times with 0.4ml Wash Buffer, followed by 4 washes in 0.4ml Binding Buffer, with centrifugation following each wash.

The antigen (protein) sample was pre-cleared with Protein-L/G as described in section 2.11.1. 250µl was added to the gel/antibody complex, along with 250µl of Binding Buffer. This solution was incubated overnight at 4°C on a rocking platform. The following day, the sample was centrifuged, and excess solution discarded. The gel/antibody-antigen complex was then washed 3 times in 0.4ml Immunoprecipitation Buffer, with centrifugation after each wash. The antigen-antibody complex was then cleaved with the addition of 200µl of an IgM/IgG Elution Buffer to the solution, followed by 5 minute incubation at room temperature. This was repeated twice more, with each 200µl fraction being

retained (the antigen should be eluted within the first 3 fractions). The high pH of the fractions was neutralised with the addition of 5µl of a Tris-HCl, pH 8.8, solution. The gel was then regenerated by washing, in triplicate, with 0.4ml Immunoprecipitation Buffer, centrifuging and discarding excess solution, between every wash. The gel was then stored at 4°C in 0.5ml Binding Buffer. The gel-antibody complex can be re-used up to 10 times without significant loss in binding capacity.

Eluted fractions were prepared for Gel Electrophoresis using NuPAGE® LDS Sample Buffer (4X) (Invitrogen, NP0007), containing 10X NuPAGE® Sample Reducing Agent (Invitrogen, NP0009). All samples were made up to 1X concentration.

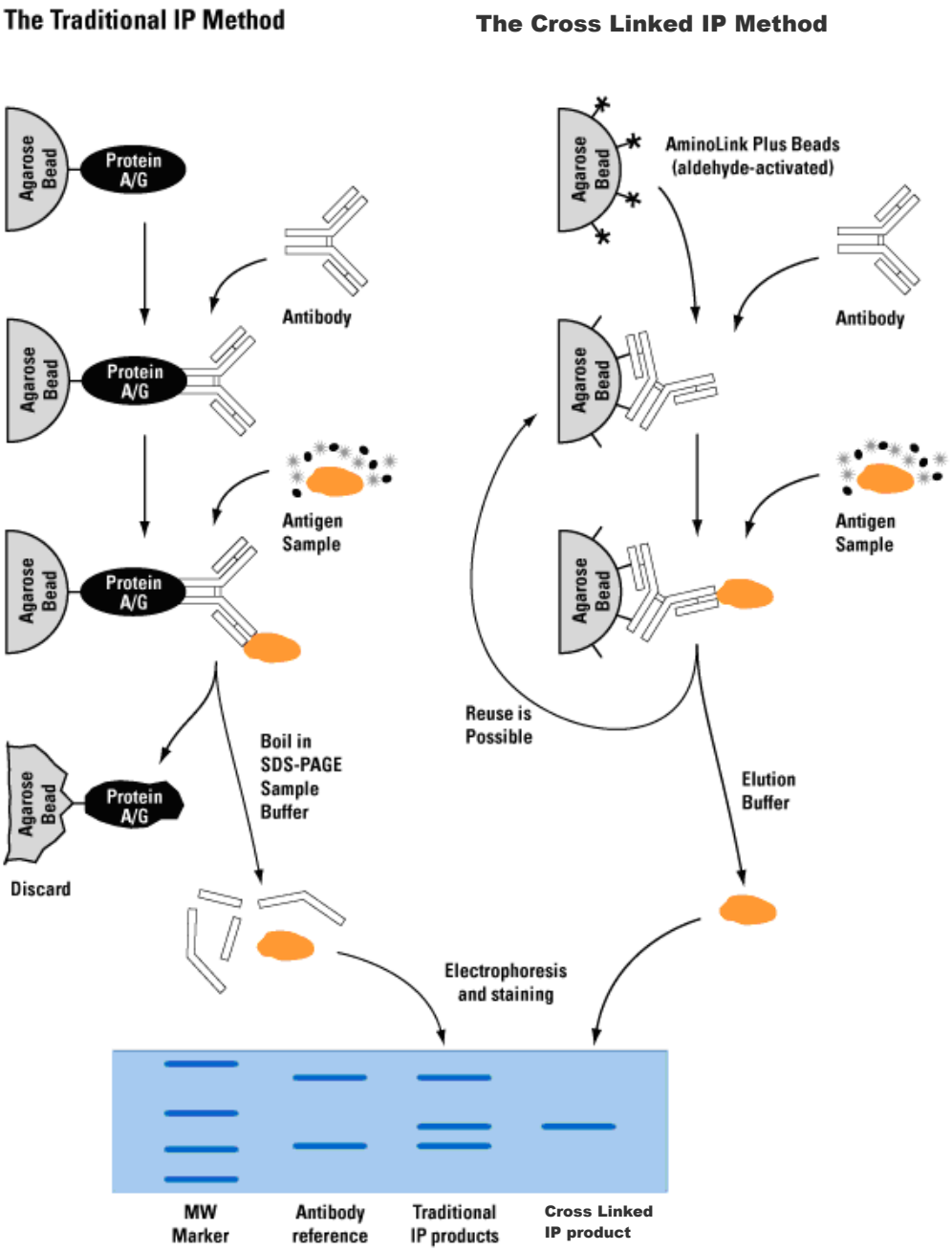

Figure 2: - Direct (Traditional) and Cross Linked Immunoprecipitation (www.piercenet.com)

2.11.3 Gel Electrophoresis of Immunoprecipitated Proteins

Immunoprecipitated proteins, along with unstained molecular weight markers (Invitrogen, LC5801), were separated on 4-12%, Bis-Tris, SDS-PAGE electrophoresis as described in section 2.10.3. Following gel electrophoresis, the gel was either stained using Brilliant blue G Colloidal Coomassie, or Western blot analysis was carried out as outlined in section 2.10.4.

2.11.4 Staining- Brilliant blue G Colloidal Coomassie and silver staining of gels for LC-MS Identification

After electrophoresis, the gels were placed in a square petri dish (Sigma, Z617679) containing fixing solution (7% glacial acetic acid in 40% (v/v) methanol (ROMIL, HL109)) for at least 1 hour. During this step a 1X working solution of Brilliant Blue G colloidal Coomassie was prepared by adding 800ml UHP to the stock bottle. When the fixing step had nearly elapsed a solution containing 4 parts of 1X working colloidal Coomassie solution and 1 part methanol was made, mixed by vortexing for 30 seconds and then placed on top of the gels. The gels were left to stain for 2 hours. To destain, a solution containing 10% acetic acid in 25% methanol was poured over the shaking gels for 60 seconds. The gels were then rinsed with 25% methanol for 30 seconds and then destained with 25% methanol for 24 hours.

Alternatively, gels were stained using a silver stain protocol. All buffers were prepared as outlined in Appendix I, Table 3:

Gels were fixed for a minimum of 2 hours, followed by three 20 minute washes in 35% Ethanol. Gels were then sensitised for 2 minutes, and washed in UHP for 5 minutes, in triplicate. Staining was then carried out, for 20 minutes with the Silver Nitrate solution, followed by two 1 minute washes in UHP. Gels were then developed until bands were visible to the naked eye. Staining was then stopped through a 5 minute wash with the stop solution.

2.12 Protein Identification Using LC-MS/MS

LC-MS/MS was performed on an Ultimate 3000 nanoLC system (Dionex), interfaced to an LTQ Orbitrap XL (Thermo Fisher Scientific).

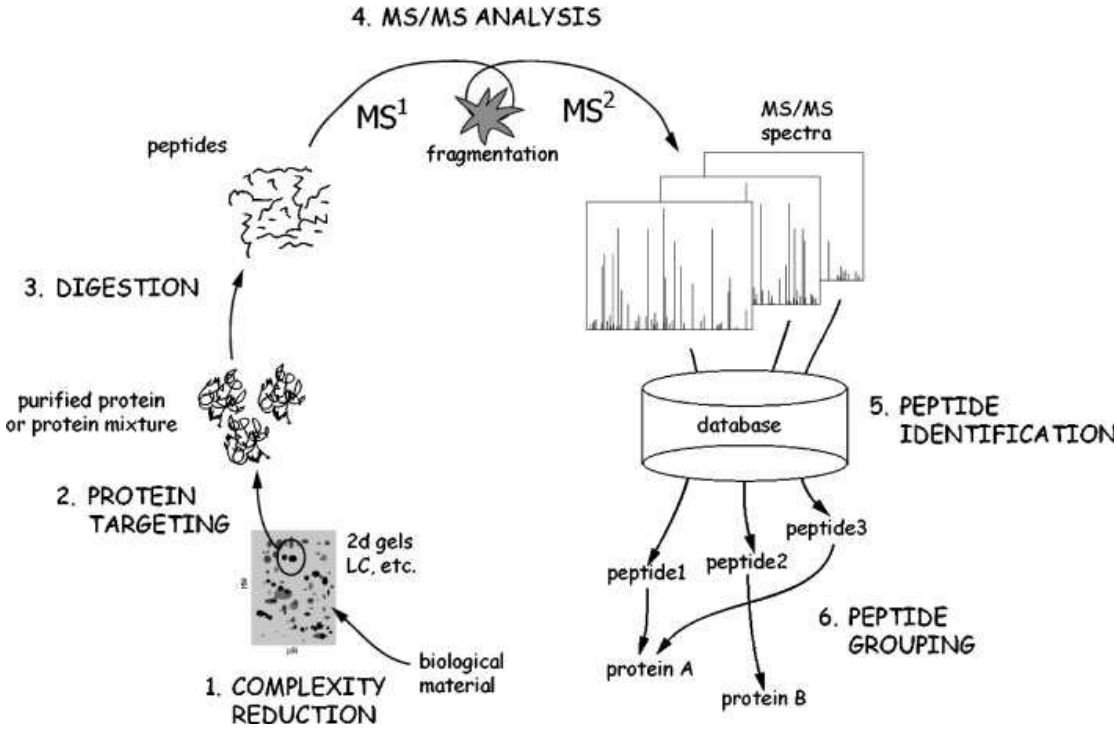

Figure 2.1: - Standard workflow for protein identification based on tandem mass spectrometry. (1) and (2), protein sample complexity reduced using separation techniques; (3), proteins are enzymatically digested; (4), resulting peptides undergo tandem mass spectrometric analysis yielding a collection of MS/MS spectra; (5) Identification of peptides is achieved through correlation of the MS/MS spectra with theoretical peptides; (6), a list of identified proteins is produced (6) (Hernandez *et al.*, 2005).

Protein bands were excised from the Coomassie-stained gel and destained with a solution containing 50% methanol and 50 mM NH_4HCO_3. Samples were then dehydrated by the addition of 70% acetonitrile (ACN) and swelled by rehydration in a digestion buffer containing 40 mM NH_4HCO_3 and 12.5 ng/µL of trypsin (Promega, sequencing grade) at 37 °C overnight. Peptides were extracted with three changes of 50% ACN/ 0.1% formic acid (Fluka) and dried down in a vacuum centrifuge. Tryptic peptides were re-dissolved in 10µL of 0.1% formic acid. 5µL of sample was loaded onto a trapping column packed with C18, PepMAP100 (Dionex) at a flow rate of 20µL/min in 0.1% formic acid. After 5 minutes of washing, peptides were eluted into a C18 PepMAP100 nanocolumn (15 cm×75µm ID, 3µm particles) (Dionex) at a flow rate of 350 nL/min. Peptides were separated using the mobile phase gradient: from 5 to 50% of solvent B in 30 min, and from 50 to 90% B in 5 min. Solvent A was 98:2 H_2O:ACN (v/v)

containing 0.1% formic acid; solvent B was 2:98 H_2O:ACN (v/v) containing 0.1% formic acid.

LC-MS/MS data was acquired in data-dependent acquisition (DDA) mode controlled by Xcalibur 2.0.7 software (Thermo Fisher Scientific). A typical DDA cycle consisted of an MS scan within *m*/*z* 300–2000 performed under the target mass resolution of 60,000 (full width at half maximum) followed by MS/MS fragmentation of the six most intense precursor ions under normalised collision energy of 35% in the linear trap.

2.12.1 Bioinformatic Interpretation of Mass Spectrometry Data

Bioinformatics is the application of computer science and statistics to the management of biological data such as genomics and proteomics. It allows for the determination of proteomic signatures responsible for important clinical-pathological features, and the identification of proteins/antigens that may be significant candidates as biomarkers and therapeutic targets in a host of diseases.

Database searches were performed using TurboSEQUEST software (Bioworks Browser version 3.3.1) (Thermo Fisher Scientific) using the human subset from the SWISS-PROT database. SWISS-PROT is a protein sequence database which provides a high level of annotations (such as the description of the function of a protein, its domains structure, post-translational modifications, variants, etc.), a minimal level of redundancy and high level of integration with other databases. It was established in 1986 by Amos Bairoch in the Department of Medical Biochemistry at the University of Geneva (Per Kraulis, 2001). The following filters were applied: for charge state 1, X_{Corr}>1.5; for charge state 2, X_{Corr}>2.5; for charge state 3, X_{Corr}>3.5.

LC-MS/MS analysis and bioinformatic interpretation of data was carried out with the help of Michael Henry and Dr. Paul Dowling.

2.13 Immunohistochemical Analysis

All immunohistochemical studies on formalin-fixed paraffin-embedded tissue sections were performed following the method of Hsu *et al.*, (1981) using an avidin-biotin horseradish peroxidase (HRP) conjugated kit (ABC) plus an appropriate secondary antibody. Formalin-fixed paraffin-embedded tissue was kindly provided by Tallaght Hospital (AMNCH), Mount Carmel Hospital, Beaumont Hospital, Royal Victoria Eye & Ear Hospital and St. Vincent's Hospital, Dublin. 5µm sections of tissue blocks were cut using a microtome, mounted onto poly-l-lysine coated slides. Slides were stored at room temperature until required.

All immunohistochemical staining was performed using the Dako Autostainer (Dako, S3800). Deparaffinisation and antigen retrieval was performed using Epitope Retrieval 3-in-1 Solution (pH 9) (Dako, S2375) and the PT Link system (Dako, PT101), whereby slides are heated to 97°C for 20 minutes, then cooled to 65°C. The slides are then immersed in Wash buffer (Dako, S3006). On the Autostainer, slides were blocked for 10 minutes with 200µl HRP Block (Dako, S2023). Cells were washed with Wash buffer, and 200µl of MAb was added to the slides for 20 minutes. Slides were washed again with Wash buffer, and then incubated with 200µl Real EnVision DAB (Dako, K4065) for 30 minutes. Each slide was also run with Negative Control Reagent(1X TBS/0.05% Tween-20), to allow evaluation of non-specific staining and allow better interpretation of specific staining at the antigen site. Staining was performed using MAbs generated in this study. All slides were counterstained with haematoxylin for 5 minutes, and rinsed with deionised water, followed by wash buffer. All slides were then dehydrated in graded alcohols (2 x 3 minutes each in 70% IMS, 90% IMS and 100% IMS), and cleared in xylene (2 x 5 minutes), and mounted with coverslips using DPX mountant (Sigma, 44581).

2.14 RNA interference (RNAi)

RNAi using small interfering RNA's (siRNAs) was carried out to silence specific genes. The siRNAs used were chemically synthesised (Ambion Inc). These siRNAs were 21-23 bps in length and were introduced to the cells via reverse transfection with the transfection agent siPORT^{TM} *Neo*FX^{TM} (Ambion Inc., 4511).

2.14.1 Transfection optimisation

In order to determine the optimal conditions for siRNA transfection, optimisation with kinesin siRNA (Ambion Inc., 16704) was carried out for each cell line. There were a number of different parameters that had to be determined to establish an optimised protocol for the siRNA transfection of MiaPaCa-2 and its single cell population clones.

Cell suspensions were prepared at 1 X 10^5, 3 X 10^5 and 5 X 10^5 cells per ml. Solutions of negative control and kinesin siRNAs at a final concentration of 30nM were prepared in optiMEM (Gibco^{TM}, 31985047). NeoFX solutions at a range of concentrations were prepared in optiMEM in duplicate and incubated at room temperature for 10 minutes. After incubation, either negative control or kinesin siRNA solution was added to each neoFX concentration. These solutions were mixed well and incubated for a further 10 minutes at room temperature. 100µl of the siRNA/neoFX solutions were added to each well of a 6-well plate. 1 ml of the relevant cell concentrations were added to each well. The plates were mixed gently and incubated at 37°C for 24 hours. After 24 hours, the transfection mixture was removed from the cells and the plates were fed with fresh medium. The plates were assayed for changes in proliferation at 72 hours using the acid phosphatase assay (Section 2.4.1). Optimal conditions for siRNA transfection were determined as the combination of conditions, which gave the greatest reduction in cell number after kinesin siRNA transfection and also the least cell kill in the presence of transfection reagent. Western blot analysis was used to establish the optimum conditions for a siRNA transfection. The optimised conditions for the cell lines are shown in Table 2.16.

Cell Line	Seeding Density per 96-Well Plate	Seeding Density per 6-Well Plate	Volume NeoFX per 96 well (μl)	Volume NeoFX per 6 well (μl)
MiaPaCa-2 clone 3	$2.5x10^3$	$3x10^5$	0.2	2
DLKP-M	$2.5x10^3$	$3x10^5$	0.2	2

Table 2.14: - Optimised conditions for siRNA transfection

2.14.2 siRNA functional analysis of targets identified in MiaPaCa-2 clone 3 and DLKP-M

Two - three pre-designed siRNAs were chosen for each of the protein/gene targets and transfected into cells. Two siRNAs were used if a validated siRNA was available. Validated siRNAs have been verified by real-time RT-PCR to reduce gene expression of >70% 48 hours post-transfection. For each set of siRNA transfections carried out, control, non-transfected cells and a scrambled (SCR) siRNA transfected control were used. Scrambled siRNA are sequences that do not have homology to any genomic sequence. The scrambled non-targeting siRNA used in this study is commercially produced, and guarantees siRNA with a sequence that does not target any gene product. It has also been functionally proven to have no significant effects on cell proliferation, morphology and viability. For each set of experiments investigating the effect of siRNA, the cells transfected with target-specific siRNAs were compared to cells transfected with scrambled siRNA. This took account of any effects due to the siRNA transfection procedure, reagents, and also any random effects of the scrambled siRNA. Kinesin was used as a control to assess the efficiency of the siRNA transfection. Kinesin plays an important role in cell division; facilitating cellular mitosis. Therefore, transfection of siRNA kinesin resulted in cell cycle arrest and confirmed efficient transfection. Western blots (section 2.10.4) were used to determine if siRNA had an efficient knock-down effect at a Protein-Level. (Appendix I, Table 5 outlines the list of siRNAs and IDs used in this thesis)

2.14.3 Proliferation assays on siRNA transfected cells

As described in table 2.12, cells were seeded using 0.2µl NeoFX to transfect 30nM siRNA in a cell density of 2.5 X 103 per well of a 96-well plate. After 24 hrs, transfection medium was replaced with fresh media and cells were allowed to grow until they reached 80-90% confluency, a total of 5 days. Cell number was assessed using the acid phosphatase assay (section 2.4.1). All experiments were carried out independently at least three times.

2.14.4 Invasion assays on siRNA transfected cells

Using the optimised conditions in Table 2.16, each of the siRNAs was tested to see changes in invasion of the cells after transfection. Two-three separate siRNAs were used for each target gene (Appendix I, Table 5). All siRNAs were purchased from Ambion Inc.

To assay for changes in invasive capacity, siRNA experiments in 6-well plates were set up using 2µl NeoFX to transfect 30nM siRNA at a cell density of 3 X 10^5 per well of a 6-well plate. Transfection medium was removed after 24 hours and replaced with fresh growth medium. The transfected cells were assayed for changes in invasion capacity at 48 hours using the *in vitro* invasion assay described in Section 2.5.2. All experiments were carried out independently at least three times.

2.14.5 Motility assays on siRNA transfected cells

Motility assays were carried out as described in section 2.5.3

2.15 Statistical analysis

Analysis of the difference of comparisons, as well as untreated versus siRNA treated mean invasion and motility counts, adherence absorbance, Anoikis and percentage survival calculated, were performed using a student t-test (two-tailed with equal variance), on Microsoft Excel. This t-test method was used because the 2 sample sizes are equal, and it is assumed that the two distributions have the same variance, e.g. SNB-19 invasion assay:

Control (Hybridoma Media)	MAb 7B7 G5 (2)	
31.5	28.9	
53.1	27.3	n = 1
37.2	27.4	
34.2	23.6	
21.2	15	n = 2
29	17.3	
25.9	16.9	
23.1	22.9	n = 3
25	22.3	

Table 2.15: - Mean cell counts from invasion assay of SNB-19 glioma cells n the presence of hybridoma media (control) and MAb 7B7 G5(2). Counts of inserts over biological triplicates. 3 inserts per biological experiment

Using Microsoft Excels T Test function with the above figures, a p value of 0.029 is achieved, making it significant. The P value measures the probability that the differences between the control and test samples would be observed by chance

*, A p value of ≤ 0.05 was deemed significant

**, A p value ≤ 0.01 was deemed more significant

***, A p value ≤ 0.005 was deemed highly significant

Error bars were plotted using plus and minus the standard deviation on triplicate inserts interexperimentally.

In the siRNA experiments, siRNA scrambled transfected cells were used as control compared to siRNA treated samples. This was to ensure no ‘off-target’ effects of the siRNA transfection procedure. Non-treated controls were used to ensure scrambled siRNA was having no effect and to normalise data.

Effects of less than 20% are taken as “little to no effect”, however, statistical analyses are still carried out, and therefore an experiment that shows little to no effect can still be significant or non-significant.

CHAPTER 3

GENERATION OF MONOCLONAL ANTIBODIES DIRECTED AGAINST MIAPACA-2 CLONE 3

3.1 Background

An initial primary immunisation, and 4 booster immunisations were carried out with the pancreatic cell line, MiaPaCa-2 clone 3, an invasive variant of the MiaPaCa-2 parent cell line (Walsh *et al*., 2008), A final boost was carried out 3 days prior to fusion.

3.2 Fusion Results

Following fusion with MiaPaCa-2 clone 3 cells, as described in section 2.3.3, 335 hybridoma supernatants (77.5% fusion efficiency) were screened directly for any effect on the invasive capacity on MiaPaCa-2 clone 3 cells, and by live and fixed cell immunofluorescence.

3.3 Preliminary Characterisation of Hybridoma Supernatants

3.3.1 Screening Directly for Effects on Invasion

All resulting hybridomas were screened using a newly developed 96-well invasion assay method (section 2.5.2.) against the parent cell line, MiaPaCa-2 clone 3. Supernatants showing an increase or decrease in invasion levels were identified by three independent witnesses through microscopic evaluation. Controls comprised of cells with no antibody supernatant (hybridoma media added in place), with invasion levels in all cases being compared to this hybridoma medium control.

25 supernatants (duplicate samples) were re-screened twice (96-well invasion assay). MAbs 8B3, 7B7, 1E5, 7C3, 7B7, 9D6, 5B1 & 6E2, which all exhibited a decrease in invasion, and MAbs 7C7 & 7B6, which both showed an increase in invasion, were then re-screened, in triplicate, using 24 well invasion assays, again on the invasive MiaPaCa-2 clone 3 and the low invasive MiaPaCa-2 clone 8 cells. MAbs 7B7 and 6E2 appeared to have the most consistent inhibition of invasion, and were chosen for further characterisation. As can be seen in Figure 3.3.1, MAb 7B7 supernatants harvested at various time points, from T25cm and

T75cm flasks, show a consistent inhibitive effect on invasion levels in invasive MiaPaCa-2 clone 3 cells. Preliminary results also indicated that MAb 7B7 marginally decreased invasion (by observation only; not quantified) in MiaPaCa-2 clone 8 cells, which exhibit very low levels of invasion (results not shown).

MAbs 7B7 & 6E2 were then cloned out by limiting dilutions (section 2.3.6), and re-screened using both 96 and 24 well invasion assays (figure 3.3.2). Using invasive MiaPaCa-2 clone 3 pancreatic cells, clones G5 and G5 (2) exhibited a consistent inhibitive effect on invasion (figure 3.3.3). It was decided at this point that MAb 7B7 G5 (2) would be chosen for further characterisation. Significant inhibition of the 7B7 G5 (2) supernatant was observed (in triplicate, independent experiments) following the freezing down, and thawing back, of the hybridoma, indicating the stability of this MAb. Isotyping of MAb 7B7 G5 (2) determined it to be an IgM antibody (Figure 3.3). Isostrip analysis was carried out as described in section 2.3.7

Figure 3.3: - Isostrip analysis of MAb 7B7 G5 (2), indicating that it is an IgM subclass antibody (Isostrip, Roche Diagnostics, GmbH, 1493027)

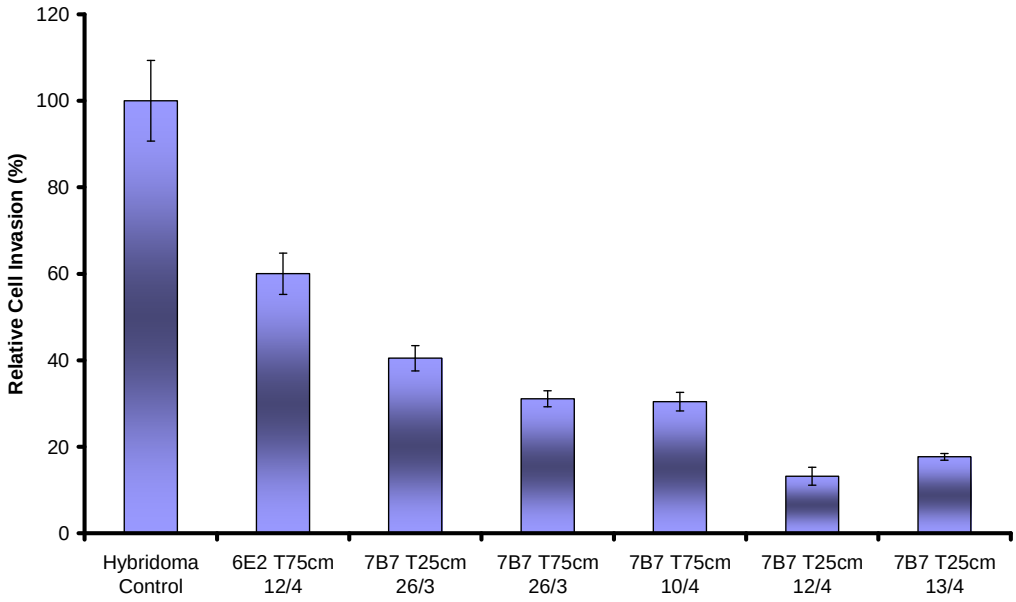

Figure 3.3.1: - Representative histogram showing inhibitory effects of MAbs 6E2 and 7B7, harvested from T25cm^3 and T75cm^3 flasks over different dates, on MiaPaCa-2 clone 3 invasion after 48 hours. MAb 6E2 successfully inhibits invasion by 40%, while MAb 7B7 inhibits invasion by up to 86%. Error bars calculated using ± standard deviation.

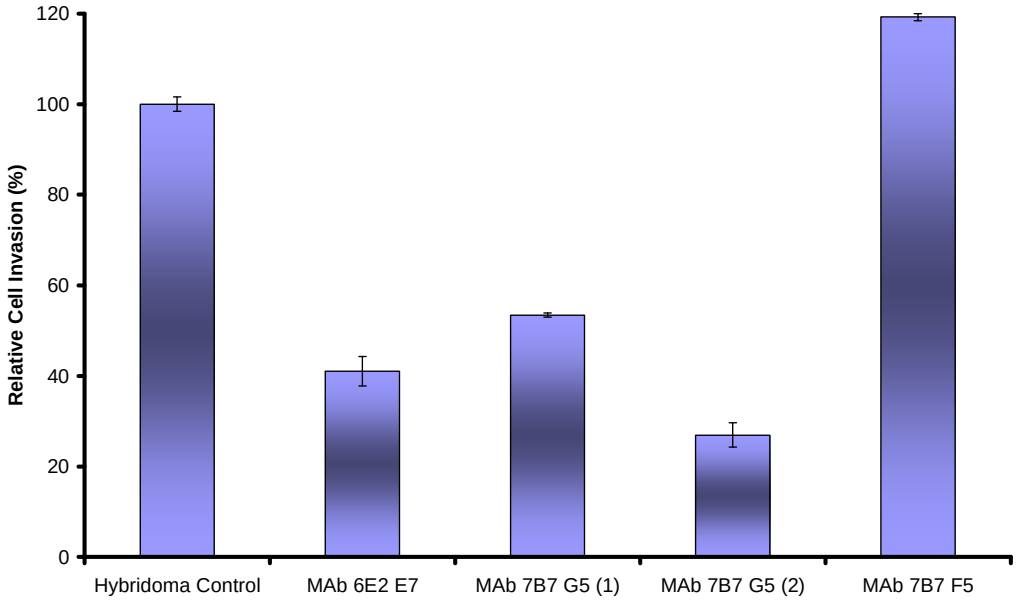

Figure 3.3.2: - Representative histogram showing inhibitory effects of MAbs 6E2 and 7B7 clones, on MiaPaCa-2 clone 3 invasion after 48 hours. Clone 6E2 E7 successfully inhibits invasion by 39%, while 7B7 G5 (2) inhibits invasion by up to 77%. Error bars calculated using ± standard deviation.

A.

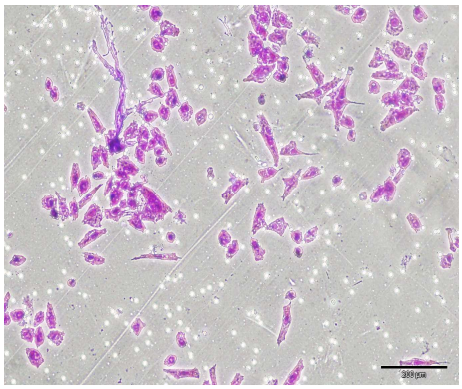

B.

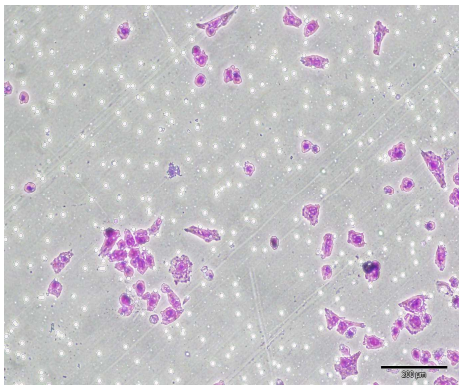

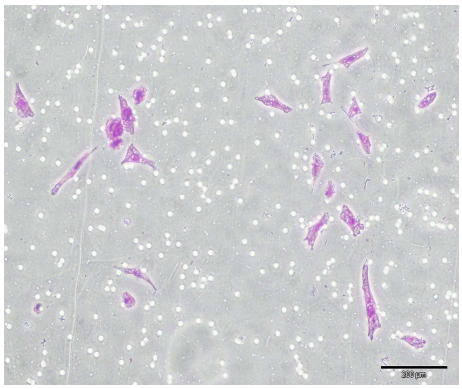

C.

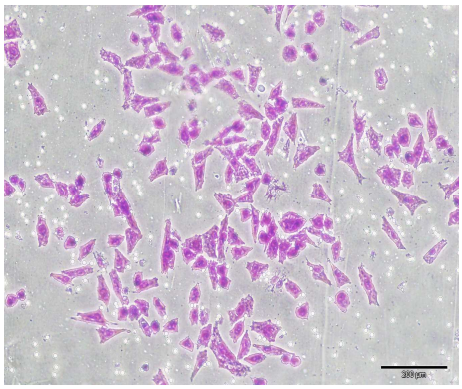

D.

Figure 3.3.3: - Representative photomicrographs showing invasion of MiaPaCa-2 clone 3 cells after 48 hours with addition of (A) hybridoma media (Control – no MAb), (B) MAb 6E5 E7, (C) MAb 7B7 G5 (2) and (D) MAb 7B7 F5. A decrease in invasion can be observed following addition of (B) MAb 6E5 clone E7 and (C) MAb 7B7 clone G5 (2) when compared to the control insert (A). No inhibition of invasion is observed with MAb 7B7 clone F5 (D). Magnification, 100X. Scale Bar, 200µm

3.3.2 Immunofluorescence Assay

Following 2 preliminary screenings, 22 hybridoma supernatants showing strong reactivity by immunofluorescence with MiaPaCa-2 clone 3 were chosen for repeat screenings. The cellular staining observed varied between strong membrane-like staining to more intracellular-like staining; some nuclear reactivity was also observed with a small number of hybridomas. Following repeated screenings, hybridomas 8F4, 3E2, 5B5, 1E5, 9D6 & 7B7 were chosen for further characterisation. Preliminary results using immunofluorescence indicated that MAbs 9D6 & 3E2 exhibited stronger reactivity with MiaPaCa-2 clone 8 cells (low level invasive variant). MAbs 7B7 & 8F4 appeared to show stronger reactivity with clone 3 compared to clone 8. MAb 8F4 showed very strong membrane positivity, not observed with any of the other antibodies, indicating that this MAb was recognising a membrane epitope. Representative photomicrographs showing MAbs 3E2, 7B7, 8F4 & 9D6 reactivity in MiaPaCa-2 clone 3 and clone 8 cells can be observed in Figure 3.3.4. Immunofluorescence assays were carried out as described in section 2.9.1 and 2.9.2

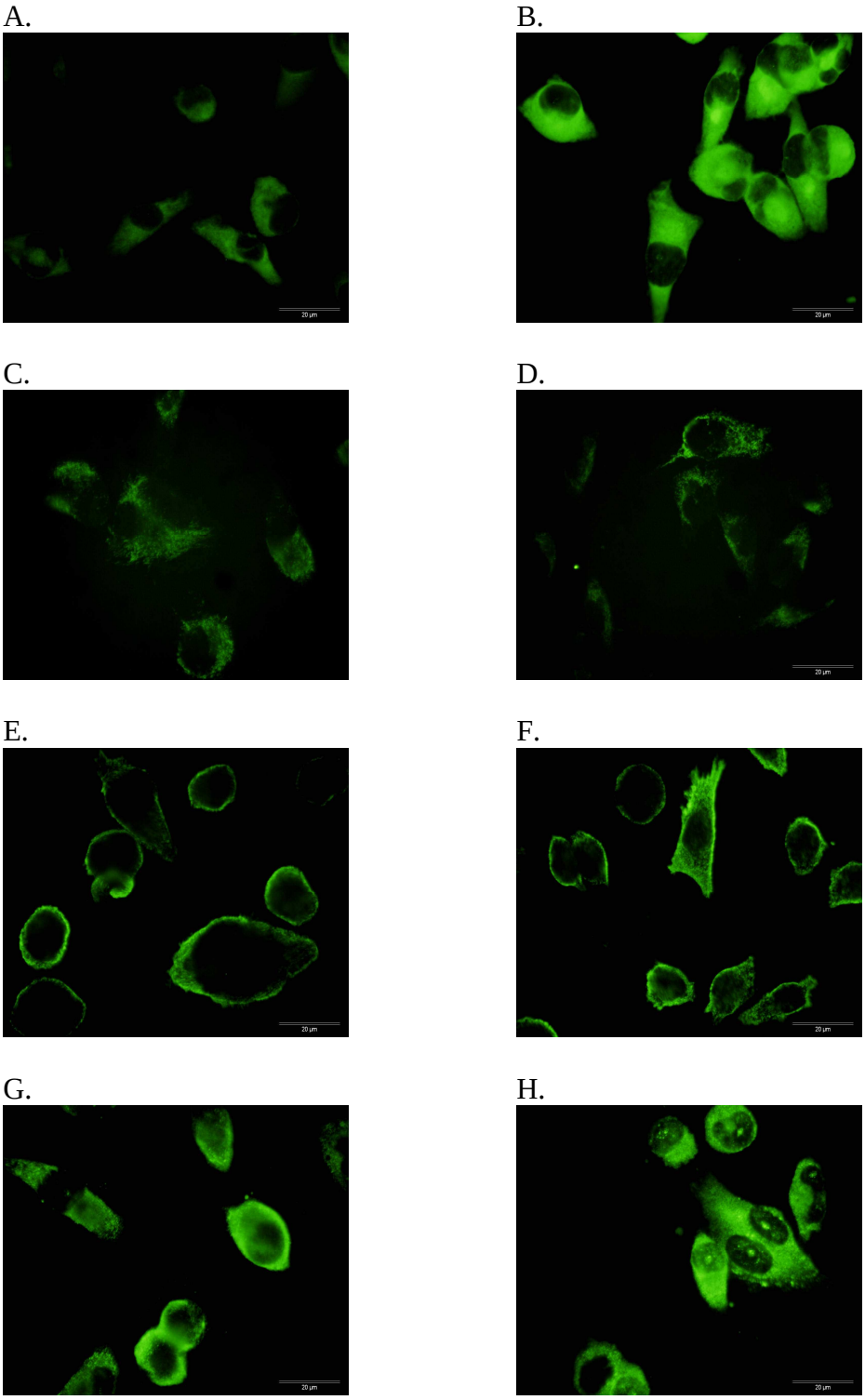

Figure 3.3.4: - Immunofluorescence analysis of MiaPaCa-2 clone 8 (A, C, E & G) and MiaPaCa-2 clone 3 (B, D, F & H) stained with MAbs 3E2 (A, B), 7B7 (C, D), 8F4 (E, F) and 9D6 (G, H). Magnification, 40X. Scale bar, 20µm.

3.4 Investigation of Functional Effect of MAb 7B7 G5 (2) in Invasive Cancer Models *In Vitro.*

MAb 7B7 G5 (2) underwent further testing to observe its effects on a number of cellular processes, including:

- Proliferation: to observe what effect the MAb has on the cancer cells ability to grow.
- Invasion & Motility: to assess the MAb's effect on cellular invasion/motility
- Adhesion: to assess the MAb's impact on the adhesive abilities of a number of cell lines to ECM proteins
- Anoikis: Anoikis is a specific form of apoptosis induced by the loss or alteration of cell-cell or cell-matrix anchorage. An *in vitro* anoikis assay was used to assess any impact this MAb has on anoikis resistance.
- MMP activity: to observe what effect, if any, this MAb has on the activity of MMP-2 and MMP-9 *in vitro*.
- Cell Morphology: to observe if incubation with this MAb affects the morphology of invasive cancer cells. Highly invasive cells usually display a spindle shaped elongated morphology.

3.4.1 MAb 7B7 G5 (2) Effect on Proliferation on the Invasive Pancreatic Cell Line MiaPaCa-2 clone 3

The primary goal of this work was to examine the effects of MAb 7B7 G5 (2) on invasion and motility. To ensure that any changes observed in the assays were not secondary to effects on cell proliferation or survival, initial experiments were carried out to determine the effects MAb 7B7 G5 (2) had on proliferation/survival of the MiaPaCa-2 clone 3 cell line. Proliferation assays were carried out as described in section 2.4.

Figure 3.4 shows that MAb 7B7 G5 (2) had no impact on MiaPaCa-2 clone 3 cell proliferation/survival after a 5 day growth assay. This suggests that the MAb has no toxic, growth inhibitory or stimulatory effect on this cell line over the course of the assay.

Statistical analyses were carried out on the average absorbancy readings of the control Vs test wells, over biological triplicates.

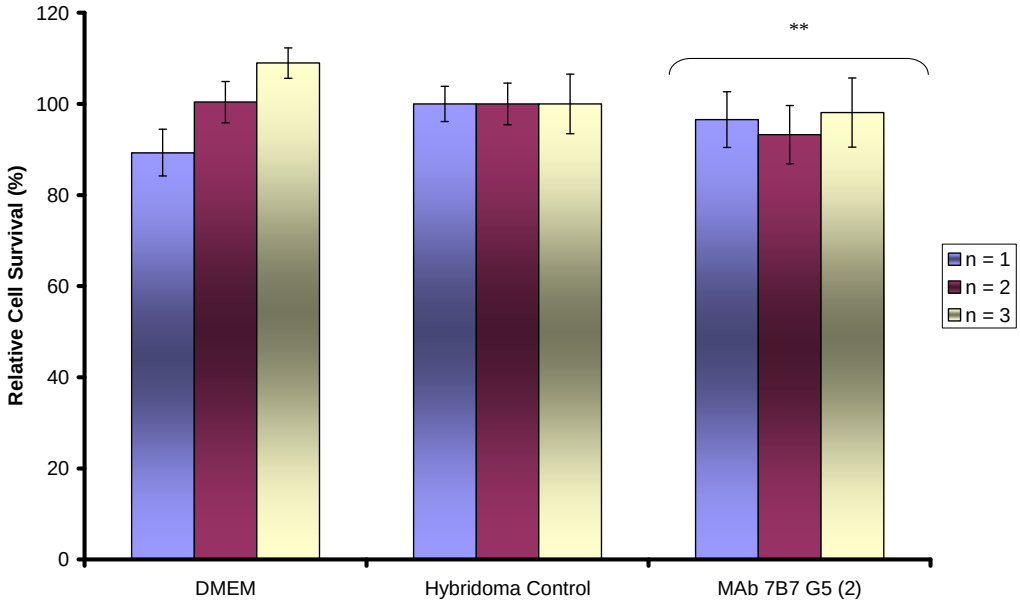

Figure 3.4: - Histogram of MAb 7B7 G5 (2) showing negligible inhibition of proliferation compared to control hybridoma medium (no MAb) representing 100% proliferation, after 96 hours. Statistics; * $p \leq 0.05$, ** $p \leq 0.01$, *** $p \leq 0.005$, Student's t-test. n = 3. Error bars calculated using ± standard deviation.

3.4.2 MAb 7B7 G5 (2) Effect on Invasion on Invasive Cancer Cell Lines

In order to ascertain what effect MAb 7B7 G5 (2) has on cell invasion and motility, Invasion and Motility assays were carried out (as described in section 2.5.2 & 2.5.3.) on a range of invasive cancer cell lines. Cells were incubated with the MAb, and after 24-48 hrs, depending on the cell line, levels of cellular invasion/motility were quantified.

Figure 3.4.2 shows that MAb 7B7 G5 (2) significantly inhibited invasion in the MiaPaCa-2 clone 3 cell line. A dose response was also observed (MAb diluted 1:2). However, no such inhibition was noted with the BxPc-3 cell line. Significant inhibition of invasion was also observed in the H1299 and DLKP-M lung cancer cell lines, the MiaPaCa-2 clone 3 pancreatic cell line, the MDA-231 and SKBR-3 cell lines, the SNB-19 glioma cell line and the HCT-116 colon cell line. Inhibition of invasion was also observed in the Lox IMVI melanoma cell line, and the DLKP-I lung cancer cell line. No inhibition was observed in the MDA-MB-157 breast cell line, the BxPc-3 pancreatic cell line or the C/68 prostate cell line. These results indicate that MAb 7B7 G5 (2) can successfully inhibit the invasion process in a number of cell types.

Figure 3.4.3 shows that MAb 7B7 G5 (2) significantly reduces cell motility in the MiaPaCa-2 clone 3 cell line, by levels similar to those seen the invasion assay. A dose response is also observed in this assay. Motility assays carried out on the SNB-19 glioma cell line (Figure 3.4.8) show that MAb 7B7 G5 (2) does not significantly reduce motility in this cell line. This may indicate that the inhibition of invasion observed with this MAb is unrelated to inhibition of cell motility.

Statistical analyses were carried out with the average cell counts of control Vs sample inserts over biological triplicates (section 2.15).

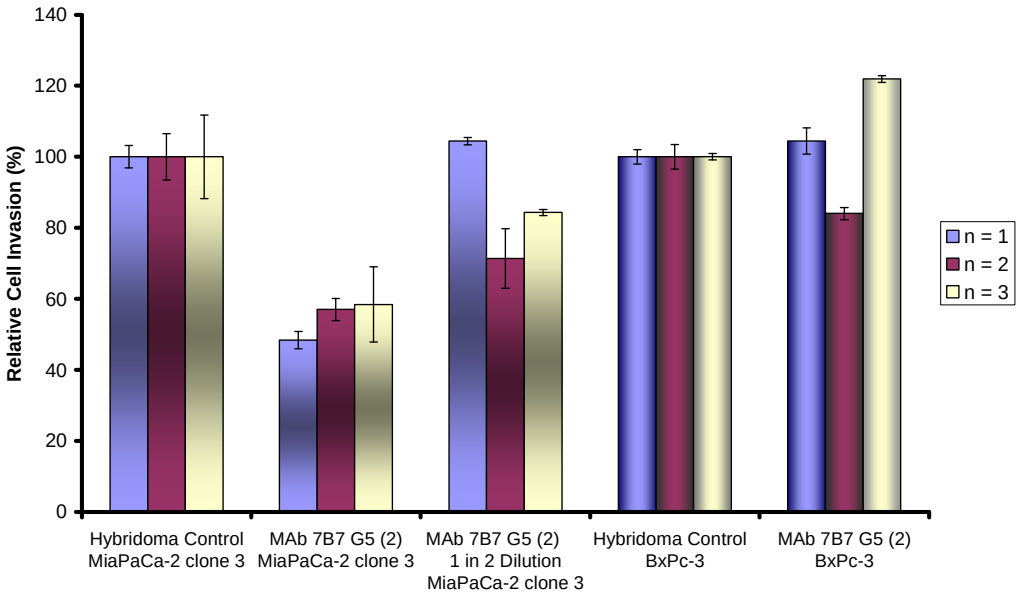

Figure 3.4.1: - Histogram of MAb 7B7 G5 (2) showing inhibition of invasion in MiaPaCa-2 clone 3, but little/no inhibition in BxPc-3 compared to control hybridoma medium (no MAb) representing 100% invasion, after 48 hours.

A dose response inhibitive effect is also observed in the MiaPaCa-2 clone 3 cell line, with 1:2 dilutions of MAb inhibiting invasion by up to 28.7% compared to control hybridoma medium (no MAb). Statistics; * $p \leq 0.05$, ** $p \leq 0.01$, *** $p \leq 0.005$, Student's t-test. $n = 3$. Error bars calculated using ± standard deviation.

Hybridoma Medium Control *MAb 7B7 G5 (2)*

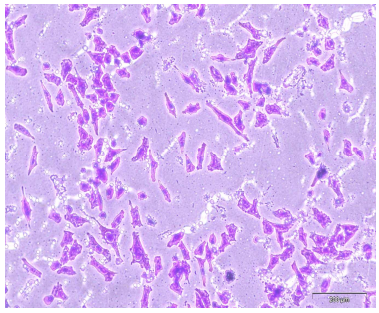

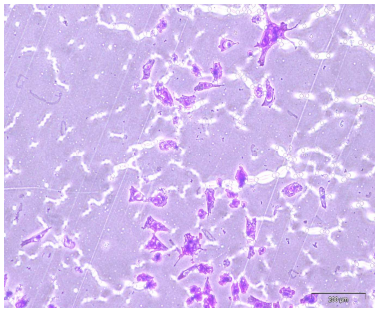

MiaPaCa-2 clone 3

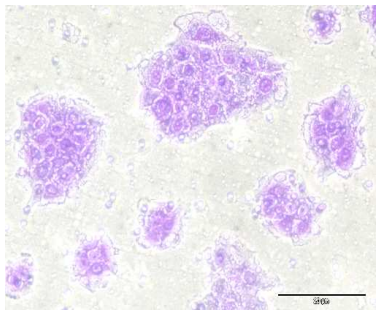

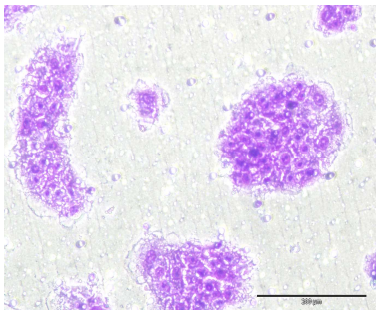

BxPc-3

Figure 3.4.2: - Representative photomicrographs showing invasion status of MiaPaCa-2 clone 3 cells following incubation with MAb 7B7 G5 (2). A decrease in invasion can be observed following addition of MAb 7B7 G5 (2) (b) compared to control insert (a) (no antibody supernatant). Magnification, 100X. Scale Bar, 200µm

3.4.3 MAb 7B7 G5 (2) Effect on Motility on the Pancreatic Cell Line MiaPaCa-2 clone 3

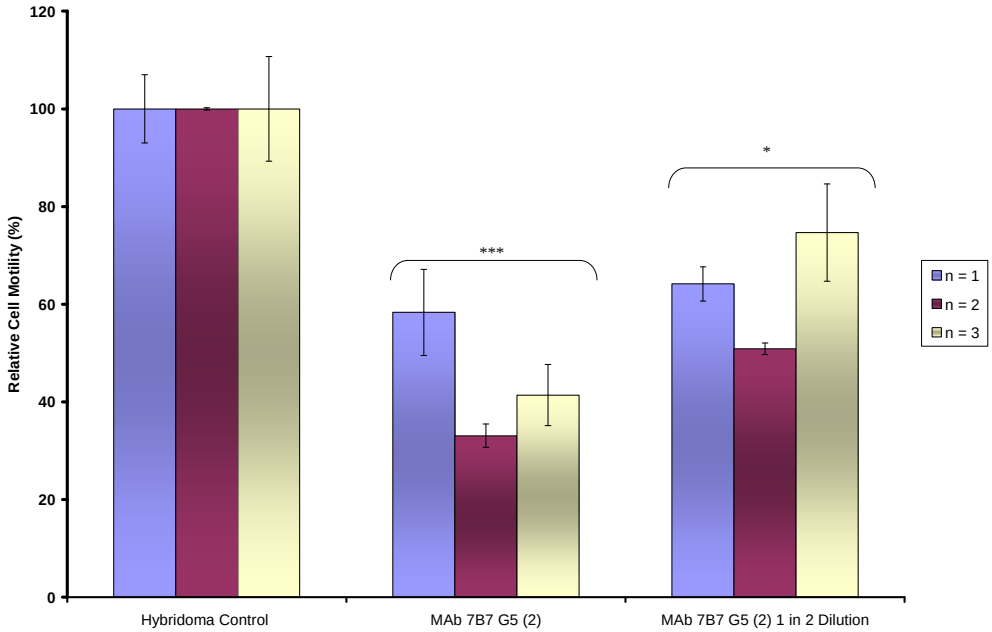

Hybridoma Medium Control

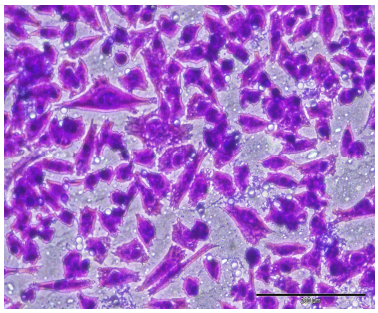

MAb 7B7 G5 (2)

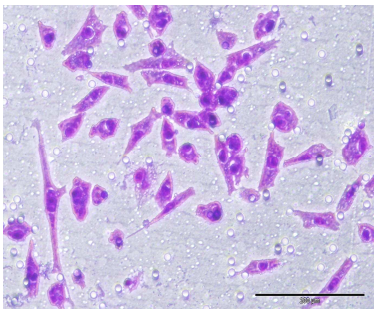

Figure 3.4.3 - Histogram and representative photomicrographs of MAb 7B7 G5 (2) showing significant inhibition of motility compared to control hybridoma medium (no MAb) representing 100% motility, after 24 hours.

A significant dose response inhibitive effect is also observed on all dates with 1:2 dilutions of the MAb showing less inhibition compared to control hybridoma medium (no MAb). Statistics; * $p \leq 0.05$, ** $p \leq 0.01$, *** $p \leq 0.005$, Student's t-test. $n = 3$. Error bars calculated using ± standard deviation. Magnification, 200X. Scale Bar, 200µm.

3.4.4 MAb 7B7 G5 (2) Effect on Invasion on the Large-Cell Lung Cancer Cell Line H1299 and Invasive Variants of NSCLC DLKP, DLKP-I & DLKP-M

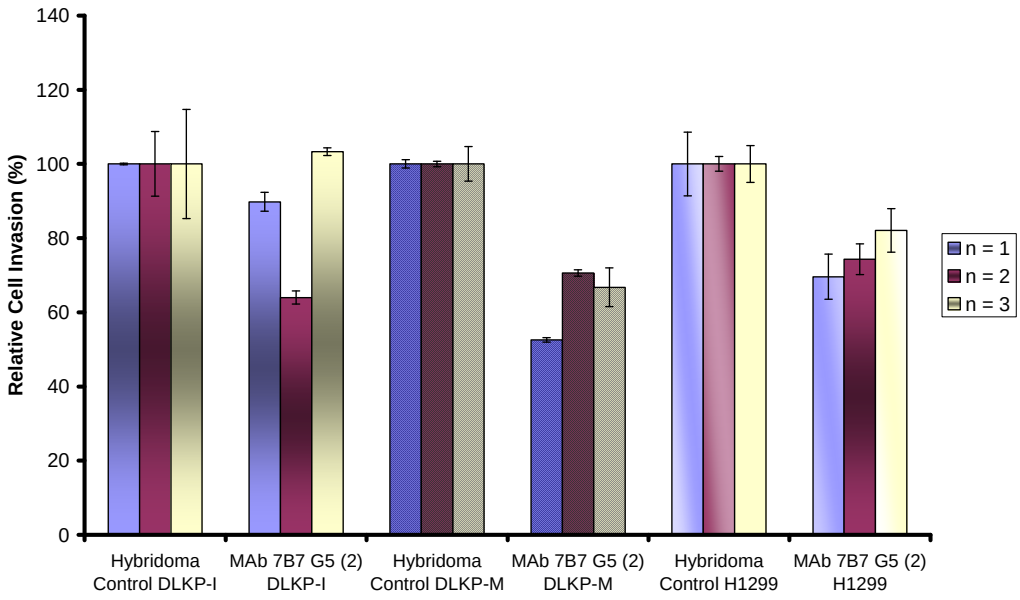

Figure 3.4.4: - Histogram of MAb 7B7 G5 (2) showing inhibition of invasion in DLKP-I, DLKP-M and H1299 compared to control hybridoma medium (no MAb) representing 100% invasion after 24 hours. Inhibition of invasion observed in the DLKP-I cell line did not reach statistical significance. Statistics; * $p \leq 0.05$, ** $p \leq 0.01$, *** $p \leq 0.005$, Student's t-test. $n = 3$. Error bars calculated using ± standard deviation.

Hybridoma Medium Control *MAb 7B7 G5 (2)*

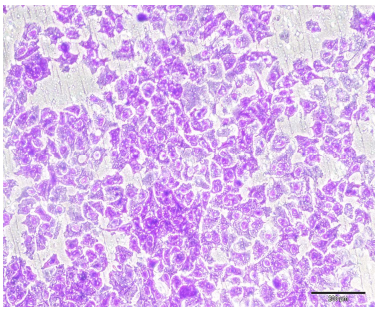

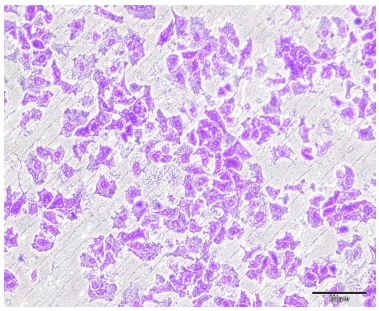

DLKP-I

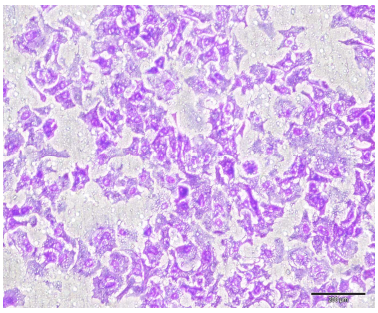

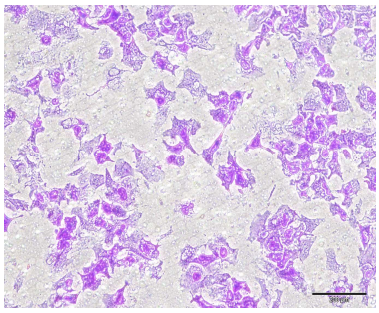

DLKP-M

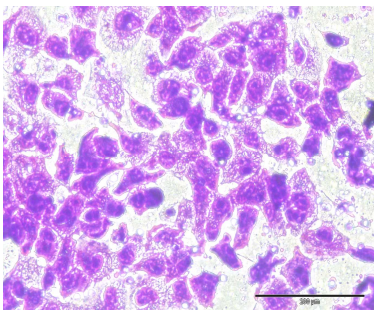

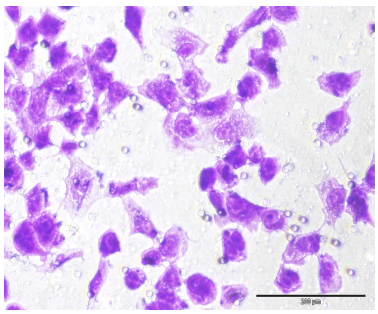

H1299

Figure 3.4.5: - Representative photomicrographs showing invasion status of DLKP-I, DLKP-M and H1299 cells following incubation with MAb 7B7 G5 (2). A decrease in invasion can be observed following addition of MAb 7B7 G5 (2) (b) compared to control insert (a) (no antibody supernatant) in all three cell lines. Magnification, 100X. Scale Bar, 200µm.

3.4.5 MAb 7B7 G5 (2) Effect on Invasion on the NSCLC DLKP-M: - Dose Response

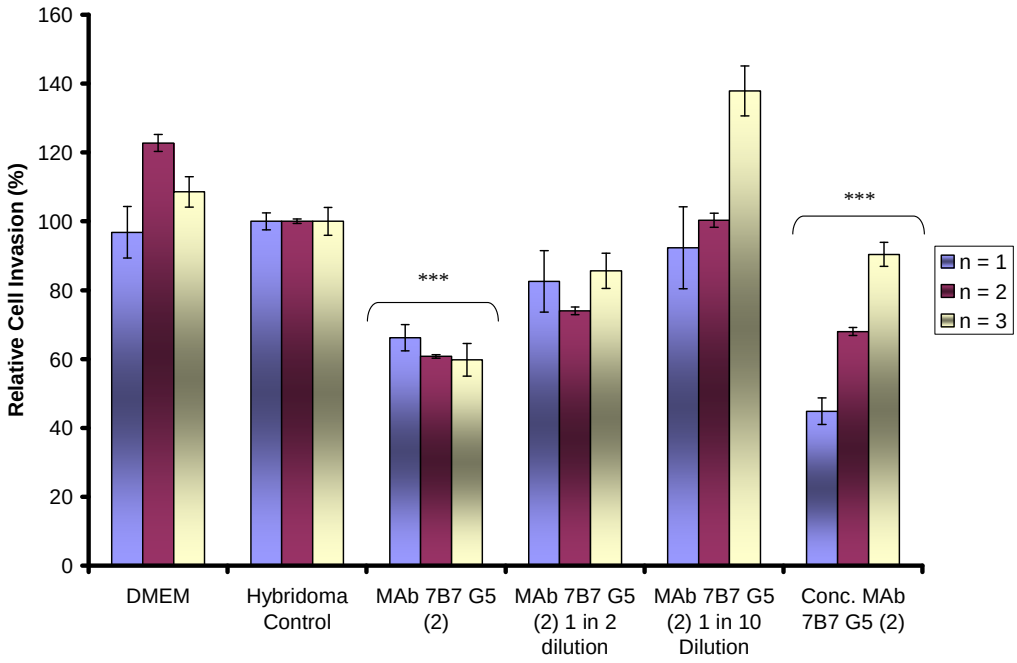

Figure 3.4.6: - Histogram of MAb 7B7 G5 (2) showing significant inhibition of invasion compared to control hybridoma medium (no MAb) representing 100% invasion) after 24 hours. Statistics; * $p \leq 0.05$, ** $p \leq 0.01$, *** $p \leq 0.005$, Student's t-test. *n = 3.* Error bars calculated using ± standard deviation.

A dose response inhibitive effect is also observed with 1:2 and 1:10 dilutions of the MAb showing less inhibition compared to MAb 7B7 G5 (2). A slight dose response with concentrated MAb (concentrated 2x using Millipore Ultrafree-15 centrifuge filter units) is also observed on one date (63.2% inhibition of invasion compared to control hybridoma medium (no MAb) representing 100% invasion).

3.4.6 MAb 7B7 G5 (2) Effect on Invasion on the Invasive, Triple Negative Breast cancer Cell Lines MDA-MB-231, MDA-MB-157 and the HER-2 Over Expressing Breast Cell Line, SKBR-3

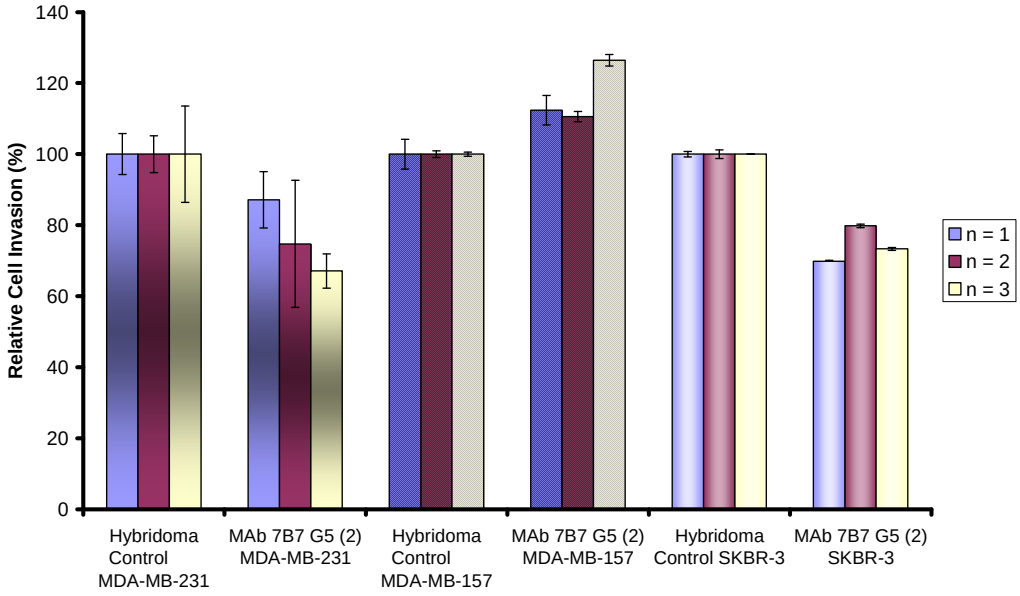

Figure 3.4.7: - Histogram of MAb 7B7 G5 (2) showing inhibition of invasion in MDA-MB-231, SKBR-3, but an increase in invasion in MDA-MB-157, compared to control hybridoma medium (no MAb) representing 100% invasion, after 24 hours. Statistics; * $p \leq 0.05$, ** $p \leq 0.01$, *** $p \leq 0.005$, Student's t-test. *n = 3.* Error bars calculated using ± standard deviation.

Hybridoma Medium Control *MAb 7B7 G5 (2)*

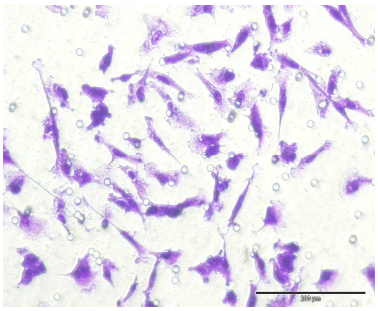

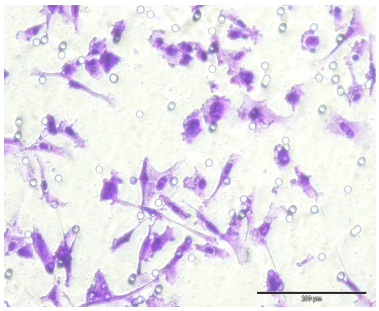

MDA-MB-231

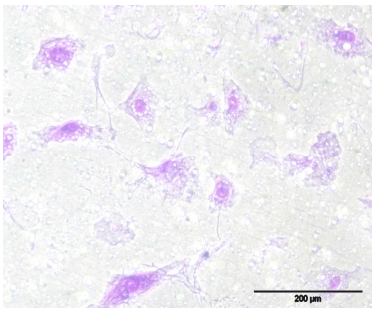

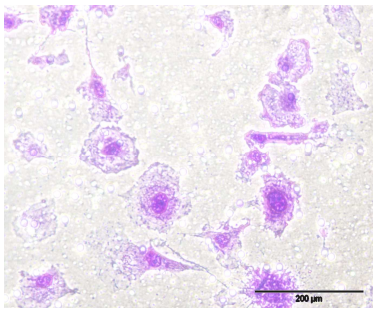

MDA-MB-157

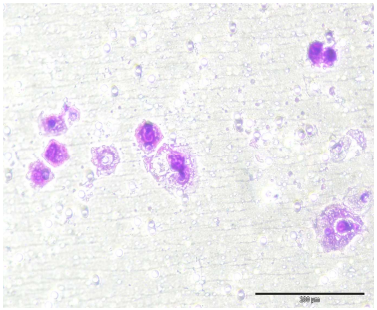

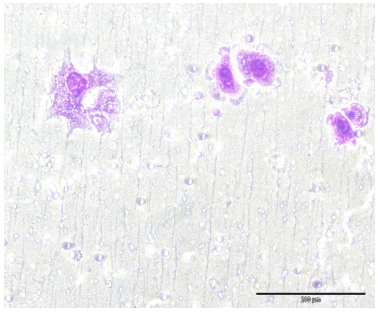

SKBR-3

Figure 3.4.8: - Representative photomicrographs showing invasion status of MDA-MDA-231 MDA-MB-157 and SKBR-3 cells following incubation with MAb 7B7 G5 (2). A decrease in invasion can be observed following addition of MAb 7B7 G5 (2) (b) compared to control insert (a) (no antibody supernatant) in the MDA-MB-231 and SKBR-3 cell lines. However, a slight increase in invasion is observed in the MDA-MB-157 cell line. Magnification, 100X. Scale Bar, 200µm.

3.4.7 MAb 7B7 G5 (2) Effect on Invasion on the Invasive Glioma Cell Line SNB-19.

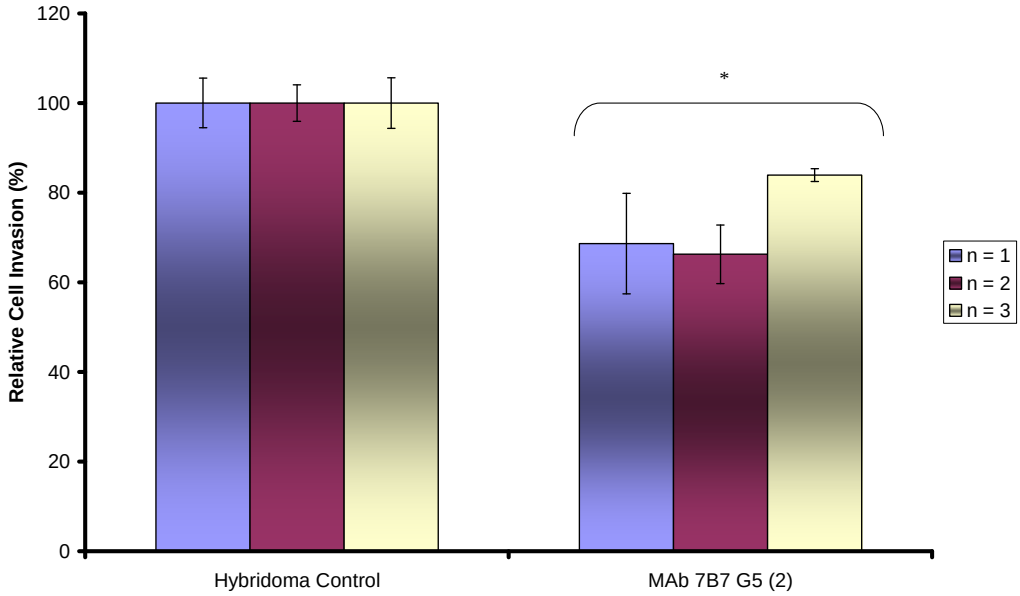

Hybridoma Medium Control

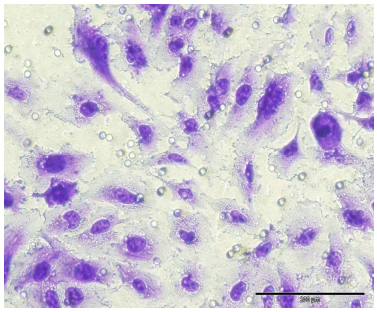

MAb 7B7 G5 (2)

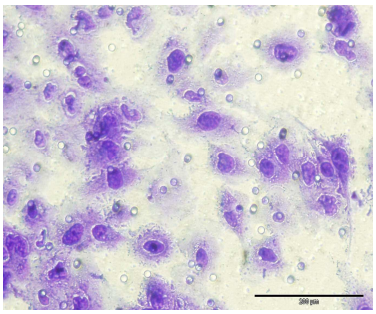

Figure 3.4.9: - Histogram and representative photomicrographs of MAb 7B7 G5 (2) showing significant inhibition of invasion compared to control hybridoma medium (no MAb) representing 100% invasion, after 24 hours. Statistics; * $p \leq 0.05$, ** $p \leq 0.01$, *** $p \leq 0.005$, Student's t-test. *n = 3.* Error bars calculated using ± standard deviation. Magnification, 100X. Scale Bar, 200µm.

3.4.8 MAb 7B7 G5 (2) Inhibition of Motility on Invasive Glioma Cell Line SNB-19

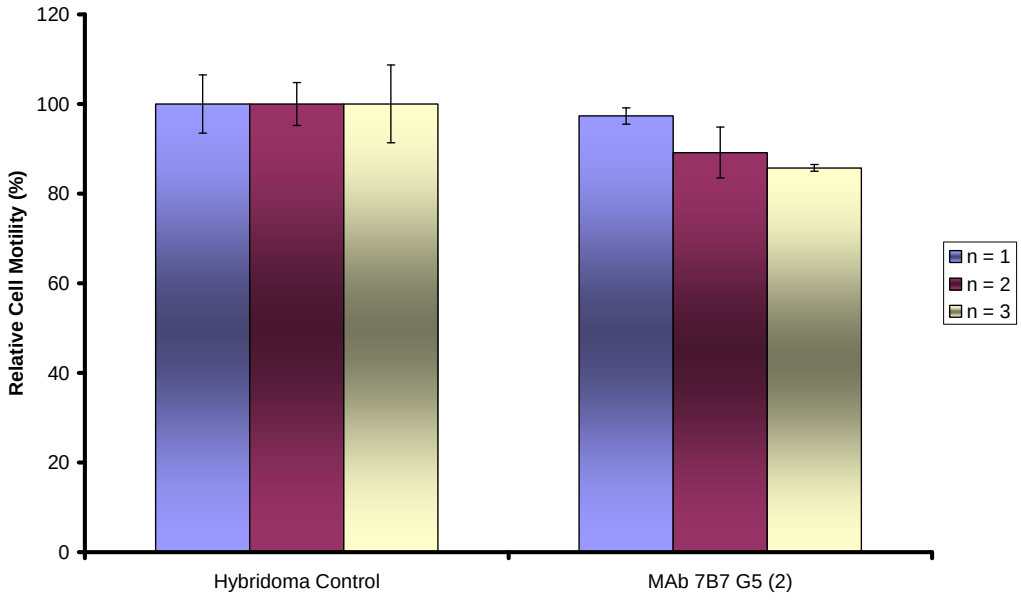

Hybridoma Medium Control

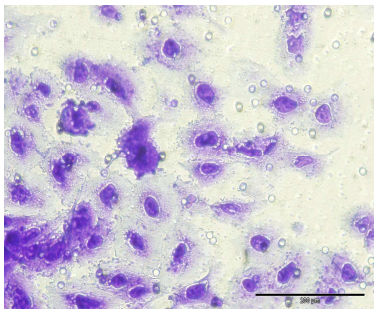

MAb 7B7 G5 (2)

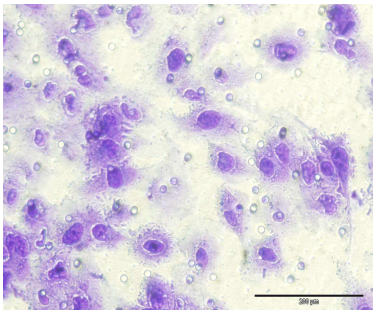

Figure 3.4.10 - Histogram and representative photomicrographs of MAb 7B7 G5 (2) showing inhibition of motility compared to control hybridoma medium (no MAb) representing 100% motility, after 24 hours. Inhibitive effect did not reach statistical significance. Statistics; * $p \leq 0.05$, ** $p \leq 0.01$, *** $p \leq 0.005$, Student's t-test. $n = 3$. Error bars calculated using ± standard deviation. Magnification, 100X. Scale Bar, 200µm.

3.4.9 MAb 7B7 G5 (2) Effect on Invasion on the Invasive Melanoma Cell Line Lox IMVI

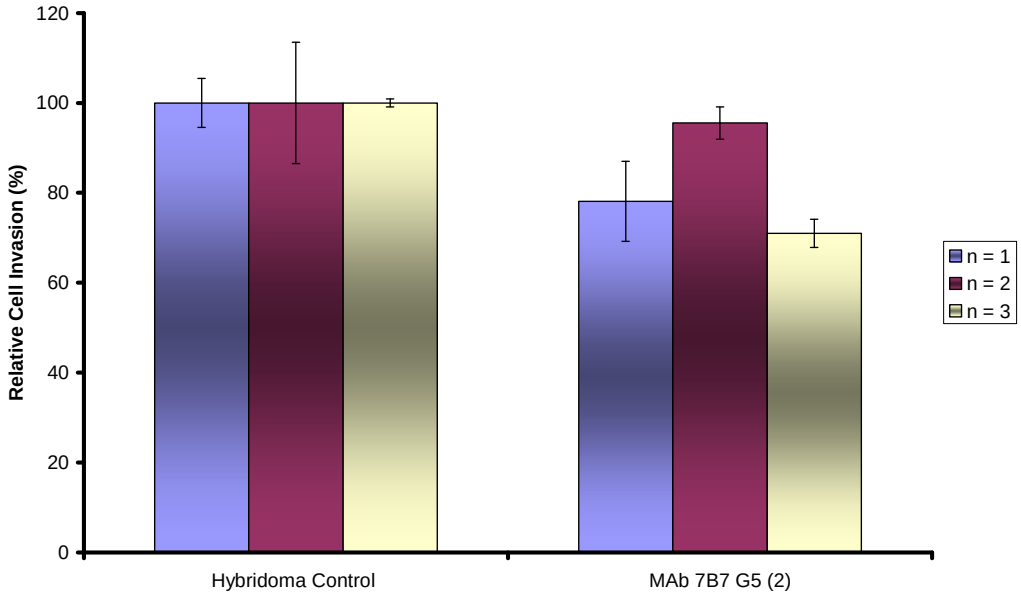

Hybridoma Medium Control

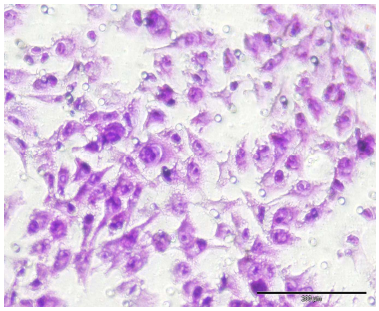

MAb 7B7 G5 (2)

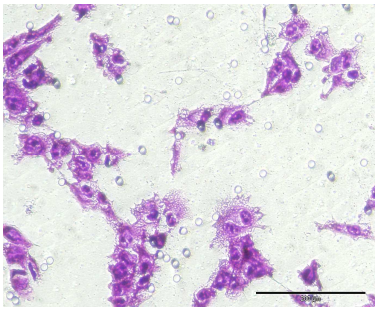

Figure 3.4.11: - Histogram and and representative photomicrographs of MAb 7B7 G5 (2) showing inhibition of invasion compared to control hybridoma medium (no MAb) representing 100% invasion, after 24 hours. Inhibitive effect did not reach statistical significance. Statistics; * $p \leq 0.05$, ** $p \leq 0.01$, *** $p \leq 0.005$, Student's t-test. *n = 3.* Error bars calculated using ± standard deviation. Magnification, 100X. Scale Bar, 200µm.

3.4.10 MAb 7B7 G5 (2) Effect on Invasion on the Invasive Prostate Cell line C/68

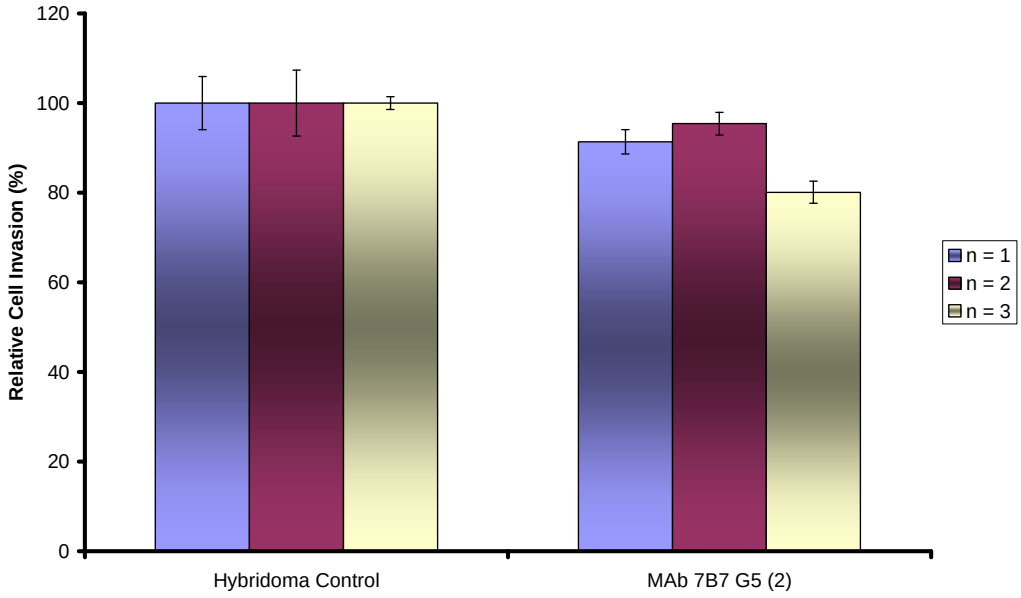

Hybridoma Medium Control

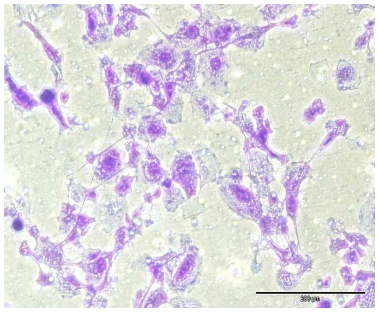

MAb 7B7 G5 (2)

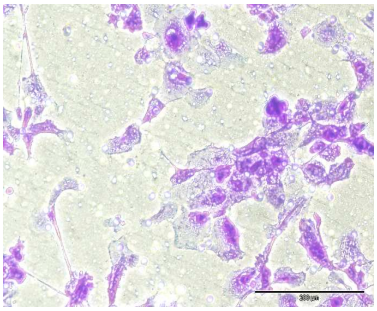

Figure 3.4.12: - Histogram and representative photomicrographs of MAb 7B7 G5 (2) showing inhibition of invasion compared to control hybridoma medium (no MAb) representing 100% invasion, after 24 hours. Inhibitive effect did not reach statistical significance. Statistics; * $p \leq 0.05$, ** $p \leq 0.01$, *** $p \leq 0.005$, Student's t-test. $n = 3$. Error bars calculated using ± standard deviation. Magnification, 100X. Scale Bar, 200µm.

3.4.11 MAb 7B7 G5 (2) Effect on Invasion on the Invasive Colorectal Cell line HCT-116

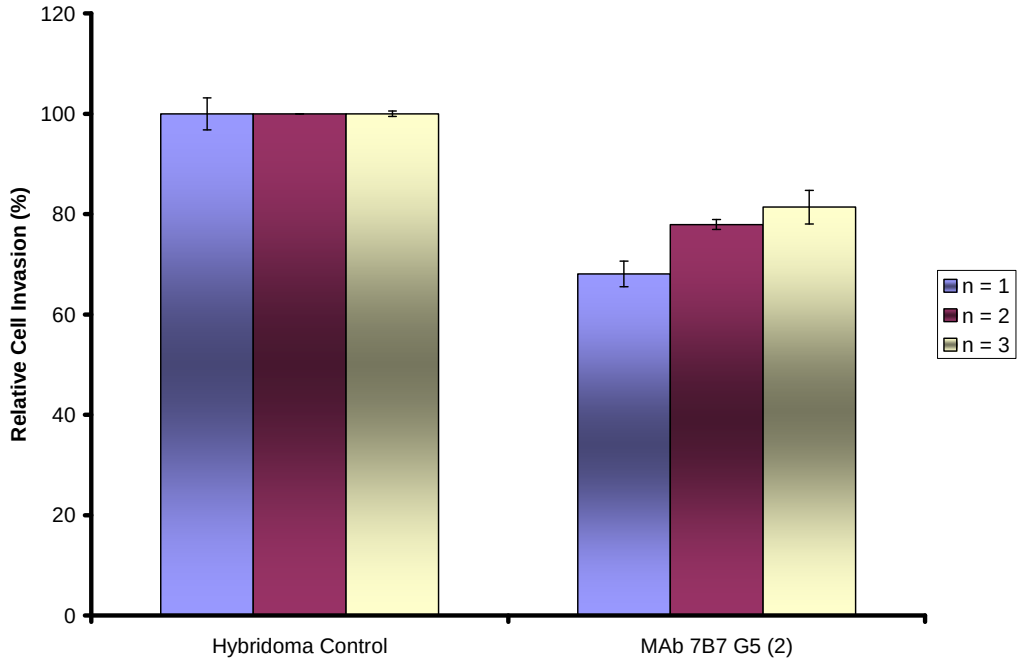

Hybridoma Medium Control *MAb 7B7 G5 (2)*

Figure 3.4.13: - Histogram and representative photomicrographs of MAb 7B7 G5 (2) showing inhibition of invasion compared to control hybridoma medium (no MAb) representing 100% invasion, after 24 hours. Statistics; * $p \leq 0.05$, ** $p \leq 0.01$, *** $p \leq 0.005$, Student's t-test. *n = 3.* Error bars calculated using ± standard deviation. Magnification, 100X. Scale Bar, 200µm.

Cancer Type	Cell Line	Mean Inhibition Levels	P value
Breast	MDA-MB-157	11.4% *increase*	0.67
	MDA-MD-231	23%	0.16
	SKBR-3	25.6%	0.22
Lung	DLKP-I	12.9%	0.57
	DLKP-M	32.2%	0.22
	H1299	30.6%	0.08
Pancreatic	MiaPaCa-2 clone 3	45.4%	0.33
	BxPc-3	3.4% *increase*	0.64
Melanoma	Lox IMVI	18.47%	0.71
Glioma	SNB-19	27%	0.02
Prostate	C/68	11%	0.7
Colon	HCT-116	24.2%	0.11

Table 3.4: - Effect of MAb 7B7 G5 (2) on invasion levels in a panel of cell lines.

3.4.12 MAb 7B7 G5 (2) Effect on Adhesion to Fibronectin & Matrigel on the Invasive Pancreatic Cancer Cell Line MiaPaCa-2 clone 3

Adhesion assays were carried out in order to investigate what effect MAb 7B7 G5 (2) had on the ability of cancer cells to attach to ECM proteins. Adhesion to ECM proteins, especially fibronectin represents an important step in metastasis (Shaw *et al*., 1996). The effect of the MAb on the ability of MiaPaCa-2 clone 3 cells to adhere to fibronectin was investigated, as was the ability of DLKP-M cells to adhere to matrigel in the presence of the MAb. Adhesion assays were performed as described in section 2.5.4

In Figure 3.4.12, MAb 7B7 G5 (2) reduced adhesion of MiaPaCa-2 clone 3 cells to fibronectin *in vitro* was observed. A significant decrease in adherence of DLKP-M cells to matrigel was also observed (Figure 3.4.13). These results indicate that MAb 7B7 G5 (2) can interfere with the ability of cancer cells to attach to components of the ECM.

Statistical analyse were carried out on the average absorbancy reading of control Vs sample wells over biological triplicates.

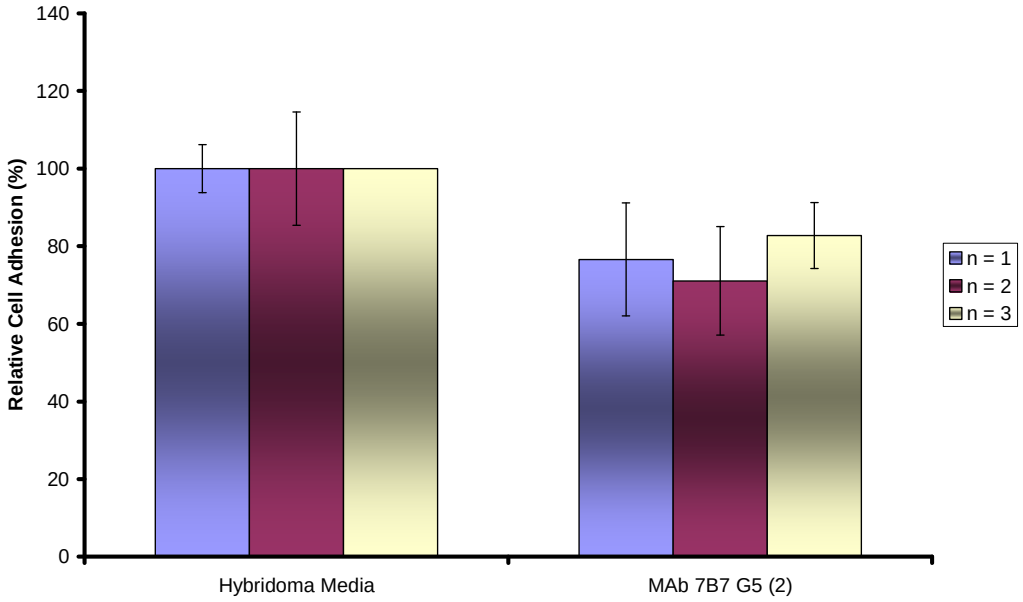

Figure 3.4.14: - Adhesion of MiaPaCa-2 clone 3 to ECM protein, fibronectin. Results are expressed as percentage adhesion to fibronectin in the presence of MAb 7B7 G5 (2), compared to adhesion to fibronectin in the presence of control hybridoma medium (no MAb). Cells grown in the presence of MAb 7B7 G5 (2) for 24 hrs, showed a decrease in adhesion to fibronectin. Statistical significance was not achieved. Statistics; * $p \leq 0.05$, ** $p \leq 0.01$, *** $p \leq 0.005$, Student's t-test. *n = 3.* Error bars calculated using ± standard deviation.

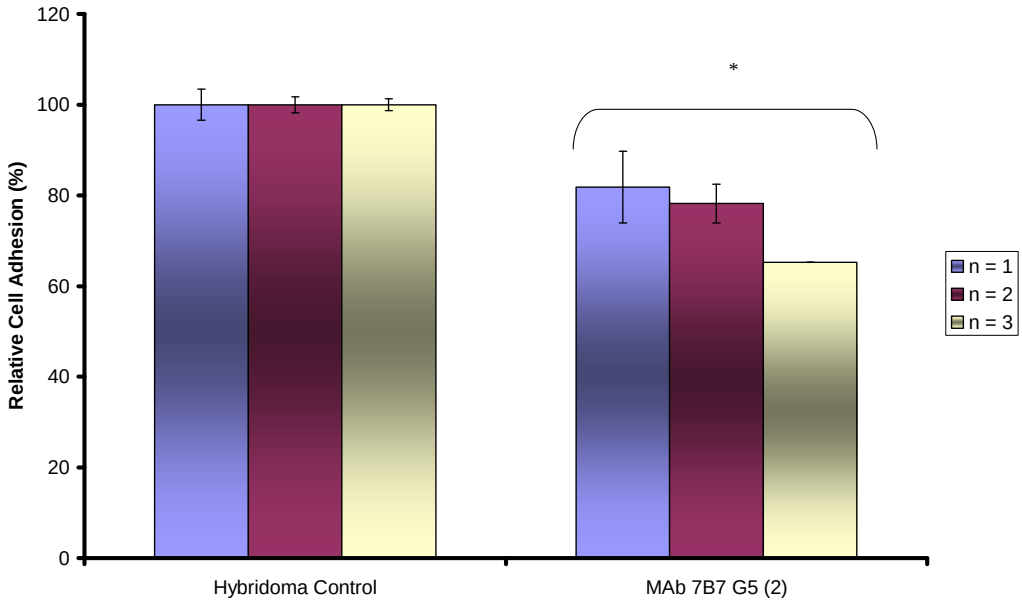

Figure 3.4.15: - Adhesion of DLKP-M to extracellular matrix protein, matrigel. Results are expressed as percentage adhesion to matrigel in the presence of MAb 7B7 G5 (2), compared to adhesion to matrigel in the presence of control hybridoma medium (no MAb). Cells grown in the presence of MAb 7B7 G5 (2) for 24 hrs, showed a significant decrease in adhesion to matrigel. Statistics; * $p \leq 0.05$, ** $p \leq 0.01$, *** $p \leq 0.005$, Student's t-test. *n = 3.* Error bars calculated using ± standard deviation.

3.4.13 MAb 7B7 G5 (2) Effect on Anoikis on the Invasive Pancreatic Cancer Cell Line MiaPaCa-2 clone 3 and on the Invasive NSCLC DLKP-M Cell Line

To determine whether MAb 7B7 G5 (2) effects anoikis resistance *in vitro*, Anoikis assays were carried out on the MiaPaCa-2 clone 3 and DLKP-M cell lines. Anoikis is a specific form of apoptosis induced by the loss or alteration of cell-cell or cell-matrix anchorage. MiaPaCa-2 clone 3 has been shown to have a high level of anoikis resistance (Walsh *et al*., 2009), while DLKP-M has been shown to be 50% resistant to anoikis (Dr. Keenan, NICB, unpublished results). In this study, the effect of MAb 7B7 G5 (2) on the above cell lines growing in anoikis-inducing conditions was investigated. Anoikis assays were carried out as described in section 2.6.

Figure 3.4.14 shows that MAb 7B7 G5 (2) has little/no effect on the cells when there are growing in Anoikis-inducing conditions. The cells do not display any increased or decreased levels of anoikis resistance, indicating that MAb 7B7 G5 (2) does not effect this cellular process.

Statistical analyse were carried out on the average absorbancy reading of control Vs sample wells over biological triplicates.

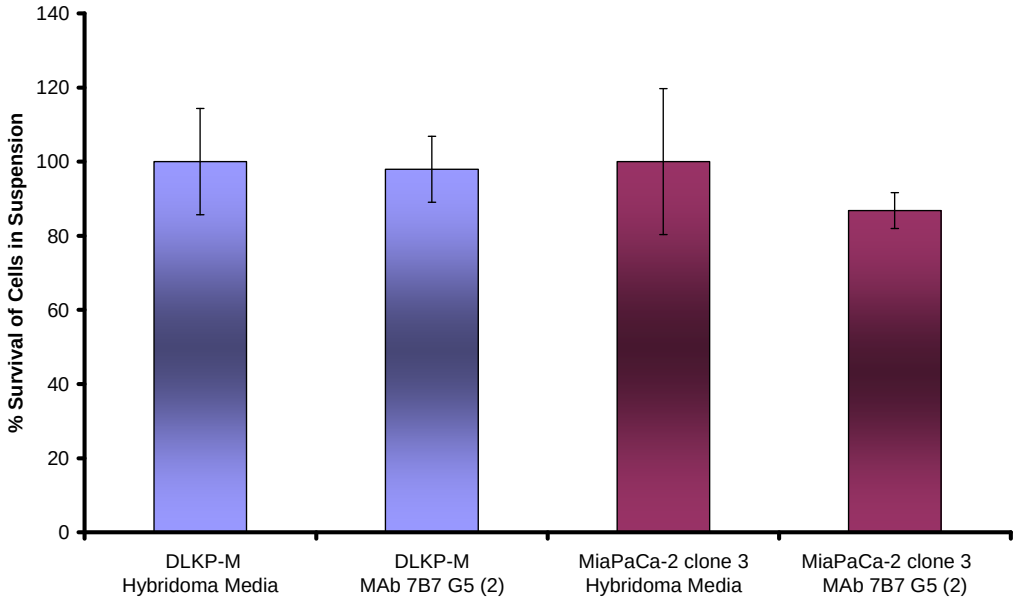

Figure 3.4.16: - Representative histogram showing percentage survival of non-adherent cells (24 hrs poly-HEMA treated plastic). The presence of MAb 7B7 G5 (2) has a slight effect on cell survivability when compared to cells growing in the presence of hybridoma medium (no MAb). Statistical significance was not achieved in this experiment. Data shown is mean ± standard deviation (n = 3).

3.4.14 Morphological Change of MiaPaCa-2 clone 3 Cells Incubated with MAb 7B7 G5 (2)

MiaPaCa-2 clone 3 cells display an elongated, splindle-like morphology, which is associated with an invasive phenotype. To investigate whether MAb 7B7 G5 (2) effects cell morphology, MiaPaCa-2 clone 3 cells were incubated with the MAb for 24hrs, after which, cell morphology was observed. This assay was carried out as described in section 2.8.

Figure 3.4.15 shows the effect MAb 7B7 G5 (2) has on the MiaPaCa-2 clone 3 cells, compared to cells grown in the absence of the MAb. It is quite clear that the cells have lost their elongated, spindle-like shape, and exhibit a more rounded appearance, similar to the less invasive MiaPaCa-2 clone 8 cell morphology. As a spindle-like cell morphology has been linked to cell invasion (Yilmaz *et al*., 2007), this change may indicate that the invasive capabilities of the MiaPaca-2 clone 3 cells have been diminished following incubation with MAb 7B7 G5 (2).

A.

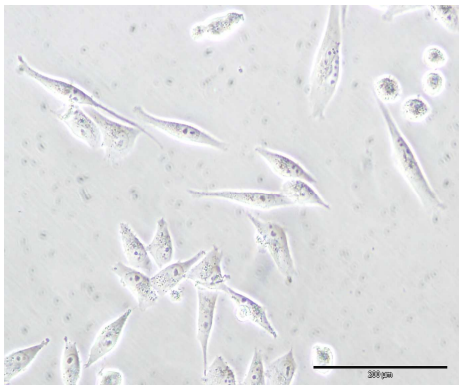

B.

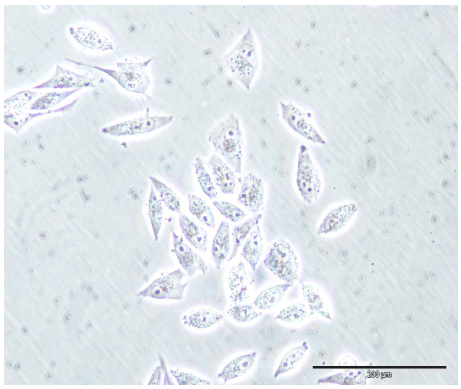

Figure 3.4.17: - Representative photomicrographs showing morphology of MiaPaCa-2 clone 3 cells following incubation with MAb 7B7 G5 (2). Cells incubated with MAb 7B7 G5 (2) (B) have lost their elongated, splindle-like morphology, which is associated with an invasive phenotype, and have become more rounded. Cells incubated with hybridoma media (A) retain their normal morphology. Magnification, 100X. Scale Bar, 200µm.

3.4.15 MAb 7B7 G5 (2) Effect on MMP Activity in the Invasive Breast Cancer Cell Line MDA-MB-231

Zymography assays were carried out in order to investigate the effect of MAb 7B7 G5 (2) has on MMP-9 expression. MMP-9 is involved in the degradation of proteins in the extracellular matrix and plays a crucial role in localised degradation of the basement membrane, and subsequent cellular invasion. MDA-MB-231 was chosen for this study, as it is known to express MMP-9 (Hegedus *et al*., 2008). Conditioned media from cells incubated with the MAb was collected, as described in section 2.7.1. This was then separated on a zymography gel, which was then subsequently stained. The zymography assay was carried out as described in section 2.7.2.

Figure 3.4.16 shows that MAb 7B7 G5 (2) greatly decreases the activity of active MMP-9 in the MDA-MB-231 cell line, when compared to cells grown in the absence of the MAb. This is also clearly observed in the zymography gel. This preliminary result indicates that MAb 7B7 G5 (2) inhibits the activity of MMP-9 *in vitro* (see Appendix VI for complete zymograpgy gel).

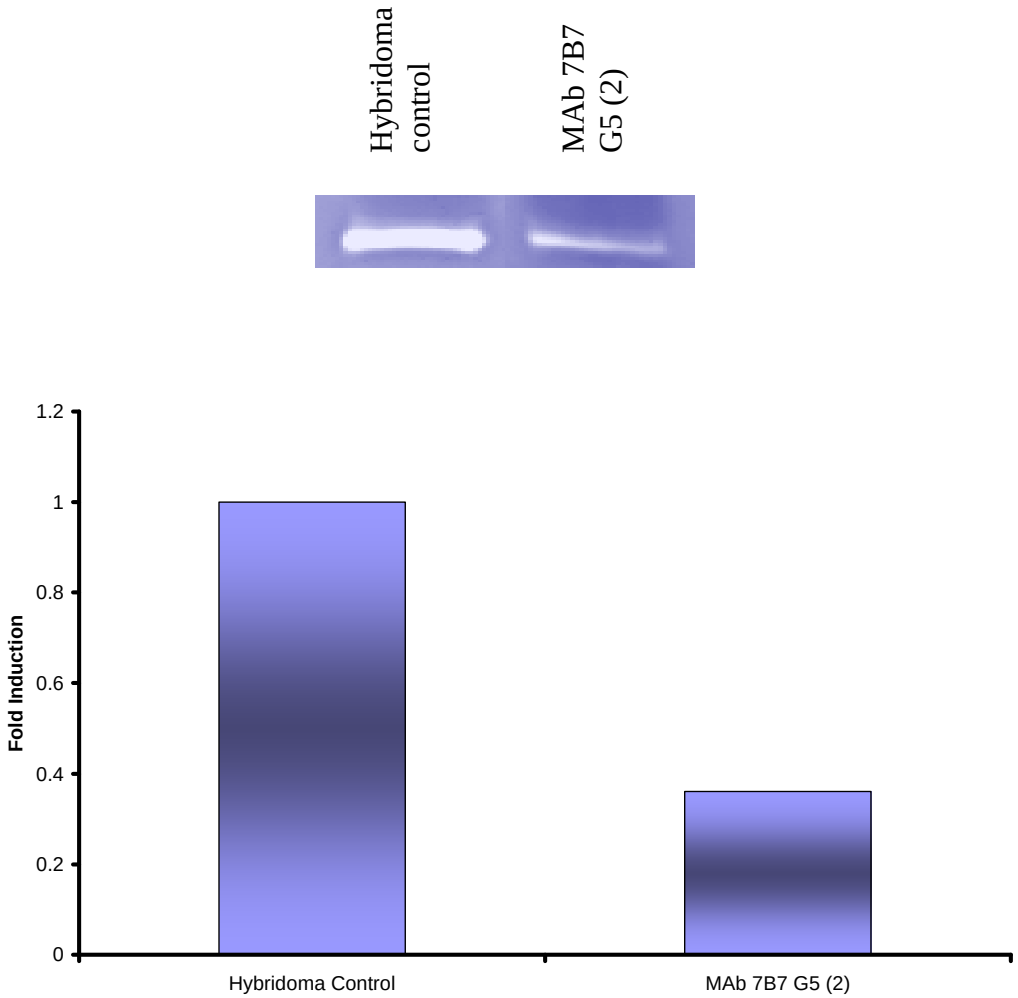

Figure 3.4.18: - Graph and zymography gel showing effect of MAb 7B7 G5 (2) on MMP-9 activity in the MDA-MB-231 breast cell line. Cells incubated with MAb 7B7 G5 (2) show a decrease in the activity of MMP-9 when compared to control hybridoma medium (no MAb) representing normal MMP-9 activity.

3.5 Immunofluorescence Studies of MAb 7B7 G5 (2) In a Panel of Cancer Cell Lines

A.

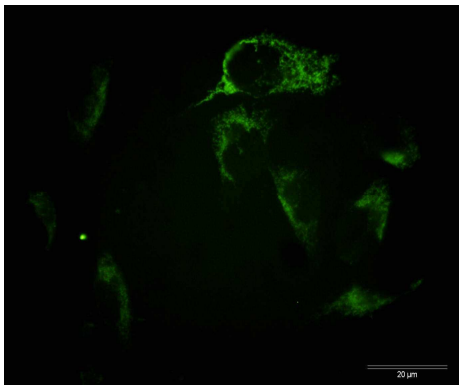

B.

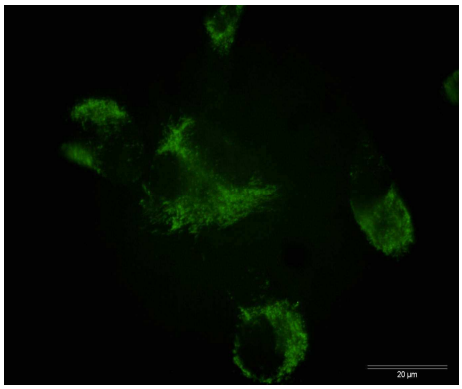

C.

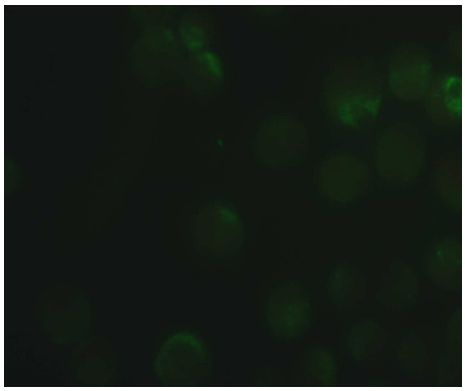

D.

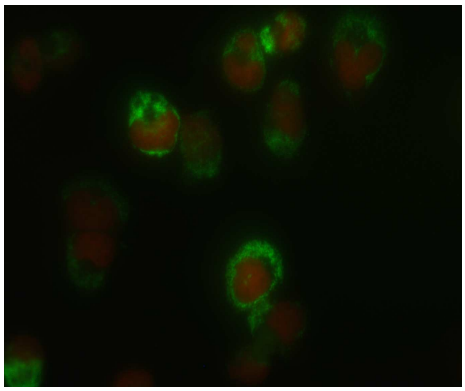

Figure 3.5: - Immunofluorescence analysis of MAb 7B7 G5 (2) on MiaPaCa-2 clone 3, clone 8 pancreatic cancer cells, and DLKP-SQ and a Mitoxantrone resistant variant, DLKP-Mitox-6p cancer cell lines (Joyce, H., unpublished). Cytoplasmic/membrane reactivity is observed in the invasive MiaPaCa-2 clone 3 cells (A), while less intense positivity is observed in MiaPaCa-2 clone 8 cells (B), which exhibit low levels of invasion. Intense reactivity with MAb 7B7 G5 (2) is observed in the invasive DLKP-Mitox-6p cell line (D), compared to the parental DLKP-SQ cell line (C), which exhibits low levels of invasion. Magnification, 630X (A & B), 400X (C & D). Scale Bar, 10µm , 20µm. (D counter stained with Propidium Iodide).

3.6 Western Blotting Analysis

Western blotting analysis of whole cell lysates of MiaPaCa-2 clone 3 cells, followed by probing with MAb 7B7 G5 (2) did not produce any specific reactive bands.

3.7 Immunoprecipitation Studies

In order to try and identify the target antigens, immunoprecipitation studies were carried out on a variety of cell lines. MiaPaCa-2 clone 3 was the primary cell line used, due to the initial invasion/motility assays carried out with that cell line. Protein-L agarose beads were used to pull out the reactive antigens from cell lysates of MiaPaCa-2 clone 3 cells for MAb 7B7 G5 (2). Following separation on 4-12% Bis-Tris SDS-PAGE, a number of bands were identified (Figure 3.1.12). These were compared to bands pulled out using control mouse IgM, and those bands only present with the 7B7 G5 (2) MAb were identified through liquid chromatography mass spectrometry (LC-MS) analysis (Dionex Ultimate 3000 LC system, LTQ-Orbitrap mass spectrometer), LC-MS sequencing using LCMS/LTQ mass spectrometry and TurboSEQUEST software using the human subset from the SWISS-PROT database.

Two different methods of immunoprecipitation were carried out in order to facilitate identification of the antigen of interest. The first method, termed Direct IP (section 2.11.1.), involves incubating the antibody/cell lysates complex with Protein-L agarose beads, then separating the solution, containing both antigen and antibody fragments, on SDS-PAGE. In the second method, known as Cross-Linked IP (section 2.11.2.), a purified form of the MAb (section 2.3.8) is covalently bound to the agarose beads, which is then incubated with the cell lysate. The antibody-antigen complex is then eluted leaving the antibody bound to the agarose beads, resulting in an antigen-only solution (i.e. no antibody interference). When separated on SDS-PAGE, any resulting bands will be free of antibody fragments, allowing for easier antigen identification through mass spectrometry. Controls for both immunoprecipitation methods consisted of control mouse IgG/IgM antibodies.

3.7.1 MAb 7B7 G5 (2) – Direct Immunoprecipitation Method

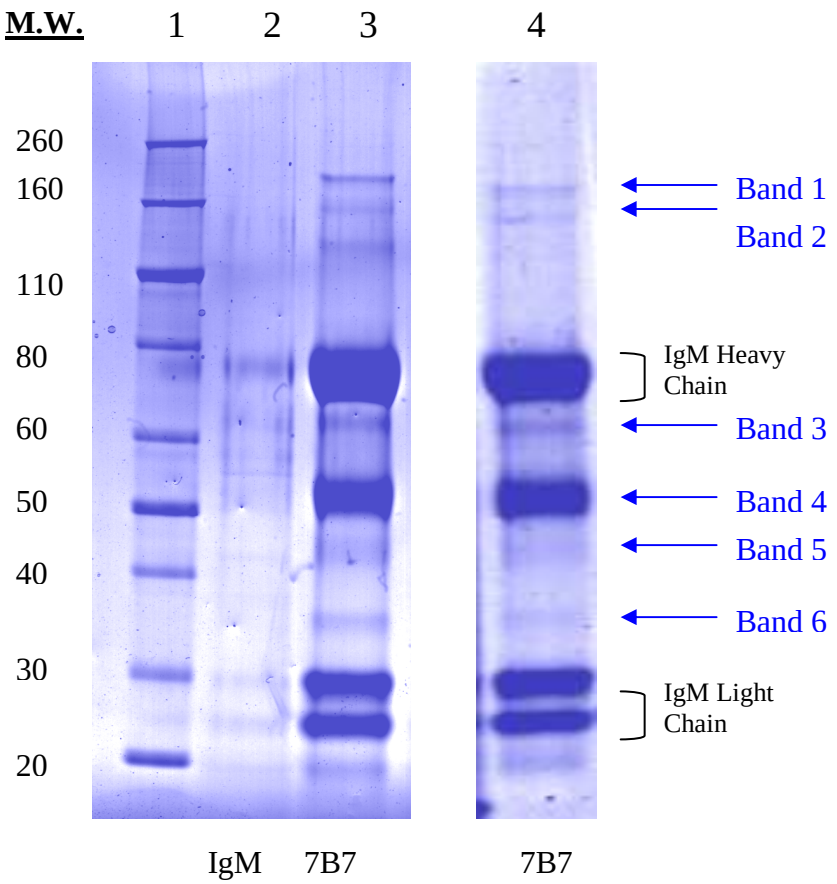

Figure 3.7: - Direct Immunoprecipitation of cell lysates with 7B7 G5 (2) MAb and control mouse IgM.
A representative SDS-PAGE gel of MiaPaCa-2 clone 3 and Lox IMVI cells immunoprecipitated with MAb 7B7 G5 (2) and separated on SDS-PAGE, and stained with 0.25% Coomassie Blue. Lane 1: molecular weight markers. Lane 2: MiaPaCa-2 clone 3 immunoprecipitated using control mouse IgM. Lane 3: MiaPaCa-2 clone 3 immunoprecipitated with MAb 7B7 G5 (2). Lane 4: Lox IMVI immunoprecipitated with MAb 7B7 G5 (2). Five bands of MAb 7B7 G5 (2) target proteins are observed; at approx. 200 kDa, 160 kDa, 65 kDa, 45 kDa and 35 kDa. These 5 bands were not present in the control IgM, were observed in triplicate experiments, and in 3 different cell lines. Each band was excised, digested with trypsin and run through an LCMS/LTQ-Orbitrap Mass Spectrometer for identification (section 2.12).

3.7.2 Purification of MAb 7B7 G5 (2)

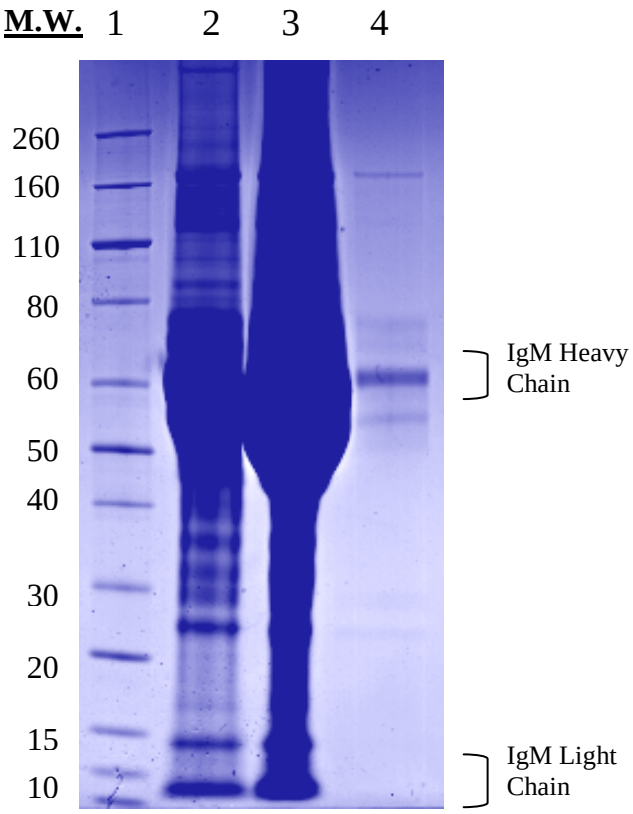

Figure 3.7.1: **-** Representative SDS-PAGE gel showing successful purification of 7B7 G5 (2) MAb, using the Pierce NAb Spin Purification Kit (section 2.3.8). Lane 1: Molecular Weight marker. Lane 2: Unpurified MAb 7B7 G5 (2). Lane 3: Concentrated, unpurified MAb 7B7 G5 (2). Lane 4: Purified MAb 7B7 G5 (2). Purified MAb is required for cross-linked immunoprecipitation.

3.7.3 MAb 7B7 G5 (2) - Cross Linked Immunoprecipitation Method

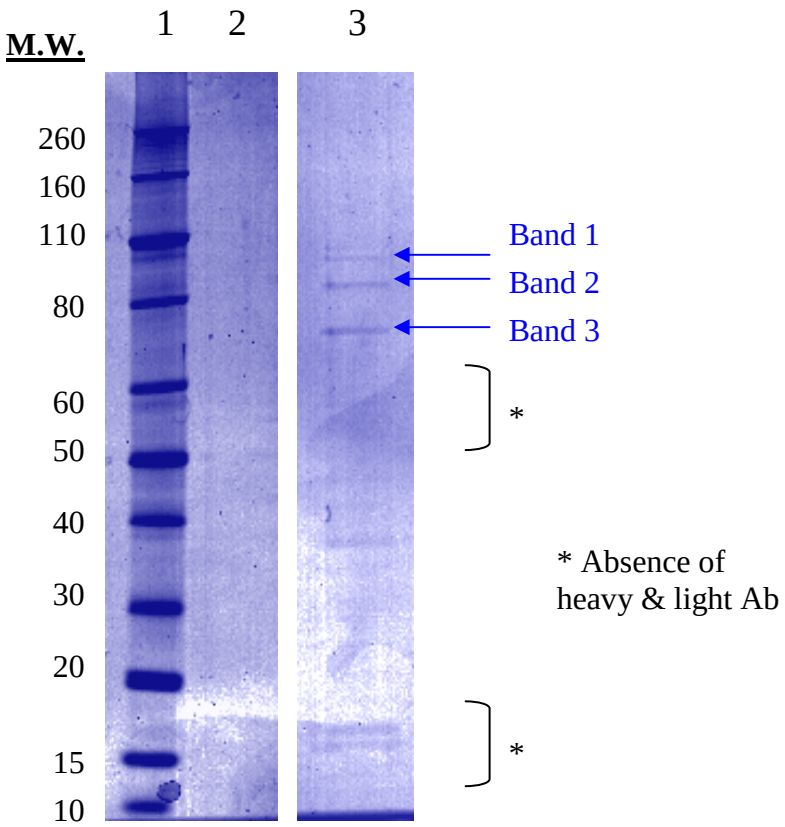

Figure 3.7.2: - Immunoprecipitates of MiaPaCa-2 clone 3 cells separated by SDS-PAGE, and stained with 0.25% Coomassie Blue. Lane 1: molecular weight markers. Lane 2: Unbound MAb 7B7 G5 (2). Lane 3: MiaPaCa-2 clone 3 immunoprecipitated with MAb 7B7 G5 (2). Three bands of antigen recognition and/or interacting proteins are observed; at approx. 100 kDa, 80 kDa, and 70 kDa. No antibody heavy and light chains are present. Each band was excised and run through an LCMS/LTQ Mass Spectrometer for identification (section 2.12). Non-binding agarose beads were used as a control.

3.8 Western Blot Analysis of MAb 7B7 G5 (2) Immunoprecipitates

Western blotting analysis was then carried with MAb 7B7 G5 (2) immunoprecipitates, in order to establish MAb reactivity, if any, with the antigens pulled out through the immunoprecipitation process. No reactive bands were observed.

3.9 Mass Spectrometry Identification of MAb 7B7 G5 (2) Target Proteins

Following separation of immunoprecipitates on 4-12% Bis-Tris SDS-PAGE, the gels were stained with 0.25% Coomassie Blue and destained accordingly. Bands of interest were excised from the gel, digested with trypsin, and subjected to LC-MS analysis. Identification was achieved using the SWISS-PROT SEQUEST database (section 2.12.1).

Positive identification was deemed valid if:

- proteins were observed in duplicate or more, from 2 or more independent experiments
- a minimum of 2 peptide sequences was obtained
- molecular weight of protein matched molecular weight of band on gel
- proteins achieved a high XC score, indicating excellent confidence in the identification (the minimum acceptable Xcorr for identified peptides was 1.5 for 1+ peptides, 2.5 for 2+ peptides and 3.5 for 3+ peptides).
- proteins were unique to MAb 7B7 G5 (2) (i.e. not found with other MAbs)

Criteria for a valid identification is described in full in section 2.12.1

Protein Name	Band	Gene Symbol	SWISSPROT Protein AC Number	MW (kDa)
ATP-dependent DNA helicase 2 subunit 2	2 (Cross Linked I.P.)	XRCC5	P13010	82.65
ATP-dependent DNA helicase 2 subunit 1	3 Cross Linked I.P.)	XRCC6	P32807	69.79

Table 3.9: **-** Proteins identified using the above criteria, from excised bands immunoprecipitated with MAb 7B7 G5 (2), through mass spectrometry. Band number refers to highlighted bands on gel represented in figures 3.7 and 3.7.2.

Direct immunoprecipitation of MAb 7B7 G5 (2) only gave two positive results. The band at approx. 36 kDa was identified as Elongation Factor 1-Alpha 1. However, this protein was also immunoprecipitated out with another antibody (MAb 9E1 24 (6)). All other bands were identified as Mouse IgM. In order to obtain a clear identification, it was necessary to remove the IgM components from the immunoprecipitates. This was achieved using the cross linked IP method, as described in section 2.11.2. A representative gel can be observed in Figure 3.7.2. From this, three bands of interest were observed. The top band (approx. 110 kDa), identified as Nucleolin, was also observed in a control IP, so was disregarded. The band at approx. 80 kDa was identified as ATP-dependent DNA helicase 2 subunit 2. The band at approx. 69 kDa was identified as ATP-dependent DNA helicase 2 subunit 1. All proteomic data is included in Appendix II & III).

All other bands observed were either identified as Mouse IgM, or were present in the control mouse IgM immunoprecipitates, and were thus disregarded.

3.9.1 Identification of MAb 7B7 G5 (2) Target Proteins by LC-MS Analysis of 7B7 G5 (2) Immunoprecipitates.

ATP-dependent DNA helicase 2 subunit 1

Scan(s)	Peptide	MH+	z	Type	P (pro) P (pep)	Score XC
KU70_HUMAN RecName: Full=**ATP-dependent DNA helicase 2 subunit 1**; AltName: Full=ATP-dependent DNA helicase II 70 kDa subunit; AltName: Full=Lupus Ku autoantigen protein p70; Short=Ku70; AltName: Full=70 kDa subunit of Ku antigen; AltName: Full=Thyroid-lupu					1.24E-09	50.24
976	R.QIILEKEETEELKR.F	1757.96436	2	CID	4.76E-07	3.81
1017	**R.IM*LFTNEDNPHGNDSAK.A**	1918.85997	2	CID	1.24E-09	4.77
1244	R.TFNTSTGGLLLPSDTKR.S	1807.95483	2	CID	4.40E-08	3.71
1540	K.KPGGFDISLFYR.D	1399.73682	2	CID	1.99E-06	3.39
1650	R.DSLIFLVDASK.A	1207.65686	2	CID	3.27E-05	3.02

Table 3.9.1: - Identification of Protein ATP-dependent DNA helicase 2 subunit 1, obtained using SEQUEST Human protein database

Peptides were identified using Bioworks 3.3.1 software. A representative results (experiments were carried out at least 3 times) is shown above, where 5 peptides corresponding to Human ATP-dependent DNA helicase 2 subunit 1 were identified. All 5 peptides showed high XC scores indicating excellent confidence in this identification. (Note: the minimum acceptable Xcorr for identified peptides was 1.5 for 1+ peptides, 2.5 for 2+ peptides and 3.5 for 3+ peptides).

MSGWESYYKTEGDEEAEEEQEENLEASGDYKYSGRDSLIFLVDASKAMFESQSEDELTPFDMSIQCI
QSVYISKIISSDRDLLAVVFYGTEKDKNSVNFKNIYVLQELDNPGAKRILELDQFKGQQGQKRFQD
MMGHGSDYSLSEVLWVCANLFSDVQFKMSHK**RIMLFTNEDNPHGN**DSAKASRARTKAGDLRDT
GIFLDLMHLKKPGGFDISLFYRDIISIAEDEDLRVHFEESSKLEDLLRKVRAKETRKRALSRLKLKLN
KDIVISVGIYNLVQKALKPPPIKLYRETNEPVKTKTRTFNTSTGGLLLPSDTKRSQIYGSRQIILEKEET
EELKRFDDPGLMLMGFKPLVLLKKHHYLRPSLFVYPEESLVIGSSTLFSALLIKCLEKEVAALCRYT
PRRNIPPYFVALVPQEEELDDQKIQVTPPGFQLVFLPFADDKRKMPFTEKIMATPEQVGKMKAIVEK
LRFTYRSDSFENPVLQQHFRNLEALALDLMEPEQAVDLTLPKVEAMNKRLGSLVDEFKELVYPPDY
NPEGKVTKRKHDNEGSGSKRPKVEYSEEELKTHISKGTLGKFTVPMLKEACRAYGLKSGLKKQEL
LEALTKHFQD

Figure 3.9: - Total amino acid sequence of Human ATP-dependent DNA helicase 2 subunit 1 protein presented above. Scan of 1017 peptide sequence, which shows the highest XC score (4.77) is highlighted

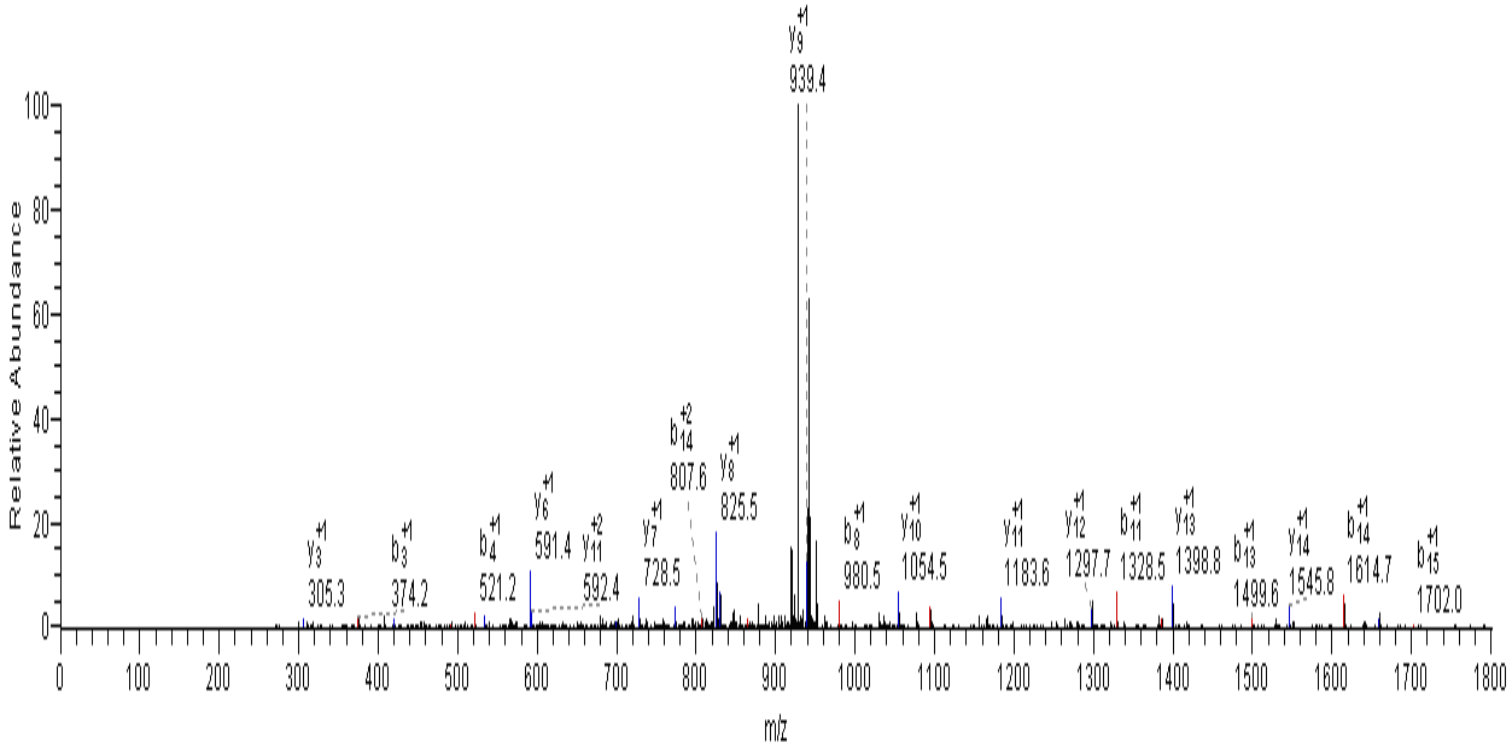

Figure 3.9.1: - The MS-MS spectrum for scan 1017 showing b (indicated in red) & y (indicated in blue) fragment ion series overlay.

ATP-dependent DNA helicase 2 subunit 2

Scan(s)	Peptide	MH+	z	Type	P (pro) P (pep)	Score XC
KU86_HUMAN RecName: Full=**ATP-dependent DNA helicase 2** subunit 2; AltName: Full=ATP-dependent DNA helicase II 80 kDa subunit; AltName: Full=Lupus Ku autoantigen protein p86; AltName: Full=86 kDa subunit of Ku antigen; AltName: Full=Ku86; AltName: Full=Ku80					**2.08E-07**	**30.21**
1257	R.YGSDIVPFSK.V	1112.56226	2	CID	9.87E-07	3.03
1390	**R.HIEIFTDLSSR.F**	1317.67969	2	CID	2.08E-07	3.16
1605	K.SQLDIIIHSLK.K	1266.74158	2	CID	5.48E-06	3.11

Table 3.9.2: - Identification of Protein ATP-dependent DNA helicase 2 subunit 2, obtained using SEQUEST Human protein database

Peptides were identified using Bioworks 3.3.1 software. A representative result (experiments were carried out at least 3 times) is shown above, where 3 peptides corresponding to Human ATP-dependent DNA helicase 2 subunit 2 were identified. All 3 peptides showed high XC scores indicating excellent confidence in this identification.

MVRSGNKAAVVLCMDVGFTMSNSIPGIESPFEQAKKVITMFVQRQVFAENKDEIALVLFGTDGTDN
PLSGGDQYQNITVHRHLMLPDFDLLEDIESKIQPGSQQADFLDALIVSMDVIQHETIGKKFEK**RHIEI**
FTDLSSRFSKSQLDIIIHSLKKCDISLQFFLPFSLGKEDGSGDRGDGPFRLGGHGPSFPLKGITEQQKE
GLEIVKMVMISLEGEDGLDEIYSFSESLRKLCVFKKIERHSIHWPCRLTIGSNLSIRIAAYKSILQERV
KKTWTVVDAKTLKKEDIQKETVYCLNDDDETEVLKEDIIQGFRYGSDIVPFSKVDEEQMKYKSEG
KCFSVLGFCKSSQVQRRFFMGNQVLKVFAARDDEAAAVALSSLIHALDDLDMVAIVRYAYDKRA
NPQVGVAFPHIKHNYECLVYVQLPFMEDLRQYMFSSLKNSKKYAPTEAQLNAVDALIDSMSLAKK
DEKTDTLEDLFPTTKIPNPRFQRLFQCLLHRALHPREPLPPIQQHIWNMLNPPAEVTTKSQIPLSKIKT
LFPLIEAKKKDQVTAQEIFQDNHEDGPTAKKLKTEQGGAHFSVSSLAEGSVTSVGSVNPAENFRVL
VKQKKASFEEASNQLINHIEQFLDTNETPYFMKSIDCIR

Figure 3.9.2: - Total amino acid sequence of Human ATP-dependent DNA helicase 2 subunit 2 protein presented above. Scan of 1390 peptide sequence, which shows the highest XC score (3.16) is highlighted

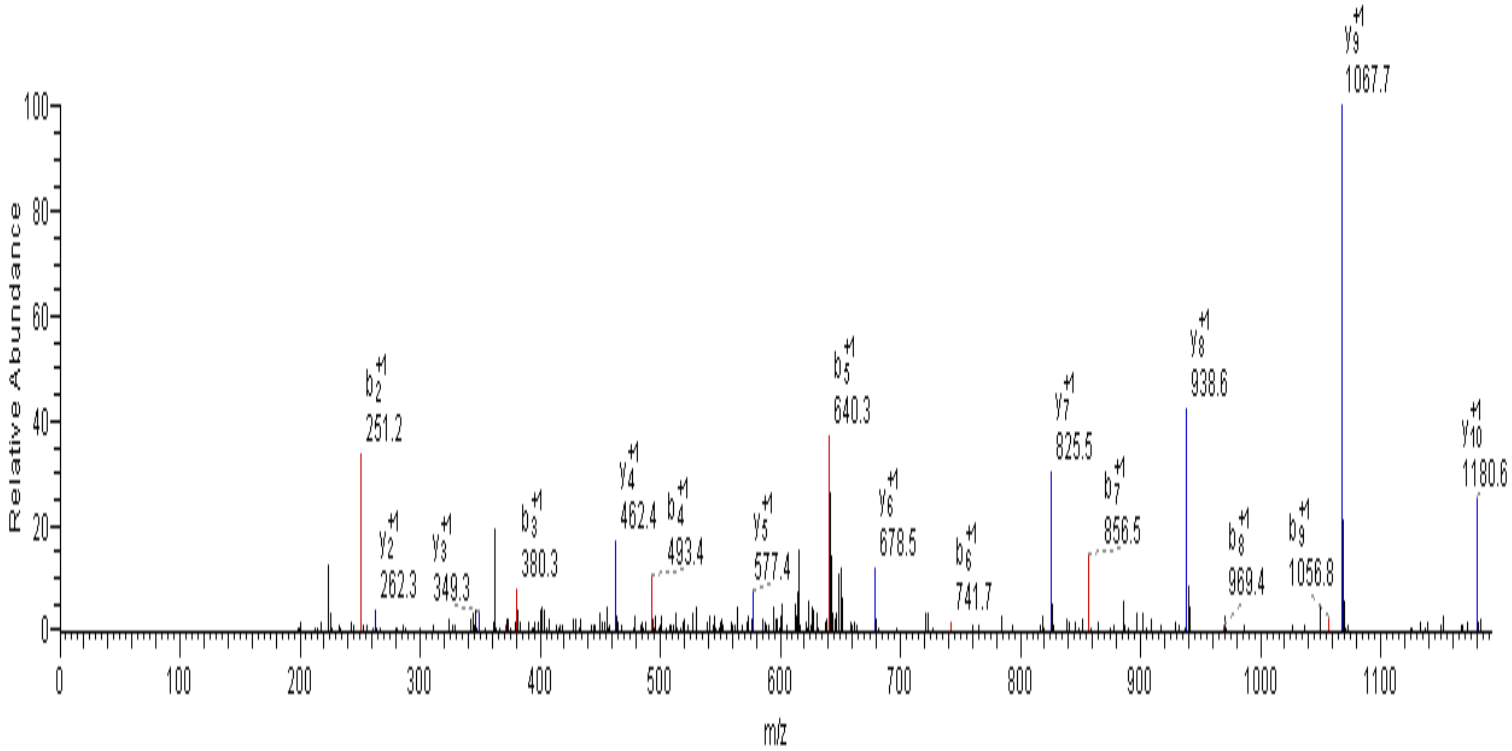

Figure 3.9.3: - The MS-MS spectrum for scan 1390 showing b (indicated in red) & y (indicated in blue) fragment ion series overlay.

3.10 Western Blot Validation of MAb 7B7 G5 (2) Target Proteins

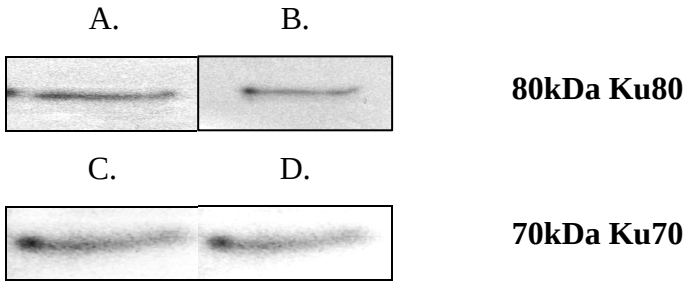

Figure 3.10: **-** Western Blot analysis of (A) DLKP-A Cross Linked I.P. sample, and (B) MiaPaCa-2 clone 3 Cross Linked I.P. sample, separated by SDS-PAGE and probed with an ATP dependent DNA helicase 2 subunit 1 antibody (Ku80). A reactive band at the expected weight of 80 kDa is detected in all immunoprecipitates, confirming this protein band as ATP dependent DNA helicase 2 subunit 1. *n = 3*.

(C & D): Western Blot analysis of DLKP-A Cross Linked I.P. sample and MiaPaCa-2 clone 3 Cross Linked I.P. samples probed with ATP dependent DNA helicase 2 subunit 2 antibody (Ku70). A reactive band at the expected weight of 70 kDa is detected in both immunoprecipitates, confirming this protein band as ATP dependent DNA helicase 2 subunit 2. *n = 3*.

3.11 siRNA Functional Analysis of MAb 7B7 G5 (2) Target Proteins

To investigate any functional role of the identified MAb 7B7 G5 (2) target proteins in cancer cell invasion, siRNA silencing of the respective targets was carried out using Ambion Inc. Silencer® Select siRNAs. Two or three (where available) siRNAs specific to each target were investigated.

The conditions for siRNA transfection were optimised in 96- and 6-well plates using kinesin as a positive control, and scrambled siRNA as a siRNA transfection control (section 2.14.1). For each set of siRNA transfections carried out, a non-transfected cell line and a scrambled (SCR) siRNA transfected control were used. Kinesin (Kin) was used as a control for efficient transfection as Kin siRNA reduces proliferation in the cells.

- 48hrs post-transfection, cells were lysed (RIPA), analysed by SDS-PAGE, and probed with specific antibodies to respective targets to test effect of knockdown on Protein-Levels.

- Proliferation assays (section 2.14.3) were carried out on transfected cells to assess the impact of knockdown on proliferation levels in the cells, to ensure that any inhibition in invasion was not just due to a decrease in the cell number.

- Invasion assays (section 2.14.4) were carried out on transfected cells to confirm whether or not these targets were involved in invasion.

- Motility assays (section 2.14.5) were carried out on transfected cells to confirm whether or not these targets were involved in motility.

3.11.1 Investigation of Ku70 in Cancer Cell Invasion

Ku70 knockdown was carried out in the MiaPaCa-2 clone 3 and DLKP-M cell lines.

Silencing of the Ku70 gene by two different siRNAs significantly reduced the invasive capacity of MiaPaCa-2 clone 3 and DLKP-M cells:

- MiaPaCa-2 clone 3 invasion was significantly inhibited, by an average of 37.4%, following siRNA transfection with Ku70A, and an average of 24.9% following siRNA transfection by Ku70B.
- DLKP-M invasion was inhibited by an average of 17.2% following siRNA transfection with Ku70A, and significantly inhibited by an average of 38.6% following siRNA transfection with Ku70B.

Motility was also significantly inhibited in the MiaPaCa-2 clone 3 cell line following siRNA transfection with Ku70B, by an average of 35.7%

No significant affect on proliferation in either the MiaPaCa-2 clone 3 or DLKP-M cell lines was observed following transfection of siRNAs, indicating that the observed inhibition of invasion was not due to any reduced proliferative capacity of the cells. Protein knockdown was confirmed by Western Blot analysis (Figures 3.11 & 3.11.6).

Statistical analyses for proliferation assays were carried out on the average absorbancy readings of the control Vs test wells, over biological triplicates.

Statistical analyses for invasion assays were carried out with the average cell counts of control Vs sample inserts over biological triplicates (section 2.15).

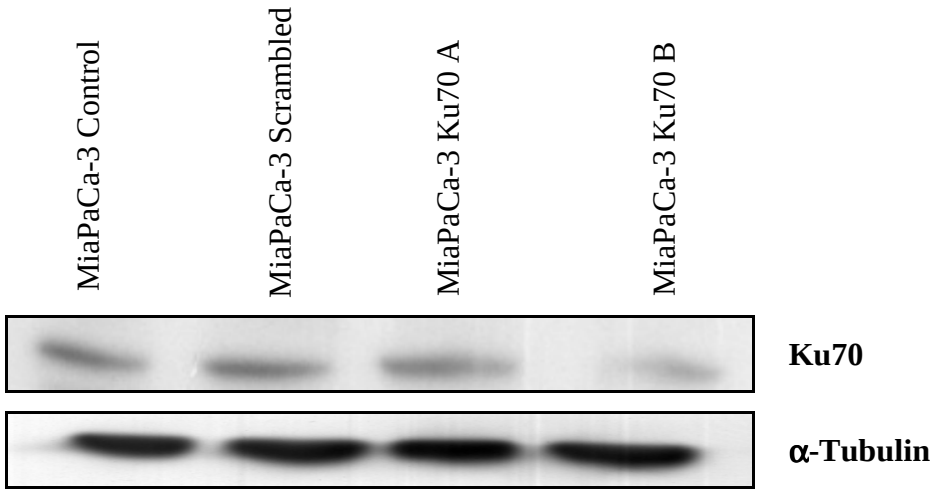

Figure 3.11: - Western Blot analysis of whole cell (RIPA) lysates of MiaPaCa-2 clone 3 transfected cells, separated on SDS-PAGE, and probed with an ATP-dependent DNA helicase 2 subunit 2 antibody. A reduction in the levels of Ku70 can be seen when compared to the control MiaPaCa-2 clone 3 cell lysate (untransfected). α-Tubulin was used as a loading control. (15μg protein per lane loaded) *n = 3*.

- **Effect of siRNA Ku70 on MiaPaCa-2 clone 3 Proliferation**

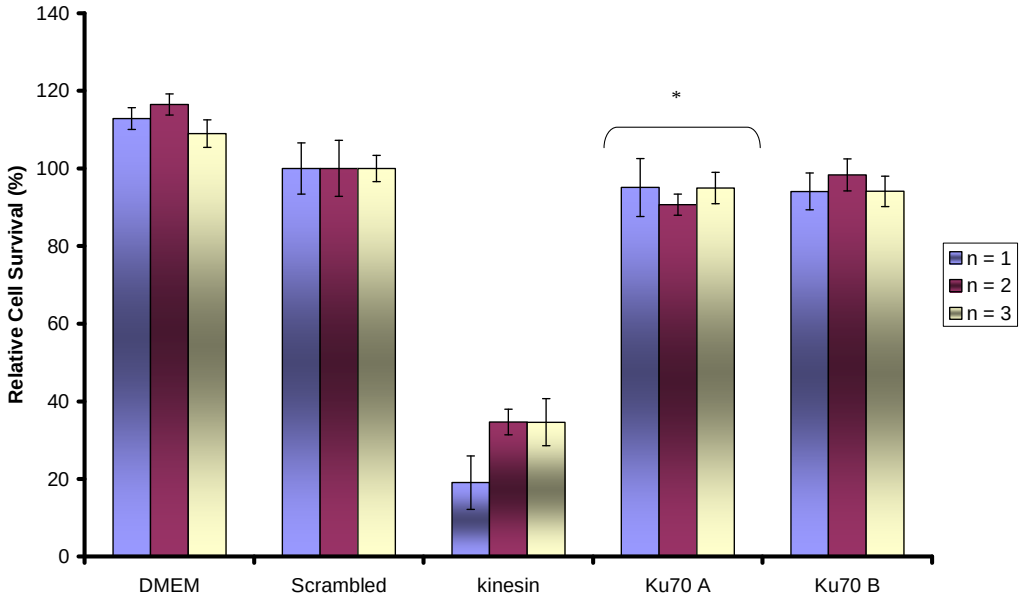

Figure 3.11.1: **-** Histogram showing proliferation assay of MiaPaCa-2 clone 3 scrambled, kinesin and transfected with siRNAs A, & B targeting Ku70. Results graphed as % survival relative to scrambled transfected cells (control). Loss of Ku70 did not affect proliferation in this cell line; therefore any inhibition of invasion is not due to cell kill. Statistics performed using student t-test compared to scrambled control; * $p \leq 0.05$, ** $p \leq 0.01$, *** $p \leq 0.005$, $n = 3$.

- **Knockdown of Ku70 reduces invasion in MiaPaCa 2-clone 3**

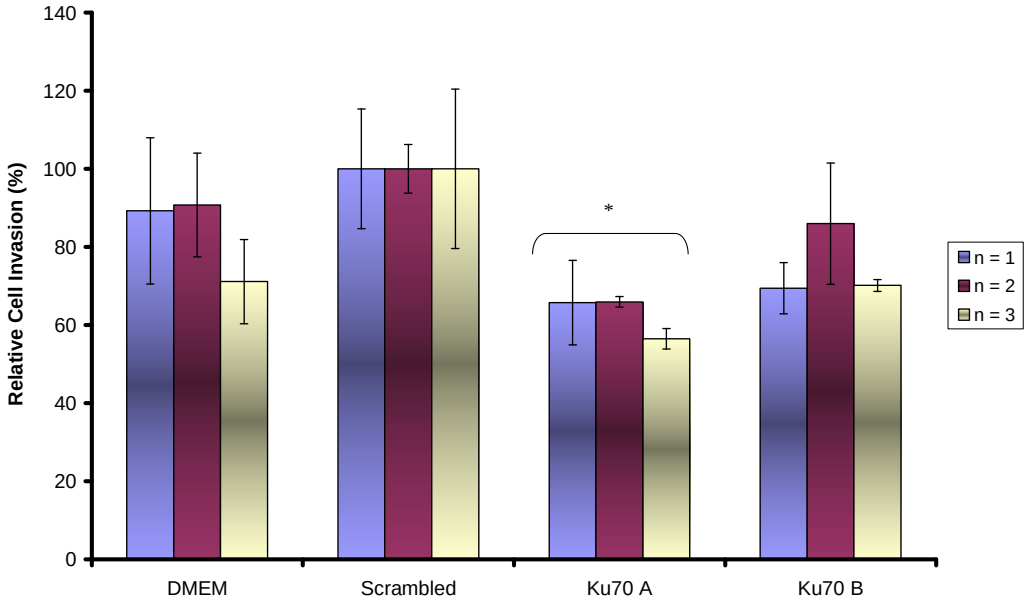

Figure 3.11.2: - Histogram showing effect of Ku70 knockdown on invasive behaviour of MiaPaCa-2 clone 3 cells. Forty-eight hours post-transfection with Ku70 siRNAs, invasion assays on MiaPaCa-2 clone 3 cells were performed. Ku70-A siRNA transfected cells show a significant decrease in invasion levels, while Ku70-B siRNA transfected cells also show a decrease in invasion levels, but not significantly so. Statistics performed using student t-test compared to scrambled control; * $p \leq 0.05$, ** $p \leq 0.01$, *** $p \leq 0.005$, *n = 3*.

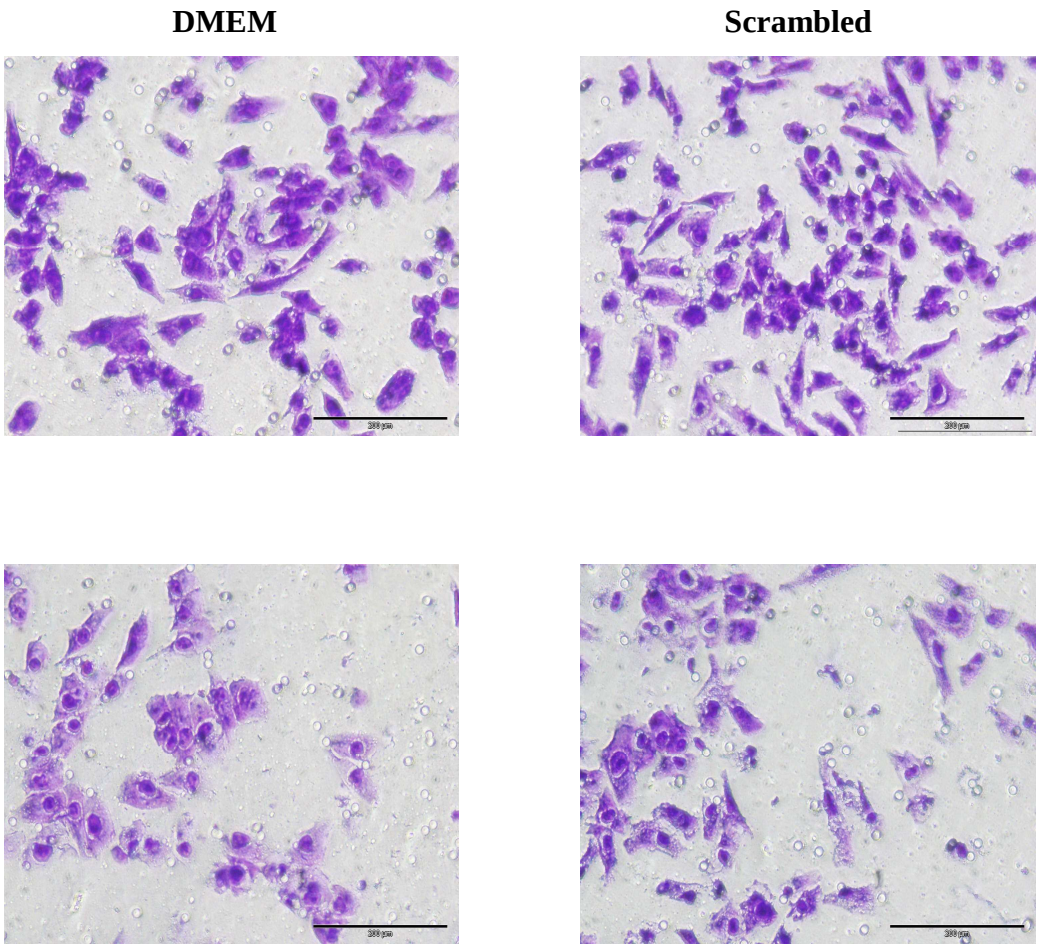

Figure 3.11.3: - Representative photomicrographs showing invasion status of MiaPaCa-2 clone 3 cells after 48hrs, untreated (DMEM), transfected with scrambled siRNA (Control), transfected with Ku70-A siRNA and Ku70-B. A decrease in invasion can be observed following transfection with Ku70 siRNAs when compared to the control insert (scrambled). Magnification, 100X, scale bar, 200 μm.

- **Knockdown of Ku70 reduces motility in MiaPaCa 2-clone 3**

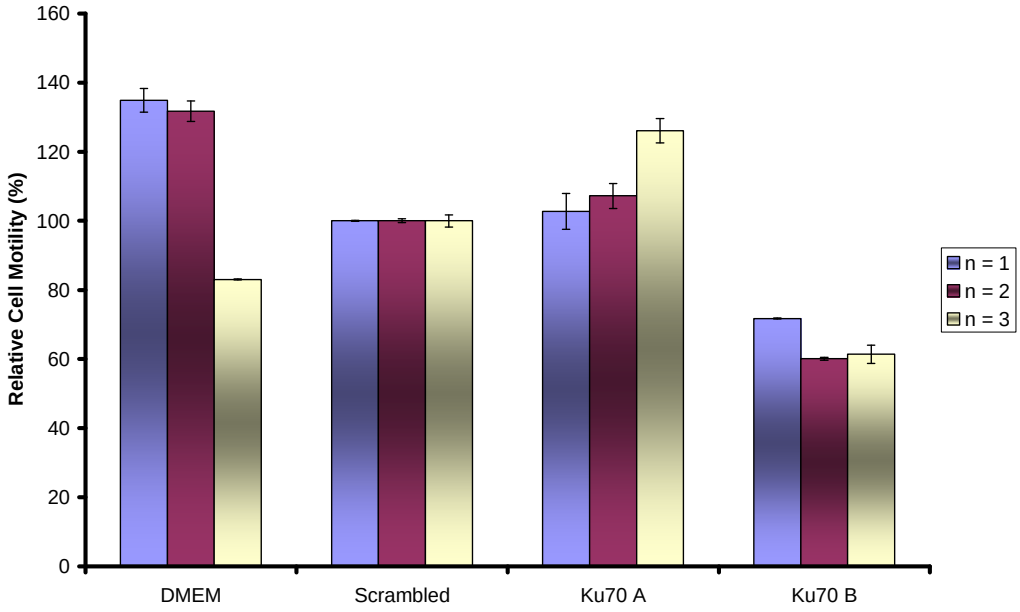

Figure 3.11.4: - Histogram showing effect of Ku70 knockdown on motile behaviour of MiaPaCa-2 clone 3 cells. Forty-eight hours post-transfection with Ku70 siRNAs, motility assays on MiaPaCa-2 clone 3 cells were performed. Ku70 B siRNA transfected cells show a decrease in motility levels. Statistics performed using student t-test compared to scrambled control; * $p \leq 0.05$, ** $p \leq 0.01$, *** $p \leq 0.005$, $n = 3$.

DMEM **Scrambled**

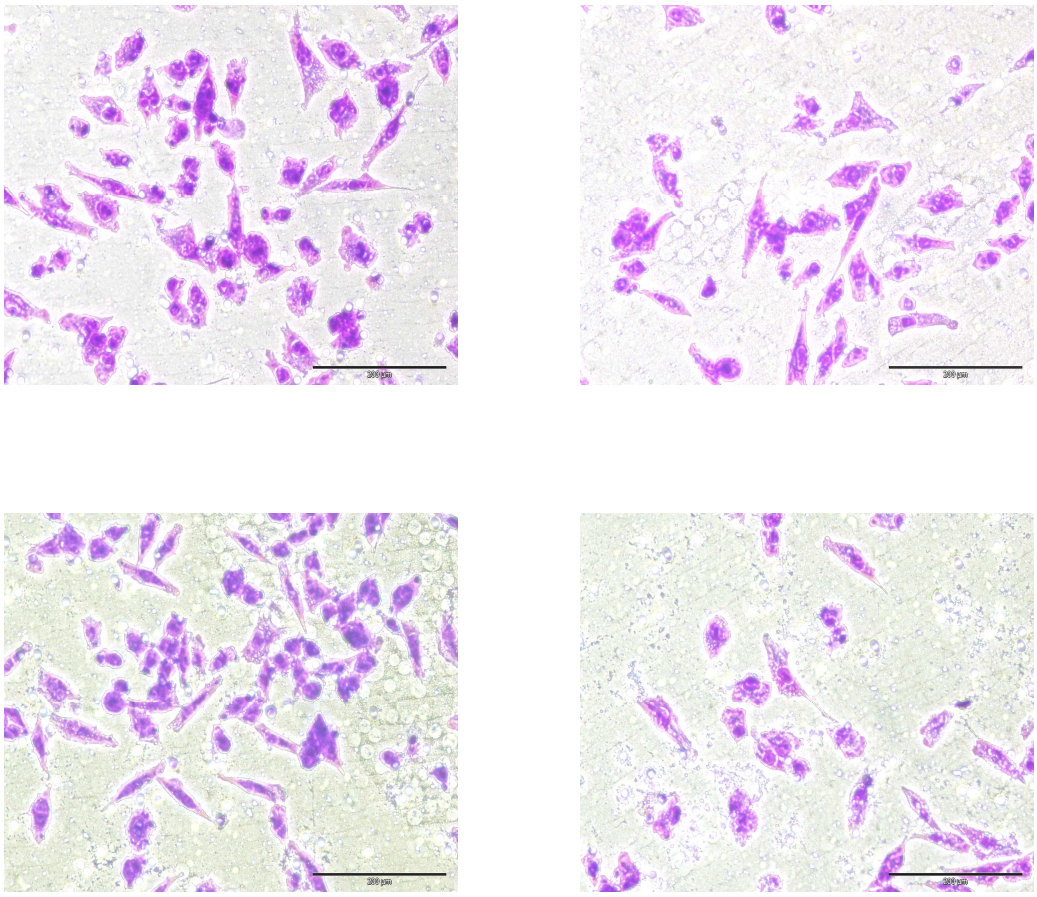

Ku70 A **Ku70 B**

Figure 3.11.5: - Representative photomicrographs showing motility status of MiaPaCa-2 clone 3 cells after 48hrs, untreated (DMEM), transfected with scrambled siRNA (Control), transfected with Ku70-A siRNA and Ku70-B. A decrease in motility can be observed following transfection with Ku70 siRNA B, but not A, when compared to the control insert (Scrambled). Magnification, 100X, scale bar, 200 μm.

- **Effect of Ku70 siRNA transfection in DLKP-M**

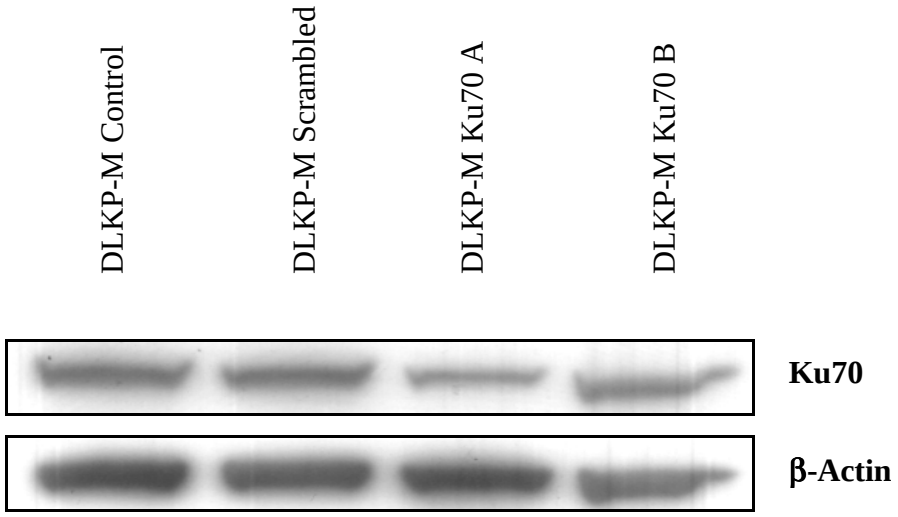

Figure 3.11.6: - Western Blot analysis of whole cell (RIPA) lysates of DLKP-M transfected cells, separated on SDS-PAGE, and probed with an ATP-dependent DNA helicase 2 subunit 2 antibody. A reduction in the levels of Ku70 can be seen when compared to the control DLKP-M cell lysate (untransfected). β-Actin was used as a loading control. (15μg protein per lane loaded) *n = 3*.

- **Effect of siRNA Ku70 on DLKP-M Proliferation**

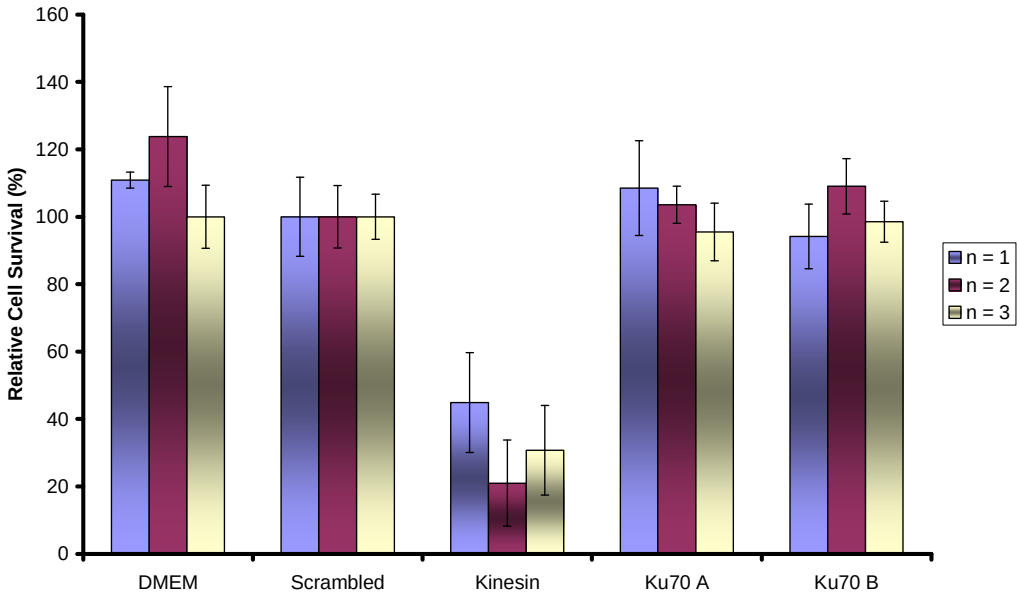

Figure 3.11.7: - Histogram showing proliferation assay of DLKP-M scrambled, kinesin and transfected with siRNAs A, & B targeting Ku70. Results graphed as % survival relative to scrambled transfected cells (control). Loss of Ku70 did not affect proliferation in this cell line; therefore any inhibition of invasion is not due to cell kill. Statistics performed using student t-test compared to scrambled control; * $p \leq 0.05$, ** $p \leq 0.01$, *** $p \leq 0.005$, *n = 3.*

Knockdown of Ku70 reduces invasion in DLKP-M

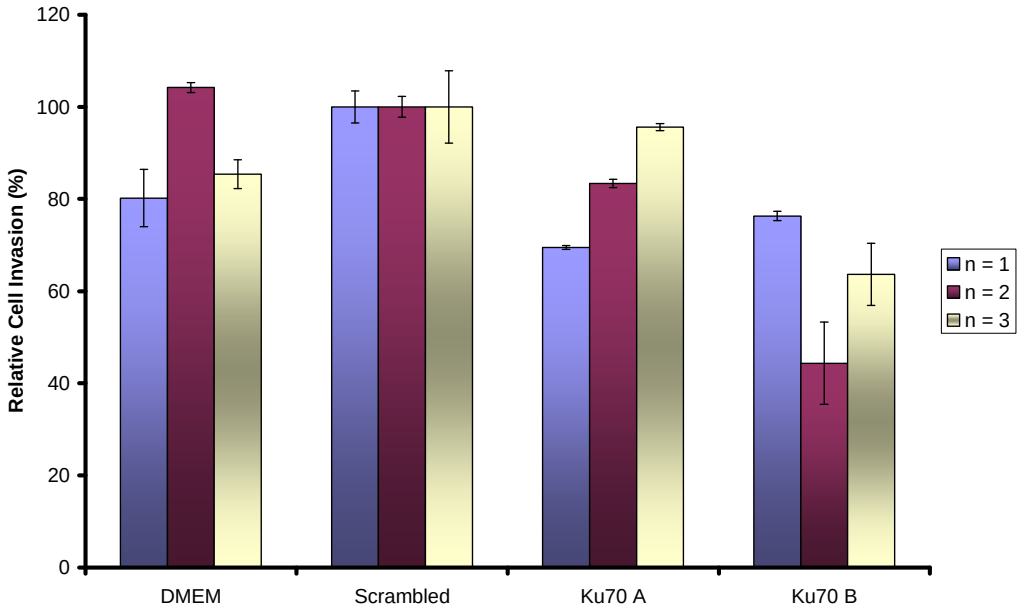

Figure 3.11.8: - Histogram showing effect of Ku70 knockdown on invasive behaviour of DLKP-M cells. Forty-eight hours post-transfection with Ku70 siRNAs, invasion assays on DLKP-M cells were performed. Ku70-A and Ku70-B siRNA transfected cells show a decrease in invasion levels. Statistics performed using student t-test compared to scrambled control; * $p \leq 0.05$, ** $p \leq 0.01$, *** $p \leq 0.005$, $n = 3$.

DMEM **Scrambled**

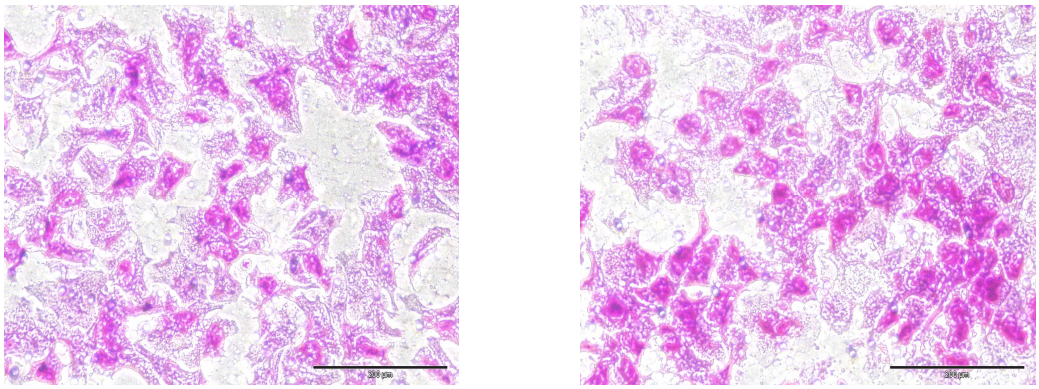

Ku70 A **Ku70 B**

Figure 3.11.9: - Representative photomicrographs showing invasion status of DLKP-M cells after 48hrs, untreated (DMEM), transfected with scrambled siRNA (Control), transfected with Ku70-A siRNA and Ku70-B. A decrease in invasion can be observed following transfection with Ku70 siRNA B, but not A, when compared to the control insert (Scrambled). Magnification, 100X, scale bar, 200 µm.

3.11.2 Investigation of Ku80 in Cancer Cell Invasion

Ku80 knockdown was successfully carried out in the MiaPaCa-2 clone and DLKP-M cell lines.

Silencing of the Ku80 gene by two different siRNAs significantly reduced the invasive capacity of the MiaPaCa-2 clone 3 and DLKP-M cells:

- MiaPaCa-2 clone 3 invasion was significantly inhibited by an average of 31.7% following siRNA transfection with Ku80A, and an average of 50.8% following siRNA transfection by Ku80C
- DLKP-M invasion was inhibited by an average of 16% following siRNA transfection with Ku70A, and an average of 38.4% following siRNA transfection with Ku80C

Motility was also inhibited in the MiaPaCa-2 clone 3 cell line following siRNA transfection with Ku80A by an average of 21%, and significantly inhibited with Ku80C, by an average of 53.7%.

No significant affect on proliferation in either the MiaPaCa-2 clone 3 or DLKP-M cell lines was observed following transfection of both siRNAs, indicating that the observed inhibition of invasion was not due to any reduced proliferative capacity of the cells. Protein knockdown was confirmed by Western blot analysis (Figures 3.11.10 & 3.11.16)

- **Effect of Ku80 siRNA transfection in MiaPaCa-2 clone 3**

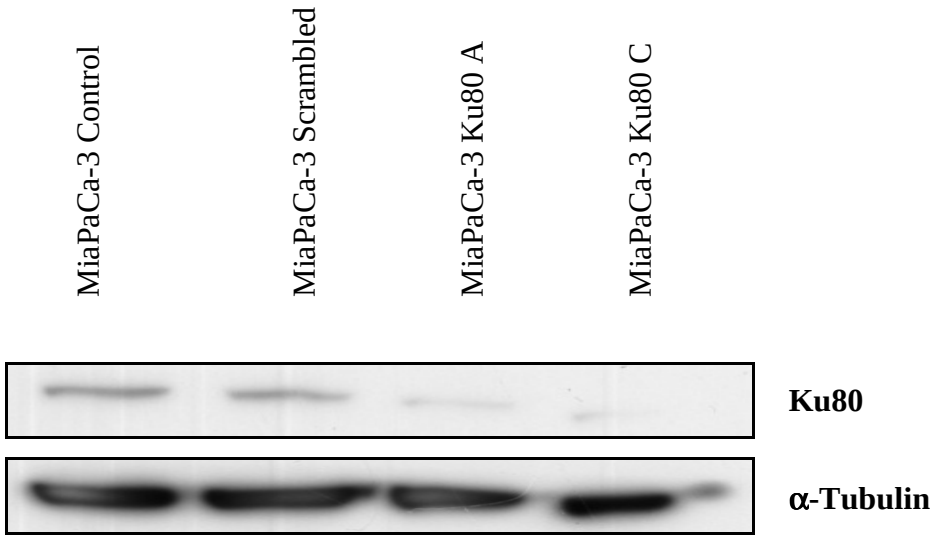

Figure 3.11.10: - Western Blot analysis of whole cell (RIPA) lysates of MiaPaCa-2 clone 3 transfected cells, separated on SDS-PAGE, and probed with an ATP-dependent DNA helicase 2 subunit 1 antibody. A reduction in the levels of Ku80 can be seen when compared to the control MiaPaCa-2 clone 3 cell lysate (untransfected). α-Tubulin was used as a loading control. (15μg protein per lane loaded) *n = 3*.

- **Effect of siRNA Ku80 on MiaPaCa-2 clone 3 Proliferation**

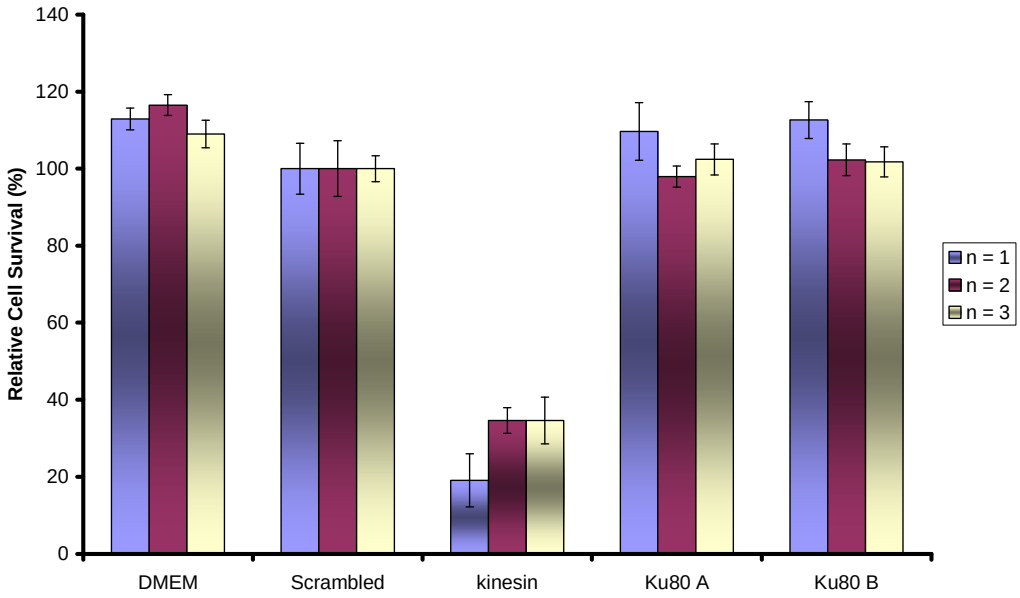

Figure 3.11.11: - Histogram showing proliferation assay of MiaPaCa-2 clone 3 cells, scrambled, kinesin and transfected with siRNAs A, & B targeting Ku80. Results graphed as % survival relative to scrambled transfected cells (control). Loss of Ku80 did not affect proliferation in this cell line; therefore any inhibition of invasion is not due to cell kill. Statistics performed using student t-test compared to scrambled control; * $p \leq 0.05$, ** $p \leq 0.01$, *** $p \leq 0.005$, $n = 3$.

- **Knockdown of Ku80 reduces invasion in MiaPaCa-2 clone 3**

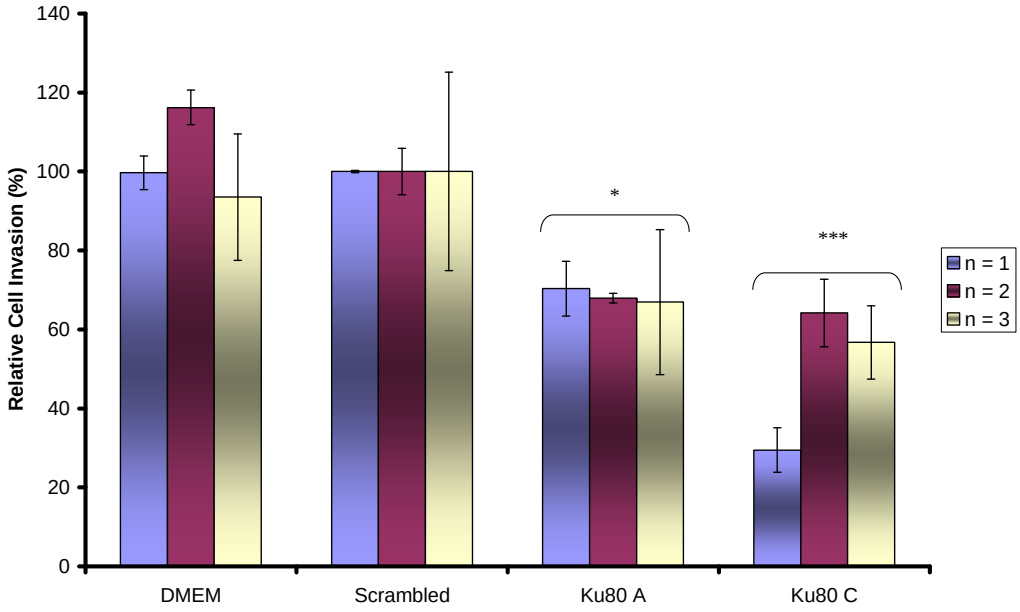

Figure 3.11.12 - Histogram showing effect of Ku80 knockdown on invasive behaviour of MiaPaCa-2 clone 3 cells. Forty-eight hours post-transfection with Ku80 siRNAs, invasion assays on MiaPaCa-2 clone 3 cells were performed. Both Ku80-A and Ku80-C siRNA transfected cells show a significant decrease in invasion levels. Statistics performed using student t-test compared to scrambled control; * $p \leq 0.05$, ** $p \leq 0.01$, *** $p \leq 0.005$, *n = 3.*

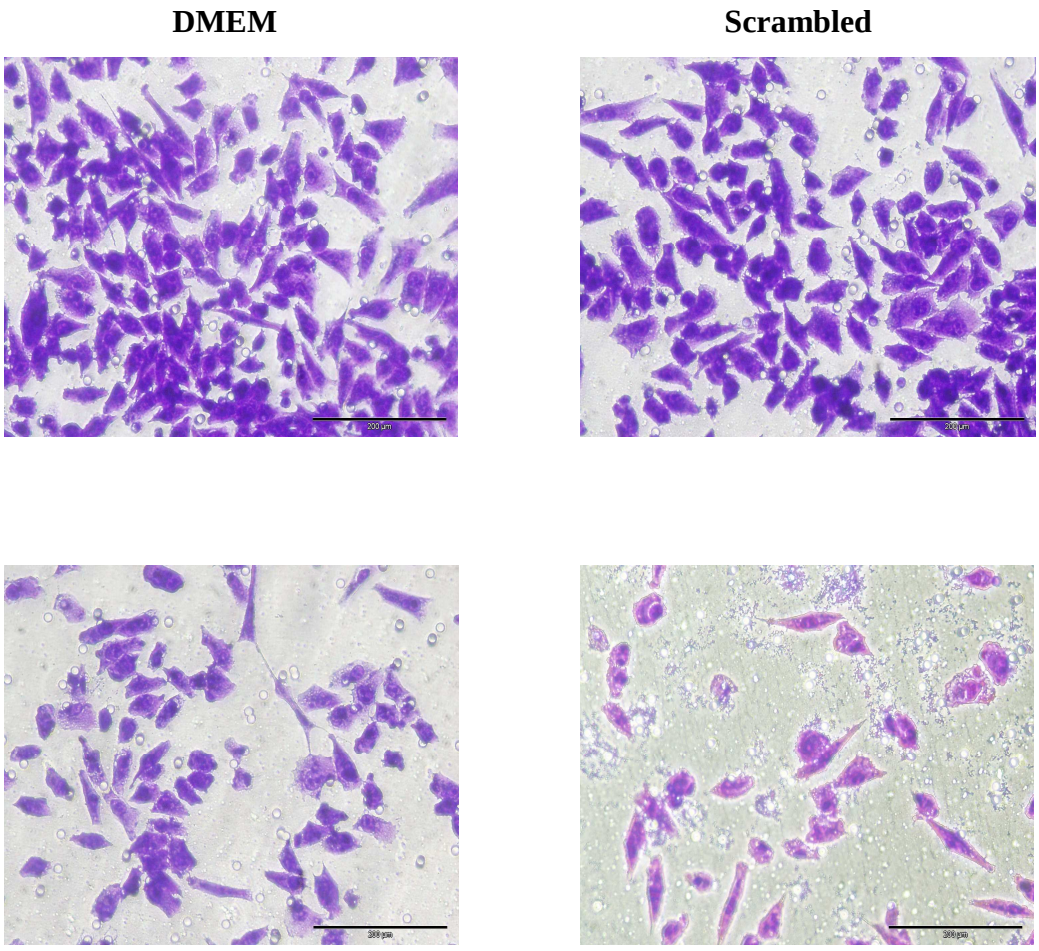

Figure 3.11.13: - Representative photomicrographs showing invasion status of MiaPaCa-2 clone 3 cells after 48hrs untreated (DMEM), transfected with scrambled siRNA (Control), transfected with Ku80-A siRNA, transfected with Ku80-C siRNA. A decrease in invasion can be observed following transfection with Ku80 siRNAs when compared to the control insert (Scrambled).
Magnification, 100X, scale bar, 200 μm.

- **Knockdown of Ku80 reduces Motility in MiaPaCa-2 clone 3**

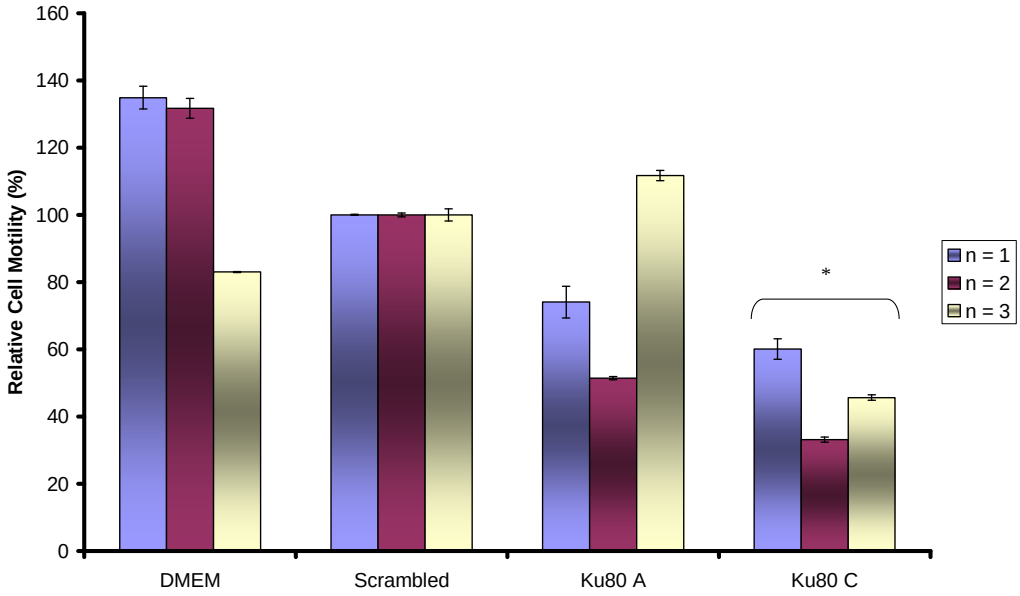

Figure 3.11.14: - Histogram showing effect of Ku80 knockdown on motile behaviour of MiaPaCa-2 clone 3 cells. Forty-eight hours post-transfection with Ku80 siRNAs, motility assays on MiaPaCa-2 clone 3 cells were performed. Ku80-A siRNA transfected cells show a decrease in motility levels while Ku80-C siRNA transfected cells also show a significant decrease in motility levels. Statistics performed using student t-test compared to scrambled control; * $p \leq 0.05$, ** $p \leq 0.01$, *** $p \leq 0.005$, *n = 3.*

DMEM **Scrambled**

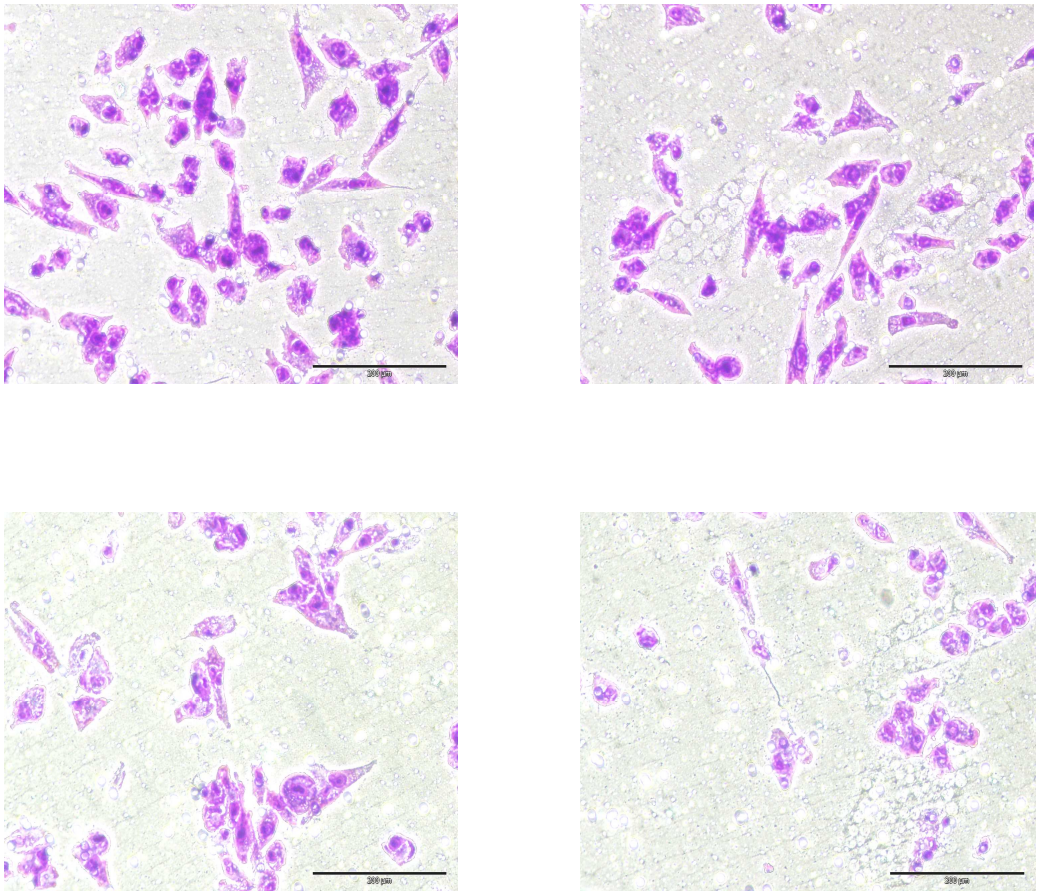

Ku80 A **Ku80 C**

Figure 3.11.15: - Representative photomicrographs showing motility status of MiaPaCa-2 clone 3 cells after 24hrs, untreated (DMEM), transfected with scrambled siRNA (Control), transfected with Ku80-A siRNA, transfected with Ku80-C siRNA. A decrease in motility can be observed following transfection with Ku80 siRNAs when compared to the control insert (Scrambled).
Magnification, 100X, scale bar, 200 μm.

- **Effect of Ku80 siRNA transfection in DLKP-M**

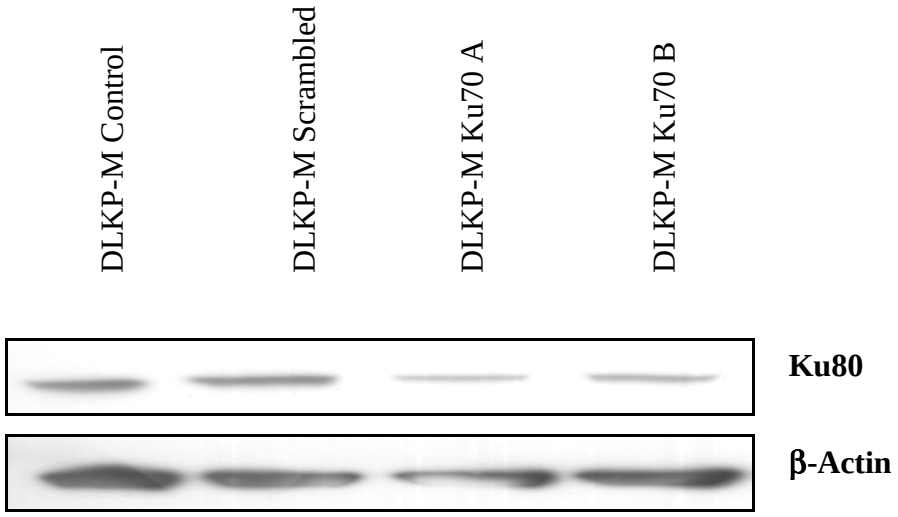

Figure 3.11.16: - Western Blot analysis of whole cell (RIPA) lysates of DLKP-M transfected cells, separated on SDS-PAGE, and probed with an ATP-dependent DNA helicase 2 subunit 1 antibody. A reduction in the levels of Ku80 can be seen when compared to the control MiaPaCa-2 clone 3 cell lysate (untransfected). β-Actin was used as a loading control. (15µg protein per lane loaded) *n = 3*.

- **Effect of siRNA Ku80 on DLKP-M Proliferation**

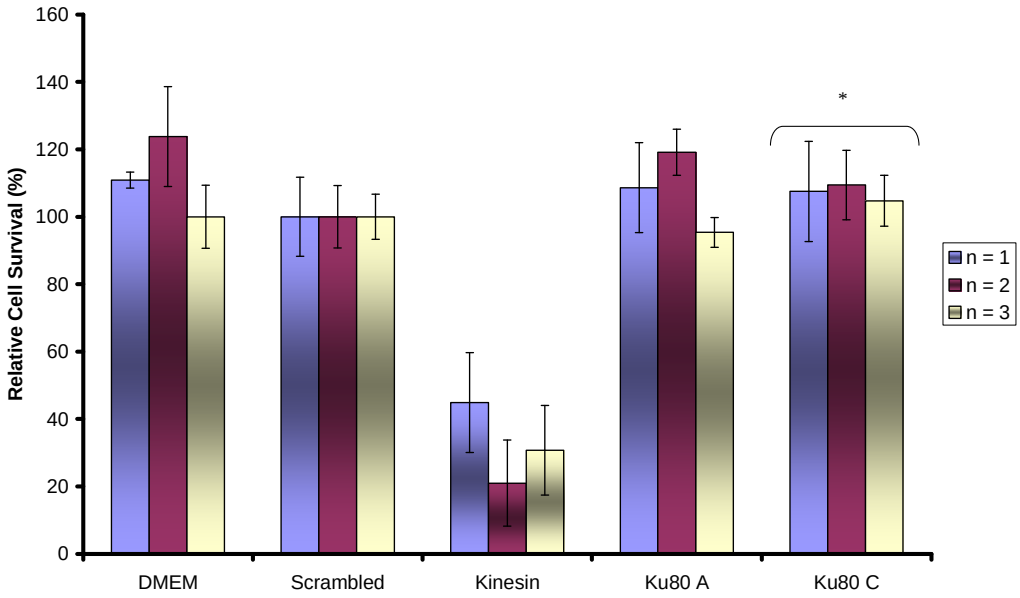

Figure 3.11.17: - Histogram showing proliferation assay of DLKP-M scrambled, kinesin and transfected with siRNAs A, & B targeting Ku80. Results graphed as % survival relative to scrambled transfected cells (control). Loss of Ku80 did not affect proliferation in this cell line; therefore any inhibition of invasion is not due to cell kill. Statistics performed using student t-test compared to scrambled control; * $p \leq 0.05$, ** $p \leq 0.01$, *** $p \leq 0.005$, *n = 3*.

- **Knockdown of Ku80 reduces invasion in DLKP-M**

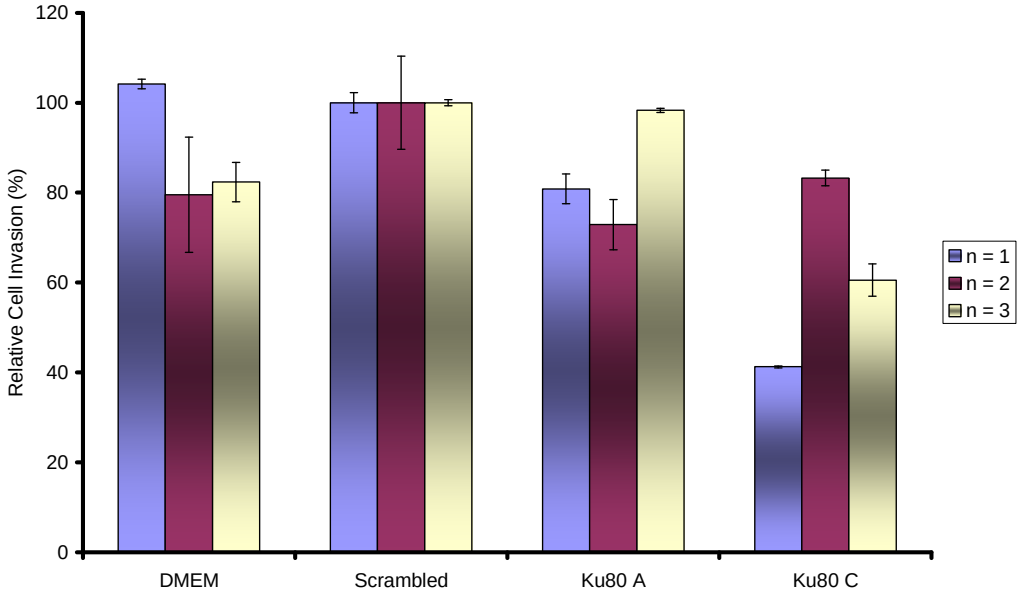

Figure 3.11.18: - Histogram showing effect of Ku80 knockdown on invasive behaviour of DLKP-M cells. Forty-eight hours post-transfection with Ku80 siRNAs, invasion assays on DLKP-M cells were performed. Ku80-A siRNA transfected cells show a small decrease in invasion levels, while Ku80-C siRNA transfected cells show a larger decrease in invasion levels. Statistics performed using student t-test compared to scrambled control; * $p \leq 0.05$, ** $p \leq 0.01$, *** $p \leq 0.005$, *n = 3.*

DMEM **Scrambled**

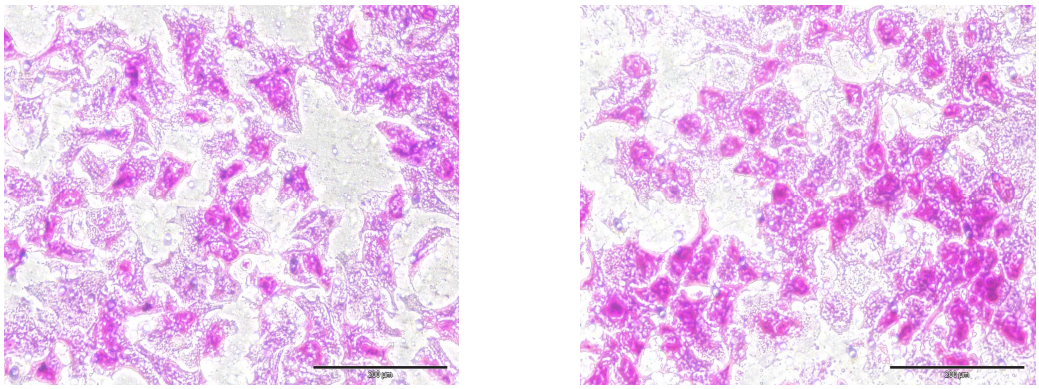

Ku80 A **Ku80 C**

Figure 3.11.19: - Representative photomicrographs showing invasion status of DLKP-M cells after 48hrs, untreated (DMEM), transfected with scrambled siRNA (Control), transfected with Ku80-A siRNA and Ku80-C. A decrease in invasion can be observed following transfection with Ku80 siRNA C, but not A, when compared to the control insert (B). Magnification, 100X, scale bar, 200 μm.

- **Effect of Ku70 siRNA transfection on Ku80 Expression in MiaPaCa-2 clone 3**

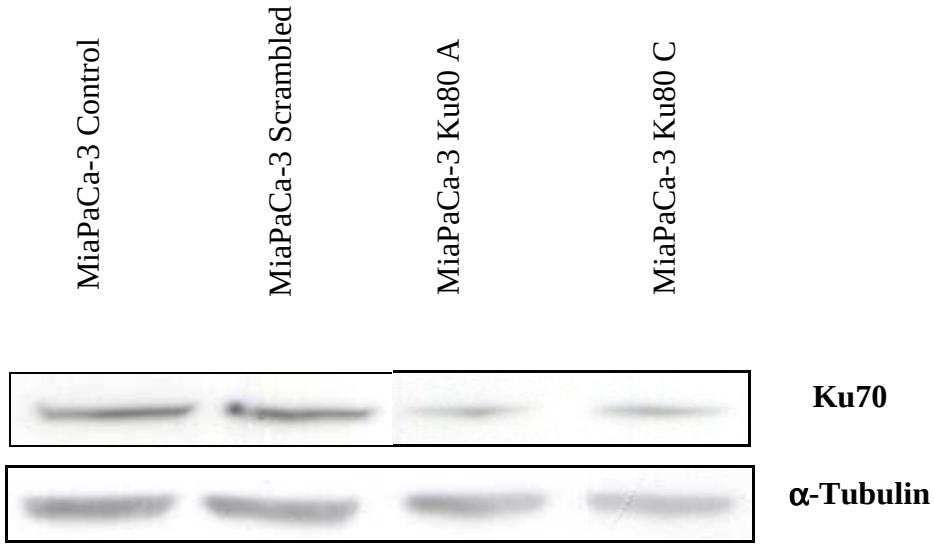

Figure 3.11.20: - Western Blot analysis of whole cell (RIPA) lysates of MiaPaCa-2 clone 3 transfected cells, separated by SDS-PAGE, probed with an ATP-dependent DNA helicase 2 subunit 2 antibody (Ku70). A reduction in the levels of Ku70 can be seen in cells transfected with siRNAs targeting Ku80, when compared to the control MiaPaCa-2 clone 3 cell lysate (untransfected). α-Tubulin was used as a loading control. (15μg protein per lane loaded) *n = 3*.

- **Effect of Ku80 siRNA transfection on Ku70 Expression in MiaPaCa-2 clone 3**

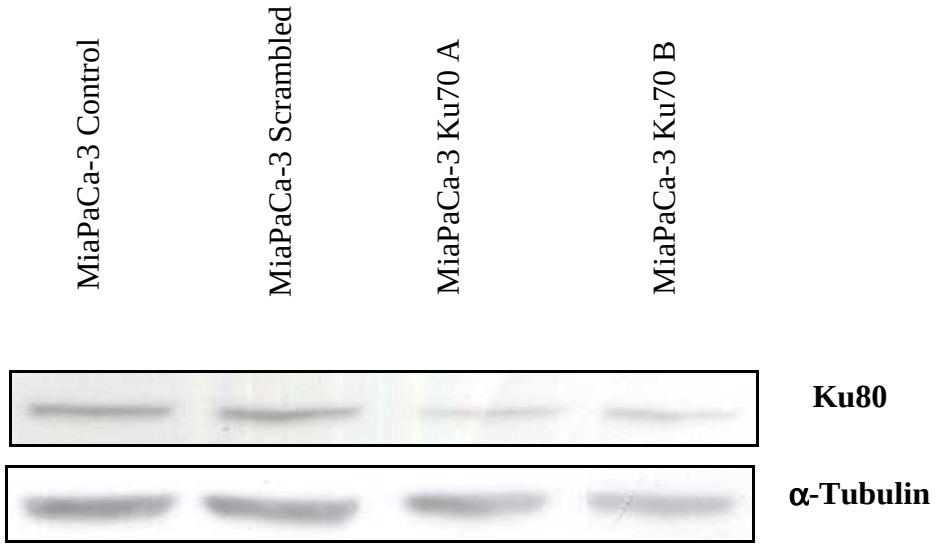

Figure 3.11.21: - Western Blot analysis of whole cell (RIPA) lysates of MiaPaCa-2 clone 3 transfected cells, separated by SDS-PAGE, probed with an ATP-dependent DNA helicase 2 subunit 1 antibody (Ku80). A reduction in the levels of Ku80 can be seen in cells transfected with siRNAs targeting Ku80, when compared to the control MiaPaCa-2 clone 3 cell lysate (untransfected). α-Tubulin was used as a loading control. (15µg protein per lane loaded) *n = 3*.

3.11.3 Expression of MAb 7B7 G5 (2) in MiaPaCa-2 clone 3 Transfected with Ku70 & Ku80 siRNAs

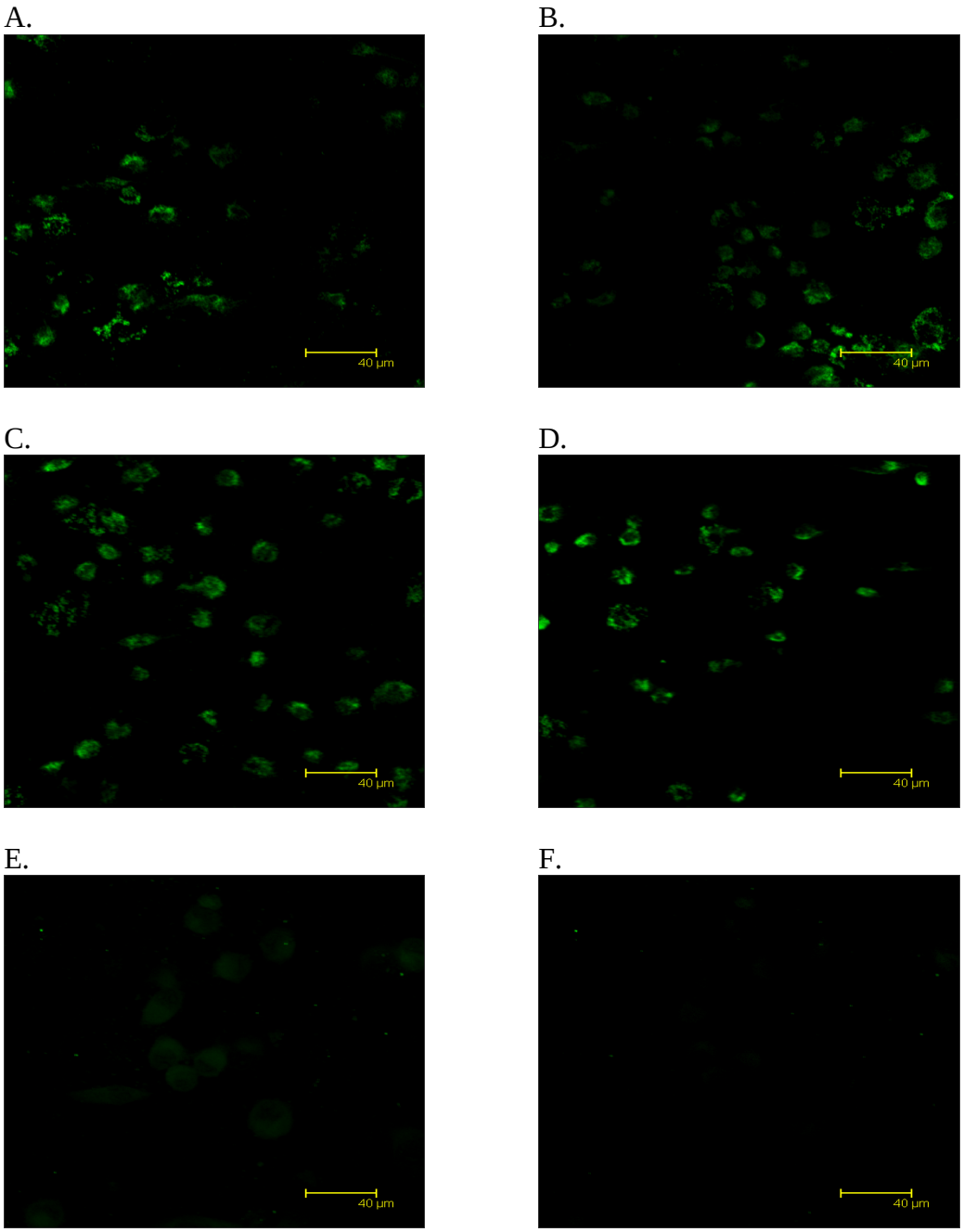

Figure 3.11.22: - Immunofluorescence analysis of MAb 7B7 G5 (2) of MiaPaCa-2 clone 3 pancreatic cancer cells (A) untransfected, (B) transfected with scrambled control, (C) transfected with Ku70A siRNA, (D) transfected with Ku70B siRNA, (E). transfected with Ku80A siRNA, (F) transfected with Ku80C siRNA. Reactivity is observed in the untransfected cells, scrambled control, and in cells transfected with Ku70 A and B (A, B, C & D), while little/no staining is observed in Ku80 transfected MiaPaCa-2 clone 3 cells (E & F). Magnification, 630X, A & B, 400X C & D. Scale Bar, 20µm

3.12 Western Blot Validation of MAb 7B7 G5 (2) Target Proteins in a Panel of Cell Lines

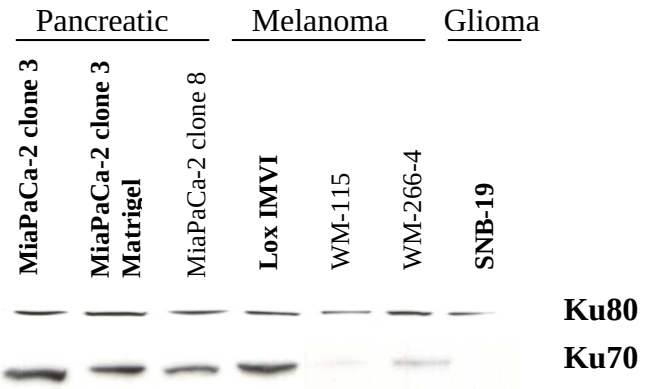

Figure 3.12: **-** Western blot analysis of pancreatic cancer cell lines, MiaPaCa-2 clone 3, MiaPaCa-2 clone 3 grown on Matrigel*, MiaPaCa-2 clone 8; Melanoma cell lines Lox IMVI, WM-115 (primary cancer), its metastatic counterpart, WM-266-4, and SNB-19 glioma cell line probed with antibodies specific for Ku80 and Ku70. Ku80 shows strong expression in all cell lines, except for SNB-19 and WM-115, which show reduced levels of expression. Ku70 has lower expression in the MiaPaCa-2 clone 8 cell line, compared to both MiaPaCa-2 clone 3 lines. In the melanoma cell lines, Ku70 shows strong expression in Lox IMVI, while expression is stronger in the metastatic WM-266-4 cell line, compared to the WM-115 primary tumour cell line. No reactive band is observed in the SNB-19 glioma cell line. *n = 3.* (See Appendix IV for representative coomassie stained gel showing equal loading). Cell lines in **bold** represent highly invasive phenotype.

* MiaPaCa-2 clone 3 cells were grown on Matrigel in order to increae the expression of proteins involved in the invasion process.

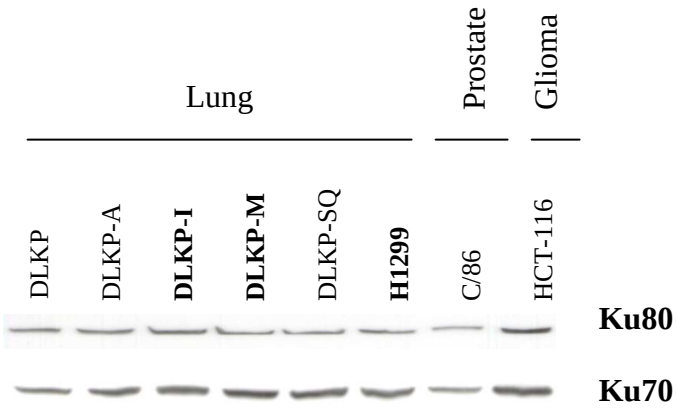

Figure 3.12.1: - Western Blot analysis of lung cancer cell lines DLKP, DLKP-A, DLKP-I, DLKP-M, DLKP-SQ and H1299; C/68 Prostate cancer cell line and HCT-116 Colon cancer cell line probed with antibodies specific for Ku80 and Ku70. Ku80 is expressed to a lesser degree in the DLKP-M and DLKP-SQ cell lines compared to DLKP-I and H1299. C/68 also shows less expression of Ku80, while HCT-116 shows strong expression for Ku80. Levels of Ku70 expression are high in all cell lines, apart from C/68, where it is expressed to a lesser degree. *n = 3.* (See Appendix IV for representative coomassie stained gel showing equal loading). Cell lines in **bold** represent highly invasive phenotype.

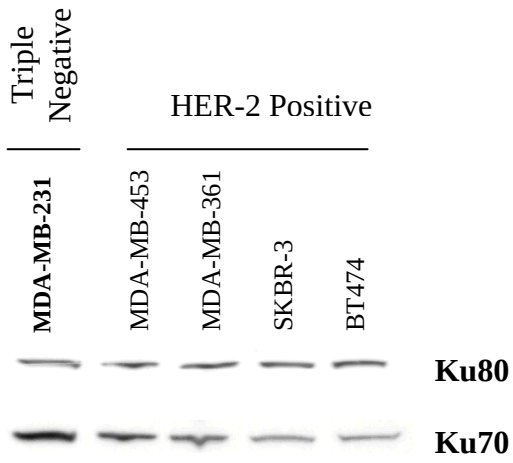

Figure 3.12.2: - Western blot analysis of HER-2 over-expressing cell lines SKBR-3, BT474, MDA-MB-453, MDA-MB-361, probed with antibodies specific for Ku80 and Ku70. Ku80 shows strong expression in all cell lines. The triple negative MDA-MB-231 cell line shows higher expression of Ku70 compared to HER2 positive cell lines. *n = 3*. (See Appendix IV for representative coomassie stained gel showing equal loading). Cell lines in **bold** represent highly invasive phenotype.

CHAPTER 4

GENERATION OF MONOCLONAL ANTIBODIES DIRECTED AGAINST MDA-MB-435-SF

4.1. Background

An initial primary immunisation, and 4 booster immunisations were carried out with MDA-MB-435-SF-Taxol10p4p-SI, a Taxol resistant variant of the parent cell line (Glynn, *et al.*, 2004), followed by a further 2 immunisations with the parent MDA-MB-435-SF cell line.

4.2 Fusion Results

Following fusion with both MDA-MB-435-SF and the Taxol variant MDA-MB-435-SF-Taxol10p4p-SI cells, as described in section 2.3.3, 436 supernatants (90.8% fusion efficiency) were screened directly for any effect on the invasive capacity on MDA-MB-435-SF cells by live and fixed cell immunofluorescence.

4.3 Preliminary Characterisation Hybridoma Supernatants

4.3.1 Screening Directly for Effects on Invasion

All resulting antibodies were screened by 96 well invasion assay method (section 2.5.2) against the parent cell line, MDA-MB-435-SF. Supernatants showing an increase or decrease in invasion levels were identified by three independent witnesses through microscopic evaluation. Controls comprised of cells with no antibody supernatant (hybridoma media added in place), with invasion levels in all cases being compared to this hybridoma medium control.

Six supernatants were chosen on the basis of a slight increase in invasion observed in relation to invasion observed with the control cells (no supernatant added) (i.e. MDA-MB-435 SF), and six supernatants that appeared to have a slight reduction in invasion were also chosen. The levels of invasion observed in MDA-MB-435-SF cells were overall very low, which made it very difficult to observe any real reduction in invasion. 24 well invasion assays were then carried out on Lox-IMVI melanoma cells. An incubation step (antibody supernatant incubated with the cell suspension at 4°C for at least 20 minutes prior to addition to invasion insert) was included in all screenings, except for the initial assays

carried out with 96-well plates. Quantification of inhibition levels of invasion was carried out through staining and counting, as described in section 2.5.2. Six antibodies that produced an inhibitory effect on cell invasion, MAbs 4E5, 3E2, 9E1, 102C, 1D2 and 104D, were chosen for further screening and characterisation.

Antibodies 4E5 & 9E1 were shown to have a consistent effect on invasion in the invasive Lox IMVI melanoma cell line (figures 4.3.1 & 4.3.2). Effects observed with MAbs 102C and 104D were not as consistent. Further analysis with MAb 9E1 indicated that this MAb consistently inhibited invasion levels in a number of *in vitro* models (the invasive LOX-IMVI melanoma cell line & the highly invasive MiaPaCa-2 clone 3 pancreatic cell line). This MAb was chosen for further characterisation.

MAb 9E1 was then cloned out by limiting dilutions (section 2.3.6), and re-screened using both 96 and 24 well invasion assays Preliminary results with MiaPaCa-2 clone 3 cells showed that clone 24 (6) exhibited consistent inhibitive effects on invasion after 48 hours, and so was chosen for further characterisation. Isotyping of MAb 9E1 24 (6) determined it to be an IgG1 antibody. Isostrip analysis was carried out as described in section 2.3.7

Figure 4.3: - Isostrip analysis of MAb 9E1 24 (26), indicating that it is an IgG1 subclass antibody (Isostrip, Roche Diagnostics, GmbH, 1493027)

A.

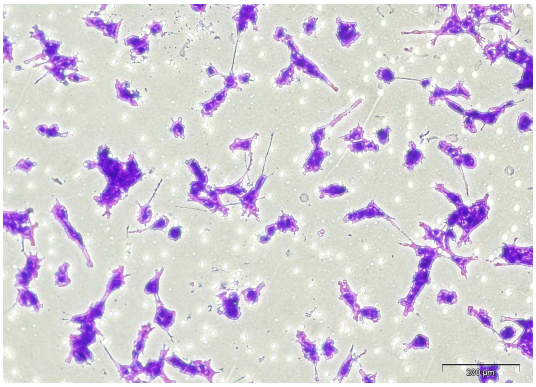

B.

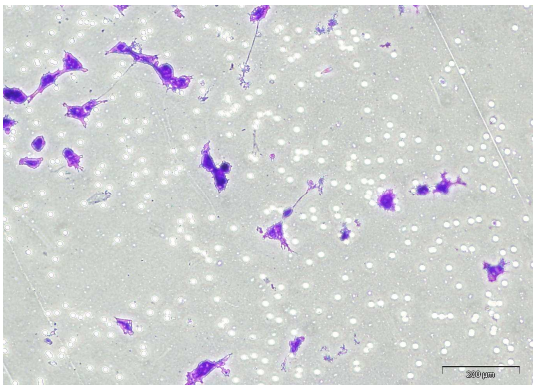

C.

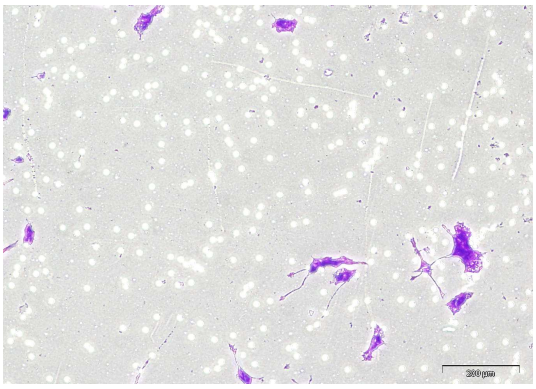

Figure 4.3.1: - Representative photomicrographs showing invasion status of LOX-IMVI melanoma cells following incubation with MAb 9E1. A decrease in invasion can be observed following incubation of cells with MAb (B) compared to control insert (A) (no MAb). A decrease in invasion is also observed following pre-incubation of cells for 5 hrs at 4°C with MAb 9E1 (C). Magnification, 100X. Scale Bar, 200µm

A.

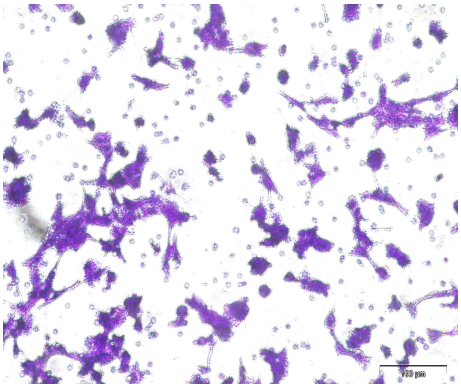

B.

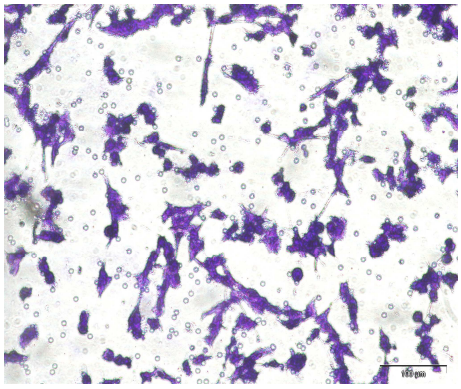

C.

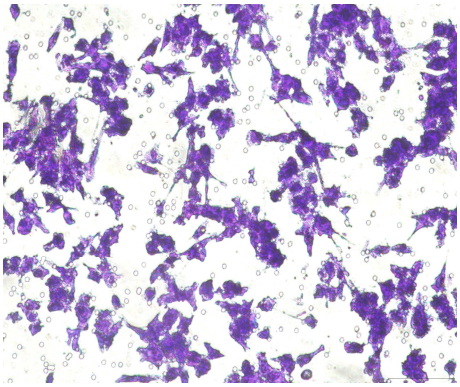

D.

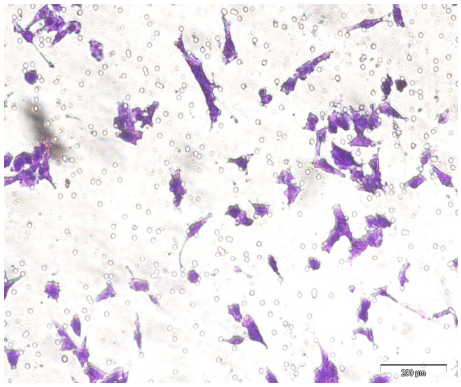

Figure 4.3.2: - Representative photomicrographs invasion status of LOX-IMVI melanoma cells following pre-incubation of cells (20 mins, 4°C) with test MAbs 7F4 (B), 7E4 (C) & 4E5 (D). A decrease in invasion can be observed following incubation with MAb 4E5 (D) compared to control insert (A) (no MAb). MAb 7F4 (B) did not appear to have any effect on invasion while there was possibly an increase in invasion following incubation with MAb 7E4 (C). Magnification, 100X. Scale Bar, 200µm.

4.3.2 Immunofluorescence Assays

Fifteen supernatants were selected on the basis of their reactivity with MDA-MB-435 SF cells using live cell immunofluorescence (approx 50% of test supernatants showed some reactivity, chosen supernatants were representative of all observed staining patterns). This staining varied between intense staining localised to the membrane of cells to more intracellular like staining. A number of supernatants resulted in a “punctuation” type of staining associated with cells. From these 15 supernatants, 4 were chosen for further characterisation. MAbs 4E5 & 7E4 showed positive staining to the inner plasma membrane on both live and fixed MDA-MB-435 SF cells. An intracellular like staining was observed, along with some inner plasma membrane positivity, on the same fixed cells with MAb 9E1, while MAb 104D showed intense membrane reactivity on preparations of live cells. Immunofluorescence analysis was carried out as described in section 2.9.1 & 2.9.2.

A.

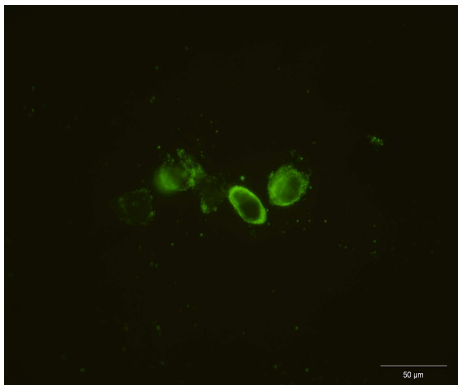

B.

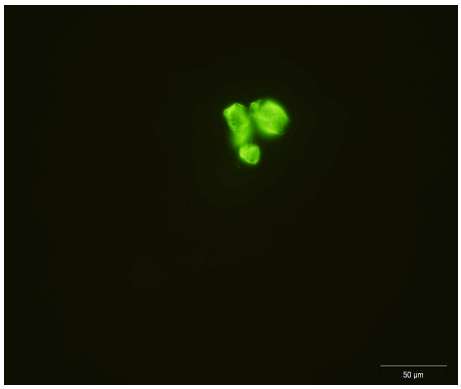

C.

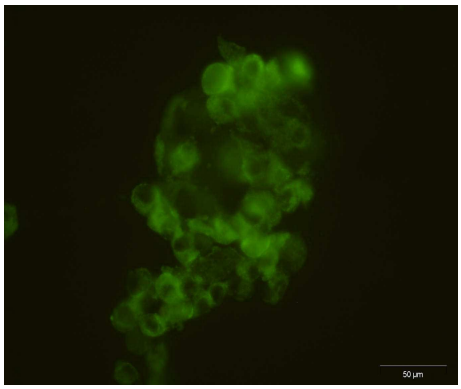

D.

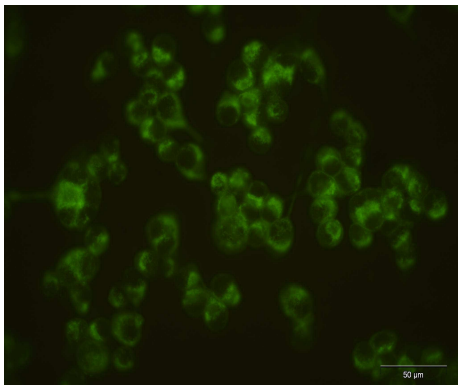

Figure 4.3.3: **-** Immunofluorescence analyses of MAb 4E5 reactivity on fixed (A) and live (B) MDA-MB-435-SF cells showing a positive staining localised to the inner plasma membrane. MAb 9E1 reactivity is also observed with MDA-MB-435-SF (C) and MDA-MB-435-SF clone 10 (highly motile variant of the MDA-MB-435-SF cell line, Joyce, H., unpublished). Magnification, 40X, scale bar = 50µm.

4.4 Investigation of Functional Effect of MAb 9E1 24 (6) in Invasive Cancer Models *In Vitro.*

MAb 9E1 24 (6) underwent further testing to observe its effects on a number of cellular processes, including:

- Proliferation: to observe what effect the MAb has on the cancer cells ability to grow.
- Invasion & Motility: to assess the MAb's effect on cellular invasion/motility
- Adhesion: to assess the MAb's impact on the adhesive abilities of a number of cell lines to ECM proteins
- Anoikis: Anoikis is a specific form of apoptosis induced by the loss or alteration of cell-cell or cell-matrix anchorage. An *in vitro* anoikis assay was used to assess any impact this MAb has on anoikis resistance.
- MMP activity: to observe what effect, if any, this MAb has on the activity of MMP-2 and MMP-9 *in vitro*.
- Cell Morphology: to observe if incubation with this MAb affects the morphology of invasive cancer cells. Highly invasive cells usually display a spindle shaped elongated morphology.

4.4.1 MAb 9E1 24 (6) Effect on Proliferation on the Invasive Pancreatic Cell Line MiaPaCa-2 clone 3

The primary goal of this work was to examine the effects of MAb 9E1 24 (6) on invasion and motility. To ensure that any changes observed in the assays were not secondary to effects on cell proliferation or survival, initial experiments were carried out to determine the effects MAb 9E1 24 (6) had on proliferation/survival of the MiaPaCa-2 clone 3 cell line. Proliferation assays were carried out as described in section 2.4.

Figure 4.4 shows that MAb 9E1 24 (6) had no impact on MiaPaCa-2 clone 3 cell proliferation/survival after a 5 day growth assay. This suggests that the MAb has no toxic, growth inhibitory or stimulatory effect on this cell line over the course of the assay.

Statistical analyses were carried out on the average absorbancy readings of the control Vs test wells, over biological triplicates.

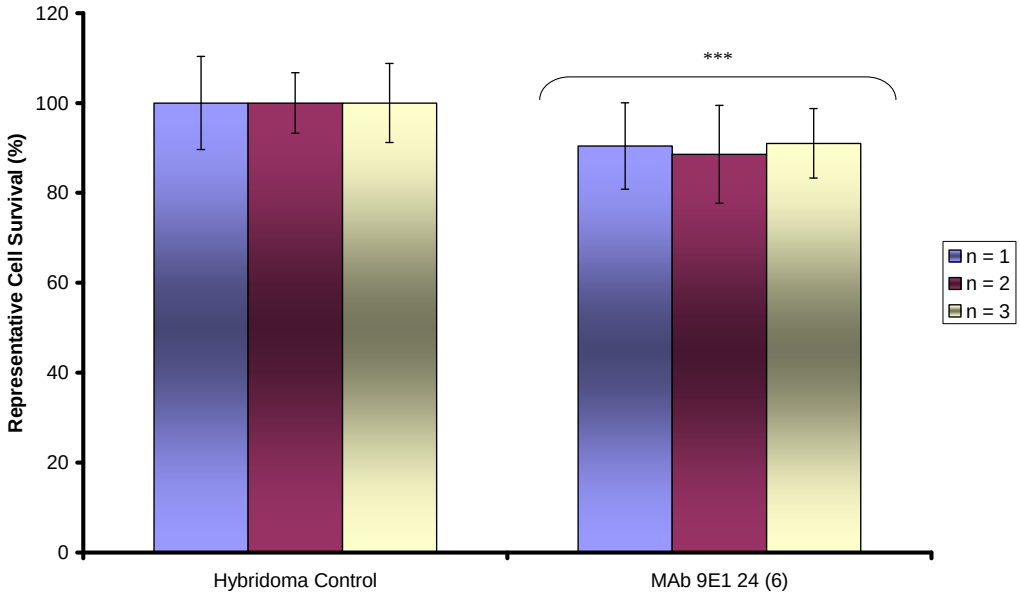

Figure 4.4: - Histogram of MAb 9E1 24 (6) showing little inhibition of proliferation in MiaPaCa-2 clone 3 compared to control hybridoma medium (no MAb) representing 100% proliferation after 96 hours. Statistics; * $p \leq 0.05$, ** $p \leq 0.01$, *** $p \leq 0.005$, Student's t-test. *n = 3.* Error bars calculated using ± standard deviation.

4.4.2 MAb 9E1 24 (6) Effect on Invasion on Invasive Cancer Cell Lines

In order to ascertain what effect MAb 9E1 24 (6) has on cell invasion and motility, Invasion and Motility assays were carried out (as described in section 2.5.2 & 2.5.3.) on a range of invasive cancer cell lines. Cells were incubated with the MAb, and after 24-48 hrs, depending on the cell line, levels of cellular invasion/motility were quantified.

Figure 4.4.2 shows that MAb 9E1 24 (6) significantly inhibited invasion in the MiaPaCa-2 clone 3 cell line. However, no such inhibition was noted with the BxPc-3 cell line. Significant inhibition of invasion was also observed in the DLKP-I, DLKP-M and H1299 lung cancer cell lines, the MDA-MD-231 breast cancer cell line, the Lox IMVI melanoma cell line and the c/68 prostate cell line. Inhibition of invasion was also observed in the SKBR-3 breast cancer cell line. No inhibition was observed in the SNB-19 glioma cell line or the BxPc-3 pancreatic cell line. In the HCT-116 colon cancer cell line, a significant *increase* in cell invasion was observed upon exposure to MAb 9E1 24 (6). An increase in invasion was also observed in the MDA-MB-157 breast cancer cell line. These results indicate that MAb 9E1 24 (6) can successfully inhibit the invasion process in a number of cell types, but can also increase cell invasion in others.

Figure 4.4.3 shows that MAb 9E1 24 (6) significantly reduces cell motility in the MiaPaCa-2 clone 3 cell line, by but to a lesser extent than those seen in the invasion assay.

Statistical analyses were carried out with the average cell counts of control Vs sample inserts over biological triplicates (section 2.15).

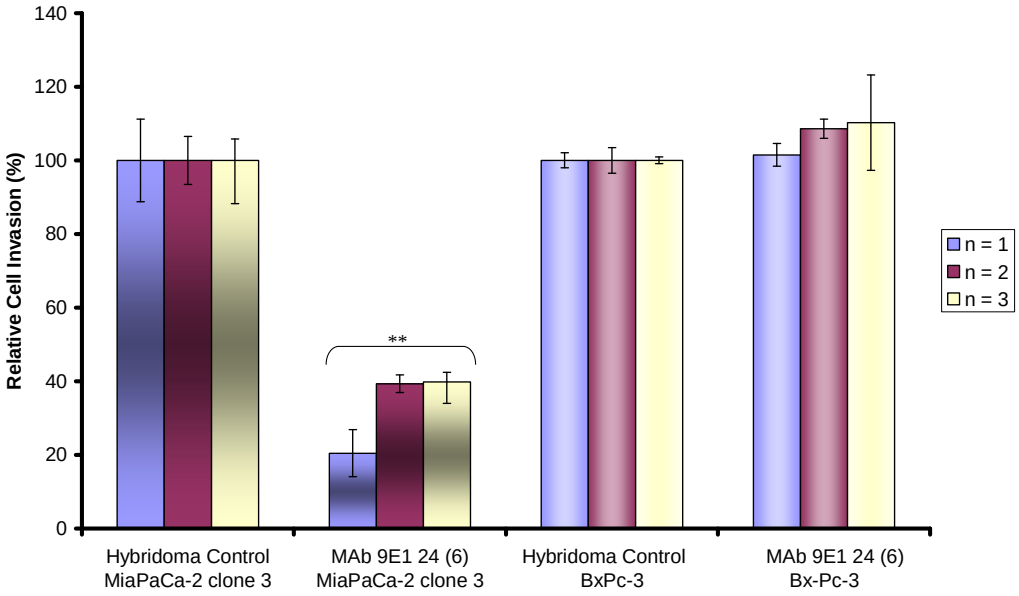

Figure 4.4.1: - Histogram of MAb 9E1 24 (6) showing significant inhibition of invasion in MiaPaCa-2 clone 3, but no inhibition in BxPc-3, compared to control hybridoma medium (no MAb) representing 100% invasion, after 48 hours. Statistics; * $p \leq 0.05$, ** $p \leq 0.01$, *** $p \leq 0.005$, Student's t-test. *n = 3.* Error bars calculated using ± standard deviation.

Hybridoma Medium Control *MAb 9E1 24 (6)*

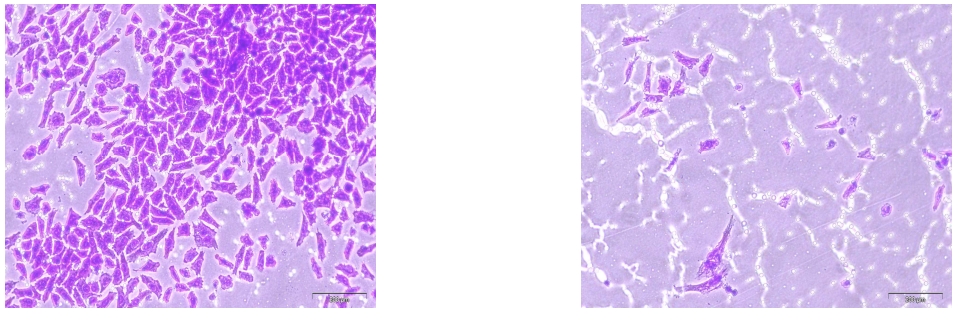

MiaPaCa-2 clone 3

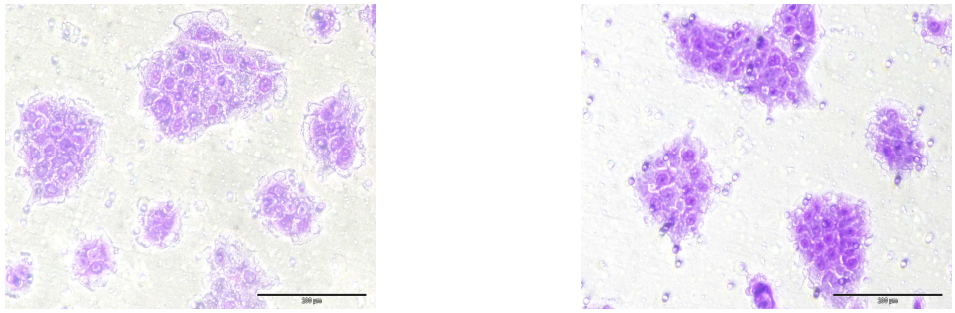

BxPc-3

Figure 4.4.2: - Representative photomicrographs showing invasion status of MiaPaCa-2 clone 3 and BxPc-3 cells following incubation with MAb 9E1 24 (6) for 48 hours. A decrease in invasion can be observed in MiaPaCa-2 clone 3 following addition of MAb 9E1 24 (6) (b) compared to control insert (a) (no antibody supernatant). No inhibitory effect is seen in BxPc-3. Magnification, 100X. Scale Bar, 200µm.

4.4.3 MAb 9E1 24 (6) Inhibition of Motility on the Pancreatic Cell Line MiaPaCa-2 clone 3

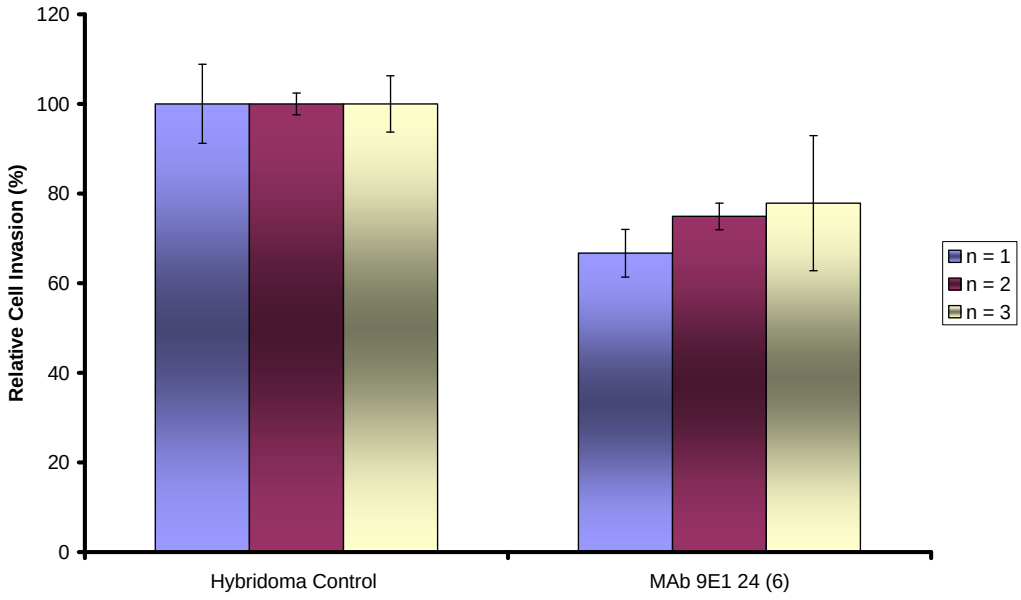

Figure 4.4.3: - Histogram of MAb 9E1 24 (6) showing inhibition of motility in MiaPaCa-2 clone 3 compared to control hybridoma medium (no MAb) representing 100% motility after 24 hours. Statistics; * $p \leq 0.05$, ** $p \leq 0.01$, *** $p \leq 0.005$, Student's t-test. *n = 3.* Error bars calculated using ± standard deviation.

4.4.4 MAb 9E1 24 (6) Effect on Invasion on the Large-Cell Lung Cancer Cell Line H1299 and Invasive Variants of the NSCLC DLKP Cell Line DLKP-I & DLKP-M

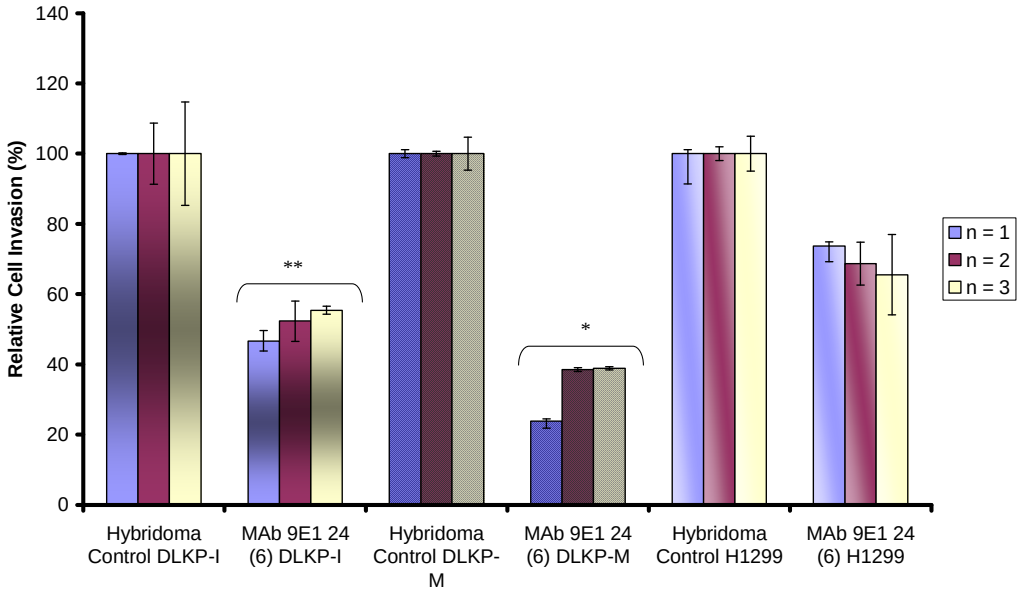

Figure 4.4.4: - Histogram of MAb 9E1 24 (6) showing significant inhibition of invasion in DLKP-I and DLKP-M compared to control hybridoma medium (no MAb) representing 100% invasion after 24 hours. Inhibition of invasion observed in the H1299 cell line did not reach statistical significance. Statistics; * $p \leq 0.05$, ** $p \leq 0.01$, *** $p \leq 0.005$, Student's t-test. $n = 3$. Error bars calculated using ± standard deviation.

Hybridoma Medium Control *MAb 9E1 24 (6)*

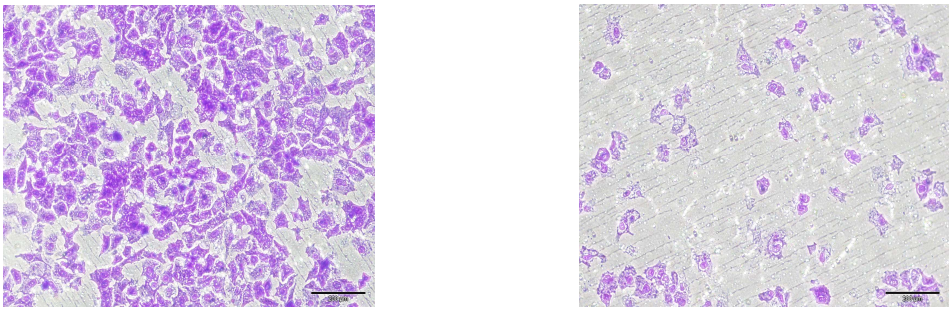

DLKP-I

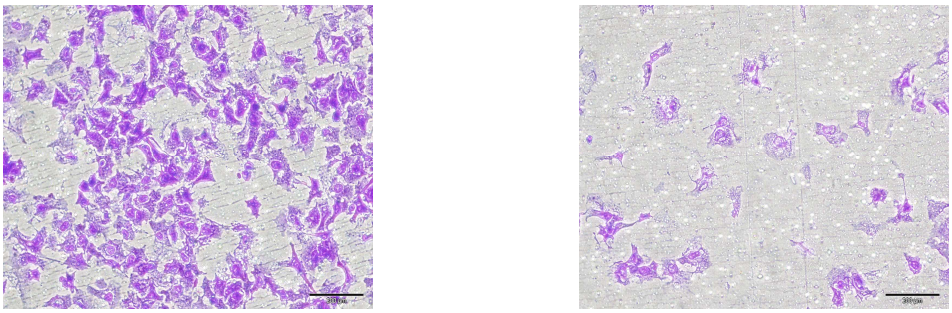

DLKP-M

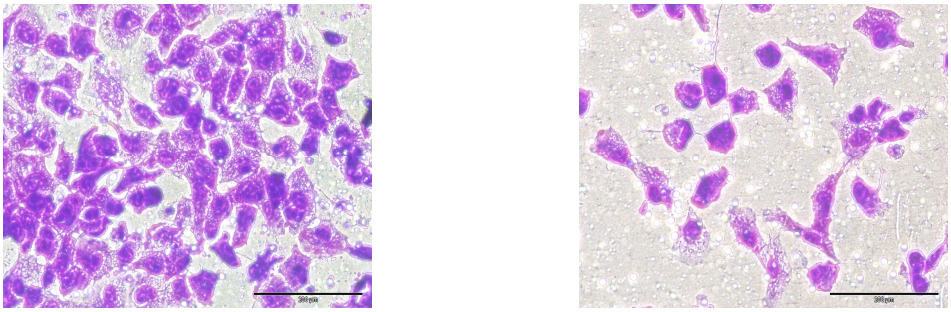

H1299

Figure 4.4.5: - Representative photomicrographs showing invasion status of DLKP-I, DLKP-M and H1299 cells following 24hr incubation with MAb 9E1 G5 (2). A decrease in invasion can be observed following addition of MAb 9E1 24 (6) (b) compared to control insert (a) (no MAb) in all three cell lines. Magnification, DLKP-I & DLKP-M, 100X; H1299, 200X. Scale Bar, 200µm.

4.4.5 MAb 9E1 24 (6) Effect on Invasion on the DLKP-M Lung Cancer Cell Line: - Dose Response

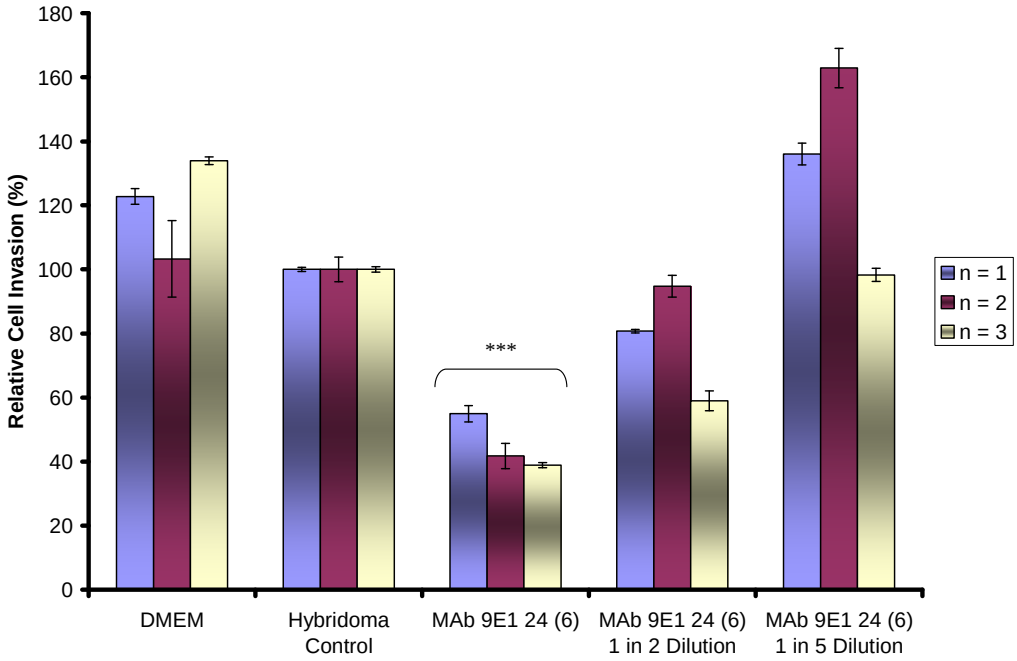

Figure 4.4.6: - Histogram of MAb 9E1 24 (6) showing significant inhibition of invasion in DLKP-M compared to control hybridoma medium (no MAb) representing 100% invasion after 24 hours. Statistics; * $p \leq 0.05$, Student's t-test. *n = 3.* Error bars calculated using ± standard deviation.

A dose response inhibitive effect is also observed with 1:2 and 1:5 dilutions of MAb showing less inhibition compared to neat MAb.

4.4.6 MAb 9E1 24 (6) Effect on Invasion on the Invasive, Triple Negative Breast cancer Cell Lines MDA-MB-231, MDA-MB-157 and the HER-2 Over Expressing Breast Cell Line, SKBR-3

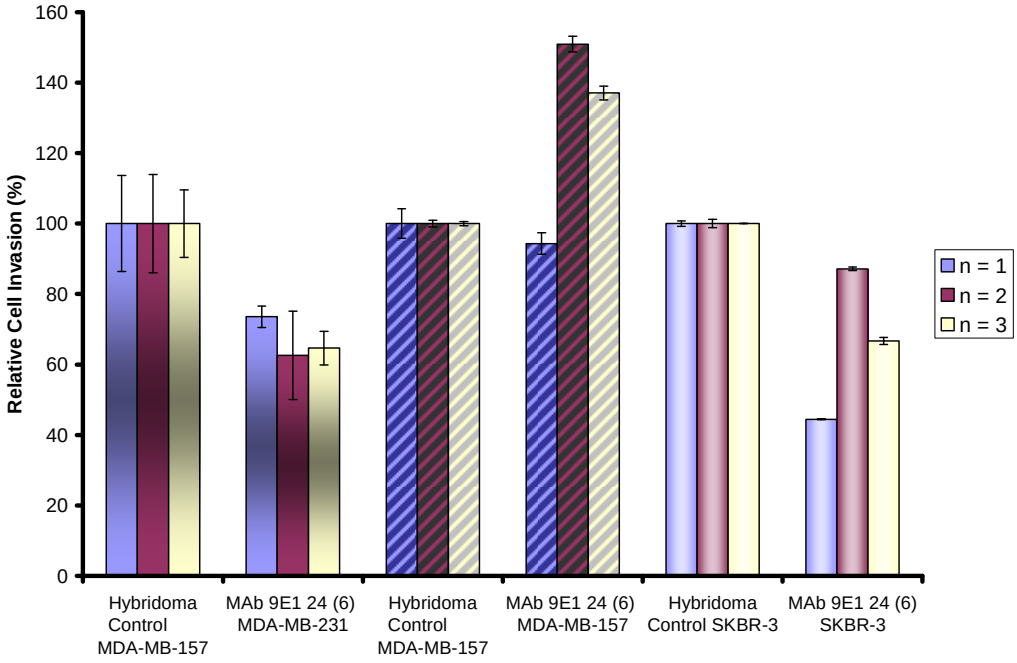

Figure 4.4.7: - Histogram of MAb 9E1 24 (6) showing inhibition of invasion in MDA-MB-231, but an increase in invasion in MDA-MB-157, and inhibition of invasion in SKBR-3, compared to control hybridoma medium (no MAb) representing 100% invasion after 24 hours. Statistics; * $p \leq 0.05$, ** $p \leq 0.01$, *** $p \leq 0.005$, Student's t-test. *n = 3.* Error bars calculated using ± standard deviation.

Hybridoma Medium Control *MAb 9E1 24 (6)*

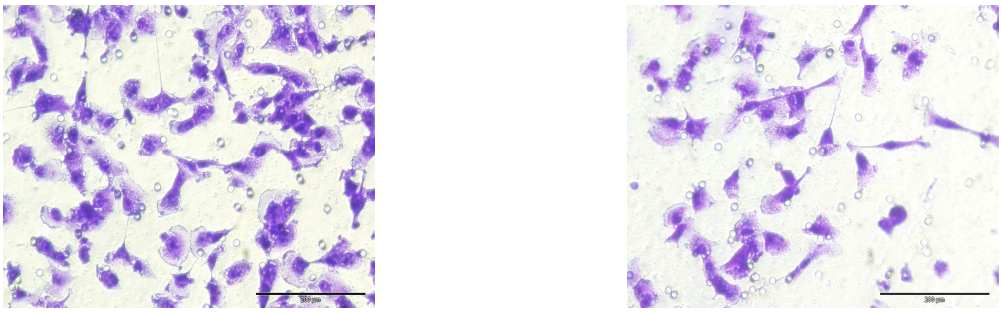

MDA-MB-231

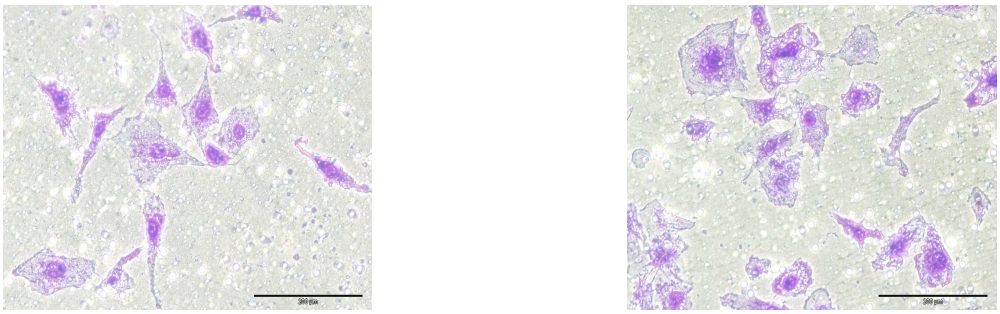

MDA-MB-157

Figure 4.4.8: - Representative photomicrographs showing invasion status of MDA-MDA-231 and MDA-MB-157 cells following incubation with MAb 9E1 24 (6). A decrease in invasion can be observed following addition of MAb 9E1 24 (6) (b) compared to control insert (a) (no MAb) in the MDA-MB-231 and SKBR-3 cell lines. However, a slight increase in invasion is observed in the MDA-MB-157 cell line. Magnification, 100X. Scale Bar, 200µm.

4.4.7 MAb 9E1 24 (6) Effect of Invasion in the Invasive Glioma Cell Line SNB-19

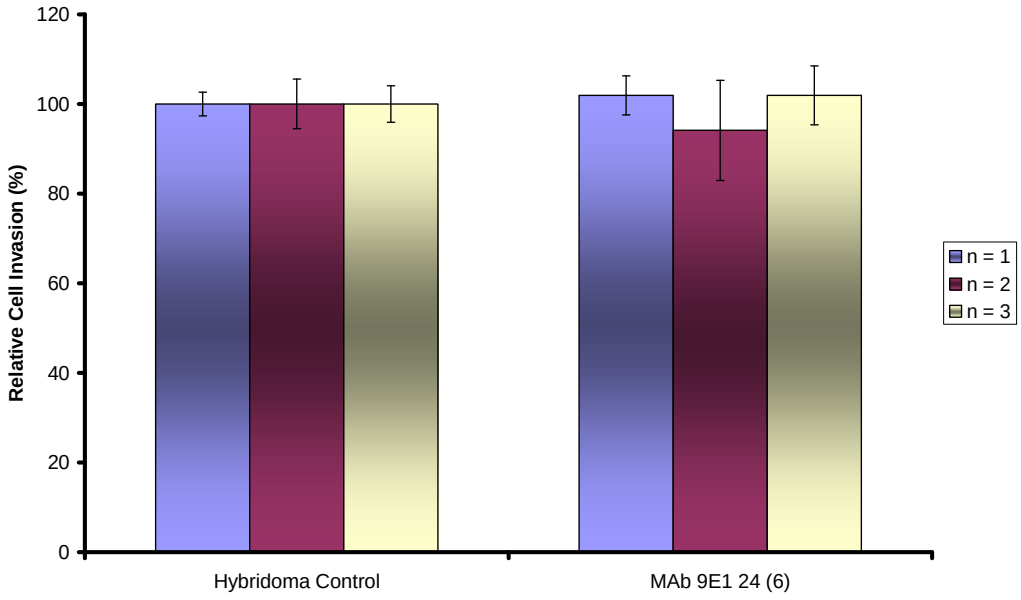

Hybridoma Medium Control *MAb 9E1 24 (6)*

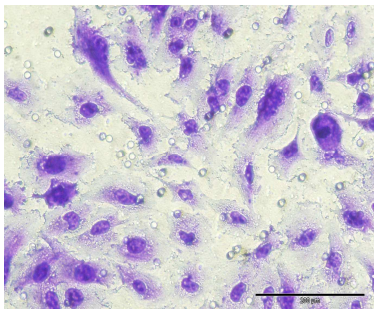

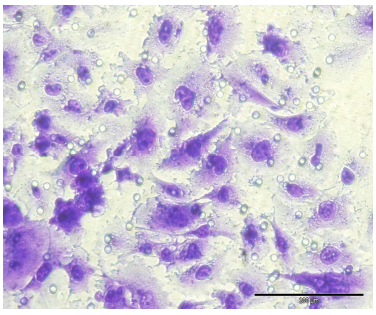

Figure 4.4.9: - Histogram and representative photomicrographs of MAb 9E1 24 (6) showing no inhibition of invasion in SNB-19 compared to control hybridoma medium (no MAb) representing 100% invasion after 24 hours. Statistics; * $p \leq 0.05$, ** $p \leq 0.01$, *** $p \leq 0.005$, Student's t-test. *n = 3.* Magnification, 100X. Scale Bar, 200µm. Error bars calculated using ± standard deviation.

4.4.8 MAb 9E1 24 (6) Effect of Invasion on the Invasive Melanoma Cell Line Lox IMVI

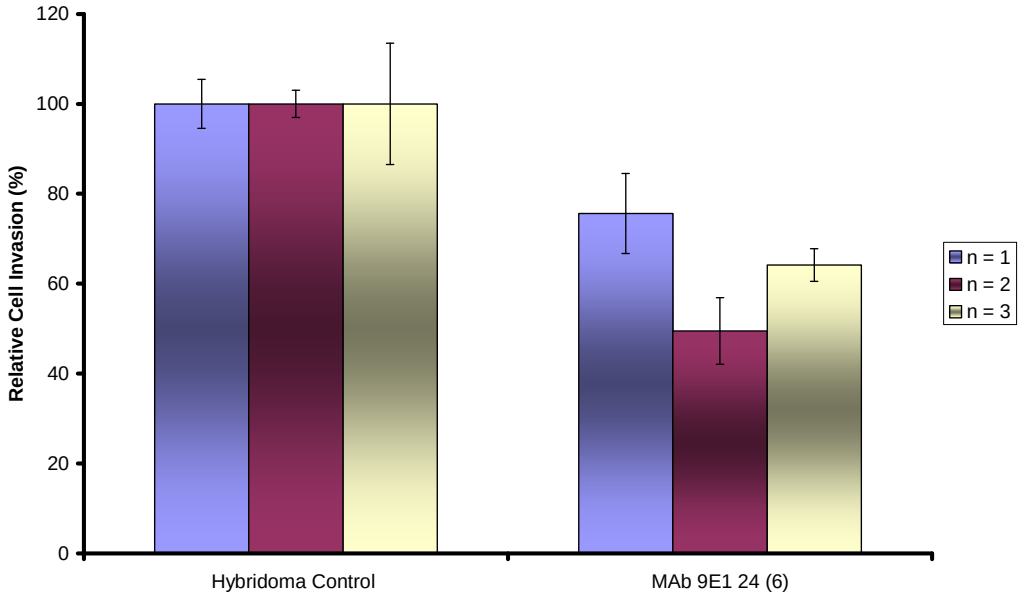

Hybridoma Medium Control

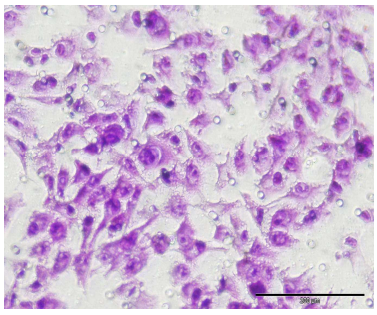

MAb 9E1 24 (6)

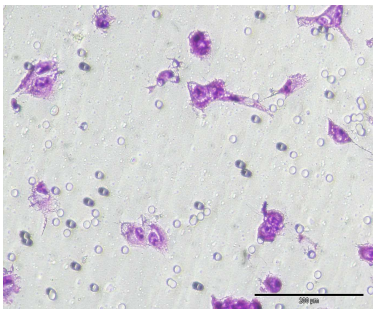

Figure 4.4.10: - Histogram and representative photomicrographs of MAb 9E1 24 (6) showing inhibition of invasion in Lox IMVI compared to control hybridoma medium (no MAb) representing 100% motility after 24hrs. Statistics; * $p \leq 0.05$, ** $p \leq 0.01$, *** $p \leq 0.005$, Student's t-test. *n = 3.* Error bars calculated using ± standard deviation. Magnification, 100X. Scale Bar, 200µm.

4.4.9 MAb 9E1 24 (6) Effect on Invasion on the Invasive Prostate Cell line C/68

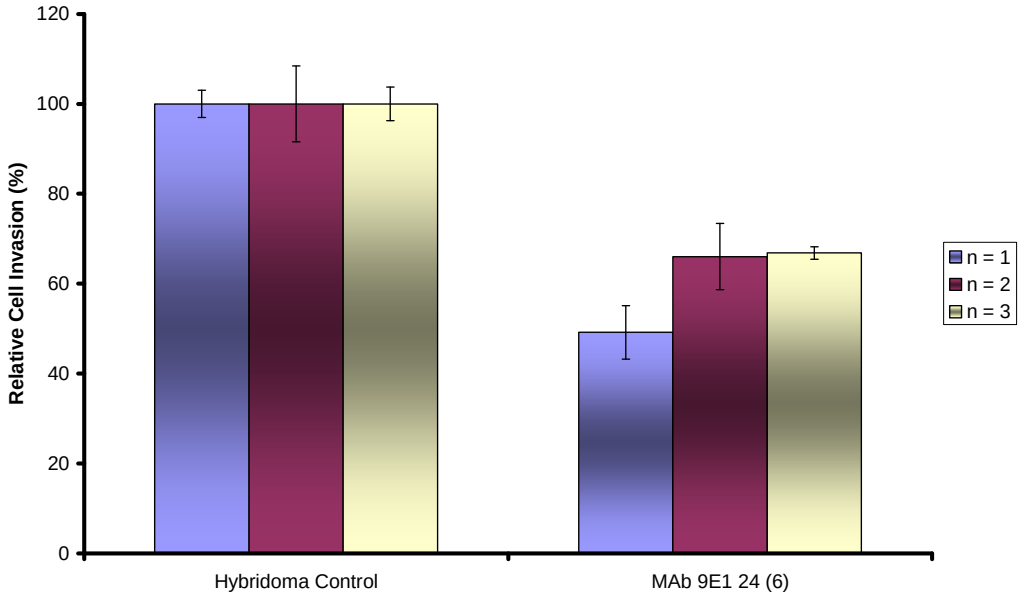

Hybridoma Medium Control *MAb 9E1 24 (6)*

Figure 4.4.11: - Histogram and representative photomicrographs of MAb 9E1 24 (6) showing inhibition of invasion in C/68 compared to control hybridoma medium (no MAb) representing 100% invasion after 24 hours. Statistics; * $p \leq 0.05$, ** $p \leq 0.01$, *** $p \leq 0.005$, Student's t-test. *n = 3.* Error bars calculated using ± standard deviation. Magnification, 100X. Scale Bar, 200µm.

4.4.10 MAb 9E1 24 (6) Effect on Invasion on the Invasive Colorectal Cell line HCT-116 – Dose Response

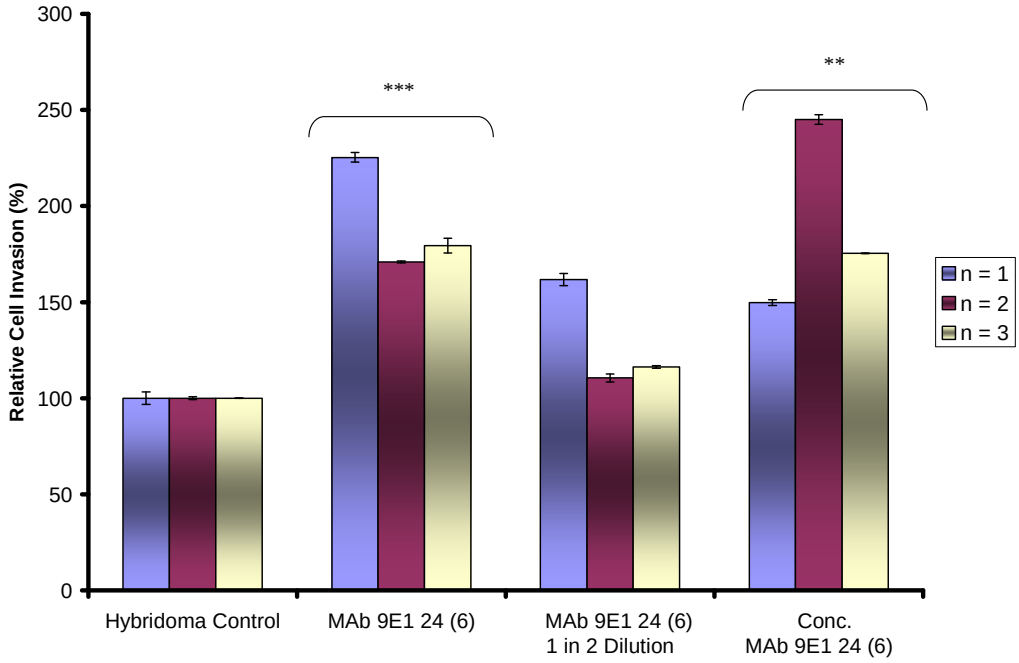

Hybridoma Medium Control

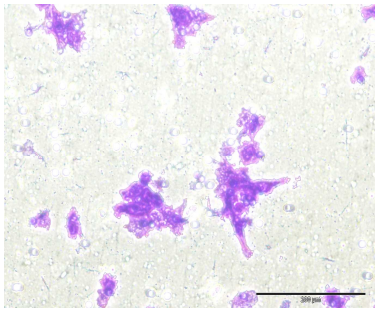

MAb 9E1 24 (6)

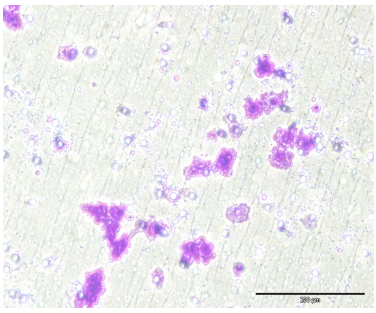

Figure 4.4.12: - Representative representative histogram and photomicrographs of MAb 9E1 24 (6) showing a significant increase in invasion in HCT-116 compared to control hybridoma medium (no MAb) representing 100% invasion after 24 hours. Statistics; * $p \leq 0.05$, ** $p \leq 0.01$, *** $p \leq 0.005$, Student's t-test. *n = 3.* Error bars calculated using ± standard deviation.

A dose response inhibitive effect is also observed on all dates with 1:2 dilutions of the MAb showing less inhibition compared to neat MAb. Magnification, 100X. Scale Bar, 200µm.

Cancer Type	Cell Line	Mean Inhibition Levels	P value
Breast	MDA-MB-157	22.6% *increase*	0.6
	MDA-MD-231	33%	0.19
	SKBR-3	33%	0.22
Lung	DLKP-I	50.8%	0.001
	DLKP-M	64%	0.02
	H1299	24.6%	0.18
Pancreatic	MiaPaCa-2 clone 3	66%	0.01
	BxPc-3	6.7% *increase*	0.64
Melanoma	Lox IMVI	36.9%	0.13
Glioma	SNB-19	0.7%	0.9
Prostate	C/68	39.3%	0.07
Colon	HCT-116	91.8% *increase*	0.0014

Table 4.4: - Effect of MAb 9E1 24 (6) on invasion levels in a panel of cell lines.

4.4.12 MAb 9E1 24 (6) Effect on Adhesion to Matrigel on the Invasive Pancreatic Cancer Cell Line MiaPaCa-2 clone 3 and the Invasive NSCLC DLKP-M Cell Line

Adhesion assays were carried out in order to investigate what effect MAb 9E1 24 (6) had on the ability of cancer cells to attach to ECM proteins. The effect of the MAb on the ability of MiaPaCa-2 clone 3 and DLKP-M cells to adhere to matrigel was investigated. Adhesion assays were performed as described in section 2.5.4.

In figure 4.4.13, MAb 9E1 24 (6) slightly reduced adhesion of MiaPaCa-2 clone 3 cells to matrigel *in vitro*. A significant decrease in adherence of DLKP-M cells to matrigel was also observed (figure 4.4.14). These results indicate that MAb 9E1 24 (6) can interfere with the ability of cancer cells to attach to components of the ECM.

Statistical analyse were carried out on the average absorbancy reading of control Vs sample wells over biological triplicates.

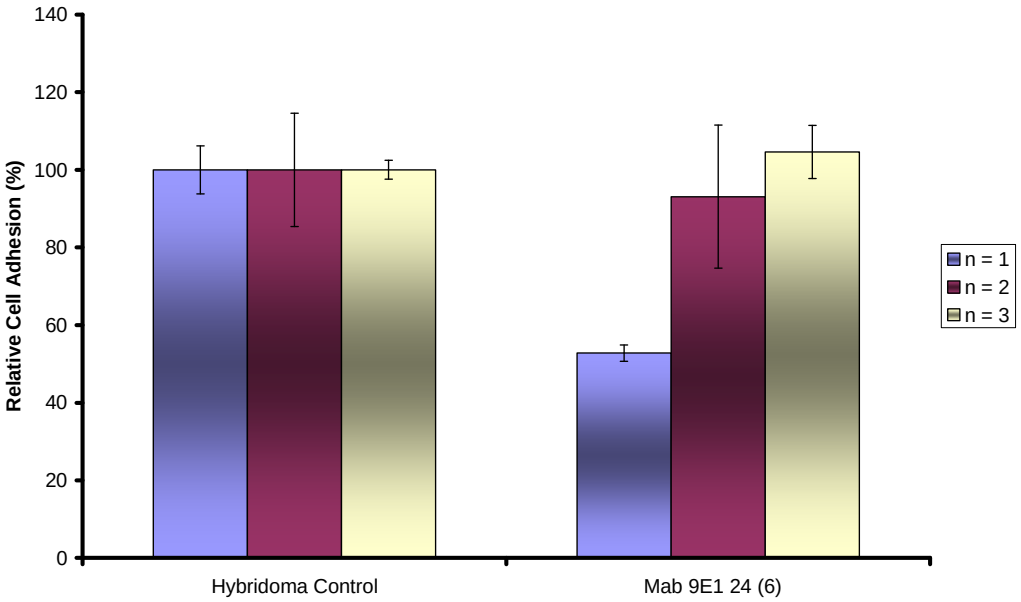

Figure 4.4.13: - Adhesion of MiaPaCa-2 clone 3 to ECM protein, fibronectin. Results are expressed as percentage adhesion to fibronectin in the presence of MAb 9E1 24 (6), compared to adhesion to fibronectin in the presence of control hybridoma medium (no MAb). Cells grown in the presence of MAb 9E1 24 (6) for 24 hrs, showed a decrease in adhesion to fibronectin when compared to the control. Statistics; * $p \leq 0.05$, ** $p \leq 0.01$, *** $p \leq 0.005$, Student's t-test. *n = 3.* Error bars calculated using ± standard deviation.

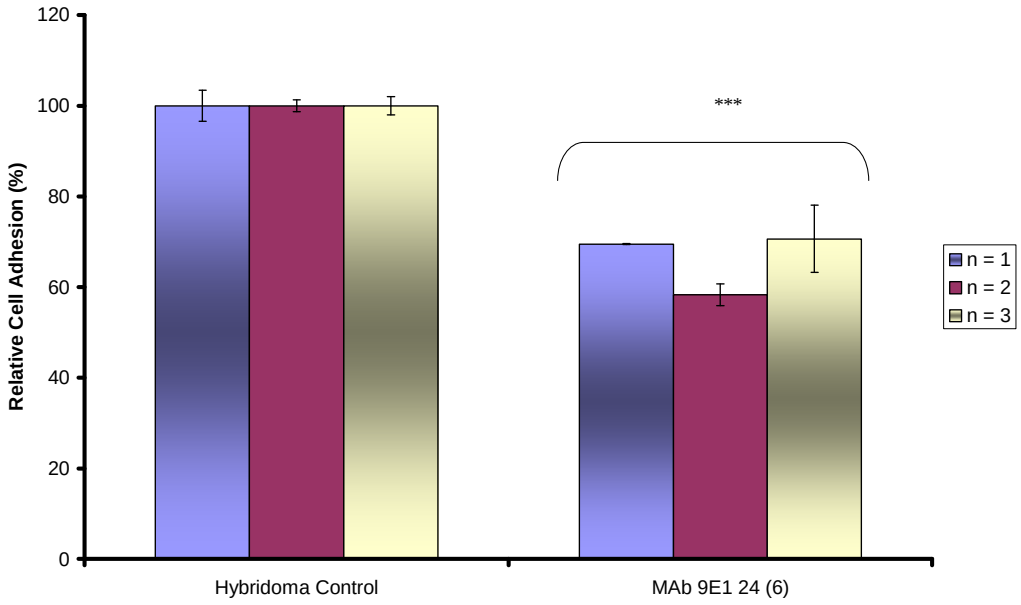

Figure 4.4.14: - Adhesion of DLKP-M to ECM protein, matrigel. Results are expressed as percentage adhesion to matrigel in the presence of MAb 9E1 24 (6), compared to adhesion to matrigel in the presence of control hybridoma medium (no MAb). Cells grown in the presence of MAb 9E1 24 (6) for 24 hrs, showed a significant decrease in adhesion to matrigel when compared to the control. Statistics; * $p \leq 0.05$, ** $p \leq 0.01$, *** $p \leq 0.005$, Student's t-test. *n = 3.* Error bars calculated using ± standard deviation.

4.4.13 MAb 9E1 24 (6) Effect on Anoikis on the Invasive Pancreatic Cancer Cell Line MiaPaCa-2 clone 3 and on the Invasive NSCLC DLKP-M Cell Line

To determine whether MAb 9E1 24 (6) effects anoikis resistance *in vitro*, Anoikis assays were carried out, on the MiaPaCa-2 clone 3 and DLKP-M cell lines. Anoikis is a specific form of apoptosis induced by the loss or alteration of cell-cell or cell-matrix anchorage. MiaPaCa-2 clone 3 has been shown to have a high level of anoikis resistance (Walsh *et al*., 2007), while DLKP-M has been shown to be 50% resistant to anoikis (Dr. Keenan, NICB, unpublished results). In this study, the effect of MAb 9E1 24 (6) on the above cell lines growing in anoikis-inducing conditions was investigated. Anoikis assays were carried out as described in section 2.6.

Figure 4.4.15 shows that MAb 9E1 24 (6) has no significant effect on the cells when there are growing in Anoikis-inducing conditions. The cells do not display any increased or decreased levels of anoikis resistance, indicating that MAb 9E1 24 (6) does not effect this cellular process.

Statistical analyse were carried out on the average absorbancy reading of control Vs sample wells over biological triplicates.

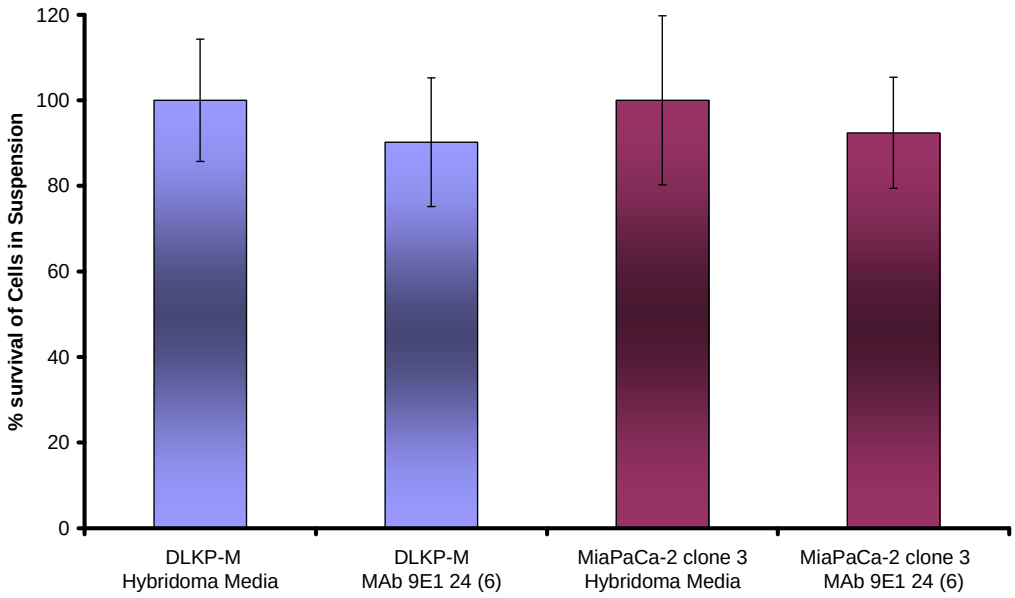

Figure 4.4.15: - Representative histogram showing percentage survival of non-adherent cells (24 hrs poly-HEMA treated plastic) incubated in the presence of MAb 9E1 24 (6). No effect on cell survivability is observed when compared to cells growing in the presence of no MAb. Statistical significance was not achieved in this experiment. Data shown is mean ± standard deviation (*n*= 3).

4.4.14 Morphological Change of MiaPaCa-2 clone 3 Cells Incubated with MAb 9E1 24 (6)

MiaPaCa-2 clone 3 cells display an elongated, splindle-like morphology, which is associated with an invasive phenotype. To investigate whether MAb 9E1 24 (6) effects cell morphology, MiaPaCa-2 clone 3 cells were incubated with the MAb for 24hrs, after which, cell morphology was observed. This assay was carried out as described in section 2.8.

Figure 4.4.16 shows the effect MAb 9E1 24 (6) has on the MiaPaCa-2 clone 3 cells, compared to cells grown in the absence of the MAb. It is quite clear that the cells have lost their elongated, spindle-like shape, and exhibit a more rounded appearance, similar to the less invasive MiaPaCa-2 clone 8 cell morphology. As a spindle-like cell morphology has been linked to cell invasion (Yilmaz *et al*., 2007), this change may indicate that the invasive capabilities of the MiaPaca-2 clone 3 cells have been diminished following incubation with MAb 9E1 24 (6).

A.

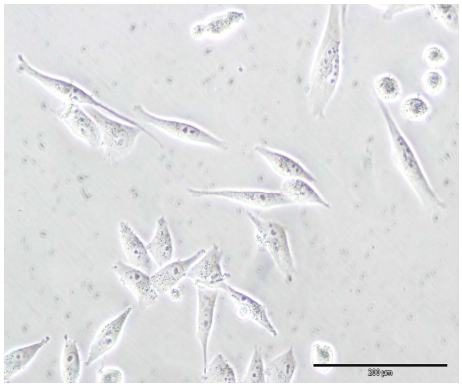

B.

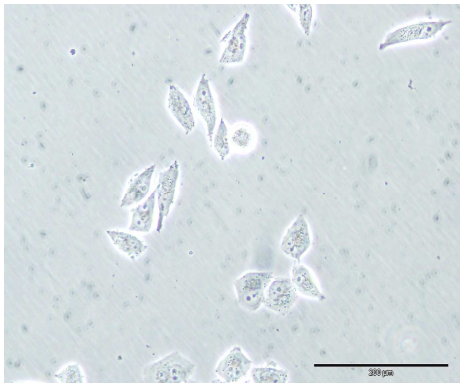

Figure 4.4.16: - Representative photomicrographs showing morphology of MiaPaCa-2 clone 3 cells following incubation with supernatant 9E1 24 (6) for 24 hours. Cells incubated with MAb 9E1 24 (6) (B) have lost their elongated, spindle-like morphology, and have become more rounded. Cells incubated with hybridoma media (A) retain their normal morphology. Magnification, 100X. Scale Bar, 200µm.

4.4.15 MAb 9E1 24 (6) Effect on MMP-9 Activity in the Invasive Breast Cancer Cell Line MDA-MB-231

Zymography assays were carried out in order to investigate the effect of MAb 9E1 24 (6) has on MMP-9 expression. MMP-9 is involved in the degradation of proteins in the ECM and plays a crucial role in localised degradation of the basement membrane, and subsequent cellular invasion. MDA-MB-231 was chosen for this study, as it is known to express MMP-9 (Hegedus *et al*., 2008). Conditioned media from cells incubated with the MAb were collected, as described in section 2.7.1. This was then separated on a zymography gel, which was then subsequently stained. The zymography assay was carried out as described in section 2.7.2.

Figure 4.4.17 shows that MAb 9E1 24 (6) decreases the activity of active MMP-9 in the MDA-MB-231 cell line, when compared to cells grown in the absence of the MAb. This is also observed in the zymography gel. This preliminary result indicates that MAb 9E1 24 (6) inhibits the activity of MMP-9 *in vitro* (see Appendix VI for complete zymograpgy gel).

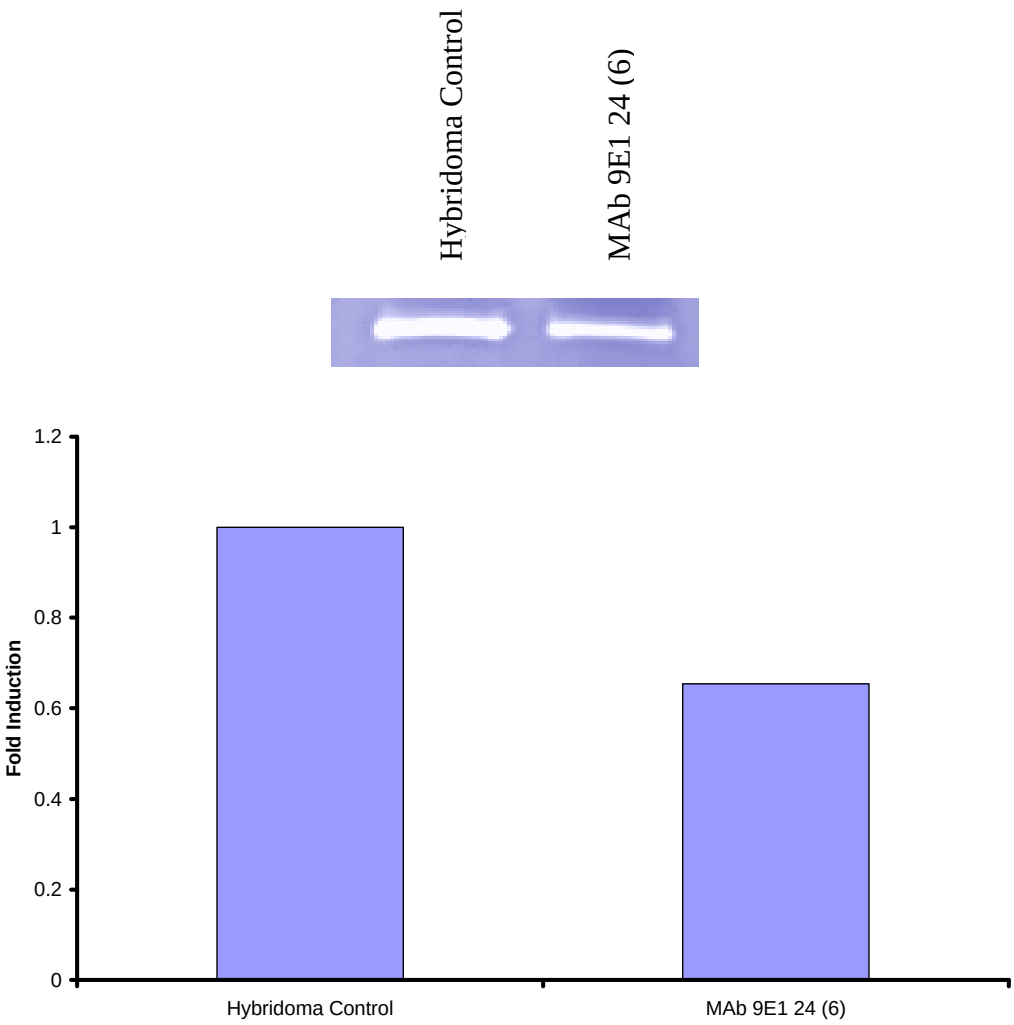

Figure 4.4.17: - Graph and zymography gel showing effect of MAb 9E1 24 (6) on MMP-9 activity in the MDA-MB-231 breast cell line. Cells incubated with MAb 9E1 24 (6) show a decrease in the activity of MMP-9 when compared to control hybridoma medium (no MAb) representing normal MMP-9 activity.

4.5 Immunofluorescence Studies of MAb 9E1 24 (6) in a Panel of Cancer Cell Lines

A.

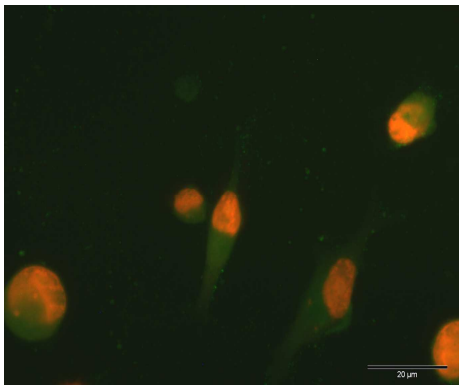

B.

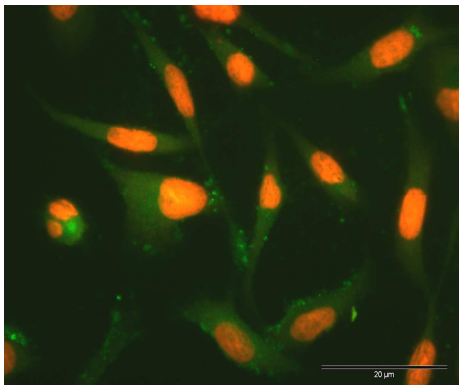

C.

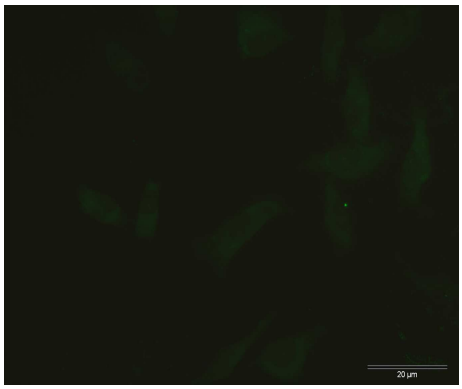

D.

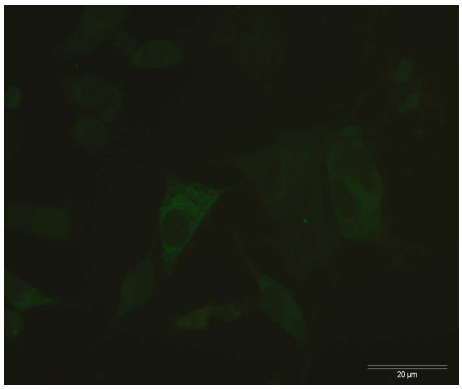

Figure 4.5: - Immunofluorescence analysis of MAb 9E1 24 (6) on MiaPaCa-2 clone 3 and clone 8 pancreatic cells. Positive staining, localised to the membrane, with some cytoplasmic reactivity, is observed in the invasive MiaPaCa-2 clone 3 cells (A & C), Staining in the poorly invasive MiaPaCa-2 clone 8 cells is slightly stronger compared to the invasive clone 3 (B & D). Magnification 400X, scale bar = 20µm. (A & B counter stained with Propidium Iodide).

A.

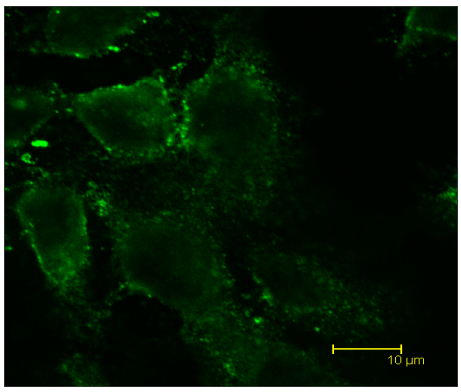

B.

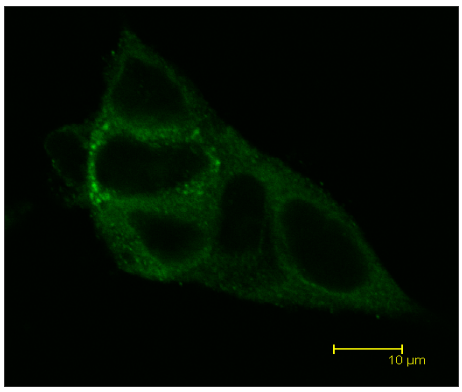

C.

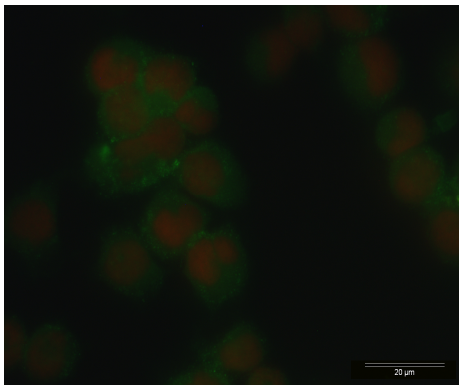

D.

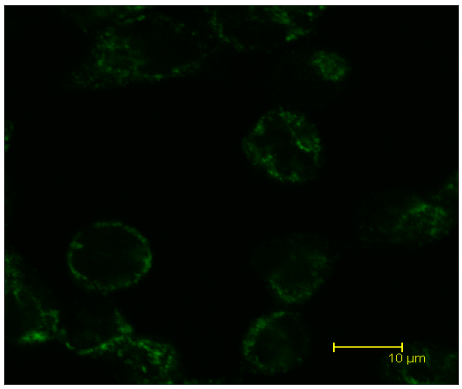

Figure 4.5.1: - Immunofluorescence analysis of (A) SKBR-3 and (B) BT474 HER-2 over expressing breast cancer cell lines; (C) DLKP-SQ and (D), DLPK-SQ-Mitox 6p lung carcinoma cells. MAb 9E1 24 (6) shows punctuate type membrane, reactivity in SKBR-3, BT474 and DLKP-SQ-Mitox-6p cells. Weak reactivity is observed in DLKP-SQ cells. Magnification, 630X, scale bar 10µm. (C counter stained with Propidium Iodide).

4.6 Western Blotting Analysis with MAb 9E1 24 (6)

Western blotting analysis was carried out on the MiaPaCa-2 clone 3 cell line (in which MAb 9E1 24 (6) showed a decrease in invasion) in order to establish the reactive antigen and its molecular weight. A selection of invasive and non-invasive cell lines, of differing cancer cell types, was also included in the analysis. Immunoblotting with MAb 9E1 24 (6) MAb on a panel of cell lines identified a very strong reactive band at approx. 75 kDa (Figures 4.6 & 4.6.1).

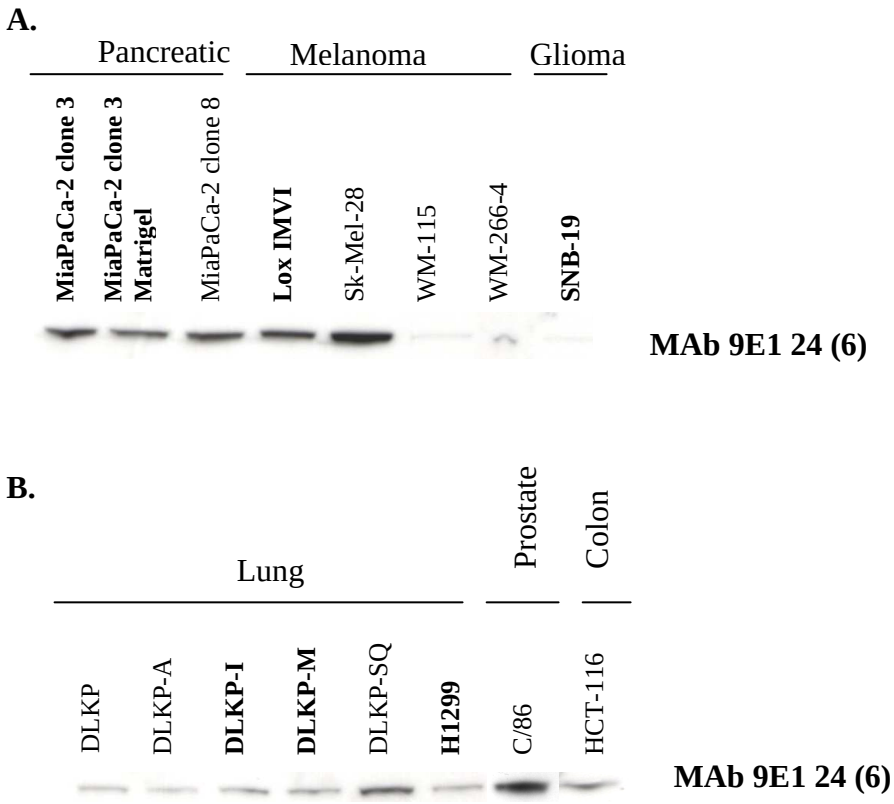

Figure 4.6: **- A.** Western blot analysis of pancreatic cancer cell lines MiaPaCa-2 clone 3, MiaPaCa-2 clone 3 grown on Matrigel, MiaPaCa-2 clone 8; Melanoma cell lines Lox IMVI, WM-115 tumour and its metastatic counterpart, WM-266-4; and SNB-19 glioma cell line probed MAb 9E1 24 (6). A reactive band at approx. 76.5 kDa can be observed in all cell lines. Reactivity in the MiaPaCa-2 clone 3 cell line is slightly stronger than in the clone 8 variant (agreeing with immunofluorescence results), while the strongest reactivity is observed in the SK-MEL-28 cell line. Very weak reactivity is observed in the WM-115, WM-266-4 and SNB-19 cell lines.

B. Western Blot analysis of lung cancer cell lines DLKP, DLKP-A, DLKP-I, DLKP-M, DLKP-SQ and H1299; C/68 Prostate cancer cell line and HCT-116 Colon cancer cell line probed MAb 9E1 24 (6). A reactive band is observed at approx. 75 kDa in all cell lines. Strong reactivity can be seen in the DLKP-SQ cell line. *n = 3.* (See Appendix IV for representative coomassie stained gel showing equal loading). Cell lines in **bold** represent highly invasive phenotype.

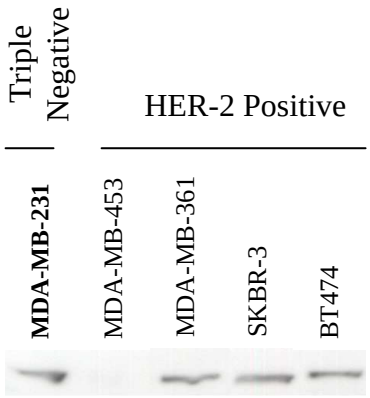

Figure 4.6.1: - Western blot analysis of HER-2 over-expressing cell lines MDA-MB-453, MDA-MB-361, SKBR-3 and BT474, and the Triple negative breast cancer cell line, MDA-MB-231; probed with MAb 9E1 24 (6). A strong reactive band can be observed at approx. 75 kDa in all cell lines, except for MDA-MB-453, where no reactive band was visible. *n = 3*. (See Appendix IV for representative coomassie stained gel showing equal loading). Cell lines in **bold** represent highly invasive phenotype.

4.7 Immunoprecipitation Studies

In order to try to identify the target antigens, immunoprecipitation studies were carried out on a panel of cell lines. MiaPaCa-2 clone 3 was the primary cell line used, due to the initial invasion/motility assays being carried out with that cell line. Protein-G agarose beads were used to pull out the reactive antigens from whole cell lysates of MiaPaCa-2 clone 3 cells for the 9E1 24 (6) MAb. Following separation on 4-12% Bis-Tris SDS-PAGE, a number of bands were identified out with this antibody (Figure 4.7). These were compared to bands pulled out using a control mouse IgG, and those bands only present with the 9E1 24 (6) MAb were identified through liquid chromatography mass spectrometry (LC-MS) analysis (Dionex Ultimate 3000 LC system, LTQ-Orbitrap mass spectrometer), LC-MS sequencing using LCMS/LTQ mass spectrometry and TurboSEQUEST software using the human subset from the SWISS-PROT database.

The direct method of immunoprecipitation was carried out in order to facilitate identification of the antigen of interest. This method (section 2.11.1.) involves incubating the antibody/cell lysate complex with the agarose beads, then separating the solution, containing both the antigen and antibody fragments, on SDS-PAGE gels.

4.7.1 MAb 9E1 24 (6) – Direct Immunoprecipitation Method

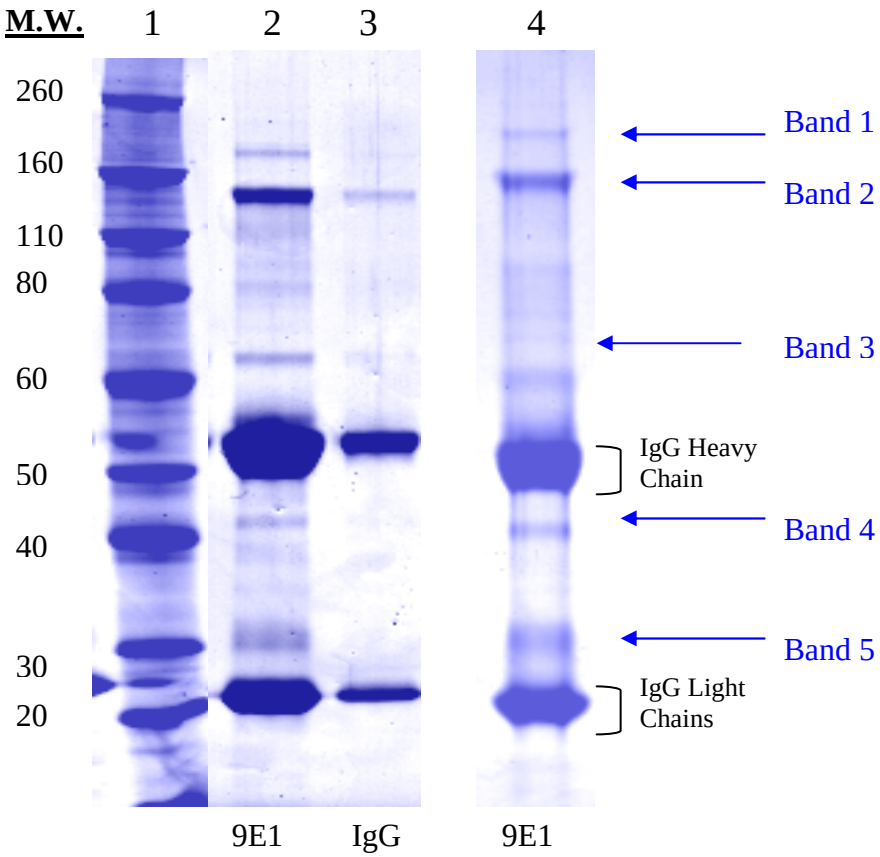

Figure 4.7: - **Direct Immunoprecipitation of cell lysates with 9E1 24 (6) MAb and control mouse IgG.**
A representative SDS-PAGE gel of MiaPaCa-2 clone 3 and H1299 cells immunoprecipitated with MAb 9E1 24 (6) and separated on 4-12% Bis-Tris SDS-PAGE, and stained with 0.25% Coomassie Blue. Lane 1: molecular weight markers. Lane 2: MiaPaCa-2 clone 3 immunoprecipitated with MAb 9E1 24 (6). Five bands of MAb 9E1 24 (6) target proteins are observed; at approx. 170 kDa, 155 kDa, 65 kDa, 42 kDa and 30 kDa. These 5 bands are not present in the control mouse IgG, have been observed in triplicate experiments, and in a number of cell lines. Each band was excised and run through an LCMS/LTQ mass spectrometer for identification. Lane 3: MiaPaCa-2 clone 3 immunoprecipitated with control mouse IgG. Lane 4: H1299 immunoprecipitated with MAb 9E1 24 (6).

4.7.2 Purification of MAb 9E1 24 (6)

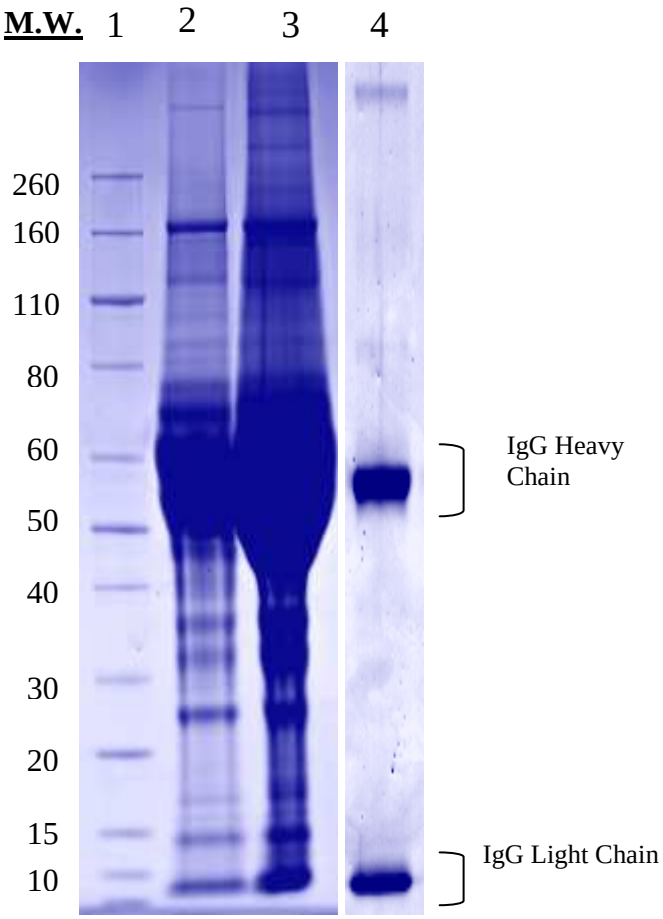

Figure 4.7.1: - Representative SDS-PAGE gel showing successful purification of 9E1 24 (6) MAb, using the Pierce NAb Spin Purification Kit (section 2.3.8). Lane 1: Molecular Weight marker. Lane 2: Unpurified MAb 9E1 24 (6). Lane 3: Concentrated, unpurified MAb 9E1 24 (6). Lane 4: Purified MAb 9E1 24 (6). Purified MAb is required for cross linked immunoprecipitation.

4.8 Mass Spectrometry Identification of MAb 9e1 24 (6) Target Proteins

Following separation of immunoprecipitates on 4-12% Bis-Tris SDS-PAGE, the gel was stained with 0.25% Coomassie Blue and destained accordingly. Bands of interest were excised from the gel, digested with trypsin, and subjected to LC-MS analysis. Identification was achieved using the SWISS-PROT SEQUEST database (section 2.12.1).

Positive identification was deemed valid if:

- protein was observed in duplicate or more, from 2 or more independent experiments
- a minimum of 2 peptide sequences was obtained
- molecular weight of protein matched molecular weight of band on gel
- molecular weight of protein matched the molecular weight of band excised from gel
- protein achieved a high XC score, indicating excellent confidence in the identification
- Proteins were unique to MAb 9E1 24 (6) (i.e. not found with other MAbs)

Criteria for a valid identification is described in full in section 2.12.1.

Protein Name	Band	Gene Symbol	SWISSPROT Protein AC Number	MW (kDa)
Annexin A6	3	ANXA6	P08133	75.87
Prohibitin	5	PHB	P35232	29.8
Protein 14-3-3 epsilon	5	YWHAE	P62258	29.1
ADP/ATP Translocase 1	5	SLC25A4	P12235	33
ADP/ATP Translocase 2	5	SLC25A5	P05141	32.87
ADP/ATP Translocase 3	5	SLC25A6	P12236	32.84
40S Ribosomal Protein 3	5	RS3	P23396	26.67
40S Ribosomal Protein S4, Y isoform 1	5	RS4Y1	P22090	29.43
40S Ribosomal Protein S4, Y isoform 2	5	RS4Y2	Q8TD47	29.27
40S Ribosomal Protein S4, X isoform	5	RPS4X	P62701	29.59

Table 4.8: - Proteins identified using above criteria, from excised bands immunoprecipitated with MAb 9E1 24 (6), through mass spectrometry. Band number refers to highlighted bands on gel represented in figure 4.7.

For MAb 9E1 24 (6), the band at approx. 75 kDa was identified as Annexin A6. The band at approx. 32 kDa was revealed to have a mixture of peptides; identified as Prohibitin, Protein 14-3-3 epsilon, and ADP-ATP Translocase 1, 2 and 3. 40S Ribosomal proteins were not studied further due to budget constraints.

All other bands observed in MAb 9E1 24 (6) were either identified as Mouse IgG, or were present in the control immunoprecipitation, and were thus disregarded.

Protein Name	Gene Symbol	SWISSPROT Protein AC Number	MW (kDa)
NAD(P)H dehydrogenase	NQO1	P15559	30.86
Glyceraldehyde-3-phosphate dehydrogenase (GAPDH)	G3P	P04406	36
Heat Shock Protein 90 kDa beta member 1	HSP90B1	Q96GW1	92.41
Fructose-bisphosphate aldolase A	ALDOA	P04075	39.39

Table 4.8.1: - Proteins identified only once, from excised bands immunoprecipitated with MAb 9E1 24 (6), through mass spectrometry.

4.8.1 Identification of MAb 9E1 24 (6) Target Proteins by LC-MS Analysis of 9E1 24 (6) Immunoprecipitates.

- **Annexin A6**

Scan(s)	Peptide	MH+	z	Type	P (pro) P (pep)	Score XC
ANXA6_HUMAN RecName: Full=**Annexin A6**; AltName: Full=Annexin-6; AltName: Full=Annexin VI; AltName: Full=Lipocortin VI; AltName: Full=p68; AltName: Full=p70; AltName: Full=Protein III; AltName: Full=Chromobindin-20; AltName: Full=67 kDa calelectrin; AltName					**4.79E-06**	**60.17**
319	K.GAGTDEKTLTR.I	1148.59058	2	CID	4.97E-05	3.40
408	R.AINEAYKEDYHK.S	1480.70667	2	CID	4.22E-05	3.01
463	K.TTGKPIEASIR.G	1172.66333	2	CID	1.95E-02	2.61
523	**K.GTVRPANDFNPDADAK.A**	1687.80347	2	CID	6.12E-03	3.46
571	-.SEISGDLAR.-	947.47925	2	CID	1.77E-02	2.11
1289	K.ALLALCGGED.-	1018.48743	1	CID	4.79E-06	2.06

Table 4.9.2: - Identification of Protein Annexin A6, obtained using SEQUEST Human protein database

Peptides were identified using Bioworks 3.3.1 software. A representative result (experiments were carried out at least 3 times) is shown above, where 6 peptides corresponding to Human Annexin A6 were identified. All 6 peptides showed high XC scores indicating excellent confidence in this identification. (Note: the minimum acceptable Xcorr for identified peptides was 1.5 for 1+ peptides, 2.5 for 2+ peptides and 3.5 for 3+ peptides).

QLVAAYKDAYERDLEADIIGDTSGHFQKMLVVLLQGTREEDDVVSEDLVQQDVQDLYEAGELKW
GTDEAQFIYILGNRSKQHLRLVFDEYLKTTGKPIEASIRGELSGDFEKLMLAVVKCIRSTPEYFAERL
FKAMKGLGTRDNTLIRIMVSRSELDMLDIREIFRTKYEKSLYSMIKNDTSGEYKKTLLKLSGGDDD
AAGQFFPEAAQVAYQMWELSAVARVEL**KGTVRPANDFNPDADAKA**LRKAMKGLGTDEDTIIDII
THRSNVQRQQIRQTFKSHFGRDLMTDLKSEISGDLARLILGLMMPPAHYDAKQLKKAMEGAGTDE
KALIEILATRTNAEIRAINEAYKEDYHKSLEDALSSDTSGHFRRILISLATGHREEGGENLDQAREDA
QVAAEILEIADTPSGDKTSLETRFMTILCTRSYPHLRRVFQEFIKMTNYDKGAGTDEKTLTRIMVSRS
EIDLLNIRREFIEKYDKSLHQAIEGDTSGDFLKALLALCGGED

Figure 4.8: - Total amino acid sequence of Human Annexin A6 protein presented above. Scan of 523 peptide sequence, which shows the highest XC score (3.46) is highlighted.

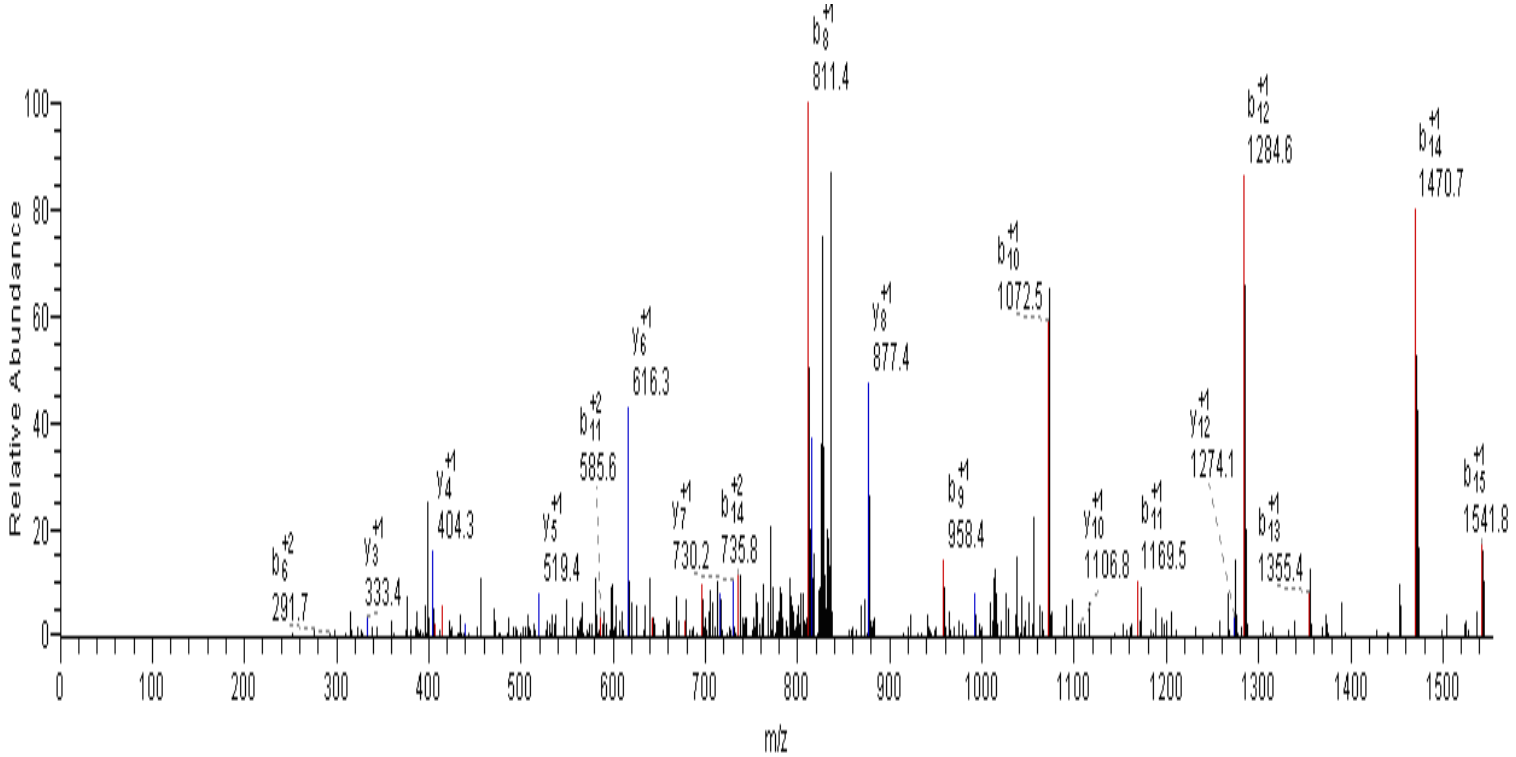

Figure 4.8.1: - The MS-MS spectrum for scan 319 showing b (indicated in red) & y (indicated in blue) fragment ion series overlay.

- **Prohibitin**

Scan(s)	Peptide	MH+	z	Type	P (pro) P (pep)	Score XC
PHB_HUMAN RecName: Full=**Prohibitin**					**1.76E-04**	**40.18**
583	K.AAIISAEGDSK.A	1061.54736	2	CID	1.00E-03	2.43
1242	R.IFTSIGEDYDER.V	1444.65906	2	CID	7.83E-04	3.28
1275	K.DLQNVNITLR.I	1185.65857	2	CID	1.91E-04	2.90
1313	**R.FDAGELITQR.E**	1149.58984	2	CID	1.76E-04	3.57

Table 4.8.3: - Identification of Protein Prohibitin, obtained using SEQUEST Human protein database.

Peptides were identified using Bioworks 3.3.1 software. A representative result (experiments were carried out at least 3 times) is shown above, where 4 peptides corresponding to Human Prohibitin were identified. All 4 peptides showed high XC scores indicating excellent confidence in this identification.

MAAKVFESIGKFGLALAVAGGVVNSALYNVDAGHRAVIFDRFRGVQDIVVGEGTHFLIP
WVQKPIIFDCRSRPRNVPVITGSKDLQNVNITLRILFRPVASQLPRIFTSIGEDYDERVLPSI
TTEILKSVVA**RFDAGELITQRE**LVSRQVSDDLTERAATFGLILDDVSLTHLTFGKEFTEA
VEAKQVAQQEAERARFVVEKAEQQKKAAIISAEGDSKAAELIANSLATAGDGLIELRKL
EAAEDIAYQLSRSRNITYLPAGQSVLLQLPQ

Figure 4.8.2: - Total amino acid sequence of Human Prohibitin protein presented above. Scan of 1313 peptide sequence, which shows the highest XC score (3.57) is highlighted.

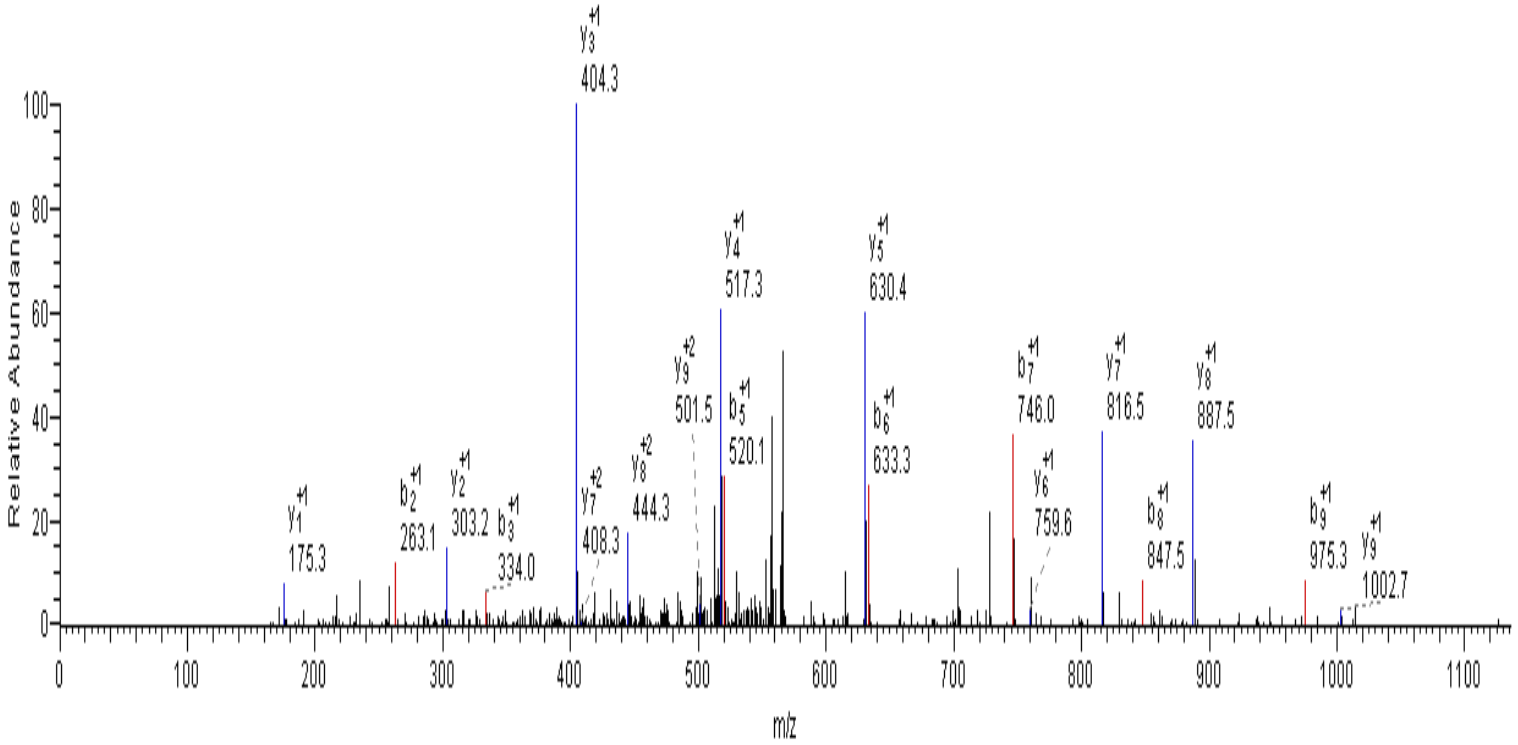

Figure 4.8.3: - The MS-MS spectrum for scan 1313 showing b (indicated in red) & y (indicated in blue) fragment ion series overlay.

- **14-3-3 protein epsilon**

Scan(s)	Peptide	MH+	z	Type	P (pro) P (pep)	Score XC
1433E_HUMAN RecName: Full=**14-3-3 protein epsilon**; Short=14-3-3E					1.27E-09	30.21
774	R.IISSIEQKEENK.G	1417.75330	2	CID	5.05E-05	3.44
1138	**K.VAGM*DVELTVEER.N**	1463.70464	2	CID	1.27E-09	4.11
1219	R.YLAEFATGNDR.K	1256.59058	2	CID	1.38E-05	2.75

Table 4.8.4: - Identification of 14-3-3 protein epsilon, obtained using SEQUEST Human protein database.

Peptides were identified using Bioworks 3.31 software. A representative result (experiments were carried out at least 3 times) is shown above, where 3 peptides corresponding to Human 14-3-3 protein epsilon were identified. All 3 peptides showed high XC scores indicating excellent confidence in this identification.

MDDREDLVYQAKLAEQAERYDEMVESMK**KVAGMDVELTVEERN**LLSVAYKNVIGAR
RASWRIISSIEQKEENKGGEDKLKMIREYRQMVETELKLICCDILDVLDKHLIPAANTGES
KVFYYKMKGDYHRYLAEFATGNDRKEAAENSLVAYKAASDIAMTELPPTHPIRLGLAL
NFSVFYYEILNSPDRACRLAKAAFDDAIAELDTLSEESYKDSTLIMQLLRDNLTLWTSDM
QGDGEEQNKEALQDVEDENQ

Figure 4.8.4: - Total amino acid sequence of Human 14-3-3 epsilon protein presented above. Scan of 1138 peptide sequence, which shows the highest XC score (4.11) is highlighted.

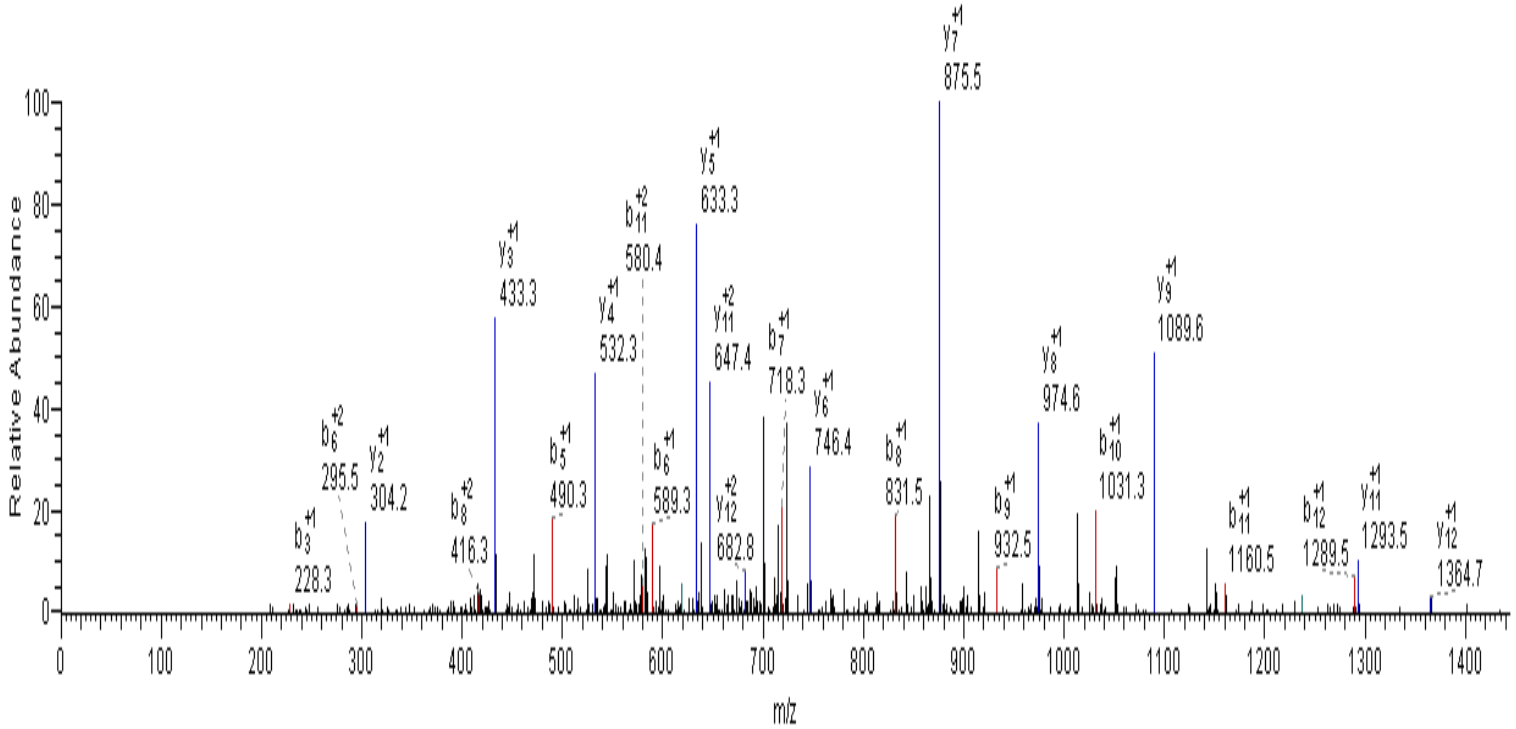

Figure 4.8.5: - The MS-MS spectrum for scan 1219 showing b (indicated in red) & y (indicated in blue) fragment ion series overlay.

4.9 Western Blot Validation of MAb 9E1 24 (6) Target Proteins

75kDa (Annexin A6)

29kDa (Protein 14-3-3 ε)

Figure 4.9: - Western Blot analysis of MiaPaCa-2 clone 3 I.P. samples, separated on SDS-PAGE, and probed with commercial Annexin A6 and Protein 14-3-3 ε-specific antibodies. Reactive bands at the expected weights of 75 kDa (Annexin A6) and 29 kDa (14-3-3ε) are detected in all immunoprecipitates, confirming these protein bands as Annexin A6 and Protein 14-3-3 ε. *n = 3*.

⇒ **Prohibitin.**

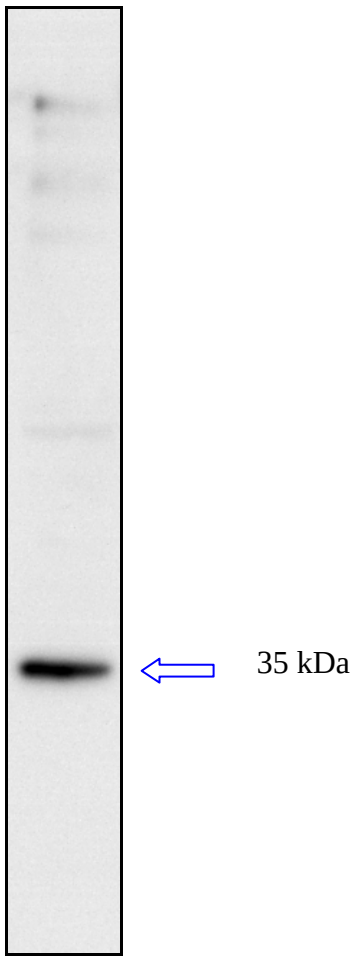

Figure 4.9.5: - Western Blot Analysis of MiaPaCa-2 clone 3 I.P. sample, separated on SDS-PAGE, and probed with an Prohibitin antibody. A reactive band at the expected weight of 35 kDa is detected by the antibody in the immunoprecipitate, confirming this protein band as Prohibitin. *n = 2.*

⇒ **Annexin A6 & MAb 9E1 24 (6).**

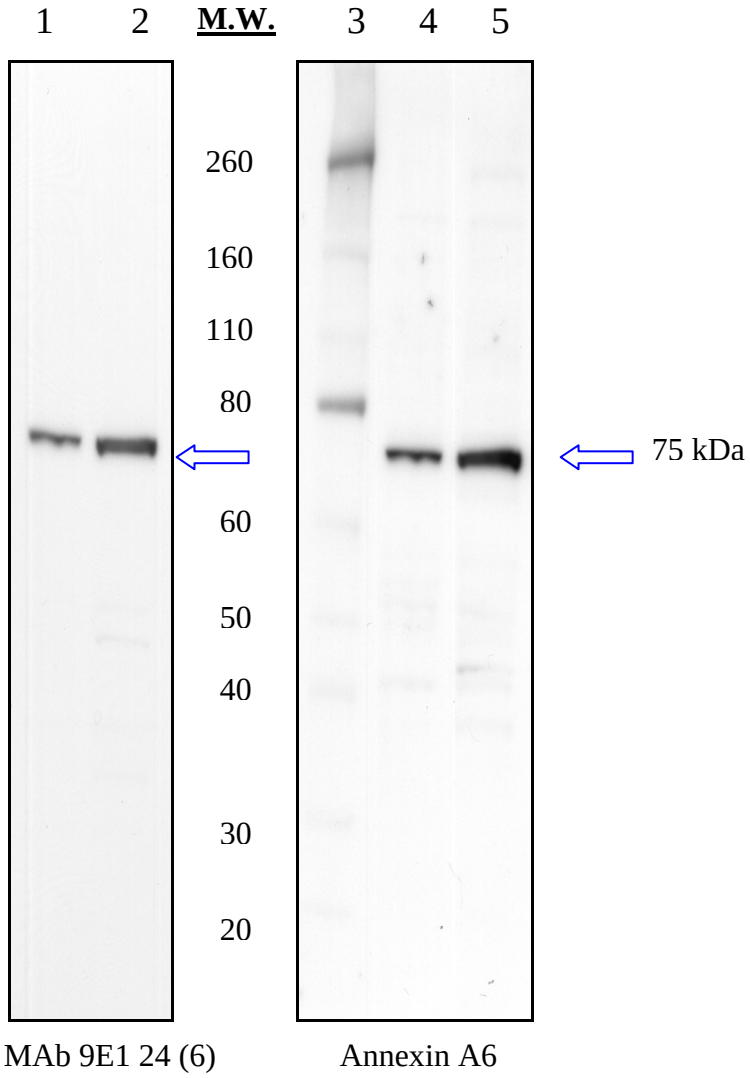

Figure 4.9.5: - Western Blot Analysis of MiaPaCa-2 clone 3 and SKBR-2 cancer cell lines, separated on SDS-PAGE, and probed with MAb 9E1 24 (6) and an Annexin A6 antibody. Reactive bands at approx. 75 kDa are detected by MAb 9E1 24 (6), while reactive bands at the expected molecular weight of 75kDa are detected by the Annexin A6 antibody. Lanes 1: MiaPaCa-2 clone 3 probed with MAb 9E1 24 (6). Lane 2: SKBR-3 probed with MAb 9E1 24 (6). Lane 3: Molecular weight markers. Lane 4: MiaPaCa-2 clone 3 probed with an Annexin A6 antibody. Lane 5: SKBR-3 probed with an Annexin A6 antibody. These results suggest that the reactive antigen of MAb 9E1 24 (6) is Annexin A6. *n = 3*.

4.10 siRNA Functional Analysis of Targets Identified Through Immunoprecipitation

After the targets for MAb 9E1 24 (6) were identified, siRNAs specific for the genes of interest were obtained, in order to see if silencing of the genes gave comparable inhibition in invasion levels to what was observed with the MAb. This would show whether the genes of interest play a role in the invasion process. The conditions for siRNA transfection were optimised in 96- and 6-well plates using kinesin as a positive control, and scrambled siRNA as a siRNA transfection control. Three siRNAs were selected for each of the targets chosen and transfected into cells (section 2.14.2). For each set of siRNA transfections carried out, a non-transfected cell line and a scrambled (SCR) siRNA transfected control were used. Kinesin (Kin) was used as a control for efficient transfection as Kin siRNA reduces proliferation in the cells.

Three siRNAs were chosen for Annexin A6, each one targeting a different region of the gene. This was in order to maximise the chance of seeing an effect on invasion and proliferation levels.

Proliferation assays (section 2.14.3) were carried out on transfected cells to assess the impact of gene silencing on proliferation levels in the cells, to ensure that any inhibition in invasion was not just due to a decrease in the cell number.

Invasion assays (section 2.14.4) were carried out on transfected cells to confirm whether or not these targets played an important role in invasion, as suggested by proteomic analysis.

Motility assays (section 2.14.5) were carried out on transfected cells to confirm whether or not these targets played an important role in motility, as suggested by proteomic analysis.

4.10.1 Investigation of the Possible Role of Annexin A6 in Cancer Cell Invasion

Annexin A6 knockdown was successfully carried out in the MiaPaCa-2 clone 3 and DLKP-M cell lines.

Silencing of the Annexin A6 gene by two different siRNAs significantly reduced the invasive capacity of the MiaPaCa-2 clone 3 and DLKP-M cells (the 3rd siRNA did not produce an effective knockdown of Annexin A6, and as such, invasion assays were not carried out on cells transfected with this siRNA):

- MiaPaCa-2 clone 3 invasion was significantly inhibited, by an average of 40% following siRNA transfection with Anx6A, and an average of 28.2% following siRNA transfection by Anx6B.
- DLKP-M invasion was inhibited by an average of 22% following siRNA transfection with Anx6A, and significantly inhibited by an average of 36.6% following siRNA transfection with Anx6B.

No significant affect on motility was observed in the MiaPaCa-2 clone 3 cell line following transfection with both siRNAs.

No significant affect on proliferation in either the MiaPaCa-2 clone 3 or DLKP-M cell lines was observed following transfection of both siRNAs, indicating that the observed inhibition of invasion was not due to any reduced proliferative capacity of the cells. Protein knockdown was confirmed by Western blot analysis (Figures 4.10 & 4.10.7).

Statistical analyses for proliferation assays were carried out on the average absorbancy readings of the control Vs test wells, over biological triplicates.

Statistical analyses for invasion assays were carried out with the average cell counts of control Vs sample inserts over biological triplicates (section 2.15).

Effect of Annexin A6 siRNA transfection in MiaPaCa-2 clone 3

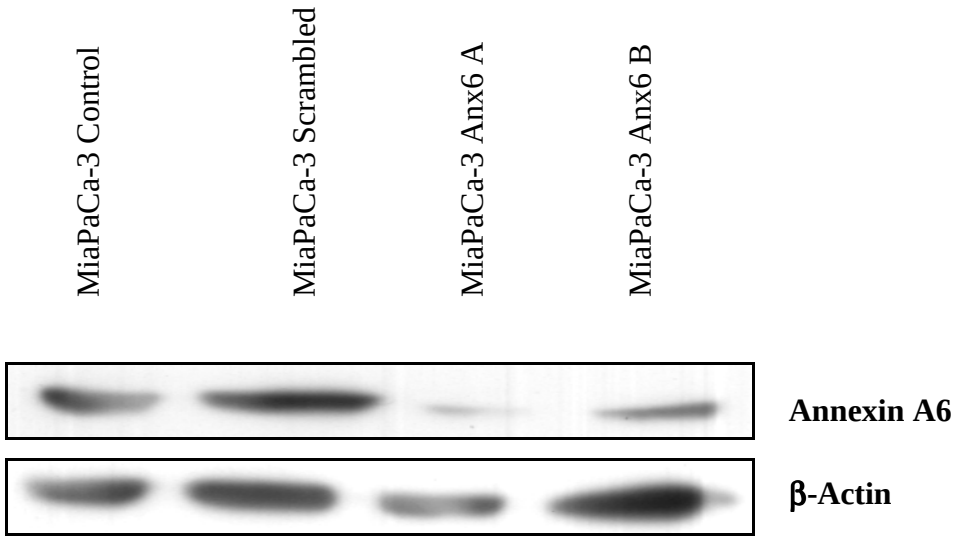

Figure 4.10: - Western Blot analysis of whole cell (RIPA) lysates of MiaPaCa-2 clone 3 transfected cells, separated on SDS-PAGE, and probed with an Annexin A6 antibody. A reduction in the levels of Annexin A6 (M.W. 75kDa) can be seen when compared to the control MiaPaCa-2 clone 3 cell lysate (untransfected). β-actin was used as a loading control. (15µg protein per lane loaded) *n = 3*.

- **Effect of siRNA Annexin A6 on MiaPaCa-2 clone 3 Proliferation**

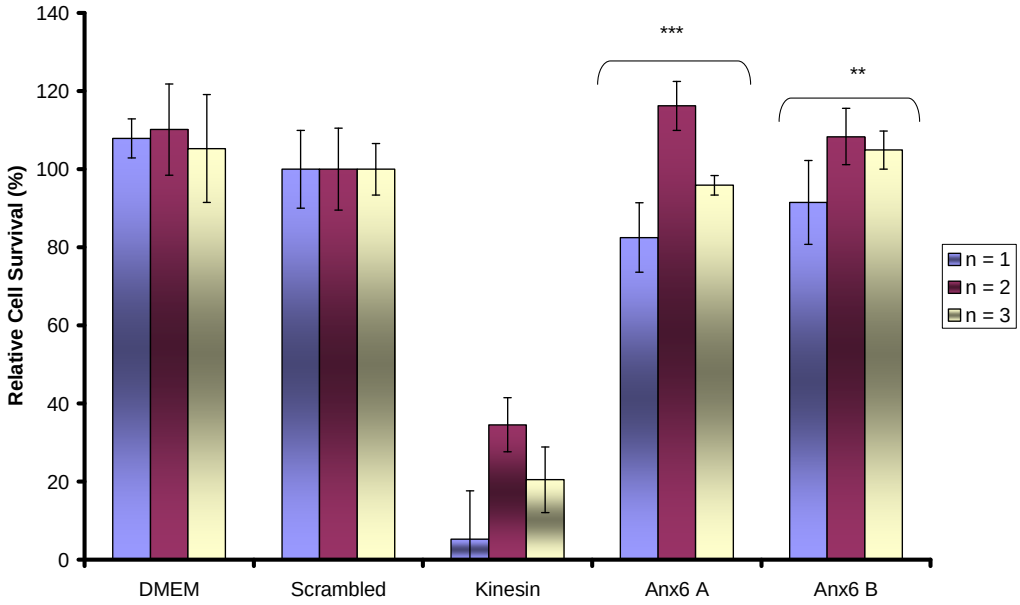

Figure 4.10.1: - Histogram showing proliferation assay of MiaPaCa-2 clone 3 scrambled, kinesin and transfected with siRNAs A, & B targeting Annexin A6. Results graphed as % survival relative to scrambled transfected cells (control). Loss of Annexin A6 did not affect proliferation in this cell line; therefore any inhibition of invasion is not due to cell kill. Statistics performed using student t-test compared to scrambled control; * $p \leq 0.05$, ** $p \leq 0.01$, *** $p \leq 0.005$, $n = 3$.

- **Knockdown of Annexin A6 reduces invasion in MiaPaCa-2 clone 3**

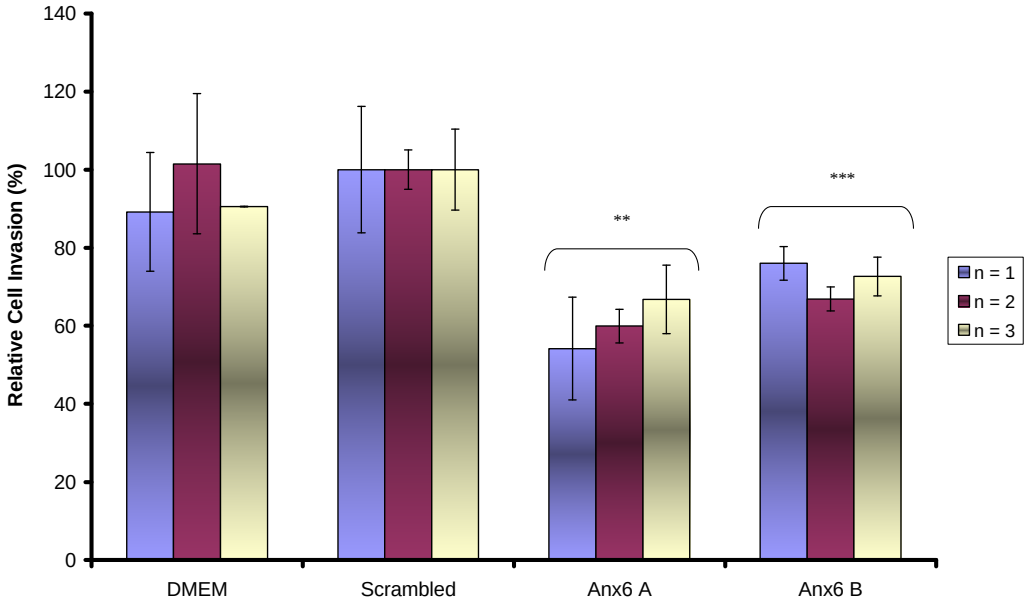

Figure 4.10.2: - Histogram showing effect of Annexin A6 knockdown on invasive behaviour of MiaPaCa-2 clone 3 cells. Forty-eight hours post-transfection with Annexin A6 siRNAs, invasion assays on MiaPaCa-2 clone 3 cells were performed. Annexin A6 siRNA A and B transfected cells show a significant decrease in invasion levels. Statistics performed using student t-test compared to scrambled control; * $p \leq 0.05$, ** $p \leq 0.01$, *** $p \leq 0.005$, $n = 3$.

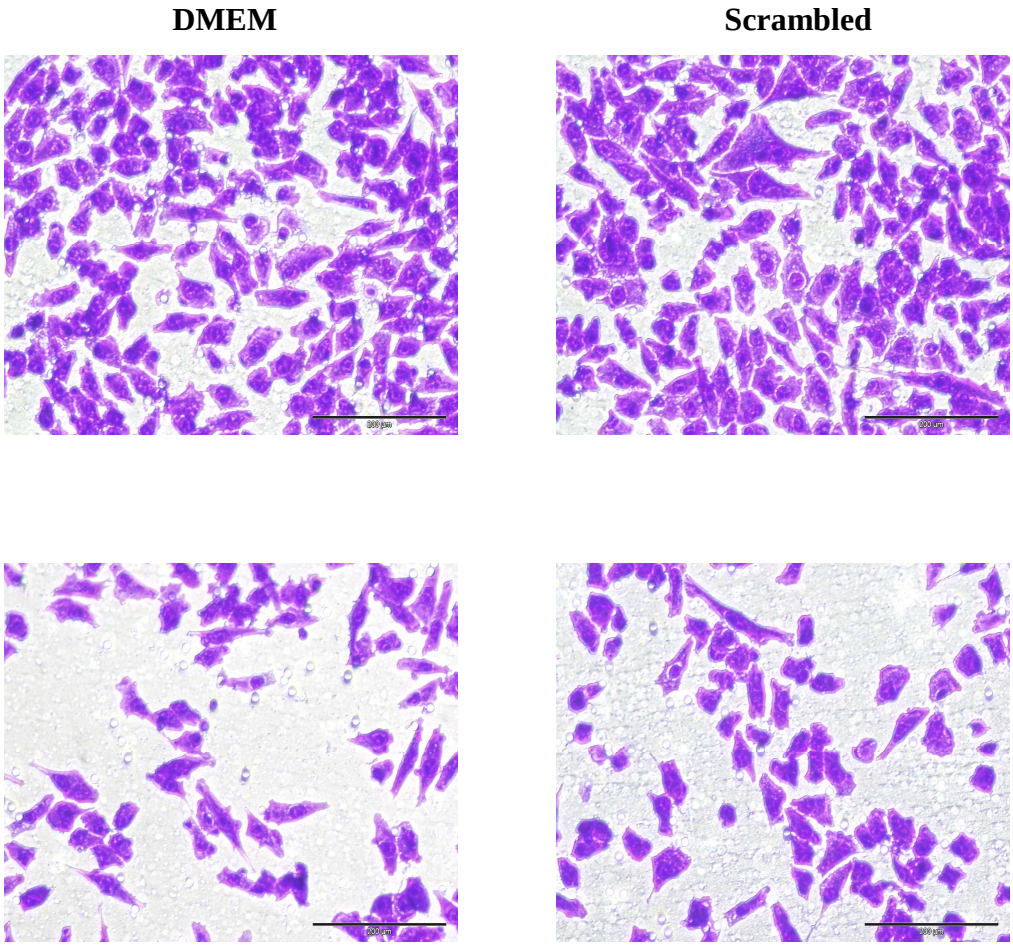

Figure 4.10.3: - Representative photomicrographs showing invasion status of MiaPaCa-2 clone 3 cells after 48hrs, untreated (DMEM), transfected with scrambled siRNA (Control), transfected with Anx6-A siRNA and Anx6-B. A decrease in invasion can be observed following transfection with both siRNAs when compared to the control insert (B). Magnification, 100X, scale bar, 200 μm.

- **Effect of siRNA Annexin A6 on MiaPaCa-2 clone 3 Motility**

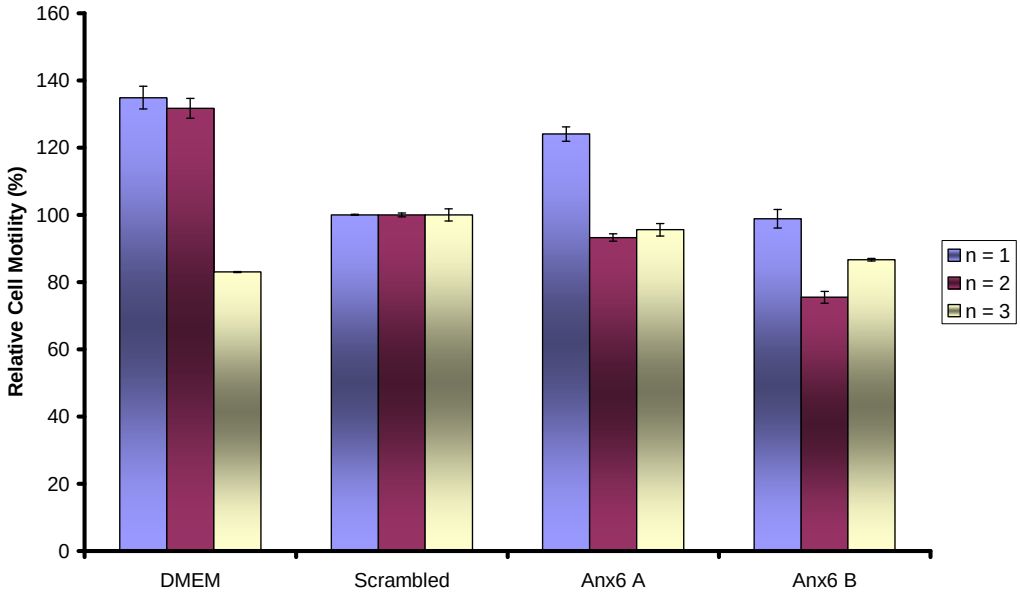

Figure 4.10.4: - Histogram showing effect of Annexin A6 knockdown on motile behaviour of MiaPaCa-2 clone 3 cells. Forty-eight hours post-transfection with Annexin A6 siRNAs, motility assays on MiaPaCa-2 clone 3 cells were performed. Annexin A6 siRNA A and B transfected cells show little decrease in motility levels. Statistics performed using student t-test compared to scrambled control; * $p \leq 0.05$, ** $p \leq 0.01$, *** $p \leq 0.005$, $n = 3$.

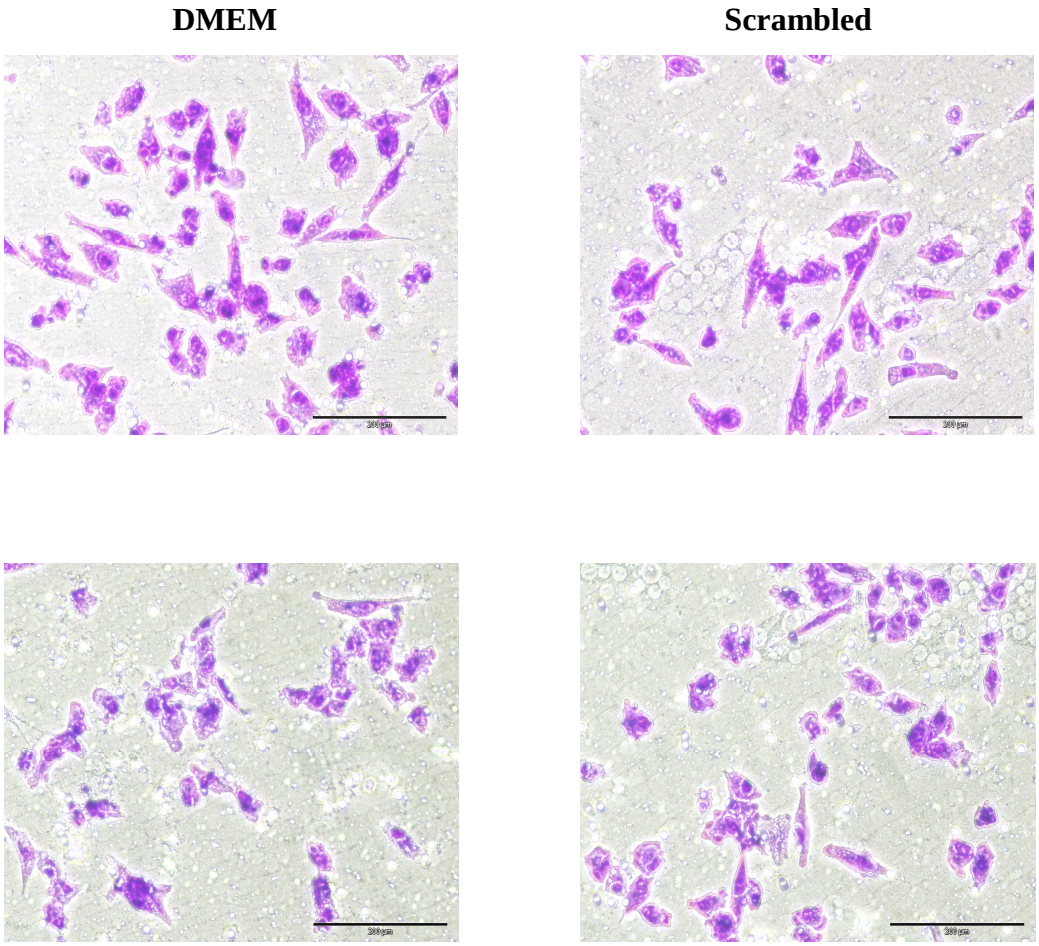

Figure 4.10.6: - Representative photomicrographs showing motility status of MiaPaCa-2 clone 3 cells after 24hrs, untreated (DMEM), transfected with scrambled siRNA (Control), transfected with Anx6-A siRNA and Anx6-B. No significant decrease in motility can be observed following transfection with both siRNAs when compared to the control insert (B). Magnification, 100X, scale bar, 200 μm.

- **Effect of Annexin A6 siRNA transfection in DLKP-M**

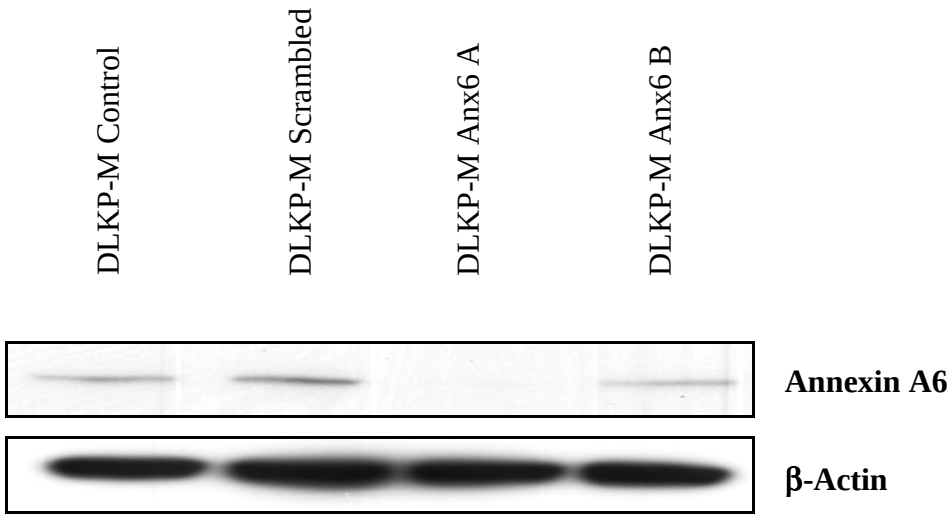

Figure 4.10.7: - Western Blot analysis of whole cell (RIPA) lysates of DLKP-M transfected cells, separated on SDS-PAGE, and probed with an Annexin A6 antibody. A reduction in the levels of Annexin A6 (M.W. 75kDa) can be seen when compared to the control DLKP-M cell lysate (untransfected). β-actin was used as a loading control. (15μg protein per lane loaded) *n = 3*.

- **Effect of siRNA Annexin A6 on DLKP-M Proliferation**

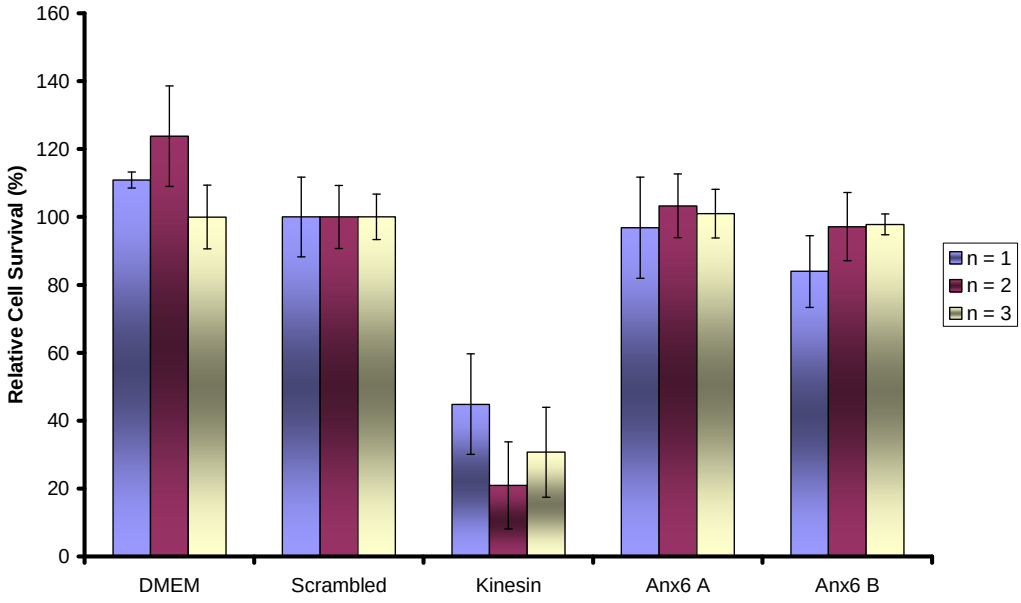

Figure 4.10.8: - Histogram showing proliferation assay of MiaPaCa-2 clone 3 scrambled, kinesin and transfected with siRNAs A, & B targeting Annexin A6. Results graphed as % survival relative to scrambled transfected cells (control). Loss of Annexin A6 did not affect proliferation in this cell line; therefore any inhibition of invasion is not due to cell kill. Statistics performed using student t-test compared to scrambled control; * $p \leq 0.05$, ** $p \leq 0.01$, *** $p \leq 0.005$, *n = 3.*

- **Knockdown of Annexin A6 reduces invasion in DLKP-M**

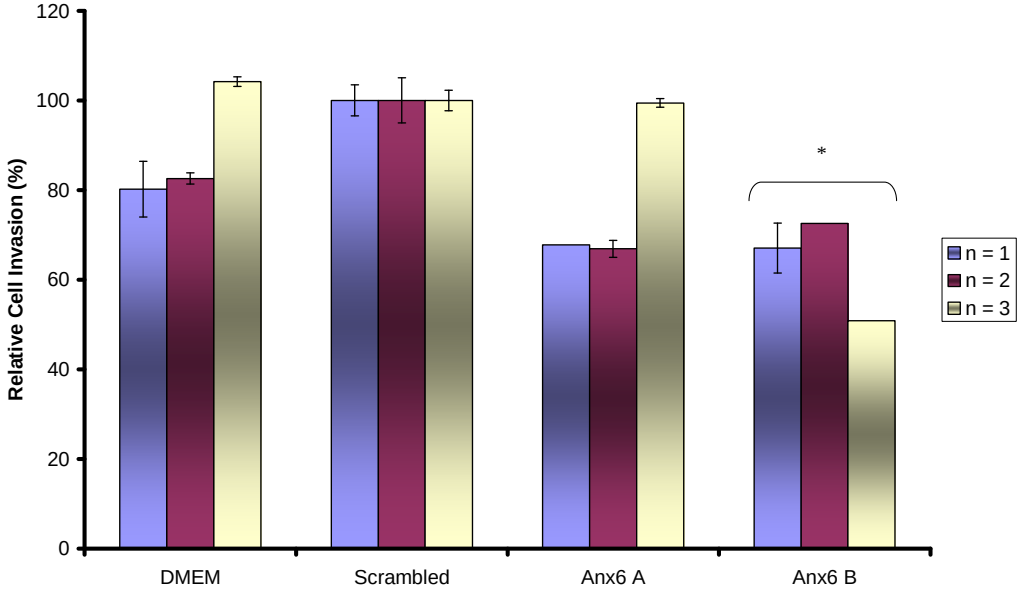

Figure 4.10.9: - Histogram showing effect of Annexin A6 knockdown on invasive behaviour of DLKP-M cells. Forty-eight hours post-transfection with Annexin A6 siRNAs, invasion assays on DLKP-M cells were performed. Annexin A6 siRNA A shows a decrease in invasion levels, while Anx6B transfected cells show a significant decrease in invasion levels. Statistics performed using student t-test compared to scrambled control; * $p \leq 0.05$, ** $p \leq 0.01$, *** $p \leq 0.005$, *n = 3.*

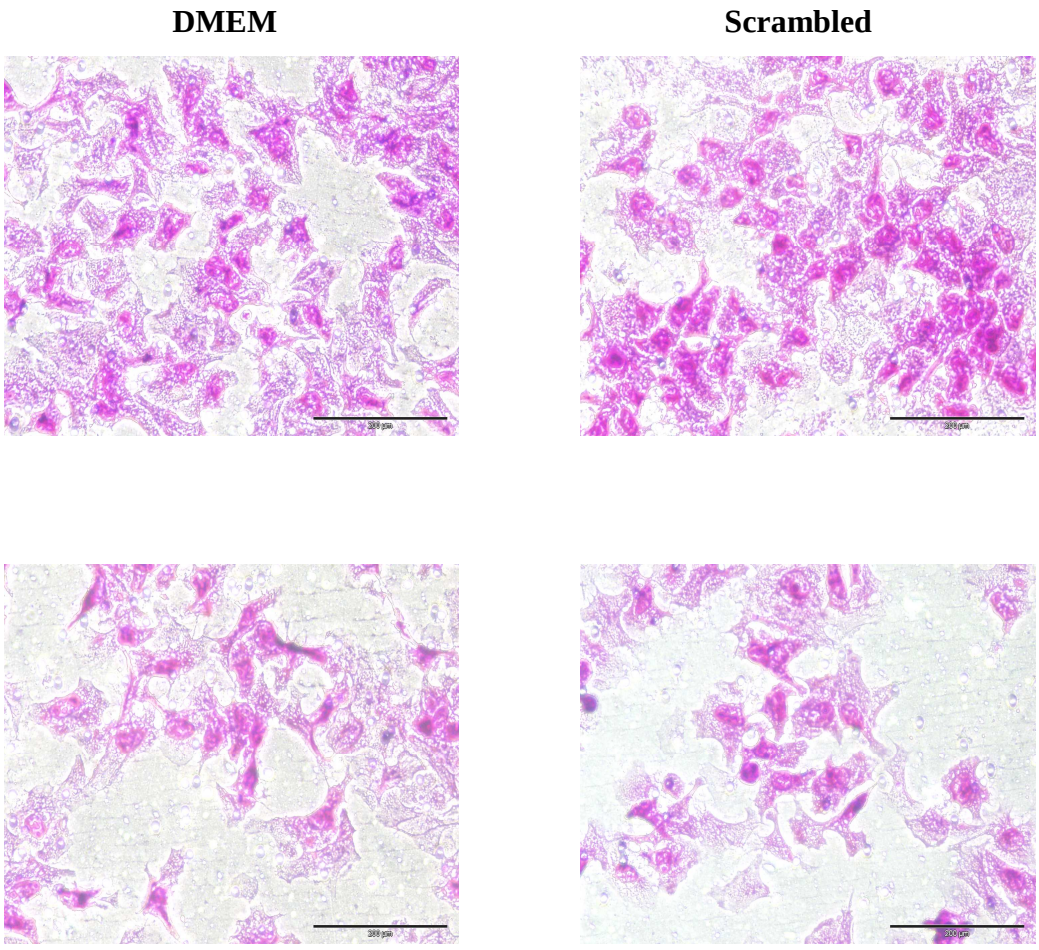

Figure 4.10.10: - Representative photomicrographs showing invasion status of DLKP-M cells after 48hrs, untreated (DMEM), transfected with scrambled siRNA (Control), transfected with Anx6-A siRNA and Anx6-B. A decrease in invasion can be observed following transfection with both Anx6 siRNA A and B, when compared to the control insert (B). Magnification, 100X, scale bar, 200 μm.

- **Effect of Annexin A6 siRNA transfection on the expression of MAb 9E1 24 (6) reactive antigen in MiaPaCa-2 clone 3**

Figure 4.10.11: - Western Blot analysis of whole cell (RIPA) lysates of MiaPaCa-2 clone 3 transfected cells, separated by SDS-PAGE, and probed with MAb 9E1 24 (6). A reduction in the levels of the reactive antigen of MAb 9E1 24 (6) (M.W. 75kDa) can be seen when compared to the control MiaPaCa-2 clone 3 cell lysate (untransfected), indicating that the reactive antigen is the Annexin A6 protein. α-tubulin was used as a loading control. (15μg protein per lane loaded) *n = 3.*

- **Effect of Annexin A6 siRNA transfection on the expression of Protein 14-3-3ε in DLKP-M**

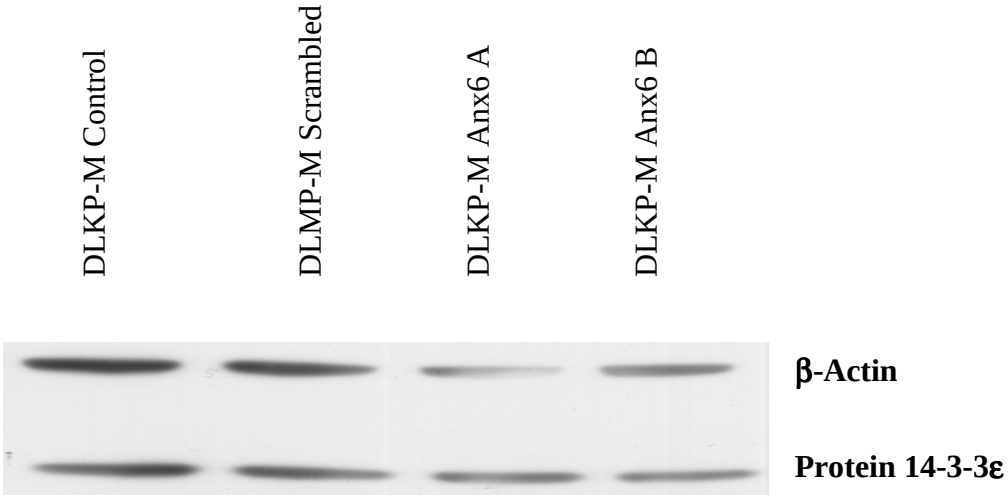

Figure 4.10.12: - Western Blot analysis of whole cell (RIPA) lysates of DLKP-M transfected cells, separated by SDS-PAGE, and probed with a commercial Protein 14-3-3ε antibody. No reduction in expression of Protein 14-3-3ε can be seen when compared to the control DLKP-M cell lysate (untransfected). β-actin was used as a loading control. (15μg protein per lane loaded) *n = 3*.

4.11 Western Blot Validation of MAb 9E1 24 (6) Target Proteins in a Panel of Cell Lines

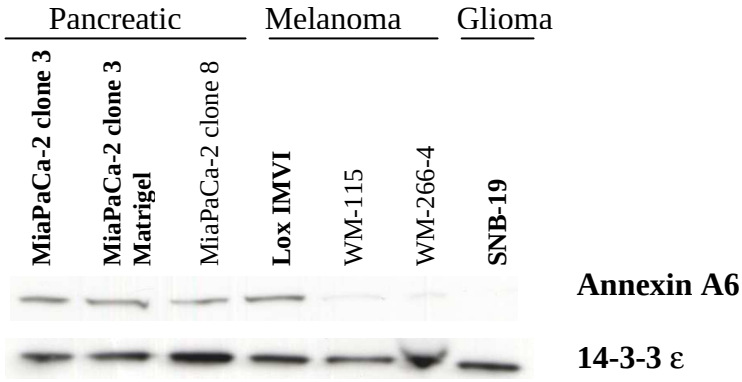

Figure 4.11: - Western blot analysis of pancreatic cancer cell lines MiaPaCa-2 clone 3, MiaPaCa-2 clone 3 grown on Matrigel, MiaPaCa-2 clone 8; Melanoma cell lines Lox IMVI, WM-115 primary cancer, and its metastatic counterpart WM-266-4 and SNB-19 glioma cell line probed with antibodies specific for Annexin A6 and Protein 14-3-3ε. Annexin A6 shows strong expression in both the MiaPaCa-2 clone 3 and MiaPaCa-2 clone 8 cell lines. Lox IMVI shows strong expression, but WM-115 and WM-266-4 show much weaker expression, while no expression is observed in SNB-19. All cell lines appear to show strong expression of Protein 14-3-3ε. *n = 3.* (See Appendix IV for representative coomassie stained gel showing equal loading). Cell lines in **bold** represent highly invasive phenotype.

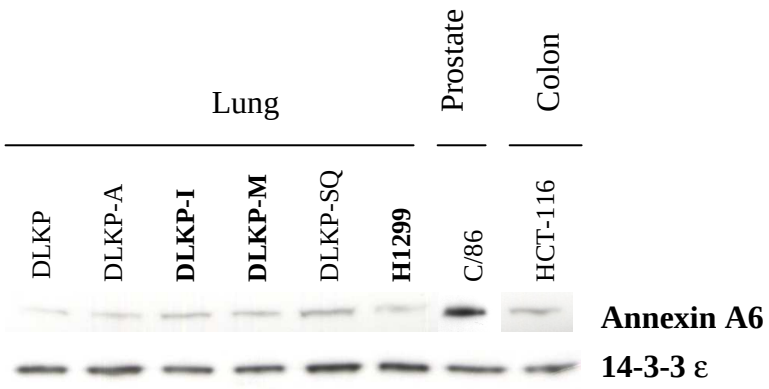

Figure 4.11.1: - Western Blot analysis of lung cancer cell lines DLKP, DLKP-A, DLKP-I, DLKP-M, DLKP-SQ and H1299; C/68 Prostate cancer cell line and HCT-116 Colon cancer cell line probed with antibodies specific for Annexin A6 and Protein 14-3-3ε. Annexin A6 expression is observed in all cell lines, apart from C/68. DLKP-SQ shows the strongest expression. Protein 14-3-3ε is expressed in all cell lines, with the strongest expression showing in the DLKP-SQ and H1299 cell lines. *n = 3.* (See representative coomassie stained gel showing equal loading). (See Appendix IV for representative coomassie stained gel showing equal loading). Cell lines in **bold** represent highly invasive phenotype.

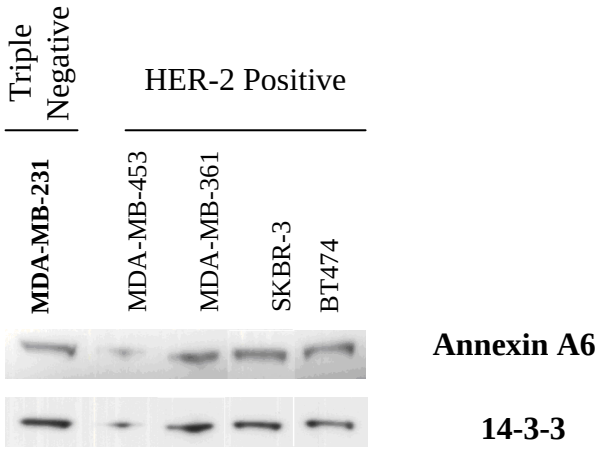

Figure 4.11.2: **-** Western blot analysis of HER-2 over expressing cell lines MDA-MB-453, MDA-MB-361, SKBR-3 and BT474, and the Triple negative breast cancer cell line, MDA-MB-231; probed with antibodies specific for Annexin A6 and Protein 14-3-3ε. Both Annexin A6 and Protein 14-3-3ε are weakly expressed in the MDA-MB-453 cell line, while strong expression is observed in all other cell lines. *n =3.* (See Appendix IV for representative coomassie stained gel showing equal loading). Cell lines in **bold** represent highly invasive phenotype.

4.12 MAb 9E1 24 (6) Expression in Normal and Malignant Tissues

Normal Tissue Type	No.	Reactivity (membrane, with some cytoplasmic positivity)
Colon	2	+
Prostate	1	+ / -
Liver	1	+ / -
Breast	2	+ +

Cancer Tissue Type	No.	Reactivity (membrane, with some cytoplasmic positivity)
Squamous Cell Carcinoma	2	+
Glioma	8	+ / -
Colon Adenocarcinoma	1	+ + +
Pancreatic Adenocarcinoma	12	+ + / + + +
Breast Carcinoma	42*	+ / - → + + +
Retinoblastoma	1	+ + +
Hodgkins Lymphoma	1	+ +
Malt Lymphoma (orbital tissue)	1	+ + +
B Cell Mantle Lymphoma (lacrimal gland)		+ + +
Basal Cell Carcinoma (eyelid)	1	+ / -
Parotid Tumour (Warthins [benign] tumour)	1	+ +

Table 4.12: - Reactivity of MAb 9E1 24 (6) in a panel of normal and cancerous tissue sections.
+++ Very intense staining; ++ Intense staining; + Weak staining; +/- Some very weak positivity.

* A range of breast tumours, representing different sub-groups of disease – HER2 positive, Triple Negative, estrogen-receptor (ER) +/- and progesterone receptor (PR) +/-, were studied. MAb 9E1 24 (6) reactivity was observed in all tumour types studied, however, negative reactivity in various subtypes was also observed.

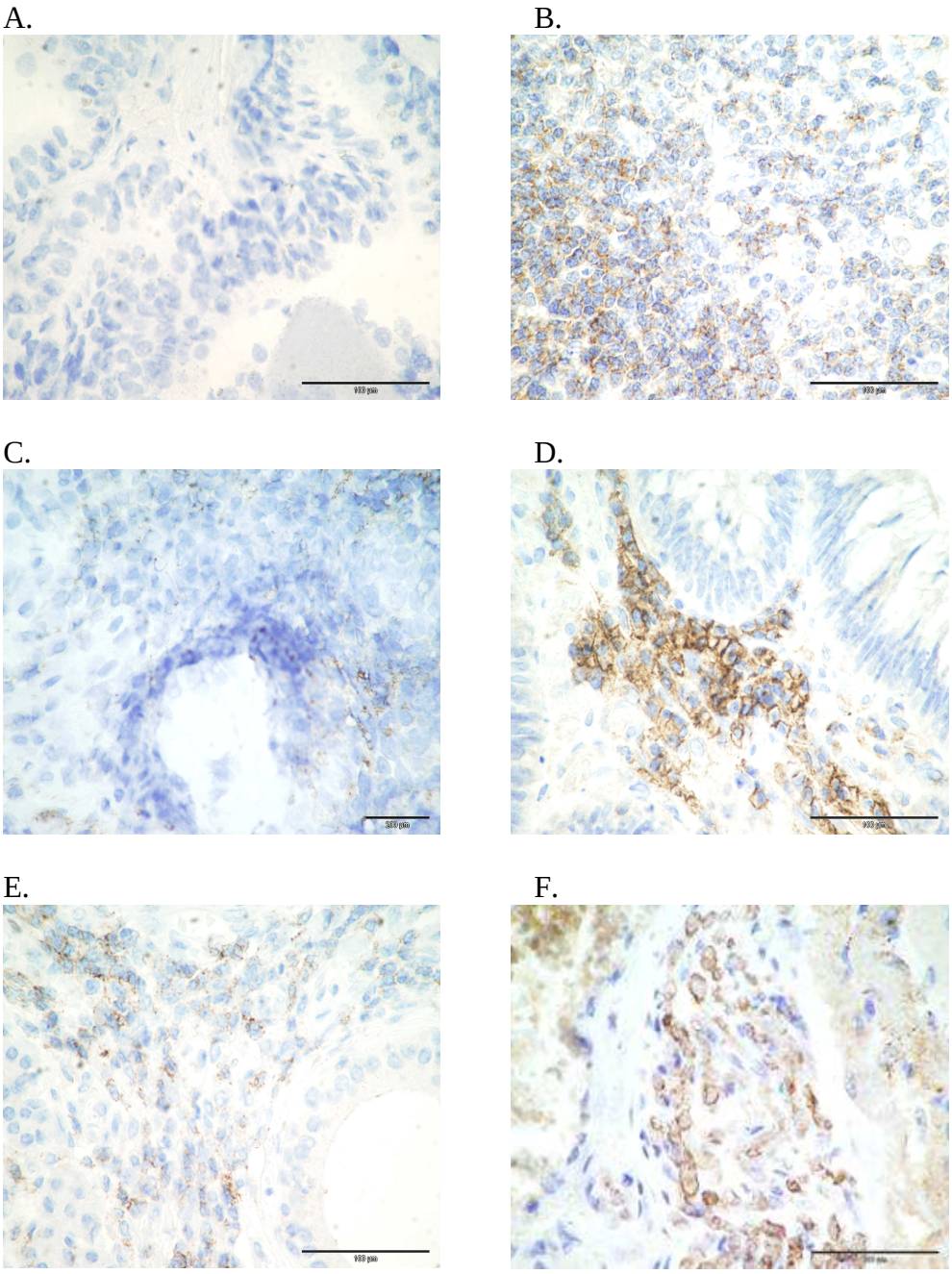

Figure 4.12: - A panel of normal, non-malignant tumour, and cancer tissues stained with MAb 9E1 24 (6). MAb shows membrane reactivity (some low level cytoplasmic reactivity also) in Hodgkins Lymphoma tissue (B), Retinoblastoma (F) and in a Warthins tumour (benign tumour of parotid gland) (E). Intense 9E1 positivity is observed in benign colon adenoma tumour (D) with weak positive staining observed in normal colon (C) and normal prostate tissue (A). Magnification, 200X, scale bar = 200µm (B) and (C). 400X, scale bar = 100µm (A), (D), (E) and (F).

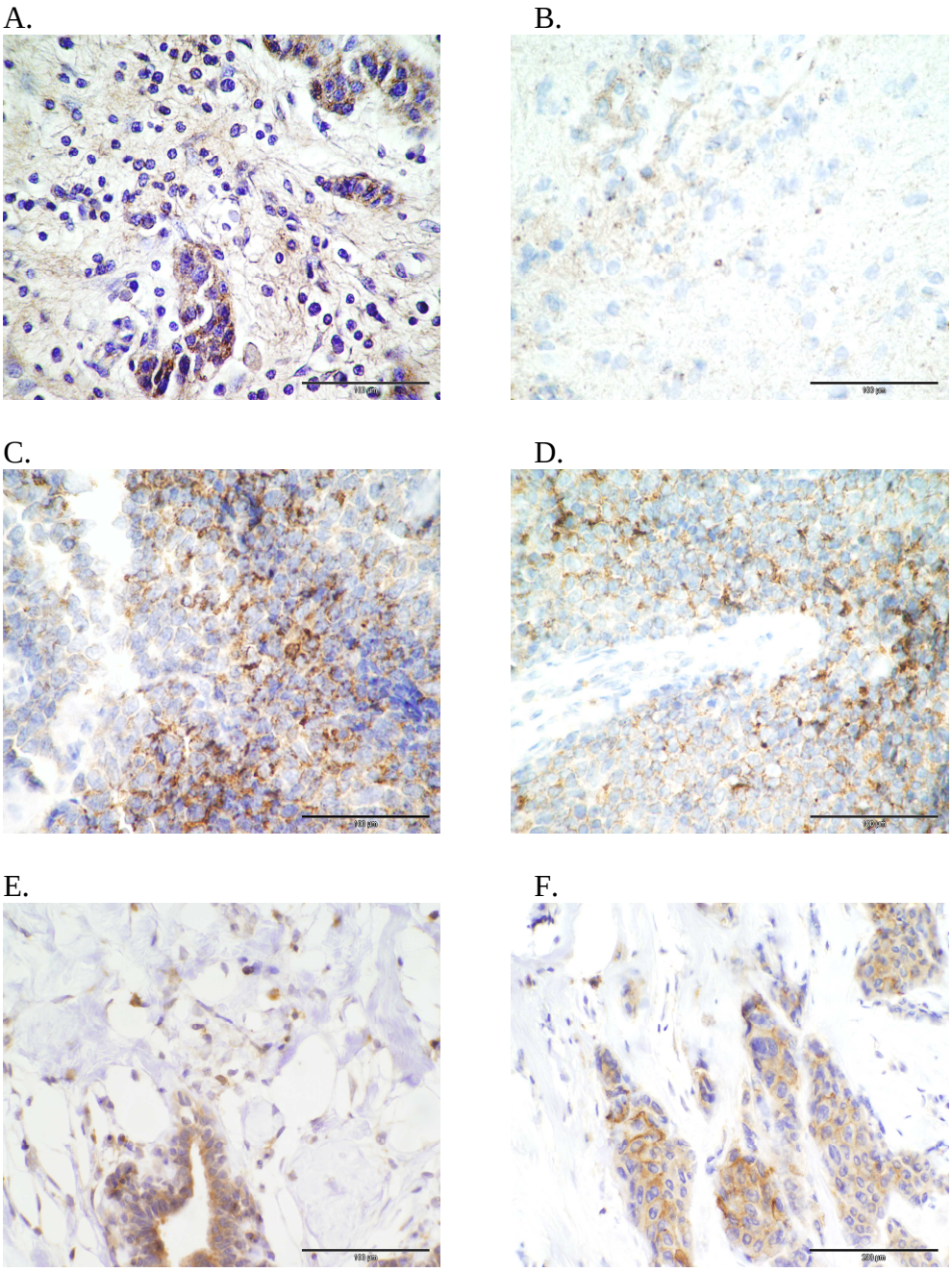

Figure 4.23.1: - A panel of normal and cancer tissues stained with MAb 9E1 24 (6). MAb positive staining is observed in pancreatic adenocarcinoma (A), B cell mantle lymphoma (C) and Malt lymphoma (orbital) tumour tissue (D). Very weak reactivity is observed in glioma (B). Normal breast tissue showing 9E1 reactivity is observed in (E) and a HER2 over expressing breast tumour showing 9E1 positivity (F). Magnification, 400X, scale bar, 100 μm, (A – E); 200X, scale bar, 200 μm (F).

4.13 Combination Studies Between MAb 7B7 G5 (2) & MAb 9E1 24 (6)

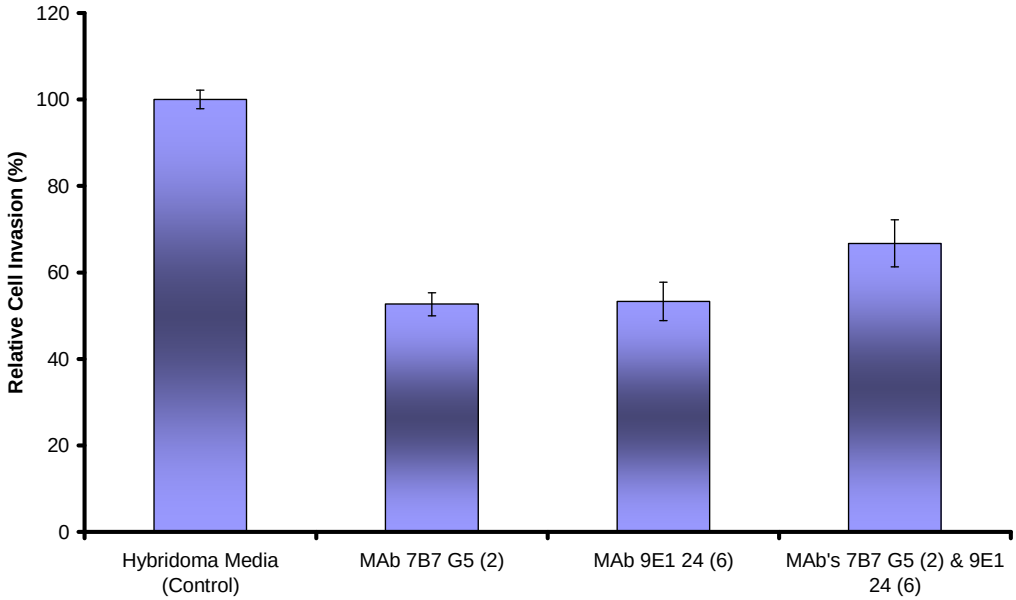

Figure 4.13: **-** Representative histogram showing inhibitory effects of MAb 7B7 G5 (2) and MAb 9E1 24 (6) individually, and in synergy, on MiaPaCa-2 clone 3 invasion after 48 hours. Both 7B7 G5 (2) and 9E1 24 (6) hybridoma neat supernatant inhibits invasion compared to the control hybridoma medium (no MAb) representing 100% invasion. However, when combined, there is no increase in inhibition levels, indicating no synergy between the two MAbs. *n = 3.* Error bars calculated using ± standard deviation.

4.14. Combination Studies with MAb 9E1 24 (6) & 7B7 G5 (2) and a Panel of Statins

Although MAbs have greatly enhanced cancer treatment, only a few are able to kill a sufficient number of malignant cells and cause tumour regression. Therefore, it is often necessary to use a combined treatment regime in order to enhance the efficacy of the anti-tumour activity.

A number of recent studies have suggested that cancer incidence rates may be lower in patients receiving statin treatment for hypercholesterolemia. Examination of the effects of statin drugs *in vitro*, on migration and invasion levels of melanoma cells was carried out. The ability of Lovastatin, Mevastatin and Simvastatin to inhibit the melanoma migration and invasion were assessed using invasion and migration assays. These compounds were then used in combination with both MAb 7B7 G5 (2) and 9E1 24 (6), in order to determine if any synergistic effect occurs in relation to inhibition of invasion.

4.14.1 Effect of Statins on the Invasion & Motility Levels on a Panel of Melanoma Cell Lines: - Lovastatin

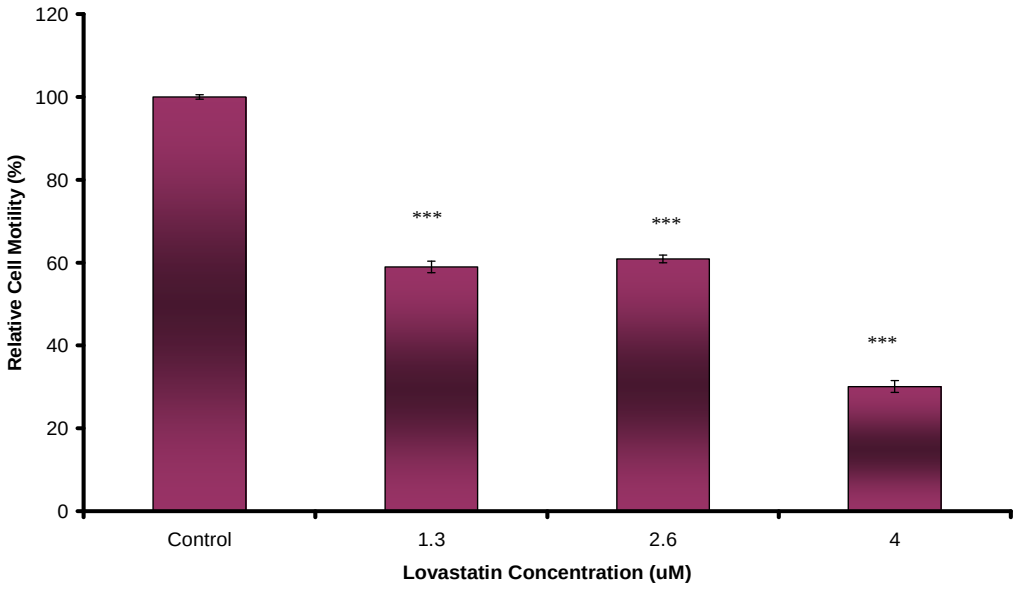

Figure 4.14: - Representative histogram of Lovastatin showing significant inhibition of HT144 cell motility at three different concentrations, compared to control (no Lovastatin) representing 100% motility, after 48hrs. Statistics; * $p \leq 0.05$, ** $p \leq 0.01$, *** $p \leq 0.005$, Student's t-test. *n = 3.* Error bars calculated using ± standard deviation.

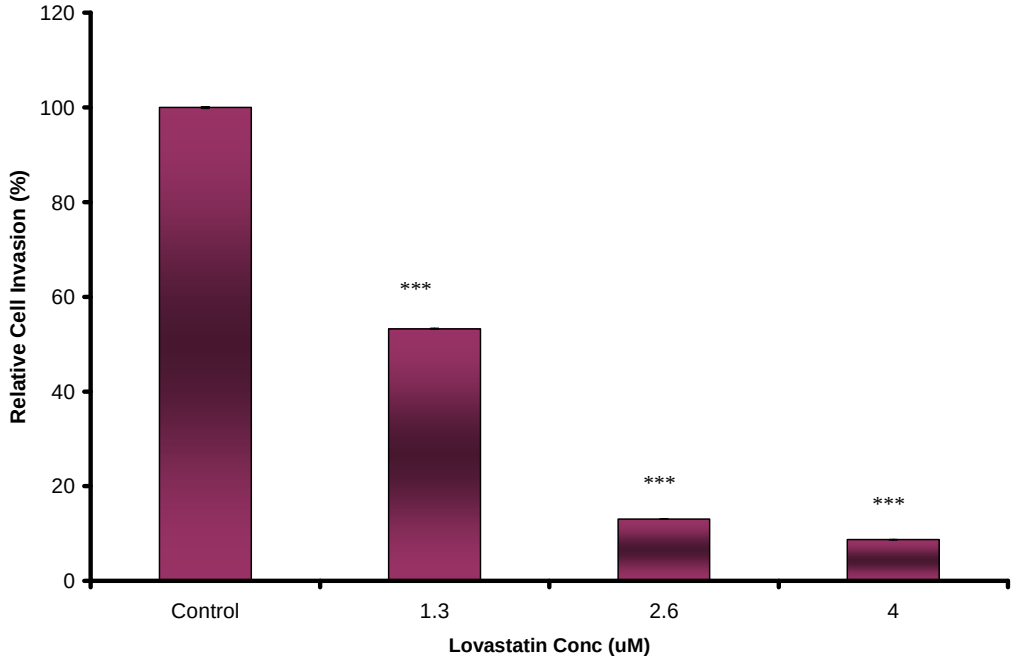

Figure 4.14.1: - Representative histogram of Lovastatin showing significant inhibition of HT144 cell invasion at three different concentrations, compared to control (no Lovastatin) representing 100% motility, after 48hrs. Statistics; * $p \leq 0.05$, ** $p \leq 0.01$, *** $p \leq 0.005$, Student's t-test. *n = 3.* Error bars calculated using ± standard deviation.

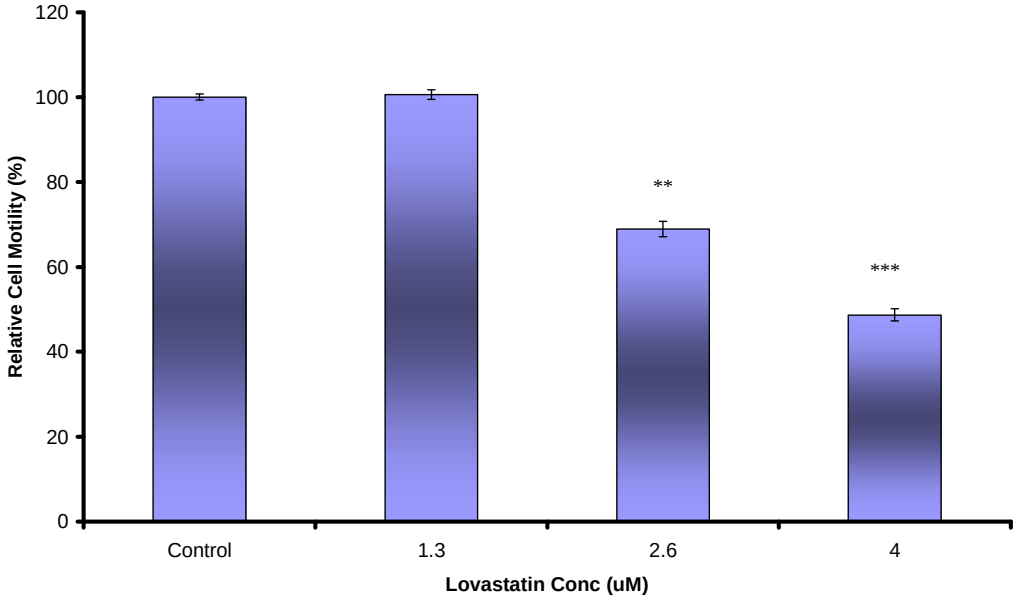

Figure 4.14.2: - Representative histogram of Lovastatin showing significant inhibition of SK-MEL-28 cell motility at two different concentrations, compared to control (no Lovastatin) representing 100% motility, after 48hrs. No effect on motility was observed with 1.3µM Lovastatin. Statistics; * $p \leq 0.05$, ** $p \leq 0.01$, *** $p \leq 0.005$, Student's t-test. *n = 3.* Error bars calculated using ± standard deviation.

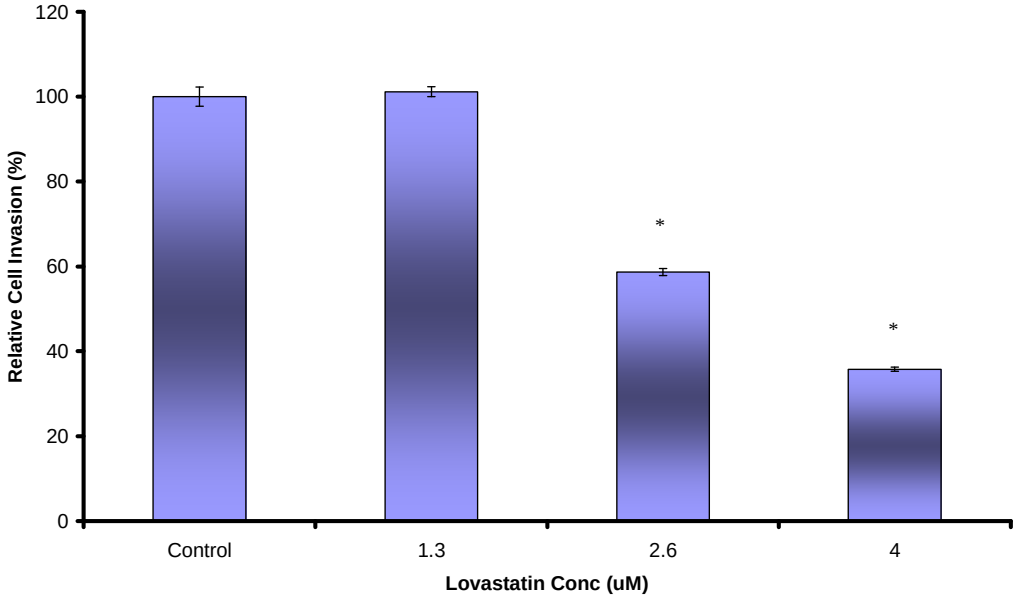

Figure 4.14.3: - Representative histogram of Lovastatin showing significant inhibition of SK-MEL-28 cell invasion at two different concentrations, compared to control (no Lovastatin) representing 100% motility, after 48hrs. No effect on invasion was observed with 1.3µM Lovastatin. Statistics; * $p \leq 0.05$, ** $p \leq 0.01$, *** $p \leq 0.005$, Student's t-test. *n = 3.* Error bars calculated using ± standard deviation.

4.14.2 Mevastatin

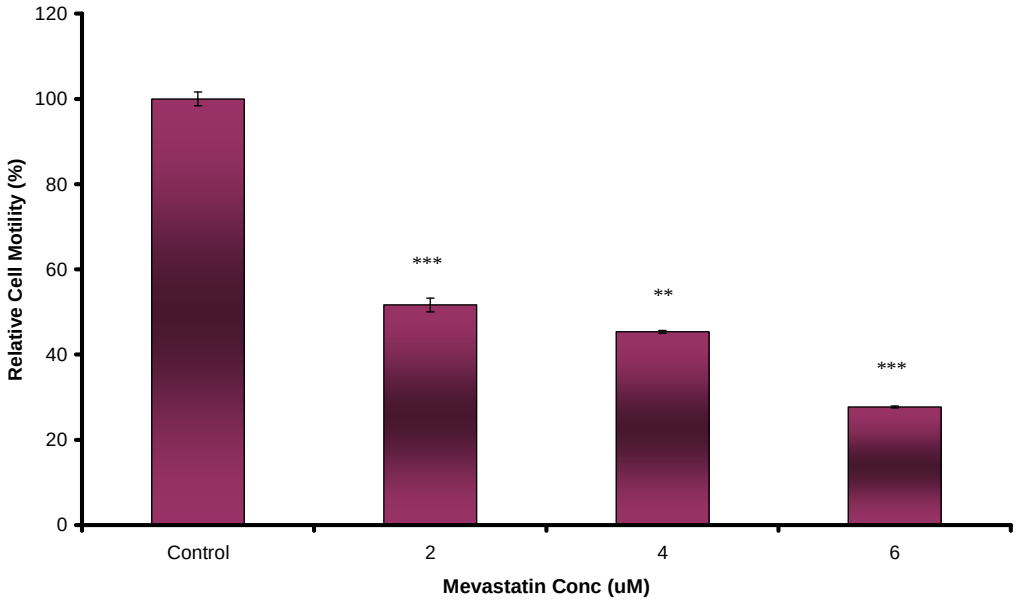

Figure 4.14.4: - Representative histogram of Mevastatin showing significant inhibition of HT144 cell motility at three different concentrations, compared to control (no Mevastatin) representing 100% motility, after 48hrs. Statistics; * $p \leq 0.05$, ** $p \leq 0.01$, *** $p \leq 0.005$, Student's t-test. *n = 3.* Error bars calculated using ± standard deviation.

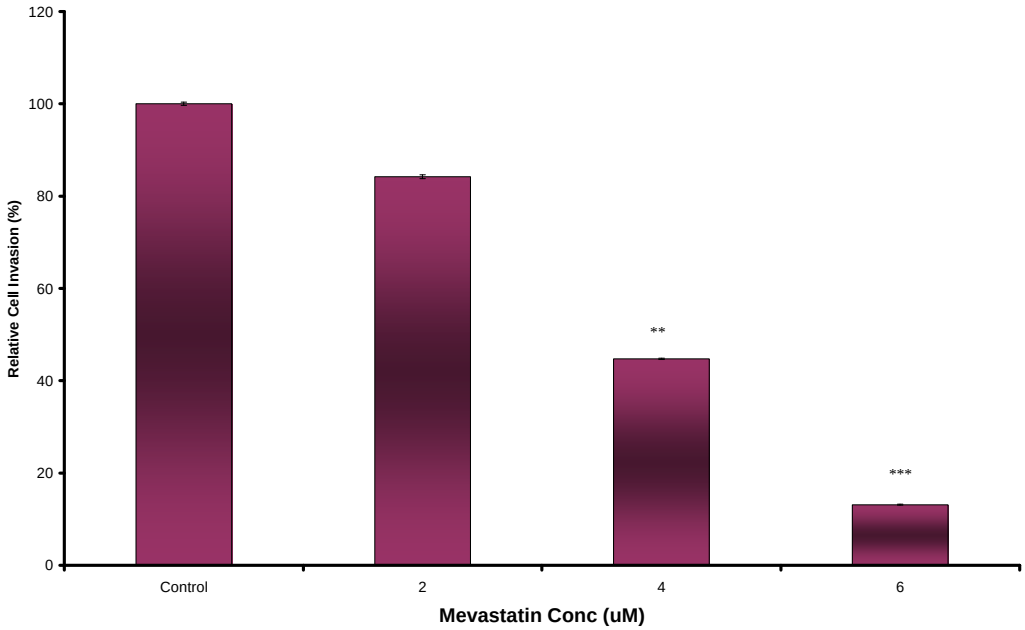

Figure 4.14.5: - Representative histogram of Mevastatin showing significant inhibition of HT144 cell invasion at two different concentrations, compared to control (no Mevastatin) representing 100% invasion, after 48hrs. Invasion was only slightly inhibited with 2µM Mevastatin. Statistics; * $p \leq 0.05$, ** $p \leq 0.01$, *** $p \leq 0.005$, Student's t-test. *n = 3.* Error bars calculated using ± standard deviation.

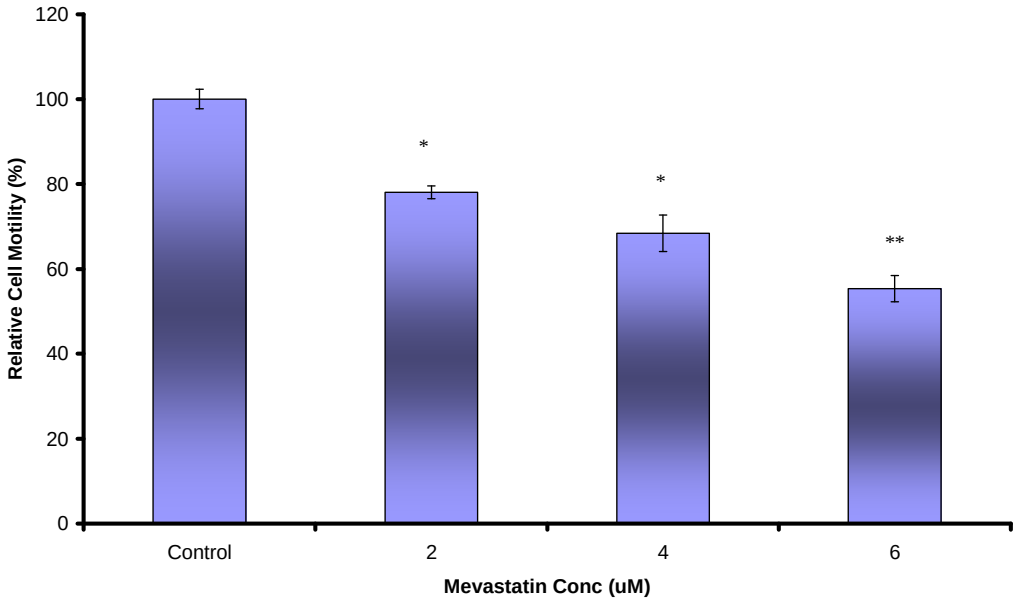

Figure 4.14.6: - Representative histogram of Mevastatin showing significant inhibition of SK-MEL-28 cell motility at three different concentrations, compared to control (no Mevastatin) representing 100% motility, after 48hrs. Statistics; * $p \leq 0.05$, ** $p \leq 0.01$, *** $p \leq 0.005$, Student's t-test. *n = 3.* Error bars calculated using ± standard deviation.

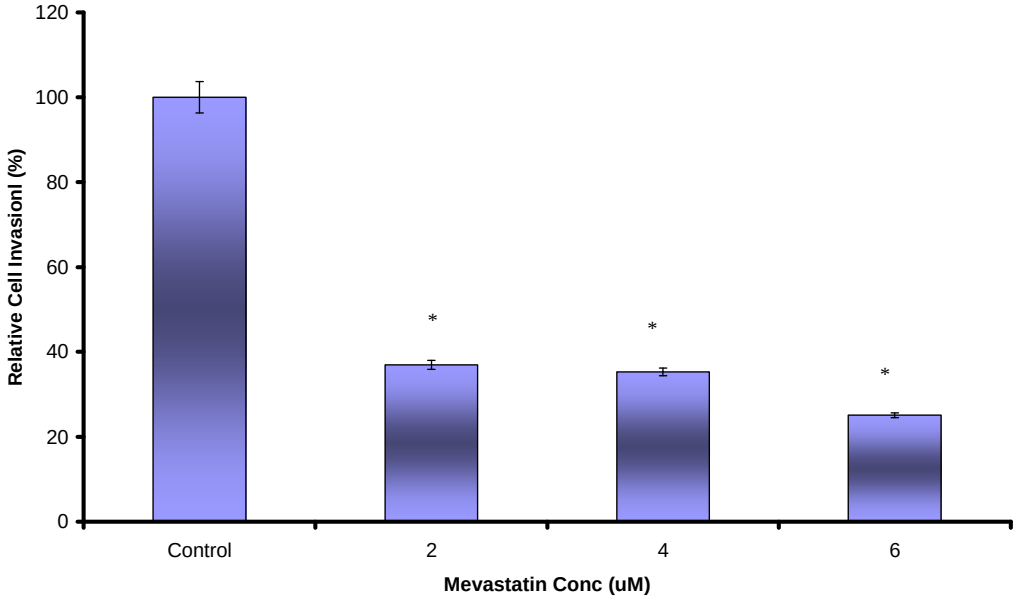

Figure 4.14.7: - Representative histogram of Mevastatin showing significant inhibition of SK-MEL-28 cell invasion at three different concentrations, compared to control (no Mevastatin) representing 100% invasion, after 48hrs. Statistics; * $p \leq 0.05$, ** $p \leq 0.01$, *** $p \leq 0.005$, Student's t-test. *n = 3.* Error bars calculated using ± standard deviation.

4.14.3 Simvastatin

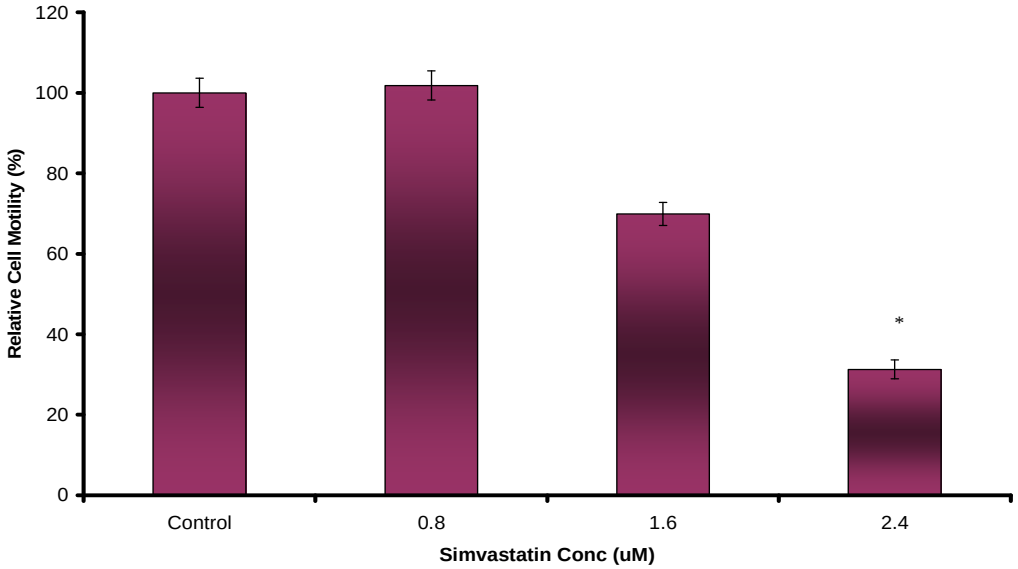

Figure 4.14.8: **-** Representative histogram of Simvastatin showing inhibition of HT144 cell motility at 1.6µM concentration, and significant inhibition at 2.4µM concentration, compared to control (no Simvastatin) representing 100% motility, after 48hrs. No effect on motility was observed with 0.8µM Simvastatin. Statistics; * $p \leq 0.05$, ** $p \leq 0.01$, *** $p \leq 0.005$, Student's t-test. *n = 3.* Error bars calculated using ± standard deviation.

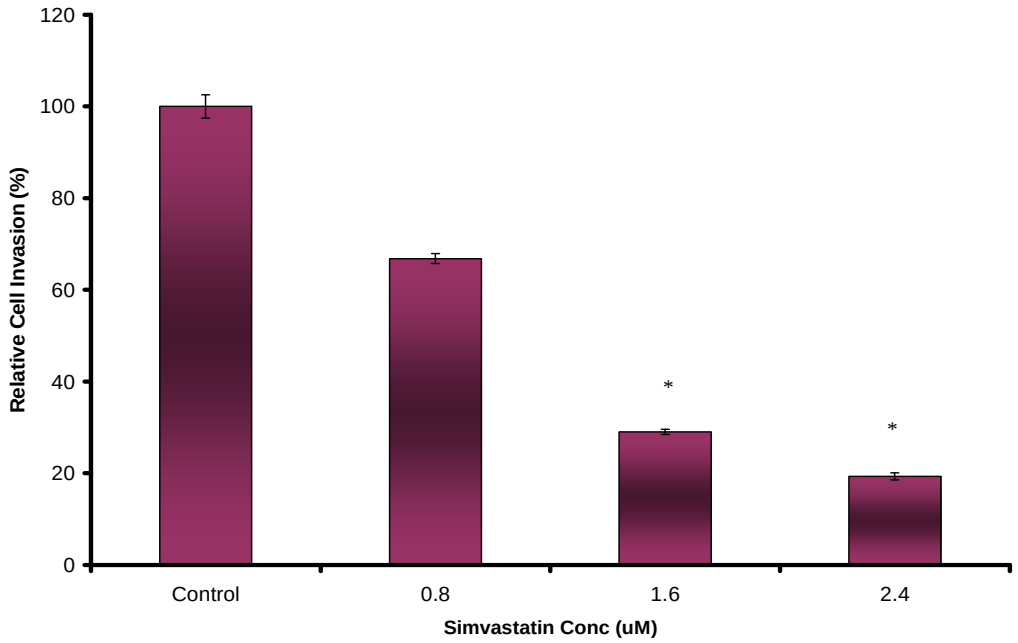

Figure 4.14.9: **-** Representative histogram of Simvastatin showing significant inhibition of HT144 cell invasion at two different concentrations, compared to control (no Simvastatin) representing 100% invasion, after 48hrs. Significance was not achieved with 2µM Mevastatin. Statistics; * $p \leq 0.05$, ** $p \leq 0.01$, *** $p \leq 0.005$, Student's t-test. *n = 3.* Error bars calculated using ± standard deviation.

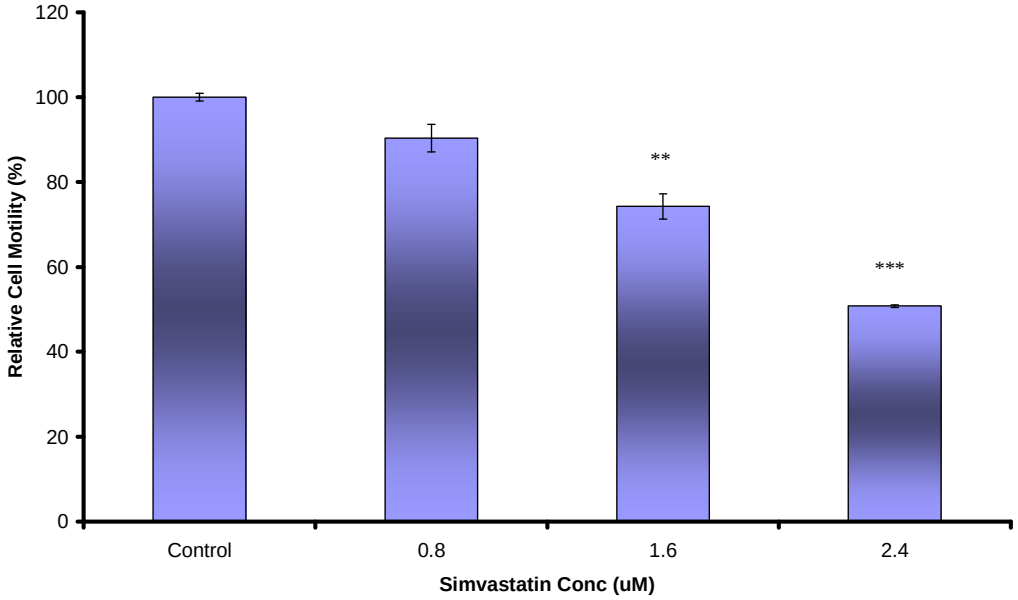

Figure 4.14.10: - Representative histogram of Simvastatin showing significant inhibition of SK-MEL-28 cell motility at two different concentrations, compared to control (no Lovastatin) representing 100% motility, after 48hrs. 0.8µM Simvastatin shows little decrease in motility levels. Statistics; * $p \leq 0.05$, ** $p \leq 0.01$, *** $p \leq 0.005$, Student's t-test. *n = 3*. Error bars calculated using ± standard deviation.

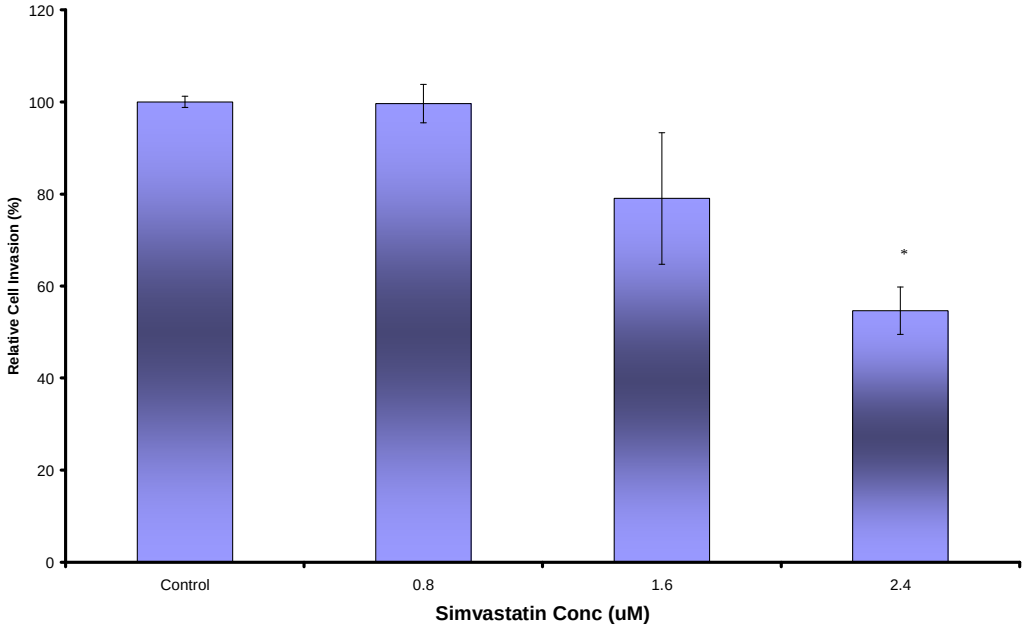

Figure 4.14.11: - Representative histogram of Simvastatin showing significant inhibition of SK-MEL-28 cell invasion at 2.4 µM concentration, compared to control (no Lovastatin) representing 100% invasion, after 48hrs. 0.8µM Simvastatin shows no decrease in invasion levels, while invasion is decreased with 1.6µM Simvastatin, but not significantly so. Statistics; * $p \leq 0.05$, ** $p \leq 0.01$, *** $p \leq 0.005$, Student's t-test. *n = 3*. Error bars calculated using ± standard deviation.

4.14.4 Effect of Statins and MAbs on Cell Invasion

4.14.4.1 MAb 7B7 G5 (2)

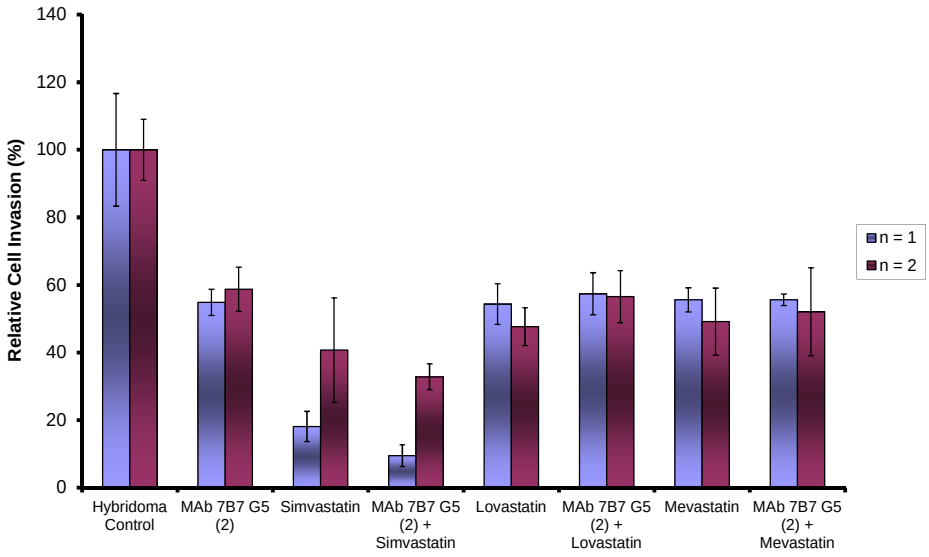

Figure 4.14.12: - Representative histogram showing significant inhibitory effects on MiaPaCa-2 clone 3 invasion by a panel of statins and MAb 7B7 G5 (2), working independently and synergistically of one another, compared to control hybridoma medium (no MAb or statins) representing 100% invasion after 48 hours. No synergistic effect was observed. Error bars calculated using ± standard deviation.

4.14.4.2 MAb 9E1 24 (6)

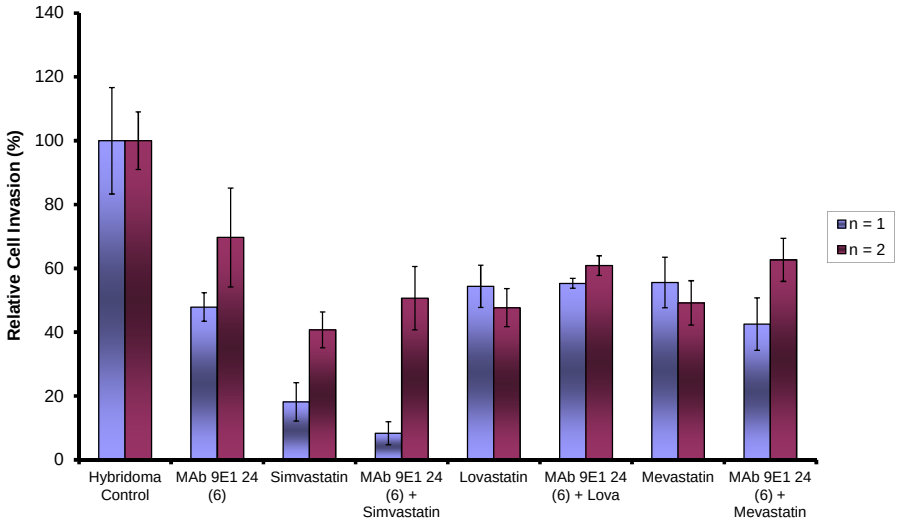

Figure 4.14.13: - Representative histogram showing significant inhibitory effects on MiaPaCa-2 clone 3 invasion by a panel of statins and MAb 9E1 24 (6), working independently and synergistically of one another. Independently, Simvastatin inhibits invasion by 75-80%, Lovastatin by 48-50%, and Mevastatin by 50-60%. When used in synergy with MAb 9E1 24 (6), there appears to be some synergy between the statins and MAb 9E1 24 (6). *n = 2.* Error bars calculated using ± standard deviation.

CHAPTER 5
DISCUSSION

The majority of deaths from cancer are due to metastatic disease. Metastasis is defined as the development of secondary tumours at a distance from a primary site of cancer. A critical step in metastatic progression is "invasion" – when cancer cells break through the ECM and enter the bloodstream/lymphatic system. While the malignant primary and secondary tumours can often be surgically removed, it is the invading cells circulating the body that cause the most harmful effects and prove to be the most difficult to target therapeutically. Successfully blocking or inhibiting these invading cells would greatly improve cancer treatment and patient prognosis. However, there are currently limited therapeutic treatments available that can successfully inhibit or prevent the invasion process.

A number of early studies involving anti-metastatic agents were carried out, however these failed to produce any clinically relevant therapeutic treatments. Early investigations involving tumour-invasion-inhibiting-factor 2 (IIF-2), a polypeptide of 21 amino acids isolated from bovine liver, successfully inhibited invasion of rat mesothelial monolayers *in vitro* (Isoai *et al*., 1990). An albumin-IIF-2 conjugate was then developed to increase the factor's half-life, and subsequent *in vivo* testing successfully inhibited colonisation of various highly metastatic tumour cells, including murine melanoma, colon adenocarcinoma, squamous cell carcinoma, forestomach carcinoma, and human fibrosarcoma (Isoai *et al*., 1994). Its anti-invasive effects appeared to be related only to an impairment of cell motility, as no inhibition of cellular adhesion or degradation of the ECM was noted. While this agent showed promising anti-invasive potential, no further studies or clinical trials were pursued.

Anti-invasion trials involving the use of MMP-inhibitors also failed to produce viable therapeutic strategies. A number of them did make it into Phase III trials, but were subsequently withdrawn. Tanamostat, an MMP-2, 3 and 9 inhibitor, was removed from Phase III trials due to patients with small cell lung cancer (SCLC) doing significantly worse than placebo-controlled patients. Prinomastat (MMP-2, 9, 13, & 14) failed to demonstrate any efficacy in any of the Phase III trials it was tested in (Fingleton, 2003). *In vivo* work carried out by Hoffman *et al*., on a new MMP inhibitor called *cis*-ACCP has shown good anti-invasion efficacy; however, it only targets MMP-2, and as such, will not be viable for a

wide range of tumour types e.g. NSCLC overexpress MMP-11 and 14 (Hoffman *et al*., 2008).

MAb therapy has emerged as an important therapeutic modality for cancer, due to the high specificity, low systemic toxicity, predictable pharmacology, ability to recruit the body's immune system and longer serum half-life of MAbs (Yan *et al*., 2008). There are a number of FDA-approved MAbs currently available for anti-tumour therapy, including Trastuzumab (Herceptin), the anti-HER2 MAb used in the treatment of HER2-overexpressing metastatic breast cancer (see Introduction – Table 1 for a full list of MAbs approved for the treatment of cancer). While these MAbs have constituted a tremendous success story for cancer treatment, they do not directly target tumour cells undergoing invasion. Some, like Trastuzumab, can limit cellular invasion, (blocking of HER2 by Trastuzumab reduced invasion *in vitro*, in the MDA-MB-435 breast cancer cell line (Sidera *et* al., 2008)); however, this is often only a side effect of their primary activity (e.g. promoting apoptosis, inhibiting cell proliferation/angiogenesis) - no MAbs are currently available that directly target the invasion process.

A number of studies are now taking place, which investigate the possibility of increasing the limited anti-invasive effects that current clinical MAbs possess. Recent work carried out by Fischgräbe *et al*., (2010) used a combination therapy of Trastuzumab and atrasentan to study the effects on SKBR-3 cell invasion. Atrasentan is an endothelin receptor antagonist, selective for subtype A (ET_A). Endothelin (ET) is a peptide containing 21 amino acids, and is involved in many normal physiological processes. They have also been shown to have a role in the growth and progression of several tumour types: in breast cancer, overexpression of ET_AR and its ligand, ET-1, correlates with decreased survival and resistance to chemotherapy (Wulfing *et al*., 2003, 2004). The authors found that dual HER2-ET_AR targeting, utilising Trastuzumab and atrasentan, was superior to either agent alone in inhibiting invasion in the SKBR-3 breast cancer cell line. Apart from enhancing the anti-invasion effects of Trastuzumab, it was also found that atrasentan enhances its anti-proliferative effects. These results suggest that the anti-tumourigenic properties of Trastuzumab, including its limited inhibitive

effects on cellular invasion, can be increased through combination therapy with other anti-cancer agents (Fischgräbe *et al*., 2010).

Another method for increasing the efficacy of current FDA-approved MAbs is to enhance their pharmacokinetic properties. Rituximab is generated in CHO (Chinese Hamster Ovary) cells, which express high levels of α1,6-fucosyltransferase (FUT8). Reduction of fucose content in Rituximab oligosaccharides, achieved through gene knockdown of FUT8 in the host CHO cells, or by generating the antibodies in other cell lines with reduced fucosylation activity (e.g. rat YB2/0 cells), results in >100-fold enhancement of ADCC activity (Shinkawa *et al*., 2003). Furthermore, engineering of the Fc region of the antibody, to increase the efficacy of binding to the neonatal Fc receptor (FcRn) (which prevents IgG degradation), increases the serum half-life of MAbs (Beck *et al*., 2010).

Studies have shown that targeting invasion-related proteins with MAbs (and other anti-cancer agents) can result in decreased cell invasion. A number of these MAbs are undergoing clinical trials (see section 1.8.5 for a comprehensive list), but as yet, none have received FDA approval.

The research carried out in this study focused on a different approach in developing MAbs. Rather than pursuing a specific molecular target known to be involved in cancer invasion, generating MAbs against this target and checking whether they can block/inhibit invasion *in vitro*, the approach used here involved the screening of MAbs directed against highly invasive cancer cells *directly* for function. Using a 96-well Boyden chamber assay, we were able to assess large numbers of MAbs for their effect on cell invasion. Those of interest were cloned and re-tested, to ensure that their activity against cell invasion was stable. Following this, the target antigens of the MAbs were immunoprecipitated, and identified through mass spectrometry analysis. Confirmation of their role in the invasion process was obtained through siRNA silencing of the antigens. Using this method, we discovered two MAbs, designated 7B7 G5 (2) [7B7] and 9E1 24 (6) [9E1], that directly target invasion-related proteins, and can successfully inhibit cell invasion in a number of cancer types.

5.1 Identification of MAbs That Can Block Cancer Invasion *In Vitro*

MAb 7B7 was generated against the highly invasive pancreatic cell line MiaPaCa-2 clone 3 (Walsh *et al.,* 2008). This cell line was chosen for immunisation because it is much more invasive than its parental cell line, displaying many differentially changed proteins, both up-regulated and down-regulated. By using this cell line as an immunogen, it was hoped that MAbs would be generated that recognise novel proteins associated with the invasion process. A second clonal variant of MiaPaCa-2 (clone 8), has significantly lower invasion levels compared to its parent cell line. Having both an invasive and non-invasive cell model available, MAbs produced could be tested to check for any increases or decreases in cell invasion.

MAb 9E1 was generated against the highly invasive breast cancer cell line, MDA-MB-435S. This is a spindle shaped variant of the parental cell line MDA-MB-435, which was isolated by Cailleau *et al.,* (1978), from the pleural effusion of a 31-year old female with metastatic ductal adenocarcinoma of the breast. A clonal population of this variant named MDA-MB-435-SF was established here in the N.I.C.B (Glynn *et al.,* 2004), which exhibited high levels of invasion. A Taxol resistant variant was then produced from this clonal variant through pulse selections, designated MDA-MB-435-SF-Taxol10p4p-SI. These two cell lines were chosen as immunogens due to their high levels of invasion and novel nature. It was hoped that any MAbs generated from this fusion would recognise new and unique proteins involved in the invasion process. However, characterisation work was not carried out with MDA-MB-435-SF, due to variations in invasion levels observed, and doubts about the origins of the parental cell line.

In 2000, gene expression analysis carried out on the National Cancer Institute's Developmental Therapeutics Program 60 (NCI60) cell line panel, found that MDA-MB-435 expressed a large number of melanoma-associated genes, and clustered with melanoma cell lines. It was proposed that the MDA-MB-435 cell line is of melanocyte origin and suggested that the patient, from whom the MDA-MB-435 cell line was derived from a pleural effusion, may have had an

undiagnosed melanoma (Ross *et al*,. 2000). While credible, a more likely explanation is that the MDA-MB-435 cells were inadvertently lost due to switching with, or contamination by, another cell line, an occurance not limited to the above cell line (Masters, 2002). Rae and colleagues subsequently presented evidence that both the MDA-MB-435 cell line and the M14 melanoma cell line were essentially identical, and that ‘‘all currently available stocks of MDA-MB-435 cells are derived from the M14 melanoma cell line and can no longer be considered a model of breast cancer’’ (Rae *et al*., 2007). Due to the uncertainty surrounding the cell line, it was decided to characterise the hybridoma supernatants on different cell lines. Recently, however, Chambers (2009) has suggested that MDA-MB-435 and M14 are identical cell lines, but are both *breast* cancer cell lines. Although identical, M14 cells have been shown to express two X chromosomes, despite the fact that they were derived from a biopsy specimen from a male patient (Wong *et al*., 1988). This has also been suggested by Hollestelle *et al*., (2009).

5.2 Functional Effects of MAbs

Following on from the discovery of the two MAbs, it was decided to characterise their effects on a number of cellular processes. Proliferation assays carried out on invasive MiaPaCa-2 clone 3 cells showed that both MAbs had no effect on cell survival or growth, suggesting that their target antigens are not involved in cell growth/survival (sections 3.4.1 & 4.4.3). These results also suggest that the decreases observed in invasion levels were a direct result of inhibition of invasion. Invasion and motility assays were also carried out on MiaPaCa-2 clone 3, resulting in significant inhibition of both processes following incubation with the MAbs. While MAb 9E1 reduced invasion levels in this cell line by up to 80% (section 4.4.2), inhibition of motility, while significant, was not as pronounced, with an average decrease of 23% observed (section 4.4.3). This suggests that the target antigen of 9E1 is playing a significant role in the invasion process, but less so in cell motility. 7B7 significantly reduced invasion, by up to 49% (section 3.4.2), while similar levels of inhibition were observed in relation to motility (section 3.4.3), suggesting that this MAb’s target antigen is involved in both the invasion and motility process. However, at this stage, it was unclear whether the decrease in invasion levels observed in this cell line was due to a decline in

cellular motility. At this point, it was decided to expand the investigation of the functional effect of both MAbs to cover a wider range of human cancer cell lines.

A panel of invasive breast cancer, lung cancer, and melanoma cell lines was investigated with 9E1 and 7B7, as were prostate, glioma and colon cancer cell lines. The levels of inhibition observed following incubation with the MAbs varied between the cell lines, with some showing little to no knockdown of invasion levels, while in some cell lines an unexpected *increase* in the levels of invasion was observed following MAb 9E1 incubation.

Motility assays were also carried out on the glioma cell line SNB-19 in the presence of 7B7 (section 3.4.8). Results show a decrease in motility levels, by up to 14.3%, while invasion is inhibited, by up to 33.8%. This suggests that the inhibition of invasion is not completely due to a decrease in motility in this cell line.

Cancer Type	Cell Line	MAb 7B7 % Inhibition (up to..)	MAb 9E1 % Inhibition (up to..)
Breast	MDA-MB-157	No Inhibition	*50.9% Increase*
	MDA-MD-231	32.9%*	37.4%*
	SKBR-3	30.2%*	55.6%
Lung	DLKP-I	35%	53.3%*
	DLKP-M	50%*	76.2%*
	H1299	30.5%*	34.5%*
Pancreatic	MiaPaCa-2 clone 3	51.7%*	79.6%
	BxPc-3	16%	No Inhibition
Melanoma	Lox	29.6%	50.6%*
Glioma	SNB-19	33.8%*	No Inhibition
Prostate	C/68	20%	50.9%*
Colon	HCT-116	32%*	*125.3% Increase**

Table 5: - **Effect of MAb 7B7 G5 (2) and 9E1 24 (6) on invasion levels in a panel of cell lines. * Significant result.**

From the results obtained, it can be stated that 9E1 has a greater inhibitory effect on cell invasion than 7B7. However, no increases in invasion were observed following incubation with 7B7. Dose response studies were also carried out with both MAbs. With regard to 7B7, a corresponding drop in inhibition levels was observed in the MiaPaCa-2 clone 3 cell line, when the MAb was diluted (section 3.4.2). Dose-response experiments with 9E1 in the DLKP-M cell line (section 4.4.5) also showed that there was a corresponding decrease in invasion levels. However, surprisingly, at low levels of the MAb (1 in 5 dilution), invasion in DLKP-M was *increased*, by up to 62%.

These results suggest that the target antigen(s) of 9E1 may be playing a dual role in the invasion process of a number of cell lines, acting as both a pro- and anti-invasive protein(s). It would also appear that at low concentration, this MAb can stimulate invasion in a cell line where higher levels of the MAb decrease cell invasion.

Cell invasion into the blood/lymph vessels depends on the interaction of the invading cells with components of the ECM and basement membrane, as does the penetration of the tumour cell into an organ at a secondary site. Adhesion assays were therefore carried out in order to observe whether the MAbs had any effect on the ability of cancer cells to adhere to matrigel and fibronectin (sections 3.4.12 & 4.4.12). Adherence of MiaPaCa-2 clone 3 to fibronectin was reduced following incubation with 7B7 (up to 29%). A significant decrease in adhesion of DLKP-M lung cancer cells to matrigel (up to 35%) was also observed. 9E1 slightly reduced adherence of MiaPaCa-2 clone 3 to fibronectin, while a significant decrease in adhesion of DLKP-M cells to matrigel (up to 42%) was observed.

Anoikis assays were carried out to determine whether the MAbs affected the ability of cancer cells to survive in suspension (sections 3.4.13 & 4.4.13). When normal cells lose contact with the ECM, and become “unanchored”, they undergo a form of programmed cell death termed “anoikis”. Cancer cells often display a resistance to this form of cell death, allowing for their survival during systemic circulation, thereby facilitating secondary tumour formation in distant

organs (Douma *et al*., 2004). Both MiaPaCa-2 clone 3 and DLKP-M cells were incubated with 7B7 and 9E1 in conditions that induce anoikis (i.e. anchorage independent growth); however, no change in survival was observed, indicating that the MAbs do not affect anoikis.

The effects of 7B7 and 9E1 on MMP activity were also investigated (sections 3.4.15 & 4.4.15). MMPs are regarded as essential molecules for tumour cells undergoing metastasis. Early studies have shown that in cancer cells, there is a clear relationship between MMPs, ECM degradation and cancer cell invasion. Inhibition of MMPs corresponds to inhibition of cell invasion; conversely, up-regulation of MMPs usually leads to increases in tumour cell invasion. These studies concluded that enhanced MMP levels result in increased tumour cell invasion (Liotta *et al*., 1980, 1986). The MDA-MB-231 breast cell line is known to have high expression levels of MMP-9 (Hegedus *et al*., 2008) and was therefore chosen for this study. We found that MDA-MB-231 cells incubated with 7B7 and 9E1 for 24hrs showed a marked decrease in MMP-9 activity, compared to MAb-free cells, suggesting that *both* MAbs can negatively affect MMP activity. However, it is still unclear if the decrease in MMP-9 activity is due to direct interaction of the MAb with MMP-9, or whether it is indirectly inactivated through inhibition of downstream signalling events. Western blot analysis of cell lysates incubated with the MAb, probed with an MMP-9 specific antibody will determine whether MMP activity is directly or indirectly affected.

Incubation of MiaPaCa-2 clone 3 cells with the MAbs also produced a definite change in cell morphology (sections 3.4.14 & 4.4.14). Under normal conditions, MiaPaCa-2 clone 3 cells exhibit a fibroblast-like phenotype, with spindle shaped elongated cells, typical of highly invasive and motile cells. However, when grown in the presence of 7B7 and 9E1, the cells lose this spindle-shaped morphology, and start to display a more rounded appearance, similar to the morphology of the low invasive variant of the MiaPaCa-2 cell line, clone 8 (Walsh *et al*., 2008). Loss of the spindle-shaped morphology might be expected in cells that have had their invasive capacity suppressed.

Preliminary immunofluorescence studies were initially carried out with both MAbs on the MiaPaCa-2 variants. Staining in the MiaPaCa-2 clone 8 cell line with 7B7 was weaker than that observed in the clone 3 variant, suggesting that its target antigen is up-regulated in the highly invasive clone 3 cell line. This staining pattern was further demonstrated in the poorly invasive DLKP-SQ compared to the highly invasive DLKP-Mitox-6p variant. With regards to any association with invasion, conflicitng results were observed with MAb 9E1. MiaPaCa-2 clone 8 appeared to show stronger reactivity than that observed in the more invasive MiaPaCa-2 clone 3 variant, while staining in the DLKP-Mitox-6p variant was slightly stronger than the DLKP-SQ. MAb 7B7 showed membrane and cytoplasmic reactivity on MiaPaCa-2 clone 3 cells (figure 3.3.2), while MAb 9E1 (figure 4.5) showed puntuated type, membrane staining on the same cell line. Some cytoplasmic reactivity was also observed. It would be likely to expect both MAbs to be reacting with a cell surface protein.

Cell surface proteins are known to be involved in several key stages of metastasis, so their expression is of fundamental importance in cancer research, and may serve as potential therapeutic targets. For example, HER2 is overexpressed at the cell surface in a range of breast tumours, and its discovery led to the development of Trastuzumab (Slamon *et al*., 2001). Furthermore, growth factor receptors expressed on the cell surface have been linked to signalling and uncontrolled cell proliferation in many cancer types, (e.g. EGFR). This has led to the development of anticancer therapies that target specific components of the EGFR signal transduction pathway e.g. Cetuximab (Raymond *et al*., 2000).

Western blot analyses were carried out in order to identify the molecular weights of the target antigens; however, 7B7 probing of a panel of cell lines did not produce any reactive bands. Therefore, we were unable to establish the molecular weights of 7B7's potential reactive antigen(s). Analysis of 9E1 did reveal a strong reactive band of approximately 75 kDa in a number of cell lines, including MiaPaCa-2 clone 3, MiaPaCa-2 clone 8 and SKBR-3 (section 4.6), indicating that this MAb was recognising a target antigen of approximately 75kDa:

Cancer Type	Cell Line	Reactivity
Pancreatic	MiaPaCa-2 clone 3	+ + +
	MiaPaCa-2 clone 3 (Matrigel)	+ + +
	MiaPaCa-2 clone 8	+ + +
Melanoma	Lox IMVI	+ + +
	SK-MEL-28	+ + +
	WM-115	+ / -
	WM-226-4	+ / -
Glioma	SNB-19	+ / -
Lung	DLKP	+ +
	DLKP-A	+
	DLKP-I	+ +
	DLKP-M	+ +
	DLKP-SQ	+ + +
	H1299	+ +
Prostate	C/68	+ + +
Colon	HCT-116	+ + +
Breast (Triple Negative)	MDA-MB-231	+ +
Breast (HER2-Positive)	MDA-MB-453	-
	MDA-MB-361	+ +
	SKBR-3	+ +
	BT474	+ +

Table 5.1: - **Western blot analysis of MAb 9E1 in a panel of cancer cell lines.**

+++ Very Strong; ++ Strong; + Intermediate; +/- Weak

Analyzing the levels of 9E1 expression in various cancer cell lines, it was found that expression in the metastatic WM-266-4 metastatic cell line was stronger than that observed in the WM-115 primary tumour. This pattern was also observed in the DLKP variants, with expression in the invasive I and M cell lines being stronger than that observed in the poorly invasive DLKP and less invasive

DLKP-A. However, the low invasive DLKP-SQ exhibited strong expression levels. (Immunofluorescence analysis showed more intense 9E1 reactivity in the DLKP-Mitox-6p cell line, compared to DLKP-SQ, however, no Western blot data is available for this cell line). SNB-19 showed little expression of the reactive antigen, which corresponds to the lack of inhibition of invasion observed in this cell line when incubated with 9E1. SKBR-3, MDA-MB-231, C/68, H1299, DLKP I and M, Lox IMVI and MiaPaCa-2 clone 3, all showed strong to very strong expression of the reactive antigen, and invasion in each was significantly inhibited following incubation with 9E1. HCT-116 also showed very strong expression. This assay shows that the main target antigen of 9E1 is expressed, to varying degrees, in a broad range of cancer cell types, both invasive and non-invasive.

5.3 Proteomic Identification of MAb Target Antigens

Immunoprecipitation studies were carried out in order to try to identify the reactive antigens of both MAbs. Immunoprecipitation is a technique which allows for the identification of a protein/antigen that reacts specifically with an antibody from a mixture of proteins so that its quantity or physical characteristics can be examined. In immunoprecipitation, the protein(s) from the cell or tissue homogenate is precipitated in an appropriate lysis buffer prior to addition of the antibody. An immune complex is then formed with the addition of the antibody to the cell lysate (which includes the antigen(s)). Once this antibody-antigen complex is formed, a protein A-, G-, or L-agarose conjugate (depending on the isoform of the antibody) is added, capturing the complex. Proteins that are bound to the antibody are precipitated, while those that are not are washed away; in order to ensure that the protein has not been non-specifically bound, an immunoprecipitation with a control antibody - mouse IgM/IgG, or an antibody with a known target protein - is run in parallel. Components of the bound immune complex are eluted from the beads, and the “immunoprecipitate” is separated according to molecular weight, using SDS-PAGE. Visualisation is achieved through colloidal blue or silver staining of the SDS-PAGE gel. The visible protein can now be excised and identified using mass spectrometry analysis.

As the MiaPaCa-2 clone 3 cell line showed the greatest inhibition of invasion following incubation with both MAbs, it was chosen to immunoprecipitate out the reactive antigens. However, subsequent immunoprecipitations were carried out on other cell lines (H1299, Lox IMVI, DLKP-I).

Immunoprecipitations were carried out using Protein-L agarose beads to pull out the reactive antigens. Protein-L was chosen due to its ability to bind onto both the IgM and IgG antibody chains, through kappa light chain interactions without interfering with the antibody's antigen-binding site (Nilson *et al*., 1996). This approach was also used in a previous study by Larkin *et al*., (2005) to immunoprecipitate the target antigen of MAb 5C3. Crude cell lysates of the cells were prepared using three lysis buffers. Lysates prepared with NP/40 resulted in gels with numerous protein bands. RIPA, and finally lysis buffer C (see section 2.10.1) produced gels with much sharper protein bands and low level background bands. (NP/40 buffer has a low denaturing level, while RIPA and lysis buffer C give lower backgrounds in immunoprecipitation, but can denature some proteins.)

Following incubation of 9E1 with the cell lysate, the antigen was immunoprecipitated using Protein-L agarose beads, and separated on a 4-12% Bis tris SDS-PAGE gel. The gel was subsequently stained with Coomassie Blue, allowing for visualisation of the bands (section 4.7.1). Five bands of interest were observed following immunoprecipitation with 9E1, each of which were excised for mass spectrometry analysis. A number of these bands were identified, but subsequently disregarded, as the same proteins had also been identified with the control IgG antibody.

Mass spectrometry (MS) is an analytical chemistry technique used for measuring mass-to-charge ratio (*m/z*) of gas-phase ions. It is the standard method used in the identification of proteins, by comparing MS data to gene and sequence databases. Basic MS instruments are comprised of three components: an ion source that confers electrical charge to the molecules, a mass analyser that separates resulting ions according to their *m/z* ratio, and a detector. In MS/MS, singly or multiply charged ions are selected according to their *m*/*z* in an initial mass

spectrometric stage. The selected precursor ions are then fragmented through collisions with an inert gas (such as helium or argon), in a process known as collisionally induced dissociation (CID). The fragmented ions formed are then mass analysed in a second mass spectrometric stage (Bonner *et al.,* 2002). An MS/MS spectrum is then produced, which represents peptides as readable entities, allowing for their interpretation and correlation with theoretical peptide sequences found in protein or genomic databases.

Extensive online searching of the peptide sequences obtained through MS/MS (section 4.9), using the SWISS-PROT database, indicated that the band excised at approx. 75 kDa was Annexin A6, with a molecular weight of 75.87 kDa. The lower band, excised at approx. 35 kDa consisted of a complex of proteins, identified as Prohibitin (M.W. = 29.8 kDa), protein 14-3-3ε (M.W. = 29.1 kDa) and 3 variants of ADP/ATP Translocase (1 – 3; M.W. = 33, 32.87, 32.84 kDa respectively). Variants of 40S Ribosomal protein were also identified. All identifications were obtained with multiple peptide sequences, matching the theoretical sequences in the protein database, high XC scores, and matching molecular weights (section 4.9.1). These criteria allowed us to accept that the identified proteins were immunoprecipitated out by the 9E1 MAb with a high degree of certainty. From this, it would appear that the MAb's target antigen is Annexin A6, as the molecular weight of this protein matches that of the reactive band seen in the Western blot analysis on a panel of cell lines probed with MAb 9E1, including MiaPaCa-2 clone 3, MiaPaCa-2 clone 8, BT474 and SKBR-3 (see figure 4.10.5). It is likely then that the other identified proteins may be interacting with this target protein.

Western blot analysis of immunoprecipitated samples probed with commercial antibodies specific for Annexin A6, Prohibitin, and the 14-3-3ε protein (section 4.10) showed a reactive band at the expected molecular weights, validating the identifications obtained through mass spectrometry analysis.

Following immunoprecipitation studies with 7B7, six bands of interest were observed which were all excised for mass spectrometry analysis (section 3.7.1).

A number of these bands were identified, but disregarded, as the same proteins were immunoprecipitated out with the control IgM antibody. All of the other bands failed to produce a positive identification, as the IgM heavy chain was contaminating the proteins. Numerous methods were employed to overcome this, including varying the cell lysate concentration, antibody concentration, MAb/lysate incubation time, antibody/antigen/Protein-L complex, Protein-L volume, and varying the incubation and washing times. All this failed to produce a positive identification. In order to obtain a positive identification, the interfering IgM heavy chain would have to be removed. It was therefore decided to carry out a cross-linked immunoprecipitation.

With cross-linked immunoprecipitation, the antibody is covalently immobilised to the agarose beads by cross-linking with disuccinmidyl suberate (DSS). The antibody/agarose complex is then added to the sample containing the antigen of interest, forming an antibody-antigen complex. As before, the bound antigens are precipitated, while those that are not are washed away. The antigen is then dissociated from the antibody, allowing the pure antigen sample to be separated on SDS-PAGE. With this method, the antigen can be identified through mass spectrometry without any interference from antibody fragments.

Prior to cross-linked immunoprecipitation, the antibody needs to be purified and dialysed. This is due to the fact that any amines (e.g. Tris or glycine), gelatine or carrier proteins will compete for binding sites to the agarose beads, thus decreasing antigen binding (section 3.7.2).

Following cross-linked immunoprecipitation (section 3.7.3), the antigen-only sample was separated on SDS-PAGE and bands were visualised with Coomassie Blue. This time, 3 bands were visible, at approx. 108 kDa, 80 kDa and 70 kDa. The 108 kDa band, identified as Nucleolin, was disregarded, as it was also identified with the control IgM antibody. The two remaining bands were excised, and analysed using a liquid chromatography- tandem mass spectrometer (LC-MS/MS).

Database searching of the peptide sequences obtained through mass spectrometry (section 3.9), using the SWISS-PROT database, indicated that the protein excised at approx. 80 kDa was ATP-dependent DNA helicase 2 subunit 2 (Ku80), with a molecular weight of 82.65 kDa. The lower band was identified as ATP-dependent DNA helicase 2 subunit 1 (Ku70), with a molecular weight of 69.79 kDa. Both identifications were obtained, in triplicate, with multiple peptide sequences, matching the theoretical sequences in the protein database, high XC scores, and matching molecular weights. These criteria allowed us to accept that the identified proteins were immunoprecipitated by the 7B7 with a high degree of certainty. As no other proteins were identified, it would appear that the MAbs target antigen is the Ku heterodimer. It was therefore decided to carry out further investigations on the Ku70 and Ku80 proteins, including siRNA silencing.

Western blot analysis of the immunoprecipitated samples with commercial antibodies targeting the Ku70 and Ku80 proteins showed a strong reactive band in both immunoprecipitates when probed with their corresponding antibody, thus validating the identifications obtained through mass spectrometry analysis (section 3.10).

5.4 Investigation of Target Antigens of MAb 9E1 24 (6)

Following identification of Annexin A6, and the strong indications that it is the target antigen of 9E1, the next step was to determine what role, if any, it plays in the invasion process. This was achieved by silencing the Annexin A6 gene using RNA interference (section 4.11). MiaPaCa-2 clone 3 and DLKP-M were chosen for this study. No other protein was chosen for siRNA silencing, due to the fact that only one reactive band was observed in Western blot analyses with 9E1, corresponding to the molecular weight of Annexin A6.

Annexin A6 is a major cellular calcium and phospholipid binding protein, and has been suggested to have tumour suppressive effects, through its ability to cause the down-regulation of the cell proliferation pathways initiated by activated Ras (Monastyrskaya *et al*., 2009). However, limited information is available with regard to its specific role, if any, in the invasion process.

Annexin A6 was successfully knocked down in both cell lines as shown by Western blot analysis. In both MiaPaCa-2 clone 3 and DLKP-M, Annexin A6 silencing did not affect cell proliferation, in agreement with proliferation results obtained with 9E1-incubated cells. (Kinesin transfected cells did however show a dramatic decrease in cell number, indicating that siRNA transfection was successful.) In relation to invasion, Annexin A6 knockdown by two siRNAs targeting the protein, significantly inhibited invasion in the MiaPaCa-2 clone 3 cell line, while siRNA-B significantly inhibited DLKP-M invasion levels. In relation to motility, no significant reduction was observed in any of the cell lines. These results indicate that Annexin A6 is involved in the invasion process of both these cell lines.

Western blot analysis on the same panel of cell lines previously probed with 9E1 was carried out with a commercial Annexin A6 antibody (section 4.12). The expression pattern observed was almost identical to that seen with 9E1 (with no expression in the SNB-19 cell line observed). Western blot analysis of 9E1 on Annexin A6 silenced MiaPaCa-2 clone 3 cells showed a significant decrease in the expression of the reactive antigen. These results give further corroboration that the main target antigen of the MAb is indeed Annexin A6. Expression levels of Protein 14-3-3ε in the same panel of cell lines were also looked at. All cell lines showed strong expression of this protein, including the WM-114, WM-266-4 and SNB-19 cell lines. Expression levels were somewhat stronger in the MiaPaCa-2 clone 8 and DLKP-SQ cell lines. Western blot analyses of Protein 14-3-3ε on Annexin A6 silenced cells were also carried out; however, expression levels remained unchanged, indicating that this protein is unaffected by the loss of Annexin A6.

Cell Line	Reactivity
MiaPaCa-2 clone 3	+ + +
MiaPaCa-2 clone 3 (Matrigel)	+ + +
MiaPaCa-2 clone 8	+ + +
Lox IMVI	+ + +
WM-115	+ / -
WM-226-4	+
SNB-19	-
DLKP	+
DLKP-A	+ +
DLKP-I	+ +

Cell Line	Reactivity
DLKP-M	+ +
DLKP-SQ	+ + +
H1299	+
C/68	+ +
HCT-116	+ + +
MDA-MB-231	+ + +
MDA-MB-453	+
MDA-MB-361	+ + +
SKBR-3	+ + +
BT474	+ + +

Table 5.2: - **Western blot analysis of Annexin A6 in a panel of cancer cell lines.**

+++ Very Strong; ++ Strong; + Intermediate; +/- Weak

The levels of Annexin A6 expression observed in this study are similar to previously published results. de Muga *et al*., (2009) carried out Western blot analyses of Annexin A6 expression on a range of normal and cancerous breast cell lines. Annexin A6 was highly expressed in the HER2 elevated breast cancer cell lines, BT474, SKBR-3 and MDA-MD-361, corresponding to results obtained in this study. However, MDA-MB-453 also showed strong expression of Annexin A6, contrary to our results. All ER-positive breast cancer cell lines tested also expressed high levels of Annexin A6, while half of ER-negative cell lines tested displayed reduced Annexin A6 expression, including MDA-MB-231 and -157 (contrary to our observation with MDA-MB-231). Expression of Annexin A6 appeared to be lower in cell lines with EGFR amplification. However, it has also been suggested to play a tumour suppressor role in these cells, by reducing the activity of Ras (de Muga *et al*., 2009).

In addition to Western blot analysis of the Annexin A6, further immunofluorescence assays (section 4.5) were carried out in order to further investigate 9E1 reactivity in various cancer cell types.

Cell Line	Reactivity
MiaPaCa-2 clone 3	+ +
MiaPaCa-2 clone 8	+ +
Lox IMVI	+
SNB-19	+ / -
DLKP-SQ	+ + +
DLKP-Mitox-4p (Matrigel)	+ / -
DLKP-Mitox-6p (Matrigel)	+ + +
H1299	+ +

Cell Line	Reactivity
C/68	+ / -
HCT-116	+ +
MDA-MB-231	+ +
MDA-MB-435	+ +
SKBR-3	+ + +
BT474	+ +
MDA-MB-157	+ +

Table 5.3: - **Immunofluorescence studies of MAb 9E1 24 (6) in a panel of cancer cell lines.**

+++ Very Strong; ++ Strong; + Intermediate; +/- Weak

Levels of positive staining observed with 9E1 agreed broadly with expression levels as shown by Western blot analysis of both 9E1 and Annexin A6 antibodies; strong staining and expression levels in the HER2-overexpressing breast cancer cell lines, SKBR-3, BT474; low reactivity and expression in the SNB-19 glioma cell line. Staining in the Lox and C/68, while detectable, was lower than expected, compared to the expression levels observed in Western blot analyses. Levels of expression did correspond with inhibition of invasion with 9E1 in some cases: low reactivity and expression in SNB-19 cells correlates with the lack of inhibition of invasion observed in this cell line; strong reactivity and expression observed in MiaPaCa-2 clone 3, H1299, HCT-116, MDA-MB-231 all correlate with significant decreases (or increases) in invasion levels following incubation with 9E1.

Immunohistochemical analysis was also carried out with 9E1 on a range of normal and tumour tissue types. In general, the normal tissues analysed with MAb 9E1 showed low levels of expression; however, some reactivity was observed in normal colon tissue, but this was much reduced compared to colon

tumour tissue. The normal breast tumour tissue analysed showed strong staining with 9E1.

9E1 reactivity in tumour tissue sections varied between the tissue types. Glioma tissue samples were very weakly positive, in agreement with results obtained with the investigation of inhibition of invasion, Western blot and immunofluorescence studies. Very intense staining was observed in the colon adenocarcinoma, retinoblastoma, Malt lymphoma and B cell lymphoma tissue samples, while the basal cell carcinoma only showed some weak positivity. Staining was also observed in a Warthins tumour, a benign tumour of the parotid gland. These results indicate that Annexin A6 is associated with both invasive and non-invasive cancer phenotypes. A large number of breast cancer samples were also tested, including HER2, ER positive, ER negative, PR positive, PR negative and Triple negative samples, with 9E1 reactivity ranging from very weak positivity to very intense staining. Although these are only preliminary results, a number of HER2 positive tumours showed 9E1 reactivity, which does reflect Western blot and immunofluorescence results obtained in this study. However, in order to confirm this pattern, a much larger study would have to be carried out.

In summary, immunoprecipitation, and mass spectrometry identification of the Annexin A6 protein, its matching molecular weight to the 9E1 reactive antigen, and the subsequent decrease of this reactive antigen in Annexin A6-silenced cells, strongly indicates that this protein is the main target antigen of MAb 9E1 24 (6). This is further corroborated by the similar expression levels observed in a panel of cell lines, probed with both the 9E1 MAb, and a commercial Annexin A6 antibody. Immunofluorescence assays, and immunohistochemical analysis indicate that it is found in a variety of tumour types, both invasive, and non-invasive, while invasion assay results suggest that it may act as both a pro- and anti-invasive protein.

5.4.1 Annexin A6

The Annexins are a family of calcium-and membrane-binding proteins characterised by their unique architecture of Ca^{2+}-binding sites, which facilitates

their peripheral docking onto negatively charged membrane surfaces through their Ca^{2+}-bound conformation, thus playing a critical role in linking the plasma membrane to the cytoskeleton (Bode *et al.*, 2008). Annexins are described as ubiquitous proteins; that is, any single cell type appears to express a range of Annexins; however, no single Annexin is expressed in all cell types (Gerke *et* al., 2002). Several of the Annexin genes are located in chromosomal regions that show high frequency of loss in specific types of cancer, indicating that these Annexins could have tumour suppressor capabilities. However, it has also been suggested that changes in the expression of some Annexins during tumourigenesis may be linked to resistance to chemotherapeutic agents (Mussunoor *et al*., 2008). Annexin A2 has been linked to the suppression of prostate cancer cell migration (Liu *et al*., 2003), while its inhibition is linked to a decrease in the invasive capacity of prostate cancer cells (Hastie *et al*., 2008). Proteomic and immunohistochemical analysis showed overexpression of Annexin A1, A2, A4 and A11 in colorectal cancer compared to normal colon, while decreased expression of Annexin A7 and A10 has been linked to prostate cancer and hepatocellular carcinoma respectively (Srivastava *et al*., 2001; Liu *et al*., 2002). These findings highlight the dichotomous role of Annexins in cancer.

Annexin A6 is highly expressed in most mammalian tissues, including skeletal muscle, liver, heart, spleen and lymph nodes. High levels are also found in endothelial and endocrine cells, secretory cells and macrophages (Grewel *et al*., 2010). Annexin A6 has the ability to interact simultaneously with membranes, proteins of the EGFR/Ras/mitogen-activated protein kinase (MAPK) pathway, endocytic machinery and the actin cytoskeleton. This enables it to provide a scaffold to (A) form membrane-bound multifactorial signalling complexes, (B) to regulate transient membrane-actin cytoskeleton interactions during endocytosis and (C) to stabilise the protein/lipid composition during membrane microdomain formation such as caveolae/membrane rafts (Grewal and Enrich, 2006, 2009).

Expression of Annexin A6 at the cell surface has been reported in numerous studies; as a receptor for chondroitin sulfate chains (Takagi *et al*., 2001), in association with S100A8/A9 in the cytoplasm (Bode *et* al., 2008) and the serum adhesive protein, fetuin-A (Sakwe *et al*., 2010). This is in agreement with the

both immunofluorescence and immunohistochemistry results obtained in this study, showing strong 9E1 reactivity to the cell membrane.

5.4.2 Annexin and Cell Proliferation

It has been shown that Annexin A6 inhibits Ras signalling in breast cancer cells. The activated Ras protein significantly enhances several facets of the malignant phenotype, including the deregulation of tumour-cell growth (Shield *et al.*, 2000). At the cell surface, binding of EGF to EGFR leads to Ras activation, which in turn engages Raf and MAPK to propagate the signal. Ras inactivation is regulated by GTPase-activating proteins (GAPs). Vila de Muga and her colleagues have shown that in a panel of breast cancer cell lines, Annexin A6 stimulates membrane recruitment of the p120GAP, in a calcium-dependent manner. By targeting p120GAP to the membrane, Annexin A6 stabilises the formation of Ras-p120GAP complexes at the plasma membrane, leading to a reduction of Ras in the cytoplasm, and therefore a decrease in activity of the Ras signalling pathway. Knockdown of Annexin A6 in MDA-MB-436 breast cancer cells resulted in increased Ras activity and cell proliferation (Vila de Muga *et al.*, 2009). This is contrary to results obtained in this study, where blocking of Annexin A6 with MAb 9E1, and silencing of its function through siRNA knockdown, did not produce any decreases in cell proliferation. This may be due to the fact that proliferation studies were only carried out with the MiaPaCa-2 clone 3 pancreatic cell line, where Ras, and therefore Annexin A6, may not play a major in cell proliferation. Proliferation assays carried out on cancer cell lines that overexpress EGFR, in the presence of MAb 9E1, may help to shed more light on the role of Annexin A6 in this process.

5.4.3 Annexin A6 and Cell Invasion

Annexin A6 has been reported to be downregulated in the transition of a non-metastatic to a metastatic phenotype in B16F10 mouse melanoma (Francia *et al.*, 1996); expressed in uveal melanoma, but absent in normal uveal melanocytes (van Ginkel *et al.*, 1998) and absent in transformed human B lymphocytes compared to normal B lymphocytes (Barel *et al.*, 1991). In a prostate cancer model, downregulation of Annexin A6 was observed during progression from a benign to a malignant state (Kopper *et al.*, 2006). These findings suggest a

tumour suppressor role for Annexin A6 in malignant progression. Some results from this study do highlight the anti-tumourigenic effects of Annexin A6, as can be observed from the increases in cell invasion in the colorectal cancer cell line HCT-116, and the breast cancer cell line MDA-MB-157, upon incubation with MAb 9E1.

However, it would appear that Annexin A6 can also act as a pro-invasive protein. In this study, inhibition of Annexin A6 using MAb 9E1 resulted in significant decreases in invasion levels in a number of cancer cell lines. siRNA knockdown experiments in the MiaPaCa-2 clone 3 pancreatic cell line, and in the DLKP-M lung cancer cell line, also showed a decrease in invasion levels upon silencing of the Annexin A6 gene, with motility levels remaining unaffected. This pro-invasive role of Annexin A6 has not been previously described, and as such, its method of action remains undefined.

One hypothetical mechanism for the role of Annexin A6 as a pro-invasive gene would be through the compartmentalisation of Caveolin-1. High levels of Annexin-A6 result in an accumulation of cholesterol in the late endocytic compartment, leading to reduced amounts of cholesterol in the Golgi and plasma membrane. This overall imbalance of cellular cholesterol is accompanied by an inhibition of Caveolin-1 export from the Golgi complex (Cubells *et al.*, 2007, 2008); therefore, inhibiting the function of Annexin A6 could result in the release of Caveolin-1 to the plasma membrane. Caveolin-1 has been linked to inhibition of invasion in a number of breast cancers. Cells expressing high levels of Caveolin-1 showed reduced capacity to invade matrigel, diminished response to laminin-1 stimulation and decreased metastasis to lung and bone, but no major changes in proliferative capacity (Sloan *et al.*, 2004; Fiucci *et al.*, 2002). Caveolin-1 is also integral to various cellular processes, including the formation of caveolae at the cell surface. A reduction in caveolae at the cell surface has been shown to enhance anchorage-independent growth, increase tumorigenicity, stimulate mitogen-activated protein kinase (MAPK) signalling, and drive cells to enter the cell cycle and become transformed (Galbiati *et al.*, 1998; Lin *et al.*, 2005). Although *in vitro* data indicate that low Caveolin-1 expression corresponds to an increase in tumour growth, Caveolin-1 is highly expressed in

some solid-tumour types *in vivo*. Contrary to the *in vitro* findings, its expression has even been associated with increased tumour-cell survival, aggressiveness, metastatic potential and suppression of apoptosis (Tahir *et al.*, 2001; Kato *et al.*, 2002) (although Bender *et al.*, (2000), and Felley-Bosco *et al.*, (2000) have published results disputing this).

Furthermore, Caveolin-1 has been shown to facilitate secretion of the serine protease Kallikrein 6 (KLK6) in the colon cancer cell line HCT-116. KLK6 has been linked to ECM degradation and increased tumour cell invasiveness (Henkhaus *et al.*, 2008), and above-average expression of it correlates with a poor prognosis in ovarian and uterine cancers (Diamandis *et al.*, 2003; Santin *et al.*, 2005). This may explain the significant increase in cell invasion observed in the HCT-116 cell line upon exposure to 9E1. The apparent dual role of Caveolin-1 as an anti- and pro-invasion protein reflects the behaviour of 9E1 observed in this study.

Another mechanism that may further clarify the role of Annexin A6 as a pro-invasive protein is through the development of clathrin-coated pits. Lin *et al.*, (1992) used an *in vitro* system to demonstrate that Annexin A6 is required for the Ca^{2+}, and ATP-dependent budding of clathrin-coated pits from the cell membrane. It was also demonstrated that Annexin A6 is required for regulating the formation of coated vesicles. Furthermore, after stimulating endocytosis at the cell surface, Annexin VI remains bound to endocytic vesicles to regulate entry of ligands into the prelysosomal compartment (Grewal *et al.*, 2000; Kamal *et al.*, 1998). Inhibition of Annexin A6, and of ATP, through ADP/ATP translocase proteins, which was also identified as a possible interacting protein, (ATP/ADP translocases catalyse the highly specific transport of ATP across a membrane in an exchange mode with ADP (Schmitz-Esser *et al.*, 2004)), by 9E1 may impede clathrin-coated pit budding. One result of this would be the degradation of clathrin-mediated endocytosis (CME). CME regulates cell transduction, as well as morphogenetic aspects of normal physiology (e.g. cell adhesion). Receptor clustering in clathrin-coated pits is followed by membrane invagination and vesicle scission (Goldstein *et al.*, 1979). Thereafter, cargos undergo sorting in the multi-vesicular body, either for degradation in lysosomes,

or for recycling. However, in tumour cells, this pathway presents multiple abnormalities. Tumour cells gain self-sufficiency in growth signals by delaying endocytosis-mediated inactivation of growth factor receptors (Orth *et al*., 2006), and adhesion molecules undergo enhanced recycling and re-distribution to propel invading protrusions (Balklava *et al*., 2007). However, this endocytic pathway is initiated at clathrin-coated invaginations of the plasma membrane (Mosesson *et al*., 2008). Disruption of the formation of clathrin-coated vesicles through inhibition of Annexin A6 may inhibit pro-tumourigenic signals further downstream. It must be stated however, that CME is only one pathway through which aberrant signalling can take place; endocytosis can be mediated by caveolae, and by clathrin and caveolae-independent pathways. Therefore inhibiting CME may not affect all endocytic tumour events.

Although no previous studies have related Annexin A6, ADP/ATP translocase and 14-3-3 (another protein identified along with Annexin A6, through immunoprecipitation assays in this study) proteins to the same process, it is plausible that all three are involved in CME. As described, Annexin A6 and ADP/ATP translocase could function together to form clathrin-coated pits. 14-3-3s were the first proteins to be identified that bind specifically to phosphorylated substrates. As endocytosis is regulated by phosphorylation, activity of these proteins at the membrane could have important functions (Shikano *et al*., 2006). Furthermore, 14-3-3 proteins form dimers that provide two binding sites for phosphoserine motifs in ligand proteins. They can therefore function as adaptor proteins, bringing two proteins that would not otherwise associate into close proximity (Hermeking, 2003). Inhibition of Annexin A6 as the main target antigen of 9E1 may be affecting these interacting proteins simultaneously.

The increase in invasion levels observed in the DLKP-M cell line upon incubation with diluted 9E1 presents an intriguing situation. This result may indicate that a necessary concentration of the MAb is required in order to inhibit invasion. Lower levels may inhibit the function of Annexin A6 in relation to Ras signalling, thereby increasing invasion, while clathrin-coated vesicle driven invasion remains unperturbed. Further studies involving known concentration levels of 9E1 will need to be carried out, in order to determine the optimal concentration of MAb needed for inhibition of invasion.

5.4.4 Annexin A6 and Cellular Adhesion

MiaPaCa-2 clone 3 pancreatic cells grown in the presence of MAb 9E1 showed significant decreases in adhesion to both fibronectin and matrigel, suggesting that Annexin A6 plays a role in cellular adhesion to these proteins. But what might this role be? Chondroitin sulfate proteoglycans (CSPGs) participate in the modulation of various cellular functions, including adhesion. Work carried out by Fthenou *et al*., (2009) showed that cleavage of cell-associated CS chains severely impaired Fibrosarcoma cell adhesion. Annexin A6 is known to facilitate attachment of cells to chondroitin sulphate chains (Takagi *et* al., 2002 – although in this study, they show that CSPGs are involved in anti-adhesive activity). Therefore, inhibiting the facilitory action of Annexin A6 may reduce cellular attachment to CS chains, and therefore reduce the level of cell adhesion.

Additionally, Annexin A6 has been shown to facilitate adhesion of breast carcinoma cells to Fetuin-A in a calcium dependent manner, further illustrating the role of Annexin A6 in cell adhesion (Madappa *et al*., 2004). This may therefore explain the significant decreases observed in cancer cell adhesion in the presence of MAb 9E1.

From the results obtained in this study, it would appear that Annexin A6 does have a hither-to unknown role to play as a pro-invasive protein, and that by blocking its function, it is possible to significantly reduce invasion levels in a number of cancer cell lines. However, further work will need to be carried out in order to fully elucidate its role in the invasion process.

5.5 Investigation of MAb 7B7 Target Antigens

Following identification of the target proteins of 7B7, the next step was to determine what role, if any, they play in the invasion process. This was achieved by carrying out siRNA knockdown of these proteins. MiaPaCa-2 clone 3 and DLKP-M were chosen for this study (section 3.11).

The Ku heterodimer has been implicated in DNA double strand break repair, telomere maintenance and apoptosis, and as such, is thought to play a crucial role

in cell survival. Its overexpression has been linked to the promotion of oncogenic phenotypes, while low expression leads to genomic instability and tumourigenesis. These observations suggest that the Ku protein may act as either a tumour suppressor or an oncoprotein (Gullo *et al*., 2006).

Ku70 was successfully knocked down in both cell lines, and reduction in protein levels was confirmed, as shown by Western blot analysis. In both MiaPaCa-2 clone 3 and DLKP-M, Ku70 silencing did not affect cell proliferation. (Kinesin transfected cells did however show a dramatic decrease in cell number, indicating that siRNA transfection was successful.) This result corresponds with the proliferation assay results observed with 7B7. In relation to invasion, Ku70 knockdown by both siRNAs significantly inhibited invasion in the MiaPaCa-2 clone 3 cell line, while siRNA-B significantly inhibited DLKP-M invasion levels. In relation to motility, MiaPaCa-2 clone 3 siRNA-B transfected cells showed a significant decrease in levels.

Ku80 silencing also gave similar results to those seen in Ku70-silenced cells. Both cell lines showed successful knockdown of Ku80; cell proliferation was unaffected, while invasion and motility was significantly decreased in the MiaPaCa-2 clone 3 cell line. Meanwhile, DLKP-M siRNA-C transfected cells showed a reduction in invasion levels.

Furthermore, Ku70 expression was reduced in Ku80 silenced cells, and *vice versa*, suggesting that the two subunits of the Ku heterodimer work in tandem. This is in agreement with previous studies (Bertolini *et al*., 2007; Mayeur *et al*., 2005). However, simultaneous silencing of both Ku70 and Ku80 did not produce a greater inhibitive effect on cell invasion - in fact, inhibition of invasion was greatly reduced. This may be due to the lack of optimisation for dual siRNA transfection: in order to maintain overall siRNA concentration levels, only half of the volume of each siRNA was used during transfection. This could explain the reduced inhibition levels observed.

From the results obtained above, it would appear that the two subunits of the Ku protein play a role in cell invasion *and* motility, and that by blocking their function, both processes can be successfully inhibited.

Due to the fact that Western blot analysis does not work with the 7B7 MAb, immunofluorescence assays were carried out on Ku70 and Ku80 silenced MiaPaCa-2 clone 3 cells. Strong staining was observed on both untransfected cells, and scrambled-siRNA transfected cells, which was taken as the control. Ku70 silenced cells did not display any reduced reactivity with 7B7, while Ku80 silenced cells displayed a marked decrease in staining. While these results are only preliminary, it may suggest that the Ku80 subunit is the main target antigen for the 7B7 MAb, and that the Ku70 subunit is merely immunoprecipitated along with it.

Western blot analysis was carried out in order to observe the expression levels of Ku70 and Ku80 in a panel of cancer cell lines. Ku80 showed strong expression in most of the cell lines tested; however, expression was weaker in the C/68 prostate cell line, corresponding to the low inhibition of invasion observed following incubation with 7B7, while Ku70 expression is low in the SNB-19 glioma cell line (possibly corresponding to the low inhibition of motility observed following incubation with 7B7). Expression was stronger in the MiaPaCa-2 clone 3 compared to the clone 8 variant, while expression was also stronger in the WM-266-4 metastatic cell line compared to the WM-115 primary cell line.

Cell Line	Reactivity	
	Ku70	Ku80
MiaPaCa-2 clone 3	+ + +	+ + +
MiaPaCa-2 clone 3 (Matrigel)	+ + +	+ + +
MiaPaCa-2 clone 8	+ +	+ +
Lox IMVI	+ + +	+ + +
WM-115	+ +	-
WM-226-4	+ + +	+ / -
SNB-19	+	+ /-
DLKP	+ +	+
DLKP-A	+ +	+ +
DLKP-I	+ +	+ +

Cell Line	Reactivity	
	Ku70	Ku80
DLKP-M	+ +	+ + +
DLKP-SQ	+ +	+ +
H1299	+ +	+ +
C/68	+	+
HCT-116	+ + +	+ + +
MDA-MB-231	+ +	+ + +
MDA-MB-453	+ +	+ +
MDA-MB-361	+ +	+ +
SKBR-3	+ +	+
BT474	+ +	+

Table 5.4: - **Levels of expression of Ku70 and Ku80 in a panel of cancer cell lines.**

+++ Very Strong; ++ Intermediate; + Weak; +/- Very Weak

Ku70 expression levels were similar to those seen with Ku80 – stronger expression in the MiaPaCa-2 clone 3 compared to the clone 8 variant (corresponding to preliminary immunofluorescence assay results); stronger expression in the WM-266-4 metastatic tumour compared to the WM-115 primary tumour. However, some differences are observed: Ku70 expression in the SNB-19 glioma cell line is negligible, there is slightly stronger expression in the DLKP-M cell line, compared to the other variants, while expression in the triple negative MDA-MB-231 breast cell line showed the strongest expression out of all the breast cancer cell lines. No data pertaining to expression levels in the triple negative MDA-MB-157 breast cancer cell line is available; therefore, any association of expression with triple negative cell lines cannot be confirmed. The differences between the expression of both proteins in the invasive and non-invasive variants of cell lines correspond to results observed in immunofluorescence studies, with 7B7 giving stronger staining on invasive cell lines, compared to low/non-invasive cell lines. Furthermore, the weaker expression levels in the C/68 cell line may explain the relative lack of inhibition

observed in this cell line; however, as 7B7 did not work on Western blotting, no direct comparisons can be made with Ku70 and Ku80. Immunohistochemical analyses were also carried out, but 7B7 did not produce any staining.

In work carried out by Nolens and his colleagues, Western blot analysis of nuclear and cytoplasmic Ku70 and Ku80 expression was carried out in a number of breast cell lines. Although our results only show whole cell expression of the Ku subunits, some results do correspond to Nolen's *et al*., e.g. Ku70 expression is weaker than Ku80 in the HER2 positive BT474 and SKBR-3 breast cancer cell lines. However, these authors reported that the expression of Ku80 versus Ku70 is weaker in the MDA-MB-231 cell line, contrary to the result obtained in this study. This discrepancy may be down to the fact that only whole cell expression of the subunits was looked at in our study (Nolens *et al*., 2009).

Results observed in immunofluorescence assays carried out on a range of cell lines stained with 7B7, are in agreement with the expression levels of Ku70 and Ku80 obtained through Western blot analysis. Stronger staining was observed in the MiaPaCa-2 clone 3 cell line, when compared to the clone 8 variant; C/68 and SNB-19 reactivity was low, while low level staining was observed in the SKBR-3 and BT474 cell lines, corresponding to the expression levels of Ku80. These results also correlate with 7B7 inhibition of invasion, with significant decreases observed in MiaPaCa-2 clone 3 and SKBR-3, no significant inhibition of invasion in the C/68 prostate cell line, and no inhibition of SNB-19 motility.

Cell Line	Reactivity	Cell Line	Reactivity
MiaPaCa-2 clone 3	+ + +	H1299	+ +
MiaPaCa-2 clone 8	+ +	C/68	+ / -
Lox IMVI		MDA-MB-231	+ +
SNB-19	+ / -	MDA-MB-435	+
DLKP-SQ	+	MDA-MB-157	+ +
DLKP-Mitox-4p (Matrigel)	+ / -	SKBR-3	+ +
DLKP-Mitox-6p (Matrigel)	++ / +++	BT474	+ +

Table 5.5: - **Levels of immunofluorescence staining of MAb 9E1 24 (6) in a panel of cancer cell lines.**

+++ Very Strong; ++ Strong; + Intermediate; +/- Weak

Positive identification and validation of the 7B7 immunoprecipitates as Ku70 and Ku80, along with the absence of any other identified proteins, indicates that the target antigens of this MAb are the subunits of the Ku heterodimer protein. Furthermore, reduced 7B7 reactivity on Ku80 siRNA-transfected cells observed in immunofluorescence assays suggests that this subunit is the main target antigen.

5.5.1 Ku Heterodimer

The Ku heterodimer consists of the two tightly associated sub-units, Ku70 and Ku80 (in *S. cerevisiae*) or Ku86 (in higher eukaryotes – the Ku80 designation is used in this study, due to the molecular weight of the identified band being 80kDa). Located mainly in the nucleus, it is an abundant protein that plays a key role in the non-homologous end joining process, which is responsible for repairing a high percentage of DNA double strand breaks (DSBs) in somatic cells of all multicellular eukaryotes (Koike *et al.*, 2008). Ku also recruits a 465-kDa DNA-dependent protein kinase catalytic subunit (DNA-PK_{cs}) to the DNA double-strand break sites stimulating the DNA-PK_{cs} kinase activity. DNA-PK_{cs} interacts with and phosphorylates a nuclear protein, XRCC4, which associates

with DNA ligase IV. DNA ligase IV is thought to catalyze DNA-end joining (Costantini *et al*., 2007).

The Ku80 subunit of the heterodimer also exists as a truncated 69kDa protein variant in several human cell lines including B cells (Muller *et al*., 1998), the leukaemia cell line, HL60 (Han *et al*., 1996) and multiple myeloma cells (Tai *et al*., 2000). This variant differs from the full-length Ku80 protein through a truncated C terminus (Sallmyr *et al*., 2002). It is suggested that this variant is formed through post translational modification after Ku80 re-entry to the nucleus, where it is proteolytically cleaved into a smaller form (Gullo *et al*., 2006).

Apart from its essential role in DNA repair, Ku has also been implicated in a number of other cellular processes, including antigen receptor gene arrangements (e.g., Variable (Diversity) Joining {V(D)J} recombination), telomere maintenance and regulation of heat shock-induced responses. It has been observed to play a role in regulation of the G2 and M phases of the cell cycle (Gullo *et al.,* 2006), and its binding to an apolipoprotein C-IV promoter stimulates the expression of the gene, facilitating the transport of lipids through the lymphatic and circulatory systems (Kim *et al*., 2008).

Ku's ability to regulate numerous intracellular functions suggests that it may be active at multiple locations within the cell. Ku proteins are primarily localised to the transcriptionally active regions of the nucleus. Furthermore, they are components of the nuclear matrix, and are diffusely distributed in the nucleoplasm (Yu *et al*., 1998). However, they have also been shown to relocate to extranuclear sites in the cells e.g. subcellular compartments including the cytoplasm and cell membranes of numerous cell types (Koike *et al*., 2008). Structurally, Ku does not contain a known plasma membrane localisation signal, but does contain a hydrophobic region, thus facilitating cell surface expression. (Zhang *et al*., 2001) As immunofluorescence studies have shown, MAb 7B7 has cytoplasmic and membrane reactivity in numerous cancer cell lines, suggesting that the MAb is binding to this subcellular Ku heterodimer.

Previous studies suggest that a delicate balance exists in Ku expression; overexpression of Ku proteins promotes oncogenic phenotypes, while low expression has been linked to genomic instability and tumourigenesis. Such studies indicate that the Ku proteins may have a role as either tumour suppressors or oncoproteins (Pucci *et al.,* 2001; Gullo *et al.,* 2006).

5.5.2 Ku and Cell Proliferation

The Ku heterodimer has been well documented as playing a crucial role in DNA double strand break repair (DSBR). Therefore, the presence of functional Ku proteins in the cell is necessary for the maintenance of genomic stability, and consequently, the survival and proliferation of cancer cells. It was shown that the hyperproliferation of cancerous gastric cells could be associated with both high expression and high nuclear levels of Ku70 and Ku86 (Lim *et al.,* 2002).

However, Uegaki *et al.,* have shown that the Ku heterodimer is not essential for cell growth. They showed that inactivation of either Ku70 or Ku80 did not cause any defects in cellular proliferation (Uegaki *et al.,* 2006). This agrees with the results seen in this study: the lack of inhibition of MiaPaCa-2 clone 3 proliferation when incubated with 7B7 may be due to the fact that the MAb only targets cell surface Ku70 and 80, and that it is the nuclear Ku heterodimer that controls cell proliferation. Work carried out by Ajmani *et al.,* (1995) showed that proliferating lymphocytes do not express cell surface Ku. However, siRNA silencing of both targets did not affect cell proliferation either, thus corroborating the results obtained by Uegaki and his colleagues.

5.5.3 Ku and Cell Invasion/Motility

From the results obtained in this study, targeting of the Ku70 and Ku80 proteins by 7B7 results in the inhibition of invasion and motility in a number of cell lines. The low levels of inhibition observed in the C/68 prostate cell line correspond to the low level of expression of both subunits of the Ku heterodimer observed in this cell line. Furthermore, inhibition of invasion was significantly decreased in the SNB-19 glioma cell line, while motility levels were relatively unchanged. Western blot analysis of this cell line showed that Ku80 was strongly expressed, while levels of Ku70 were greatly diminished. This may indicate that the

inhibitory effect 7B7 has on motility may depend on Ku70 having a role to play in the motility process, either individually or in concert with Ku80. In the MiaPaCa-2 clone 3 cell line, Ku70 expression is strong, which may correspond to the highly significant decrease in motility levels observed upon exposure to 7B7. In the case of SNB-19, Ku70 may not be involved in cell motility, and therefore, 7B7 has no inhibitory effect. No data on Ku70/80 expression levels in the BxPc-3 pancreatic cell line, or the MDA-MB-157 breast cancer cell line is available, so it is unknown if the lack of inhibition of invasion observed in these cell lines is due to the absence of these proteins.

Both Ku70 and Ku80 have been shown previously to play a role in cell invasion and motility. HER2 overexpression in breast cancers is correlated with poor patient outcome due to extensive metastatic progression. Nolens *et al*., (2009) have shown that the Ku heterodimer, through interaction with Activator protein-2 (AP-2) α and AP-2γ transcription factors, contribute to HER2 gene overexpression in breast cancer (Nolen *et al*., 2009). Furthermore, upregulation of the Ku protein has been shown to increase the ability of Kelly neuroblastoma and MCF-7 breast carcinoma cells to invade endothelial monolayers, and to enhance levels of cellular locomotion (Ginis *et al.*, 2000). This is achieved through a specific interaction with MMP-9.

MMP-9 is a Zn^{+2} dependent endopeptidase, synthesised and secreted in monomeric form as a zymogen. Its primary function is degradation of proteins in the extracellular matrix, proteolytically digesting decorin, elastin, fibrillin, laminin, gelatin (denatured collagen), and types IV, V, XI and XVI collagen. It also activates growth factors such as proTGFb and proTNFa (atlasgeneticsoncology.org*)*. High serum levels of MMP-9 have been related to rapid progression, poor overall survival and secondary metastasis in cancer patients with melanoma (Nikkola *et al*., 2005). In an experimental model for spontaneous metastasis of rat mammary carcinoma, serum and plasma levels of MMP-9 were associated with the development of metastases in the lung and lymph nodes (Nakajima *et al.*, 1993).

A number of studies have shown that secreted MMPs can localise at the cell surface through interactions with "docking" molecules (Stamenkovic, 2003), thereby allowing cells to concentrate, and activate these MMPs at the close interface between their plasma membrane and ECM, a stage essential for tumour cell invasion. In the case of cancer cells, this is a key event in promoting tumour invasion. The decrease in levels of activated MMP-9 following incubation with 7B7 observed in this study suggests that the MAb is blocking the binding of this MMP to its "docking" molecule. Both forms of the Ku heterodimer have been shown to interact with MMP-9 at the cell surface (Monferran *et al.,* 2004), thus suggesting that the Ku protein acts as the "docking" molecule for MMP-9. The presence of these MMP-binding proteins allows cells to concentrate and activate MMPs at the close interface between their plasma membrane and ECM and, in cancer cells, may be a key event in promoting tumour invasion and angiogenesis (Toth *et al.,* 1997; Bourguignon *et al.,* 1998; Olson *et al.*, 1998; Yu and Stamenkovic, 1999, 2000). Therefore, the inhibitory effect seen with 7B7 could possibly be due to its blocking of the Ku protein, and its function as a docking molecule for MMP-9. MMP-9 remains inactive, and is unable to carry out its proteolytic activities. siRNA silencing of both Ku70 and Ku80 proteins resulted in inhibited levels of invasion similar to that seen with 7B7; however, whether this is due to the inability of the cells to bind to MMP-9 is unknown. Zymography assays carried out on the conditioned media of Ku70 and Ku80 silenced cells would clarify this.

Ku80 has also been implicated in cancer cell invasion through involvement with the tyrosine kinase receptor, TrkA. TrkA overexpression has been associated with increased breast cancer cell growth and invasion, as well as survival (Lagadec *et al*., 2009). In work carried out by Lagadec *et al*., (2010), they found an increase in membrane Ku80 and Ku70 levels in TrkA-overexpressing cells. Furthermore, inhibition of Ku80 through siRNA silencing, or antibody blocking, strongly reduced TrkA-stimulated invasion, thus indicating that Ku80 was involved in this process. Suppression of Ku70, however, had no effect on cell invasion. Interestingly, simultaneous inhibition of both Ku80 and Ku70 reduced cell invasion to a similar degree of that observed with Ku80 inhibition alone.

This would suggest that the Ku80 subunit, and not Ku70, mediates TrkA-stimulated invasion (Lagadec *et al*., 2010).

5.5.4 Ku and Cellular Adhesion

Both Ku70 and Ku80 have also been shown to play a role in cell adhesion. Work carried out by Lynch *et al.,* and Teoh *et al.,* showed that a surface molecule induced by hypoxia and exposure to CD40 ligand was identified as Ku80. The role of Ku in both homotypic (same cell type) and heterotypic (different cell types) adhesion was further demonstrated by these two groups using functional antibodies directed against both subunits of the Ku protein. It was shown that Ku is involved in heterotypic adhesion of leukocytes to endothelial cells and of myeloma cells to bone marrow stroma; in the homotypic adhesion of myeloma cells and in the adhesion of fibroblasts and myeloma cells on fibronectin and collagen IV; all these phenomena are mediated by Ku upon CD40L stimulation (Lynch *et al.,* 2001; Teoh *et al.,* 1998).

So how might Ku contribute to increase cell adhesion on Fibronectin? Monferran and her colleagues showed that both Ku70 and Ku80 present a structural relationship with Integrin I domains, and the A1 and A3 domains of von Willebrand factor (VWA), domains known to be involved in cell adhesion to ECM proteins, including Fibronectin (Monferran *et al*., 2004). Results obtained in this study show that 7B7 MAb reduces cellular adhesion to both Fibronectin and Matrigel by around 30%. The possibility exists that this MAb may be blocking this Ku/VWA interaction, thus reducing cell adhesion to Fibronectin.

5.5.5 Ku and Anoikis Resistance

From the Greek word meaning “homelessness”, anoikis is an apoptotic process induced by the absence of a surface for cell adhesion. Cells that have undergone anoikis usually display nuclear fragmentation and membrane blebbing, resulting from the activation of caspase proteases, all features observed during anoikis. Caspase activation in most cells requires permeabilisation of the outer mitochondrial membrane. This releases into the cytosol a host of factors, whose combined effect is caspase activation (Valentijn *et al.,* 2004). One such factor in this caspase activation pathway is Bax. Bax is a member of the pro-apoptotic

Bcl-2 family of proteins and is localised in a physiologically inactive form in the cytoplasm (Fan *et al*., 2005). After apoptotic stimuli, Bax is translocated into the mitochondria and promotes the release of cytochrome *c*, leading to protein degradation, nuclear fragmentation, and eventual cell apoptosis. However, association between the C-terminus of Ku70 and the N-terminus of Bax in the cytoplasm results in the inactivation of Bax, thus suppressing Bax translocation to the mitochondria and eventual cell death (Sawada *et al*., 2003). This mediation between Ku70 and Bax does not require the co-operative effects of Ku80. Therefore, inhibiting Ku70 should increase the level of anoikis seen in cells, and this has been observed in numerous studies. Sawada *et al.,* (2003) showed that overexpression of Ku70 suppressed the mitochondrial translocation of Bax, and increased the relative proportion of Bax in the cytosol. Ku70 deficient mouse embryonic fibroblasts also showed increased sensitivity to apoptotic stimuli.

Anoikis assays set up with 7B7 did not show an increase in cell death, or a decrease in the number of anoikis-resistant cells. There are a number of possible reasons for this. One could be that the concentration of antibody was not sufficient in order to produce an observable effect. Another possibility was that Ku70 was successfully blocked, but that Bax translocation to the mitochondria did not take place. Sawada *et al*., (2003) have shown that even in Ku70-deficient cells, a substantial amount of Bax remained in the cytosol. This suggests that there is a multitude of steps involved in Bax activation, in addition to the dissociation of Ku70. The presence of a Bax inhibitor protein (e.g. Bax Inhibitor I) may also be acting as an anti-apoptotic agent. It is also possible that the pool of Ku70/80 available to 7B7 (primarily on the outside of the plasma membrane) does not play a role in intracellular events leading to apoptosis. One final possibility for the lack of any effect observed in relation to anoikis with 7B7 is that the Ku70-Bax association is not involved in anoikis in the DLKP-M and MiaPaCa-2 clone 3 cell lines. Other signalling pathways may be involved in Anoikis resistance in these cells, which are unaffected by 7B7, therefore no changes (within errors) would be seen in cell number when compared to the hybridoma media control.

5.5.6 Anti-Ku MAbs

There have been a number of studies carried out, using MAbs that specifically target the subunits of the Ku heterodimer. Wang *et al*., (1994) used an MAb, designated 162, to investigate the assembly of Ku70 and Ku80, and their interaction with DNA. Immunofluorescence assays carried out with this MAb indicated that it interacted with both subunits of the Ku heterodimer, but not with each individual subunit. MAb 162 also immunoprecipitated the Ku heterodimer from cells infected with a Ku70 & 80 vaccine, but did not immunoprecipitate the individual subunits from cells coinfected with only a single subunit vaccine. Furthermore, the MAb stabilised the Ku heterodimer under conditions that normally dissociate Ku70 from Ku80 (Wang *et al*., 1994).

Luk *et al*., (2005) generated a MAb, designated CLD3, through immunisation of BALB/c mice with cancerous tissue lysates from hepatocellular carcinoma (HCC) patients. Hybridomas were subsequently screened against the homologous antigens by ELISA, producing MAb CLD3. Immunofluorescence and immunohistochemistry assays were carried out to characterise the location of reactivity of the MAb in tumourigenic HCC cell lines. Immunoprecipitation assays indicated that the target antigen was the Ku heterodimer, and this was then confirmed through Western blot analysis. This antibody was able to react with the Ku70 and Ku80 subunits individually, as well as the heterodimer as a whole (Luk *et al*., 2005).

A MAb generated against multiple myeloma (MM) cells was found to recognise the Ku80 subunit only. Designated 5E2, this MAb was found to inhibit MM cell adhesion to bone marrow stromal cells. Immunoprecipitations carried out with this MAb showed that the Ku70 subunit was co-immunoprecipitated out along with the Ku80 subunit, even though the MAb did not react specifically with Ku-70 protein, as shown by Western blot. This study reveals that it is possible to immunoprecipitate out the Ku heterodimer as a whole, with a MAb that only targets one specific subunit (Teoh *et al*., 1997).

Immunofluorescence assays carried out on Ku transfected cells with 7B7 suggests that this MAb is targeting the Ku80 subunit of the heterodimer.

Simultaneous siRNA transfection with the two different subunits did not produce levels of inhibition greater than those observed when each subunit was targeted individually, but this may be due to lack of optimisation of dual siRNA transfection. However, previous studies have suggested that each subunit of Ku protein is required to stabilize the other. Therefore, targeting one subunit should be sufficient to block the activity of the complete heterodimer at the membrane (Monferran *et al*., 2004; Satoh *et al*., 1995; Li *et al*., 2002).

5.6 Combination Studies of MAb 7B7 & 9E1

The Ku heterodimer and Annexin A6 share common targets in different signalling pathways, leading to potential co-operative effects. For example, Ku70 and 80 form a complex with poly (ADP-ribose) polymerase (PARP-1), driving expression of the stress-specific S100A9 gene (Grote *et al*., 2006); expression of this gene has been associated to inflammation, and its up-regulation in various types of tumours suggests that it has a possible role in inflammation-associated cancer (Gebhardt *et al*., 2006). S100A8/A9 is also connected to Annexin A6, since both proteins are exposed on the cell surface of SKBR-3 cells upon calcium influx (Bode *et al*., 2008). Therefore, both of the MAbs generated in this study could have a possible synergistic effect. In order to investigate this, invasion assays were carried out on the MiaPaCa-2 clone 3 cell line, with a combination of the two MAbs.

Initially, there did not appear to be any further increase in the inhibition of invasion above that observed with each MAb acting individually. However, it should be noted that only half the volume of each antibody was used in the assay, (i.e. 50µl of each MAb, giving a total volume of 100µl). We have seen that our MAbs present a dose-dependent response; 9E1 at a 1 in 2 dilution gave an average inhibition of 22% in the DLKP-M cell line, while the same dilution of MAb 7B7 gave an average of 20% inhibition in the same cell line. When used in combination in the MiaPaCa-2 clone 3 cell line, invasion was inhibited by an average of 42%, suggesting that an additive effect had been achieved, rather than a synergistic one.

While invasion was significantly inhibited by both MAbs in various cancer cell lines, the effects observed differed between them. For example, 9E1 significantly inhibited invasion in the C/68 prostate cancer cell line, while 7B7 had little effect. Conversely, SNB-19 invasion was significantly reduced in the presence of 7B7, while 9E1 had no impact on invasion levels. In many cases, these differences between the MAbs can be attributed to the expression of their respective target antigens in the given cell lines. The effects of both MAbs on HCT-116 invasion highlight their differing mechanisms of actions. MAb 7B7's significant decrease in invasion levels may possibly be due to its disruption of the proteolytic action of MMP-9, while the increases observed upon incubation with MAb 9E1 may be due to the action of caveolin-1 facilitating KLK6 secretion, and thus increased ECM degradation and cell invasion. Interestingly, both MAbs had no effect on the BxPc-3 pancreatic cancer cell line.

Significant inhibition of cell motility was observed with both MAbs; however, 7B7 gave a much more pronounced decrease, with levels comparable to that observed in inhibition of invasion. Again, this may be as a result of its target antigens having a more central role in cellular motility, than Annexin A6. Cellular adhesion to matrigel was significantly decreased upon incubation with the MAbs, while adhesion to fibronectin was also inhibited. However, 7B7 gave more consistent results in relation to the former ECM protein. Similar morphological changes were observed following exposure to the MAbs, and MMP-9 activity was also decreased. The similarity in results obtained in these experiments is not unexpected, as inhibition of cellular invasion is likely to affect these cellular processes. Therefore, two separate and distinct anti-invasive agents can elicit similar responses. The absence of effect in anoikis observed with both MAbs is likely due to the complex nature of this cellular process. It is highly unlikely that a single pathway regulates anoikis. Many signals are affected depending on whether or not cells commit to an apoptotic fate, and it is an accumulation of all these pathways that decides the cell fate.

5.7 Combination Studies with MAb 9E1 24 (6) & 7B7 G5 (2) and Lovastatin, Mevastatin and Simvastatin

Although both MAbs significantly inhibited invasion in numerous cancer cell types, neither one gave complete inhibition. This is not unexpected, as it is highly unlikely that only one protein would control cell invasion. One of the reasons why cancer is such a difficult disease to treat is due to the multiple mechanisms it employs in order to continue with proliferation and colonisation. Therefore, any successful therapeutic treatments will likely involve various anti-cancer agents, working in synergy, against a myriad of targets. For this reason, combination studies were carried out in order to investigate the possibility of increasing the inhibitive effects of both MAbs. As mentioned earlier (section 1.2.7.1) statin drugs have shown some anti-tumourigenic properties in relation to melanoma, therefore it was decided to test Simvastatin, Lovastatin, and Mevastatin to observe their effects on melanoma cell invasion and migration *in vitro*. All three statins were found to inhibit melanoma cell invasion and cell motility, *in vitro,* in the two melanoma cell lines tested, at non-toxic concentrations, in a dose-dependant manner (section 4.14). These results reflect results obtained by Collisson *et al*., (2003), who described atorvastatin inhibition of invasion of the melanoma cell lines A375M, CHL, SK-MEL-28, and WM 166-4 in a dose-dependant manner, with A375M invasion being inhibited at non-toxic concentrations. Farina *et al*., (2003) described the metastatic inhibition of F311 mammary carcinoma cells in BALB/c mice following pre-treatment with a non-cytotoxic concentration of Lovastatin.

The results observed suggest that the standard doses used for cholesterol treatment may not be sufficient to directly inhibit melanoma cell invasion (the peak plasma concentration of Simvastatin achieved in patients receiving a 40mg per day does is approximately 3ng/ml (7.2nM) (Najib *et al*., 2003). Therefore, statins are unlikely to be beneficial for prevention of melanoma. However, statin treatment at higher doses may be beneficial as an adjuvant therapy to inhibit melanoma cell invasion and metastasis. Synergistic interactions have been observed between statins and several chemotherapy agents *in vitro* (Sleijfer *et al*., 2005).

Once the anti-invasion and anti-motility effects of the statins were established, synergy studies were conducted between the 9E1 and 7B7 MAbs, and Simvastatin, Lovastatin and Mevastatin. However, no increase in inhibition of invasion in the MiaPaCa-2 clone 3 cell line was observed. Incubation of both MAbs with Lovastatin and Mevastatin did not produce any noticeable synergistic effect, with inhibition of invasion remaining at levels achieved with the statins alone. Incubation of MAb 7B7 G5 (2) with Simvastatin did increase inhibition levels slightly; however, these decreases remained within experimental error. Although no apparent synergy was observed between the MAbs and the statins tested, further studies should be carried out, not only on a wider range of statins, but also on other anti-cancer agents, such as MMP inhibitors. Future cancer therapies will inevitably involve multi-drug treatments, targeting different processes, including metastasis, and as such, information on compatibility and synergy will be essential.

5.8 MAb 9E1 & 7B7: From Bench to Bedside

The research presented in this thesis is proof of principle of how MAbs can be successfully generated that specifically target invasion-related proteins, and can block cancer invasion *in vitro*. Both 9E1 and 7B7 have shown significant anti-invasion activity *in vitro* in a number of cancer models; however, if they are to be considered as future therapeutic agents for the treatment of cancer, a lengthy development process has to be initiated to produce a final product suitable for testing in humans. While *in vitro* systems of testing can offer a wide range of data pertaining to the mechanisms of action of the MAbs, they are not sufficiently complex to study the entire metastatic process: metastasis, as discussed in section 1.1, is much more than invasion, adhesion, and growth rate (Mendoza *et al*., 2010). The use of animal models (*in vivo*) allows for the testing of MAbs in a highly complex environment.

In order to investigate the effects our MAbs would have on the invasion process *in vivo*, an orthotopic mouse model would have to be used. With this model, tumour cells are implanted in their original tissue, allowing for the development of tumours that are comparable to human tumours, and leading to the emergence

of metastasis in a few weeks. In these models, bioluminescence imaging allows for the characterisation of tumour burden, and consequently, determination of the effect of the MAbs on the metastatic process (Pastuskovas *et al*., 2010; Engebraaten *et al*., 2009).

Another method of animal testing involves *ex vivo* modelling. This involves experimenting on animal tissues outside of the organism under controlled conditions, but with minimal changes to its natural environment. Recently, Mendoza *et al*., have developed an *ex vivo* pulmonary metastasis assay (PuMa) in which GFP-expressing cancer cells proliferate and progress in lung tissue, allowing for the assessment of metastatic progression up to, and beyond, a 21-day observation period. Furthermore, this assay validated *in vivo* behaviour of high- and low-metastatic human and mouse cancer cell lines (Mendoza *et al*., 2010). This method offers a simple way to study the process of metastatic progression at a secondary site, while recapturing the cellular and microenvironmental complexity of *in vivo* systems. If the MAbs show the same anti-invasion effect *in vivo*, or *ex vivo*, as was observed *in vitro*, then they could be considered for possible testing in pre-clinical trials. However, a number of factors must be considered before testing commences

As with the MAbs developed during this study, the majority of clinically interesting antibodies were raised in mice and prepared from hybridoma cells. This gave rise to the problem of immunogenicity of murine MAbs in humans, and the inevitable generation of HAMA (Human-Anti-Mouse-Antibodies). Therefore, murine-origin MAbs must undergo re-engineering to enhance their clinical utility i.e. to increase their immunogenicity. The most commonly used re-engineering techniques are chimerisation and humanisation (see section 1.8.2 - Qu *et al*., 2005). (However, murine MAbs can still be used in clinical settings e.g. lymphoma patients who are immunosuppressed rarely develop HAMAs, which interfere with repeated therapeutic MAb administration (Leonard *et al*., 2005).) Furthermore, a fully human antibody can be made against a specific target, in this case Annexin A6 and the Ku heterodimer.

Another point of consideration involves the IgM nature of 7B7. Historically, IgM monoclonal antibodies have been underrepresented in human therapeutic development due to problems with low affinity and cross reactivity (Brändlein *et al*., 2002), and their large size means they have a limited utility for therapeutics (Reichert *et al*., 2006). Although IgM is the most effective isotype for complement activation, it does not readily extravasate from vascular structures (Adams *et al*., 2005). Therefore, when choosing MAbs for clinical testing, many companies tend to shy away from those with an IgM subclass. However, Irie *et al*., (2004) have hypothesized that IgM MAbs may be more effective against cancer cells *in vivo*, due to the correlation between prolonged survival and high serum levels of IgM, but not IgG, anti-tumour antibodies in patients with metastatic melanoma, and the complete or partial regression of skin metastases of melanoma following intra-tumoural injection of human IgM antibodies. Furthermore, a number of IgM MAbs have undergone clinical trials (Azuma *et al*., 2007; Irie *et al*., 2004), highlighting the therapeutic potential of IgM-type MAbs.

There is also a hierarchy among IgG MAbs when effecting ADCC; IgG1 and IgG3 have high ADCC effector function, while IgG2 and IgG4 have low function (Lin, M.Z., *et al*., 2005). This is probably due to their differential affinities for Fc receptors (Nimmerjahn *et al*., 2005).

If it is decided to either make chimeric or humanised antibodies from our MAbs, or to make fully human antibodies against their targets, these will then have to undergo rigorous testing before they can obtain FDA or EMA approval. Pre-clinical *in vivo* characterisation must take place, in order to investigate the pharmaceutical properties, pharmacokinetics and pharmacodynamics of the administered drug. Distribution studies provide preliminary data on routes of metabolism and excretion, target organs for toxicity, and drug sanctuary sites (DeVita *et al*., 2008). Animal models for cancer drug development should include features relevant to human cancer, such as the representation of molecular targets, microenvironment, tumour natural history, angiogenesis, and metastasis (Gitler *et al*., 2004). Mice are the most commonly used vertebrate species for *in vivo* testing, due to their size, low cost, ease of handling, fast

reproduction rate, and similarity to human physiology (they share 99% of their genes with humans) (Rosenthal *et al*., 2007).

Dosing studies will be essential when testing (the chimeric/humanised/fully human) 9E1 and 7B7 *in vivo*, both in animal models and in clinical trials. As observed in the DLKP-M cell line, incubation of the cells with diluted 9E1 resulted in an increase in invasion levels. Concentrated 7B7 was also observed to increase invasion levels in the MiaPaCa-2 clone 3 cell line (results not shown). Varying dilutions of the MAbs will need to be administered in order to determine the optimal antibody concentration required for successful inhibition of invasion.

Side effects of the MAbs, both positive and negative, will also be a critical feature to investigate when conducting *in vivo* trials. The proposed target antigen of 9E1 is Annexin A6. This protein is the most abundant Annexin in the heart, and has been localised in various cell types, including muscle cells (myocytes). Overexpression of Annexin A6 has resulted in physiological alterations in contractile mechanics, leading to dilation and weakening of the heart, whereas its absence has been found to induce faster changes in Ca^{2+} removal from myocytes and increased contractility, suggesting a negative role for Annexin A6 in cardio-muscle contraction (Camors *et al*., 2005). Annexin A6 has also been implicated in regulation of the secretory process in plasma cells (Bode *et al.,* 2008; Tiacci *et al.,* 2005). This presents a situation where the administration of 9E1 could affect other physiological functions, unrelated to cancer, where Annexin A6 is involved.

Cell surface Ku proteins has been implicated in the invasion processes of cancer cells in this, and many other studies, but they are also involved in invasion of normal cells such as monocytes during recruitment to tissues, a crucial event during inflammatory responses. Inflammation is known to play a decisive role at different stages of tumour development, including initiation, promotion, malignant conversion, invasion, and metastasis (Grivennikov *et al*., 2010). Therefore, an anti-Ku antibody may have further anti-cancer effects than those identified in this study. However, the Ku heterodimer is involved in many other

cellular processes, and its inhibition could have negative side effects that could greatly influence regular physiological activities.

As undesired as they are, any negative side effects observed with either MAb *in vivo* may not necessarily result in the abandonment of clinical trials. Although animal models are designed to represent events occurring in humans, sometimes metabolic and physiological differences result in the appearance of side effects in animals which later do not materialize in humans. Even so, most therapeutic drugs available to clinicians elicit unwanted side effects. For example, Trastuzumab is linked with cardiac toxicity. In a clinical trial of Trastuzumab in HER2-positive metastatic cancer patients, an increased incidence of serious cardiac events was observed, notably when Trastuzumab was administered in combination with anthracyclines. In addition to its expression in tumour cells, the HER2 receptor is also expressed on cardiomyocytes, where it exerts a protective effect on cardiac function; therefore, interference with HER2-signaling may block this protective effect (Perez, 2008). However, if it is deemed that any beneficial effects observed with a new drug outweigh the negative side effects, or if the side effects can be managed or even reversed with standard therapy, then it may be decided that clinical trials can begin.

Clinical trials of prospective agents for cancer treatment undergo 5 phases of testing: phase 0, which establishes whether the drug or agent behaves in human subjects as was expected from preclinical studies (Lancet, 2009), through to phase IV, which involves the safety surveillance and technical support of a drug after it has been granted a license (Ebbesen *et al*., 2008). However, clinical trials involving anti-metastatic agents present a number of problems. These include the high numbers of patients required, due to the necessity to assess recurrence of metastatic disease. Measuring response rates beyond stable disease will further increase the number of patients needed.

Over the past 20 years, there has been a dramatic shift in MAbs undergoing clinical development. From the period 1990-1991, humanised MAbs accounted for 45% of all MAbs in clinical development; 30% were murine, 13.5% were chimeric while 11.5% were fully human. However, from 2000-2008, these

figures changed dramatically, with 45% of MAbs in clinical development being fully human, 39% humanised, 9% chimeric, and 7% murine (Nelson *et al*., 2010). This trend highlights the growing development of fully human MAbs in clinical trials. Furthermore, between 1997 and 2008, 131 human MAbs entered clinical trials. Of these, 30 were in Phase I, 51 in Phase II and 7 in Phase III, and a total of 7 were approved for marketing by the FDA (33 were discontinued). Among the FDA approved MAbs were Panitumumab, an anti-EGFR antibody approved for the treatment of metastatic colorectal carcinoma, and Ofatumumab, a CD20-specific MAb approved for the treatment of chronic lymphocytic leukaemia (Nelson *et al*., 2010).

In 2009, MAb-mediated cancer therapy generated total revenues of over US$18bn worldwide. From 2010, that sector will benefit from new drugs, new targets and expanding indications for existing products. With cancer incidence and prevalence rising worldwide (studies reveal that incidence rates will rise by up to 40% by 2025) the treatment of cancer will be a priority for healthcare providers, with high demand for effective and well-tolerated therapies (Visiongain, 2010). The lack of MAbs directed against invading cancer cells is a major market niche that is waiting to be exploited, and with the current trends in revenues generated by MAb based therapy, the rewards are there for anyone willing to commit resources into the development of anti-metastatic MAbs.

CHAPTER 6
CONCLUSIONS & FUTURE WORK

1. By screening directly for function, two Mabs were identified that can significantly block cancer invasion *in vitro*.

2. MAb 7B7 was generated against the highly invasive pancreatic cell line MiaPaCa-2 clone 3. Incubation with this MAb significantly reduced invasion in the MDA-MB-231 and SKBR-3 breast cancer cell lines; the DLKP-M NSCLC and H1299 ling cancer cell lines; the SNB-19 glioma cell line and the HCT-116 colon cell line. Inhibition of invasion was also observed in the Lox IMVI melanoma cell line, but significance was not reached. Invasion levels in the pancreatic cell line BxPc-3 and the prostate cell line C/68 were only slightly inhibited. MAb 7B7 also significantly inhibited motility in the MiaPaCa-2 clone 3 cell line following incubation with MAb 7B7, but not SNB-19 motility. This MAb also decreased MiaPaCa-2 clone 3 adhesion to fibronectin, and DLKP-M adhesion to matrigel. MMP-9 activity in the MDA-MB-231 breast cancer cell line was also decreased following incubation with MAb 7B7.

3. Immunofluorescence analysis of MAb 7B7 on MiaPaCa-2 clone 3 cells revealed membrane and cytoplasmic reactivity. Stronger reactivity was observed in cells exhibiting a more invasive phenotype compared to less invasive cells (MiaPaCa clone 3 versus clone 8; DLKP-Mitox-6p versus DLKP-SQ).

4. Cross-linked immunoprecipitation studies, followed by LC-MS/MS analysis, revealed the Ku70 and Ku80 subunits of the Ku heterodimer as the target proteins of 7B7. These identifications were validated through Western blot analysis using commercial antibodies directed against Ku70 and Ku80.

5. Confirmation of the role of Ku70 and Ku80 in invasion and motility was confirmed through siRNA silencing of both subunits, which resulted in significant inhibition of both of these processes.

6. Western blot analysis of Ku70 and Ku80 produced a similar pattern of expression to that observed in the immunofluorescence studies. Expression was stronger in the invasive (MiaPaca-2 clone 3, WM-266-4) versus non-invasive (MiaPaCa-2 clone 8, WM-115) cell lines. Expression levels also corresponded to invasion assay results e.g. low expression and inhibtion was observed in the SNB-19 glioma and C/68 prostate cell lines.

7. Immunofluorescence assays carried out on Ku70 and Ku80 siRNA-transfected cells revealed that 7B7 reactivity was decreased in Ku80 silenced cells, while reactivity was unchanged with Ku70 silenced cells. This suggests that the Ku80 subunit is the main target antigen of MAb 7B7.

8. MAb 9E1 was generated against the highly invasive melanoma cell line MDA-MB-435-SF. This MAb was shown to significantly inhibit cell invasion in the MiaPaCa-2 clone 3 pancreatic cancer cell line; the MDA-MB-231 breast cancer cell line; the DLKP-I, DLKP-M and H1299 NSCLC cell lines; the Lox IMVI melanoma cell line and the C/68 prostate cancer cell line. Inhibition of invasion was also observed in the SKBR-3 breast cancer cell line, but significance was not reached. Surprisingly, invasion was *increased* in the MDA-MB-157 breast cancer cell line, and in the HCT-116 colon cancer cell line. These results suggest that the target antigen(s) of this MAb can act as both a pro- and anti-invasive protein. MAb 9E1 also significantly inhibited cell motility in the MiaPaCa-2 clone 3 cell line, but to a lesser extent. Other invasion-related processes, including MiaPaCa-2 clone 3 adhesion to fibronectin, DLKP-M adhesion to matrigel, and MMP-9 activity in the MDA-MB-231, were also decreased following incubation with 9E1.

9. Immunofluorescence analysis of MAb 9E1 showed membrane “punctuate” type staining, along with some cytoplasmic reactivity, in MiaPaCa-2 clone 3 cells. Reactivity was observed in invasive and anon-invasive cancer cell types. Western blot analysis indicated that the target

antigen of 9E1 is expressed in a wide variety of cancer cell types (melanoma, lung, pancreatic, breast, and colon) and in both non-invasive and invasive tumour cell lines.

10. Immunohistochemical analysis showed that the target antigen was expresssed, to varying degrees, in a range of breast cancer sub-types (HER-2 overexpressing, triple negative, ER +/-, PR +/-), strong reactivity was observed in a number of HER-2 overexpressing tumours. 9E1 reactivity was also observed in normal breast tissue; normal liver & prostate tissue. 9E1 reactivity was also observed in Malt lymphoma (orbital tissue), Retinoblastoma, Hodgkins Lymphoma, B-Cell Mantle lymphoma and B-Cell lymphoma tumour tissues and in a number of pancreatic tumours. Very weak expression was bserved in Glioma tumour tissues; 9E1 expression was also observed in a Warthins Tumour, a benign parotid tumour.

11. Western blot analysis indicated that the target antigen of MAb 9E1 is a 75kDa protein. This matches the molecular weight of Annexin A6, which was identified through immunoprecipitation and mass spectrometry analysis. This indicates that Annexin A6 is the target antigen of MAb 9E1. A number of possible interacting proteins were also identified through immunoprecipitation studies, namely, Protein 14-3-3ε, Prohibitin and ADP/ATP translocase 1, 2 and 3.

12. siRNA silencing of Annexin A6 in MiaPaCa-2 clone 3 and DLKP-M cell lines, resulted in significant reduction of invasion in these cell lines. These results confirmed the role of Annexin A6 in cellular invasion. However, the increases in invasion observed in the HCT-116 colon cancer cell line indicate that Annexin A6 may also have an anti-invasive effect.

13. Western blot analysis of a commercial Annexin A6 antibody produced a similar pattern of expression to that observed with MAb 9E1.

Furthermore, Western blot analysis on Annexin A6-silenced cells with the 9E1 MAb revealed strongly reduced expression levels of the reactive band. These results further supports that the target antigen of 9E1 is the Annexin A6 protein.

14. Lovastatin, Mevastatin and Simvastatin all significantly decreased invasion and motility in the HT144 and SK-MEL-28 cell lines, indicating that they do have therapeutic effects against melanomas. Although the concentrations used in this study were at higher doses that those currently used for statin treatment, higher doses may be beneficial as an adjuvant therapy to inhibit melanoma cell invasion and metastasis.

15. Synergy studies carried out between the MAbs and Lovastatin, Mevastatin and Simvastain, did not produce any increase in inhibition.

Future Work Suggested

1. In order to gather more information on the MAbs (particularly MAb 7B7) effects on cancer cell motility, motility assays will have to be carried out on a wider range of cell types. This will help to determine if the inhibitory effects on invasion of the MAbs are a result of reduced cellular motility, or if the two processes are inhibited by differing mechanisms.

2. Investigate the effects of both MAbs on normal cells that are invasive e.g. HUVEC, melanocytes.

3. siRNA functional analysis studies of Prohibitin, Protein 14-3-3ε, ADP/ATP translocase 1-3 and the 40S ribosomal proteins will need to be carried out in order to investigate their role in the invasion process. If they are found to play a role in the invasion process, their expression in invasive versus non-invasive cancer cell lines will be looked at. Their role as interacting proteins will also need to be established. This will be carried out through immunoprecipitation studies using a commercial antibody targeting Annexin A6, to see if the same interacting proteins are identified.

4. More detailed localisation studies could be carried out through labelling of the MAbs.

5. The role of the identified target antigens could be looked at in other cellular processes e.g. adhesion, anoikis, MMP activity, and angiogenesis, through siRNA silencing of the identified proteins.

6. In order to further investigate if the Ku heterodimer in involved in activating MMP-9, zymography assays will be carried on Ku70 and Ku80 silenced cells.

7. While both MAbs significantly inhibit cancer invasion and motility, they do not fully inhibit both processes. Therefore, a wider investigation of any

possible synergistic effect between the MAbs and a range of anti-cancer agents, including MMP inhibitors, on invasion and motility, will be carried out.

8. Further confirmation that Annexin A6 is the main target antigen of MAb 9E1 can be determined though a competition assay. Western blots of cell lysates would be initially probed with MAb 9E1. Following treatment with this MAb, the blots would then be washed, and treated with a commercial Annexin A6 antibody. In theory, if the antibodies are recognising the same binding site (i.e. Annexin A6), this site will have been occupied following incubation of the blot with MAb 9E1. An appropriate 2° antibody against the commercial Annexin A6 antibody, (which does not react to MAb 9E1 24 (6)) theoretically should have little/no primary antibody to bind onto. Development of the blots should therefore reveal a much-reduced reactive band, if any, thus confirming that Annexin A6 is the target antigen of MAb 9E1 24.

9. Immunofluorescence assays involving MAb 7B7 competing with commercial anti-Ku antibodies for binding sites may also confirm if the Ku subunits are the target antigens for this MAb.

10. To obtain a more complete understanding of the mechanisms of actions of each MAb (and exactly how they are blocking invasion), and their interacting proteins, it will be necessary to carry out a human phospho-kinase assay. This involves analysing the phosphorylation profiles of kinases and their protein substrates of cells, following treatment with 7B7 & 9E1. A Human Phospho-Kinase Array Kit is available from R&D systems (Cat #: ARY003), which can detect the relative site-specific phosphorylation of 46 proteins.

11. Immunoprecipitation assays using a commercial Annexin A6 antibody would determine if the prohibitin, Protein 14-3-3ε, ADT/ATP Translocases and 40S Ribosomal proteins are interacting with Annexin A6.

12. A wider immunohistochemical study of triple negative, HER2 positive, ER positive, ER negative, invasive and non-invasive breast tumours, should be carried out, in order to fully ascertain the expression pattern of Annexin A6 in breast cancers, and to investigate any association with particular subsets of breast tumours (preliminary findings presented in this study in relation to HER2). The strong expression in colon and pancreatic tumours will need to be further investigated; the range of tumour types will have to be extended, and more extensive testing will need to be carried out on a range of normal tissues.

13. Immunohistochemical studies and antigen retrieval techniques, with 7B7 will need to be optimised in order to investigate the expression levels of its target antigens in a panel of normal and tumour tissues.

14. Levels of nuclear, versus cytoplasmic, Caveolin-1 in Annexin A6-silenced cells could be investigated, in order to test the hypothesis that incubation with MAb 9E1 results in de-compartmentalisation of caveolin-1 from the golgi complex. If this is found to be the case, then invasion assays on Caveolin-1 silenced cells, in the presence of this MAb, could allow us to determine if the anti-invasive effects of 9E1 are a result of the release of caveolin-1.

15. *In vitro* angiogenesis assays should be carried out in order to ascertain what effect, if any, both 7B7 and 9E1 have on the ability of cells to form new capillary blood vessels. HUVEC endothelial cells are standard model to use for this assay.

16. The effects of both MAbs will need to be investigated in *in vivo* mouse models. Implanted tumours will be established with a fluorescent tag, and an *in vivo* fluorescent imager will follow the growth and metastatic spread of the cells. Other *in vivo* processes will be observed, such as angiogenesis, CDC and ADCC.

17. MAbs that expressed strong reactivity with cancer cells in immunofluorescence assays, but gave no inhibition of invasion, could be investigated further as to any potential diagnostic use.

18. As MAb 9E1 can inhibit the pro-invasive capability of Annexin A6 in numerous cell lines, it should prove useful in further defining its role in the invasion process. This MAb may also be useful in ascertaining if certain cancer types contain a pro- or anti-invasive copy of the Annexin A6 protein.

CHAPTER 8
BIBLIOGRAPHY

4-Antibodies: Therapeutic Antibodies Overview

http://www.4-antibody.com

Abe, M., Sugiura, T., Takahashi, M., Ishii, K., Shimoda, M. and Shirasuna, K., (2008). "A novel function of CD82/KAI-1 on E-cadherin-mediated homophilic cellular adhesion of cancer cells". *Cancer letters,* **266**(2), 163-170.

Adams, G.P. and Weiner, L.M., (2005). "Monoclonal antibody therapy of cancer". *Nature biotechnology,* **23**(9), 1147-1157.

Aggarwal, S., (2009). "What's fueling the biotech engine--2008". *Nature biotechnology,* **27**(11), 987-993.

Agrez, M., Gu, X., Turton, J., Meldrum, C., Niu, J., Antalis, T. and Howard, E.W., (1999). "The alpha v beta 6 integrin induces gelatinase B secretion in colon cancer cells". *International journal of cancer. Journal international du cancer,* **81**(1), 90-97.

Ajmani, A.K., Satoh, M., Reap, E., Cohen, P.L. and Reeves, W.H., (1995). "Absence of autoantigen Ku in mature human neutrophils and human promyelocytic leukemia line (HL-60) cells and lymphocytes undergoing apoptosis". *The Journal of experimental medicine,* **181**(6), 2049-2058.

American Cancer Society: Cancer Facts and Figures 2010. Atlanta, Ga: American Cancer Society, 2010.
www.cancer.org/acs/groups/content/@nho/documents/document/acspc-024113.pdf

American Cancer Society: Monoclonal Antibodies. Last Revised: 10/12/2010
http://www.cancer.org/Treatment/TreatmentsandSideEffects/TreatmentTypes/Immunotherapy/immunotherapy-monoclonal-antibodies

Andrews, S., Reichow, S.L. and Gonen, T., (2008). "Electron crystallography of aquaporins". *IUBMB life,* **60**(7), 430-436.

Anttonen, A., Kajanti, M., Heikkila, P., Jalkanen, M. and Joensuu, H., (1999). "Syndecan-1 expression has prognostic significance in head and neck carcinoma". *British journal of cancer,* **79**(3-4), 558-564.

Anttonen, A., Heikkila, P., Kajanti, M., Jalkanen, M. and Joensuu, H., (2001). "High syndecan-1 expression is associated with favourable outcome in squamous cell lung carcinoma treated with radical surgery". *Lung cancer (Amsterdam, Netherlands),* **32**(3), 297-305.

AOCS Lipid Library: Proteolipids: Structure, Occurrence and Biology
http://lipidlibrary.aocs.org/lipids/protlip/index.htm

Araki, K., Wakabayashi, H., Shintani, K., Morikawa, J., Matsumine, A., Kusuzaki, K., Sudo, A. and Uchida, A., (2009). "Decorin suppresses bone metastasis in a breast cancer cell line". *Oncology,* **77**(2), 92-99.

Arbabi Ghahroudi, M., Desmyter, A., Wyns, L., Hamers, R. and Muyldermans, S., (1997). "Selection and identification of single domain antibody fragments from camel heavy-chain antibodies". *FEBS letters,* **414**(3), 521-526.

Atlas of Genetics and Cytogenetics in Oncology and Haematology

atlasgeneticsoncology.org

Auguste, K.I., Jin, S., Uchida, K., Yan, D., Manley, G.T., Papadopoulos, M.C. and Verkman, A.S., (2007). "Greatly impaired migration of implanted aquaporin-4-deficient astroglial cells in mouse brain toward a site of injury". *The FASEB journal :*

official publication of the Federation of American Societies for Experimental Biology, 21(1), 108-116.

Aznavoorian, S., Murphy, A.N., Stetler-Stevenson, W.G. and Liotta, L.A., (1993). "Molecular aspects of tumour cell invasion and metastasis". *Cancer,* **71**(4), 1368-1383.

Azuma, Y., Ishikawa, Y., Kawai, S., Tsunenari, T., Tsunoda, H., Igawa, T., Iida, S., Nanami, M., Suzuki, M., Irie, R.F., Tsuchiya, M. and Yamada-Okabe, H., (2007). "Recombinant human hexamer-dominant IgM monoclonal antibody to ganglioside GM3 for treatment of melanoma". *Clinical cancer research : an official journal of the American Association for Cancer Research,* **13**(9), 2745-2750.

Balklava, Z., Pant, S., Fares, H. and Grant, B.D., (2007). "Genome-wide analysis identifies a general requirement for polarity proteins in endocytic traffic". *Nature cell biology,* **9**(9), 1066-1073.

Baranwal, S. and Alahari, S.K., (2009). "Molecular mechanisms controlling E-cadherin expression in breast cancer". *Biochemical and biophysical research communications,* **384**(1), 6-11.

Barberis, D., Artigiani, S., Casazza, A., Corso, S., Giordano, S., Love, C.A., Jones, E.Y., Comoglio, P.M. and Tamagnone, L., (2004). "Plexin signaling hampers integrin-based adhesion, leading to Rho-kinase independent cell rounding, and inhibiting lamellipodia extension and cell motility". *The FASEB journal : official publication of the Federation of American Societies for Experimental Biology,* **18**(3), 592-594.

Barel, M., Gauffre, A., Lyamani, F., Fiandino, A., Hermann, J. and Frade, R., (1991). "Intracellular interaction of EBV/C3d receptor (CR2) with p68, a calcium-binding protein present in normal but not in transformed B lymphocytes". *Journal of immunology (Baltimore, Md.: 1950),* **147**(4), 1286-1291.

Baulcombe, D.C., (2006). "Short silencing RNA: the dark matter of genetics?". *Cold Spring Harbor symposia on quantitative biology,* **71**, 13-20.

Bauer, T.W., Liu, W., Fan, F., Camp, E.R., Yang, A., Somcio, R.J., Bucana, C.D., Callahan, J., Parry, G.C., Evans, D.B., Boyd, D.D., Mazar, A.P. and Ellis, L.M., (2005). "Targeting of urokinase plasminogen activator receptor in human pancreatic carcinoma cells inhibits c-Met- and insulin-like growth factor-I receptor-mediated migration and invasion and orthotopic tumour growth in mice". *Cancer research,* **65**(17), 7775-7781.

Beck, A., Wurch, T., Bailly, C. and Corvaia, N., (2010). "Strategies and challenges for the next generation of therapeutic antibodies". *Nature reviews.Immunology,* **10**(5), 345-352.

Bender, F.C., Reymond, M.A., Bron, C. and Quest, A.F., (2000). "Caveolin-1 levels are down-regulated in human colon tumors, and ectopic expression of caveolin-1 in colon carcinoma cell lines reduces cell tumorigenicity". *Cancer research,* **60**(20), 5870-5878.

Berclaz, G., Altermatt, H.J., Rohrbach, V., Kieffer, I., Dreher, E. and Andres, A.C., (2001). "Estrogen dependent expression of the receptor tyrosine kinase axl in normal and malignant human breast". *Annals of Oncology : Official Journal of the European Society for Medical Oncology / ESMO,* **12**(6), 819-824.

Berditchevski, F., Tolias, K.F., Wong, K., Carpenter, C.L. and Hemler, M.E., (1997). "A novel link between integrins, transmembrane-4 superfamily proteins (CD63 and CD81), and phosphatidylinositol 4-kinase". *The Journal of biological chemistry,* **272**(5), 2595-2598.

Bertolini, L.R., Bertolini, M., Anderson, G.B., Maga, E.A., Madden, K.R. and Murray, J.D., (2007). "Transient depletion of Ku70 and Xrcc4 by RNAi as a means to manipulate the non-homologous end-joining pathway". *Journal of Biotechnology,* **128**(2), 246-257.

Binyamin, L., Borghaei, H. and Weiner, L.M., (2006). "Cancer therapy with engineered monoclonal antibodies". *Update on Cancer Therapeutics,* **1**(2), 147-157.

Blackwell, K.L., Burstein, H.J., Storniolo, A.M., Rugo, H., Sledge, G., Koehler, M., Ellis, C., Casey, M., Vukelja, S., Bischoff, J., Baselga, J. and O'Shaughnessy, J., (2010). "Randomized study of Lapatinib alone or in combination with trastuzumab in women with ErbB2-positive, trastuzumab-refractory metastatic breast cancer". *Journal of clinical oncology : official journal of the American Society of Clinical Oncology,* **28**(7), 1124-1130.

Bode, G., Luken, A., Kerkhoff, C., Roth, J., Ludwig, S. and Nacken, W., (2008). "Interaction between S100A8/A9 and annexin A6 is involved in the calcium-induced cell surface exposition of S100A8/A9". *The Journal of biological chemistry,* **283**(46), 31776-31784.

Boja, E., Hiltke, T., Rivers, R., Kinsinger, C., Rahbar, A., Mesri, M. and Rodriguez, H., (2010). "Evolution of Clinical Proteomics and its Role in Medicine". *Journal of proteome research,* .

Bonner, P.L.R., Lill, J.R., Hill, S., Creaser, C.S. and Rees, R.C., (2002). "Electrospray mass spectrometry for the identification of MHC class I-associated peptides expressed on cancer cells". *Journal of immunological methods,* **262**(1-2), 5-19.

Bourguignon, L.Y., Gunja-Smith, Z., Iida, N., Zhu, H.B., Young, L.J., Muller, W.J. and Cardiff, R.D., (1998). "CD44v(3,8-10) is involved in cytoskeleton-mediated tumour cell migration and matrix metalloproteinase (MMP-9) association in metastatic breast cancer cells". *Journal of cellular physiology,* **176**(1), 206-215.

Bourguignon, L.Y., (2008). "Hyaluronan-mediated CD44 activation of RhoGTPase signaling and cytoskeleton function promotes tumour progression". *Seminars in cancer biology,* **18**(4), 251-259.

Braga, T., (2008). "Unveiling the Biological Role of Serglycin Proteoglycans: Studies on Serglycin Knock-Out Mice". Doctoral Thesis, Swedish University of Agricultural Science.

Brandlein, S., Lorenz, J., Ruoff, N., Hensel, F., Beyer, I., Muller, J., Neukam, K., Illert, B., Eck, M., Muller-Hermelink, H.K. and Vollmers, H.P., (2002). "Human monoclonal IgM antibodies with apoptotic activity isolated from cancer patients". *Human antibodies,* **11**(4), 107-119.

Bright RK, Vocke CD, Emmert-Buck MR, Durray PH, Solomon D, Fetsch P, Rhim JS, Linehan WM and Topalian SL (1997). "Generation and Genetic Characterisation of Immortal Human Prostate Epithelial Cell Lines derived from Primary Cancer Specimens". *Cancer Res*. **57**: 995-1002.

Brooks, S.A., Lomax-Browne, H.J., Carter, T.M., Kinch, C.E. and Hall, D.M., (2010). "Molecular interactions in cancer cell metastasis". *Acta Histochemica,* **112**(1), 3-25.

Brooks, P.C., Stromblad, S., Sanders, L.C., von Schalscha, T.L., Aimes, R.T., Stetler-Stevenson, W.G., Quigley, J.P. and Cheresh, D.A., (1996). "Localization of matrix metalloproteinase MMP-2 to the surface of invasive cells by interaction with integrin alpha v beta 3". *Cell,* **85**(5), 683-693.

Brown, A.J., (2007). "Cholesterol, statins and cancer". *Clinical and experimental pharmacology & physiology,* **34**(3), 135-141.

Cailleau, R., Olive, M. and Cruciger, Q.V., (1978). "Long-term human breast carcinoma cell lines of metastatic origin: preliminary characterization". *In vitro,* **14**(11), 911-915.

Camors, E., Monceau, V. and Charlemagne, D., (2005). "Annexins and Ca2+ handling in the heart". *Cardiovascular research,* **65**(4), 793-802.

Cancer Immunome Database
http://ludwig-sun5.unil.ch/CancerImmunomeDB/

Cao, J., Chiarelli, C., Richman, O., Zarrabi, K., Kozarekar, P. and Zucker, S., (2008). "Membrane type 1 matrix metalloproteinase induces epithelial-to-mesenchymal transition in prostate cancer". *The Journal of biological chemistry,* **283**(10), 6232-6240.

Cao, Y. and Suresh, M.R., (1998). "Bispecific antibodies as novel bioconjugates". *Bioconjugate chemistry,* **9**(6), 635-644.

Capparuccia, L. and Tamagnone, L., (2009). "Semaphorin signaling in cancer cells and in cells of the tumour microenvironment--two sides of a coin". *Journal of cell science,* **122**(Pt 11), 1723-1736.

Carter, P., (2001). "Improving the efficacy of antibody-based cancer therapies". *Nature reviews.Cancer,* **1**(2), 118-129.

Cassady, J.M., Chan, K.K., Floss, H.G. and Leistner, E., (2004). "Recent developments in the maytansinoid antitumor agents". *Chemical & pharmaceutical bulletin,* **52**(1), 1-26.

Cattaruzza, S. and Perris, R., (2005). "Proteoglycan control of cell movement during wound healing and cancer spreading". *Matrix biology : journal of the International Society for Matrix Biology,* **24**(6), 400-417.

Chames, P., Kerfelec, B. and Baty, D., (2010). "Therapeutic antibodies for the treatment of pancreatic cancer". *TheScientificWorldJournal,* **10**, 1107-1120.

Chemprep.com: Overview of Antibody
http://www.chempep.com/ChemPep-Antibody.htm

Chan, C.E., Chan, A.H., Hanson, B.J. and Ooi, E.E., (2009). "The use of antibodies in the treatment of infectious diseases". *Singapore medical journal,* **50**(7), 663-72; quiz 673.

Chen, Q., Manning, C.D., Millar, H., McCabe, F.L., Ferrante, C., Sharp, C., Shahied-Arruda, L., Doshi, P., Nakada, M.T. and Anderson, G.M., (2008). "CNTO 95, a fully human anti alphav integrin antibody, inhibits cell signaling, migration, invasion, and spontaneous metastasis of human breast cancer cells". *Clinical & experimental metastasis,* **25**(2), 139-148.

Chien, C.W., Lin, S.C., Lai, Y.Y., Lin, B.W., Lin, S.C., Lee, J.C. and Tsai, S.J., (2008). "Regulation of CD151 by hypoxia controls cell adhesion and metastasis in colorectal cancer". *Clinical cancer research : an official journal of the American Association for Cancer Research,* **14**(24), 8043-8051.

Chignard, N. and Beretta, L., (2004). "Proteomics for hepatocellular carcinoma marker discovery". *Gastroenterology,* **127**(5 Suppl 1), S120-5.

Choi, S., Kim, Y., Park, H., Han, I.O., Chung, E., Lee, S.Y., Kim, Y.B., Lee, J.W., Oh, E.S. and Yi, J.Y., (2009). "Syndecan-2 overexpression regulates adhesion and migration through cooperation with integrin alpha2". *Biochemical and biophysical research communications,* **384**(2), 231-235.

Chometon, G., Zhang, Z.G., Rubinstein, E., Boucheix, C., Mauch, C. and Aumailley, M., (2006). "Dissociation of the complex between CD151 and laminin-binding integrins permits migration of epithelial cells". *Experimental cell research,* **312**(7), 983-995.

Chow, A. Y. (2010) "Cell Cycle Control by Oncogenes and Tumor Suppressors: Driving the Transformation of Normal Cells into Cancerous Cells". *Nature Education,* **3**(9):7

Chu, F.M., Picus, J., Fracasso, P.M., Dreicer, R., Lang, Z. and Foster, B., (2010). "A phase 1, multicenter, open-label study of the safety of two dose levels of a human monoclonal antibody to human alpha(v) integrins, intetumumab, in combination with docetaxel and prednisone in patients with castrate-resistant metastatic prostate cancer". *Investigational new drugs,* .

Chung, B.I., Malkowicz, S.B., Nguyen, T.B., Libertino, J.A. and McGarvey, T.W., (2003). "Expression of the proto-oncogene Axl in renal cell carcinoma". *DNA and cell biology,* **22**(8), 533-540.

Clark, J.C., Thomas, D.M., Choong, P.F. and Dass, C.R., (2007). "RECK--a newly discovered inhibitor of metastasis with prognostic significance in multiple forms of cancer". *Cancer metastasis reviews,* **26**(3-4), 675-683.

Clynes, M., Redmond, A., Moran, E. and Gilvarry, U., (1992). "Multiple drug-resistance in variant of a human non-small cell lung carcinoma cell line, DLKP-A". *Cytotechnology,* **10**(1), 75-89.

Clynes, R.A., Towers, T.L., Presta, L.G. and Ravetch, J.V., (2000). "Inhibitory Fc receptors modulate in vivo cytoxicity against tumour targets". *Nature medicine,* **6**(4), 443-446.

Cohen IR, Murdoch AD, Naso MF, Marchetti D, Berd D, Iozzo RV., (1994). "Abnormal expression of perlecan proteoglycan in metastatic melanomas". *Cancer Research*. **54**(22), 5771–4.

Collisson, E.A., Kleer, C., Wu, M., De, A., Gambhir, S.S., Merajver, S.D. and Kolodney, M.S., (2003). "Atorvastatin prevents RhoC isoprenylation, invasion, and metastasis in human melanoma cells". *Molecular cancer therapeutics,* **2**(10), 941-948.

Costantini, S., Woodbine, L., Andreoli, L., Jeggo, P.A. and Vindigni, A., (2007). "Interaction of the Ku heterodimer with the DNA ligase IV/Xrcc4 complex and its regulation by DNA-PK". *DNA repair,* **6**(6), 712-722.

Coronella-Wood, J.A. and Hersh, E.M., (2003). "Naturally occurring B-cell responses to breast cancer". *Cancer immunology, immunotherapy : CII,* **52**(12), 715-738.

Cramer, L.P., (1997). "Molecular mechanism of actin-dependent retrograde flow in lamellipodia of motile cells". *Frontiers in bioscience : a journal and virtual library,* **2**, d260-70.

Cubells, L., Vila de Muga, S., Tebar, F., Bonventre, J.V., Balsinde, J., Pol, A., Grewal, T. and Enrich, C., (2008). "Annexin A6-induced inhibition of cytoplasmic phospholipase A2 is linked to caveolin-1 export from the Golgi". *The Journal of biological chemistry,* **283**(15), 10174-10183.

Cubells, L., Vila de Muga, S., Tebar, F., Wood, P., Evans, R., Ingelmo-Torres, M., Calvo, M., Gaus, K., Pol, A., Grewal, T. and Enrich, C., (2007). "Annexin A6-induced alterations in cholesterol transport and caveolin export from the Golgi complex". *Traffic (Copenhagen, Denmark),* **8**(11), 1568-1589.

Dale, K.M., Coleman, C.I., Henyan, N.N., Kluger, J. and White, C.M., (2006). "Statins and cancer risk: a meta-analysis". *JAMA : the journal of the American Medical Association,* **295**(1), 74-80.

Date, K., Matsumoto, K., Kuba, K., Shimura, H., Tanaka, M. and Nakamura, T., (1998). "Inhibition of tumour growth and invasion by a four-kringle antagonist (HGF/NK4) for hepatocyte growth factor". *Oncogene,* **17**(23), 3045-3054.

De Strooper, B., (2005). "Nicastrin: gatekeeper of the gamma-secretase complex". *Cell,* **122**(3), 318-320.

De Wever, O., Pauwels, P., De Craene, B., Sabbah, M., Emami, S., Redeuilh, G., Gespach, C., Bracke, M. and Berx, G., (2008). "Molecular and pathological signatures of epithelial-mesenchymal transitions at the cancer invasion front". *Histochemistry and cell biology,* **130**(3), 481-494.

Dent, R., Trudeau, M., Pritchard, K.I., Hanna, W.M., Kahn, H.K., Sawka, C.A., Lickley, L.A., Rawlinson, E., Sun, P. and Narod, S.A., (2007). "Triple-negative breast cancer: clinical features and patterns of recurrence". *Clinical cancer research : an official journal of the American Association for Cancer Research,* **13**(15 Pt 1), 4429-4434.

Depasquale, I. and Wheatley, D.N., (2006). "Action of Lovastatin (Mevinolin) on an in vitro model of angiogenesis and its co-culture with malignant melanoma cell lines". *Cancer cell international,* **6**, 9.

DeVita, V., Lawrence, T., Rosenberg, S.(2008). "Cancer: Principles and Practice of Oncology" **Eighth Edition** 978-0-7817-7207-5

Diamandis, E.P., Scorilas, A., Fracchioli, S., Van Gramberen, M., De Bruijn, H., Henrik, A., Soosaipillai, A., Grass, L., Yousef, G.M., Stenman, U.H., Massobrio, M., Van Der Zee, A.G., Vergote, I. and Katsaros, D., (2003). "Human kallikrein 6 (hK6): a new potential serum biomarker for diagnosis and prognosis of ovarian carcinoma". *Journal of clinical oncology : official journal of the American Society of Clinical Oncology,* **21**(6), 1035-1043.

Douma, S., Van Laar, T., Zevenhoven, J., Meuwissen, R., Van Garderen, E. and Peeper, D.S., (2004). "Suppression of anoikis and induction of metastasis by the neurotrophic receptor TrkB". *Nature,* **430**(7003), 1034-1039.

Dowling, P., Walsh, N. and Clynes, M., (2008). "Membrane and membrane-associated proteins involved in the aggressive phenotype displayed by highly invasive cancer cells". *Proteomics,* **8**(19), 4054-4065.

Downs, J.R., Clearfield, M., Weis, S., Whitney, E., Shapiro, D.R., Beere, P.A., Langendorfer, A., Stein, E.A., Kruyer, W. and Gotto, A.M.,Jr, (1998). "Primary prevention of acute coronary events with lovastatin in men and women with average cholesterol levels: results of AFCAPS/TexCAPS. Air Force/Texas Coronary Atherosclerosis Prevention Study". *JAMA : the journal of the American Medical Association,* **279**(20), 1615-1622.

Durrant, L.G., Harding, S.J., Green, N.H., Buckberry, L.D. and Parsons, T., (2006). "A new anticancer glycolipid monoclonal antibody, SC104, which directly induces tumour cell apoptosis". *Cancer research,* **66**(11), 5901-5909.

Durrant, L.G. and Scholefield, J.H., (2009). "Principles of cancer treatment by immunotherapy". *Surgery (Oxford),* **27**(4), 161-164.

Ebbesen, M., Jensen, T.G., Andersen, S. and Pedersen, F.S., (2008). "Ethical perspectives on RNA interference therapeutics". *International journal of medical sciences,* **5**(3), 159-168.

Editorial. (2009). "Phase 0 trials: a platform for drug development?". *Lancet,* **374**(9685), 176.

Eckert, L.B., Repasky, G.A., Ulku, A.S., McFall, A., Zhou, H., Sartor, C.I. and Der, C.J., (2004). "Involvement of Ras activation in human breast cancer cell signaling, invasion, and anoikis". *Cancer research,* **64**(13), 4585-4592.

Elbashir, S.M., Harborth, J., Lendeckel, W., Yalcin, A., Weber, K. and Tuschl, T., (2001). "Duplexes of 21-nucleotide RNAs mediate RNA interference in cultured mammalian cells". *Nature,* **411**(6836), 494-498.

Elbashir, S.M., Lendeckel, W. and Tuschl, T., (2001). "RNA interference is mediated by 21- and 22-nucleotide RNAs". *Genes & development,* **15**(2), 188-200.

Erfurt, C., Muller, E., Emmerling, S., Klotz, C., Hertl, M., Schuler, G. and Schultz, E.S., (2009). "Melanoma-associated chondroitin sulphate proteoglycan as a new target antigen for CD4+ T cells in melanoma patients". *International journal of cancer. Journal international du cancer,* **124**(10), 2341-2346.

Egeblad, M. and Werb, Z., (2002). "New functions for the matrix metalloproteinases in cancer progression". *Nature reviews.Cancer,* **2**(3), 161-174.

Engebraaten, O., Trikha, M., Juell, S., Garman-Vik, S. and Fodstad, O., (2009). "Inhibition of in vive tumour growth by the blocking of host alpha(v)beta3 and alphaII(b)beta3 integrins". *Anticancer Research,* **29**(1), 131-137.

Faassen, A.E., Schrager, J.A., Klein, D.J., Oegema, T.R., Couchman, J.R. and McCarthy, J.B., (1992). "A cell surface chondroitin sulfate proteoglycan, immunologically related to CD44, is involved in type I collagen-mediated melanoma cell motility and invasion". *The Journal of cell biology,* **116**(2), 521-531.

Fan, T.J., Han, L.H., Cong, R.S. and Liang, J., (2005). "Caspase family proteases and apoptosis". *Acta biochimica et biophysica Sinica,* **37**(11), 719-727.

Farina, H.G., Bublik, D.R., Alonso, D.F. and Gomez, D.E., (2002). "Lovastatin alters cytoskeleton organization and inhibits experimental metastasis of mammary carcinoma cells". *Clinical & experimental metastasis,* **19**(6), 551-559.

Felding-Habermann, B., (2003). "Integrin adhesion receptors in tumour metastasis". *Clinical & experimental metastasis,* **20**(3), 203-213.

Feleszko, W., Mlynarczuk, I., Olszewska, D., Jalili, A., Grzela, T., Lasek, W., Hoser, G., Korczak-Kowalska, G. and Jakobisiak, M., (2002). "Lovastatin potentiates antitumor activity of doxorubicin in murine melanoma via an apoptosis-dependent mechanism". *International journal of cancer.Journal international du cancer,* **100**(1), 111-118.

Feleszko, W., Zagozdzon, R., Golab, J. and Jakobisiak, M., (1998). "Potentiated antitumour effects of cisplatin and lovastatin against MmB16 melanoma in mice". *European journal of cancer (Oxford, England : 1990),* **34**(3), 406-411.

Felley-Bosco, E., Bender, F.C., Courjault-Gautier, F., Bron, C. and Quest, A.F., (2000). "Caveolin-1 down-regulates inducible nitric oxide synthase via the proteasome pathway in human colon carcinoma cells". *Proceedings of the National Academy of Sciences of the United States of America,* **97**(26), 14334-14339.

Fidler, I.J., (2003). "The pathogenesis of cancer metastasis: the 'seed and soil' hypothesis revisited". *Nature reviews.Cancer,* **3**(6), 453-458.

Filipovic, A., Gronau, J.H., Green, A.R., Wang, J., Vallath, S., Shao, D., Rasul, S., Ellis, I.O., Yague, E., Sturge, J. and Coombes, R.C., (2010). "Biological and clinical implications of nicastrin expression in invasive breast cancer". *Breast cancer research and treatment,* .

Filmus, J. and Selleck, S.B., (2001). "Glypicans: proteoglycans with a surprise". *The Journal of clinical investigation,* **108**(4), 497-501.

Fingleton, B., (2003). "Matrix metalloproteinase inhibitors for cancer therapy:the current situation and future prospects". *Expert opinion on therapeutic targets,* **7**(3), 385-397.

Fischgrabe, J., Gotte, M., Michels, K., Kiesel, L. and Wulfing, P., (2010). "Targeting endothelin A receptor enhances anti-proliferative and anti-invasive effects of the HER2 antibody trastuzumab in HER2-overexpressing breast cancer cells". *International journal of cancer.Journal international du cancer,* **127**(3), 696-706.

Fiucci, G., Ravid, D., Reich, R. and Liscovitch, M., (2002). "Caveolin-1 inhibits anchorage-independent growth, anoikis and invasiveness in MCF-7 human breast cancer cells". *Oncogene,* **21**(15), 2365-2375.

Flynn, S. and Stockinger, B., (2003). "Tumor and CD4 T-cell interactions: tumor escape as result of reciprocal inactivation". *Blood,* **101**(11), 4472-4478.

Fossa, A., Alsoe, L., Crameri, R., Funderud, S., Gaudernack, G. and Smeland, E.B., (2004). "Serological cloning of cancer/testis antigens expressed in prostate cancer using cDNA phage surface display". *Cancer immunology, immunotherapy : CII,* **53**(5), 431-438.

Francia, G., Mitchell, S.D., Moss, S.E., Hanby, A.M., Marshall, J.F. and Hart, I.R., (1996). "Identification by differential display of annexin-VI, a gene differentially expressed during melanoma progression". *Cancer research,* **56**(17), 3855-3858.

Franklin, M.C., Carey, K.D., Vajdos, F.F., Leahy, D.J., de Vos, A.M. and Sliwkowski, M.X., (2004). "Insights into ErbB signaling from the structure of the ErbB2-pertuzuMAb complex". *Cancer cell,* **5**(4), 317-328.

Freeman, S.R., Drake, A.L., Heilig, L.F., Graber, M., McNealy, K., Schilling, L.M. and Dellavalle, R.P., (2006). "Statins, fibrates, and melanoma risk: a systematic review and meta-analysis". *Journal of the National Cancer Institute,* **98**(21), 1538-1546.

Friedl, P. and Wolf, K., (2008). "Tube travel: the role of proteases in individual and collective cancer cell invasion". *Cancer research,* **68**(18), 7247-7249.

Friedl, P. and Wolf, K., (2003). "Tumour-cell invasion and migration: diversity and escape mechanisms". *Nature reviews.Cancer,* **3**(5), 362-374.

Funaro, A., Horenstein, A.L., Santoro, P., Cinti, C., Gregorini, A. and Malavasi, F., (2000). "Monoclonal antibodies and therapy of human cancers". *Biotechnology Advances,* **18**(5), 385-401.

Furuya, M., Kato, H., Nishimura, N., Ishiwata, I., Ikeda, H., Ito, R., Yoshiki, T. and Ishikura, H., (2005). "Down-regulation of CD9 in human ovarian carcinoma cell might contribute to peritoneal dissemination: morphologic alteration and reduced expression of beta1 integrin subsets". *Cancer research,* **65**(7), 2617-2625.

Galbiati, F., Volonte, D., Engelman, J.A., Watanabe, G., Burk, R., Pestell, R.G. and Lisanti, M.P., (1998). "Targeted downregulation of caveolin-1 is sufficient to drive cell transformation and hyperactivate the p42/44 MAP kinase cascade". *The EMBO journal,* **17**(22), 6633-6648.

Gao, C.F., Xie, Q., Zhang, Y.W., Su, Y., Zhao, P., Cao, B., Furge, K., Sun, J., Rex, K., Osgood, T., Coxon, A., Burgess, T.L. and Vande Woude, G.F., (2009). "Therapeutic potential of hepatocyte growth factor/scatter factor neutralizing antibodies: inhibition of tumour growth in both autocrine and paracrine hepatocyte growth factor/scatter factor:c-Met-driven models of leiomyosarcoma". *Molecular cancer therapeutics,* **8**(10), 2803-2810.

Gebhardt, C., Nemeth, J., Angel, P. and Hess, J., (2006). "S100A8 and S100A9 in inflammation and cancer". *Biochemical pharmacology,* **72**(11), 1622-1631.

Gerger, A., Hofmann, G., Langsenlehner, U., Renner, W., Weitzer, W., Wehrschutz, M., Wascher, T., Samonigg, H. and Krippl, P., (2009). "Integrin alpha-2 and beta-3 gene polymorphisms and colorectal cancer risk". *International journal of colorectal disease,* **24**(2), 159-163.

Gerke, V. and Moss, S.E., (2002). "Annexins: from structure to function". *Physiological Reviews,* **82**(2), 331-371.

Ginis, I. and Faller, D.V., (2000). "Hypoxia affects tumour cell invasiveness in vitro: the role of hypoxia-activated ligand HAL1/13 (Ku86 autoantigen)". *Cancer letters,* **154**(2), 163-174.

Gitler, M.S., Sausville, E.A., Hollingshead, M. and Shoemaker, R., (2004). "In vivo models for experimental therapeutics relevant to human cancer". *Cancer research,* **64**(22), 8478-8480.

Glynn, S.A., Adams, A., Gibson, B., Cronin, D., Harmey, J.H. and Clynes, M., (2006). "Low adhesiveness coupled with high superinvasiveness in vitro predicts the in vivo metastatic potential of a mouse mammary adenocarcinoma cell line". *Anticancer Research,* **26**(2A), 1001-1010.

Glynn, S.A., Gammell, P., Heenan, M., O'Connor, R., Liang, Y., Keenan, J. and Clynes, M., (2004). "A new superinvasive in vitro phenotype induced by selection of human breast carcinoma cells with the chemotherapeutic drugs paclitaxel and doxorubicin". *British journal of cancer,* **91**(10), 1800-1807.

Glynn, S.A., O'Sullivan, D., Eustace, A.J., Clynes, M. & O'Donovan, N. (2008), "The 3-hydroxy-3-methylglutaryl-coenzyme A reductase inhibitors, simvastatin, lovastatin and mevastatin inhibit proliferation and invasion of melanoma cells", *BMC cancer,* vol. 8, pp. 9.

Goldsmith, S.J., (2010). "Radioimmunotherapy of lymphoma: Bexxar and Zevalin". *Seminars in nuclear medicine,* **40**(2), 122-135.

Goldstein, J.L., Anderson, R.G. and Brown, M.S., (1979). "Coated pits, coated vesicles, and receptor-mediated endocytosis". *Nature,* **279**(5715), 679-685.

Gondi, C.S. and Rao, J.S., (2009). "Therapeutic potential of siRNA-mediated targeting of urokinase plasminogen activator, its receptor, and matrix metalloproteinases". *Methods in molecular biology (Clifton, N.J.),* **487**, 267-281.

Goodison, S., Urquidi, V. and Tarin, D., (1999). "CD44 cell adhesion molecules". *Molecular pathology : MP,* **52**(4), 189-196.

Graaf, M.R., Beiderbeck, A.B., Egberts, A.C., Richel, D.J. and Guchelaar, H.J., (2004). "The risk of cancer in users of statins". *Journal of clinical oncology : official journal of the American Society of Clinical Oncology,* **22**(12), 2388-2394.

Graaf, M.R., Richel, D.J., van Noorden, C.J. and Guchelaar, H.J., (2004). "Effects of statins and farnesyltransferase inhibitors on the development and progression of cancer". *Cancer treatment reviews,* **30**(7), 609-641.

Grewal, T. and Enrich, C., (2006). "Molecular mechanisms involved in Ras inactivation: the annexin A6-p120GAP complex". *BioEssays,* **28**(12), 1211-1220.

Grewal, T. and Enrich, C., (2009). "Annexins — Modulators of EGF receptor signalling and trafficking". *Cellular signalling,* **21**(6), 847-858.

Grewal, T., Heeren, J., Mewawala, D., Schnitgerhans, T., Wendt, D., Salomon, G., Enrich, C., Beisiegel, U. and Jackle, S., (2000). "Annexin VI stimulates endocytosis and is involved in the trafficking of low density lipoprotein to the prelysosomal compartment". *The Journal of biological chemistry,* **275**(43), 33806-33813.

Grivennikov, S.I., Greten, F.R. and Karin, M., (2010). "Immunity, inflammation, and cancer". *Cell,* **140**(6), 883-899.

Grote, J., Konig, S., Ackermann, D., Sopalla, C., Benedyk, M., Los, M. and Kerkhoff, C., (2006). "Identification of poly(ADP-ribose)polymerase-1 and Ku70/Ku80 as transcriptional regulators of S100A9 gene expression". *BMC molecular biology,* **7**, 48.

Guarino, M., Rubino, B. and Ballabio, G., (2007). "The role of epithelial-mesenchymal transition in cancer pathology". *Pathology,* **39**(3), 305-318.

Gullo, C., Au, M., Feng, G. and Teoh, G., (2006). "The biology of Ku and its potential oncogenic role in cancer". *Biochimica et biophysica acta,* **1765**(2), 223-234.

Guo, C., Liu, Q.G., Zhang, L., Song, T. and Yang, X., (2009). "Expression and clinical significance of p53, JunB and KAI1/CD82 in human hepatocellular carcinoma". *Hepatobiliary & pancreatic diseases international : HBPD INT,* **8**(4), 389-396.

Hamers-Casterman, C., Atarhouch, T., Muyldermans, S., Robinson, G., Hamers, C., Songa, E.B., Bendahman, N. and Hamers, R., (1993). "Naturally occurring antibodies devoid of light chains". *Nature,* **363**(6428), 446-448.

Hara-Chikuma, M. and Verkman, A.S., (2008). "Aquaporin-3 facilitates epidermal cell migration and proliferation during wound healing". *Journal of Molecular Medicine (Berlin, Germany),* **86**(2), 221-231.

Harmsen, M.M. and De Haard, H.J., (2007). "Properties, production, and applications of camelid single-domain antibody fragments". *Applied Microbiology and Biotechnology,* **77**(1), 13-22.

Hastie, C., Masters, J.R., Moss, S.E. and Naaby-Hansen, S., (2008). "Interferon-gamma reduces cell surface expression of annexin 2 and suppresses the invasive capacity of prostate cancer cells". *The Journal of biological chemistry,* **283**(18), 12595-12603.

Hegedus, L., Cho, H., Xie, X. and Eliceiri, G.L., (2008). "Additional MDA-MB-231 breast cancer cell matrix metalloproteinases promote invasiveness". *Journal of cellular physiology,* **216**(2), 480-485.

Heinemann, V., Di Gioia, D., Vehling-Kaiser, U., Harich, H.D., Heinrich, B., Welt, A., Ziske, C., Deutsch, G., Pihusch, R., Kolbl, H., Hegewisch-Becker, S., Michl, M. and Stemmler, H.J., (2010). "A prospective multicenter phase II study of oral and i.v. vinorelbine plus trastuzumab as first-line therapy in HER2-overexpressing metastatic breast cancer". *Annals of Oncology : Official Journal of the European Society for Medical Oncology / ESMO,* .

Hemler, M.E., (2008). "Targeting of tetraspanin proteins--potential benefits and strategies". *Nature reviews.Drug discovery,* **7**(9), 747-758.

Henkhaus, R.S., Roy, U.K., Cavallo-Medved, D., Sloane, B.F., Gerner, E.W. and Ignatenko, N.A., (2008). "Caveolin-1-mediated expression and secretion of kallikrein 6 in colon cancer cells". *Neoplasia (New York, N.Y.),* **10**(2), 140-148.

Hermeking, H., (2003). "The 14-3-3 cancer connection". *Nature reviews.Cancer,* **3**(12), 931-943.

Hernandez, P., Muller, M. and Appel, R.D., (2006). "Automated protein identification by tandem mass spectrometry: issues and strategies". *Mass spectrometry reviews,* **25**(2), 235-254.

Heuberger, J. and Birchmeier, W., (2010). "Interplay of cadherin-mediated cell adhesion and canonical Wnt signaling". *Cold Spring Harbor perspectives in biology,* **2**(2), a002915.

Hildenbrand, R., Allgayer, H., Marx, A. and Stroebel, P., (2010). "Modulators of the urokinase-type plasminogen activation system for cancer". *Expert opinion on investigational drugs,* **19**(5), 641-652.

Hoffman, A., Qadri, B., Frant, J., Katz, Y., Bhusare, S.R., Breuer, E., Hadar, R. and Reich, R., (2008). "Carbamoylphosphonate matrix metalloproteinase inhibitors 6: cis-2-aminocyclohexylcarbamoylphosphonic acid, a novel orally active antimetastatic matrix metalloproteinase-2 selective inhibitor--synthesis and pharmacodynamic and pharmacokinetic analysis". *Journal of medicinal chemistry,* **51**(5), 1406-1414.

Hoffmeister, M., Chang-Claude, J. and Brenner, H., (2007). "Individual and joint use of statins and low-dose aspirin and risk of colorectal cancer: a population-based case-control study". *International journal of cancer.Journal international du cancer,* **121**(6), 1325-1330.

Hollestelle, A., Nagel, J.H., Smid, M., Lam, S., Elstrodt, F., Wasielewski, M., Ng, S.S., French, P.J., Peeters, J.K., Rozendaal, M.J., Riaz, M., Koopman, D.G., Ten Hagen, T.L., de Leeuw, B.H., Zwarthoff, E.C., Teunisse, A., van der Spek, P.J., Klijn, J.G., Dinjens, W.N., Ethier, S.P., Clevers, H., Jochemsen, A.G., den Bakker, M.A., Foekens, J.A., Martens, J.W. and Schutte, M., (2010). "Distinct gene mutation profiles among luminal-type and basal-type breast cancer cell lines". *Breast cancer research and treatment,* **121**(1), 53-64.

Hollestelle, A. and Schutte, M., (2009). "Comment Re: MDA-MB-435 and M14 cell lines: identical but not M14 Melanoma?". *Cancer research,* **69**(19), 7893.

Honda, M., Akiyama, H., Yamada, Y., Kondo, H., Kawabe, Y., Takeya, M., Takahashi, K., Suzuki, H., Doi, T., Sakamoto, A., Ookawara, S., Mato, M., Gough, P.J., Greaves, D.R., Gordon, S., Kodama, T. and Matsushita, M., (1998). "Immunohistochemical evidence for a macrophage scavenger receptor in Mato cells and reactive microglia of ischemia and Alzheimer's disease". *Biochemical and biophysical research communications,* **245**(3), 734-740.

Hong, I.K., Jin, Y.J., Byun, H.J., Jeoung, D.I., Kim, Y.M. and Lee, H., (2006). "Homophilic interactions of Tetraspanin CD151 up-regulate motility and matrix

metalloproteinase-9 expression of human melanoma cells through adhesion-dependent c-Jun activation signaling pathways". *The Journal of biological chemistry,* **281**(34), 24279-24292.

Hood, J.D. and Cheresh, D.A., (2002). "Role of integrins in cell invasion and migration". *Nature reviews.Cancer,* **2**(2), 91-100.

Houle, C.D., Ding, X.Y., Foley, J.F., Afshari, C.A., Barrett, J.C. and Davis, B.J., (2002). "Loss of expression and altered localization of KAI1 and CD9 protein are associated with epithelial ovarian cancer progression". *Gynecologic oncology,* **86**(1), 69-78.

Hu, J. and Verkman, A.S., (2006). "Increased migration and metastatic potential of tumour cells expressing aquaporin water channels". *The FASEB journal : official publication of the Federation of American Societies for Experimental Biology,* **20**(11), 1892-1894.

Hughes, B., (2010). "Antibody-drug conjugates for cancer: poised to deliver?". *Nature reviews.Drug discovery,* **9**(9), 665-667.

Hsia, D.A., Mitra, S.K., Hauck, C.R., Streblow, D.N., Nelson, J.A., Ilic, D., Huang, S., Li, E., Nemerow, G.R., Leng, J., Spencer, K.S., Cheresh, D.A. and Schlaepfer, D.D., (2003). "Differential regulation of cell motility and invasion by FAK". *The Journal of cell biology,* **160**(5), 753-767.

Hsu, S.M., Raine, L. and Fanger, H., (1981). "The use of antiavidin antibody and avidin-biotin-peroxidase complex in immunoperoxidase technics". *American Journal of Clinical Pathology,* **75**(6), 816-821.

Huang, C.L., Ueno, M., Liu, D., Masuya, D., Nakano, J., Yokomise, H., Nakagawa, T. and Miyake, M., (2006). "MRP-1/CD9 gene transduction regulates the actin cytoskeleton through the downregulation of WAVE2". *Oncogene,* **25**(49), 6480-6488.

Hudler, P., Gorsic, M. and Komel, R., (2010). "Proteomic strategies and challenges in tumour metastasis research". *Clinical & experimental metastasis,* **27**(6), 441-451.

Hutterer, M., Knyazev, P., Abate, A., Reschke, M., Maier, H., Stefanova, N., Knyazeva, T., Barbieri, V., Reindl, M., Muigg, A., Kostron, H., Stockhammer, G. and Ullrich, A., (2008). "Axl and growth arrest-specific gene 6 are frequently overexpressed in human gliomas and predict poor prognosis in patients with glioblastoma multiforme". *Clinical cancer research : an official journal of the American Association for Cancer Research,* **14**(1), 130-138.

Ichikawa, T., Ichikawa, Y. and Isaacs, J.T., (1991). "Genetic factors and suppression of metastatic ability of prostatic cancer". *Cancer research,* **51**(14), 3788-3792.

Iida, J., Pei, D., Kang, T., Simpson, M.A., Herlyn, M., Furcht, L.T. and McCarthy, J.B., (2001). "Melanoma chondroitin sulfate proteoglycan regulates matrix metalloproteinase-dependent human melanoma invasion into type I collagen". *The Journal of biological chemistry,* **276**(22), 18786-18794.

Iida, J., Meijne, A.M., Knutson, J.R., Furcht, L.T. and McCarthy, J.B., (1996). "Cell surface chondroitin sulfate proteoglycans in tumour cell adhesion, motility and invasion". *Seminars in cancer biology,* **7**(3), 155-162.

Ikeda, H., Hideshima, T., Fulciniti, M., Lutz, R.J., Yasui, H., Okawa, Y., Kiziltepe, T., Vallet, S., Pozzi, S., Santo, L., Perrone, G., Tai, Y.T., Cirstea, D., Raje, N.S., Uherek, C., Dalken, B., Aigner, S., Osterroth, F., Munshi, N., Richardson, P. and Anderson, K.C., (2009). "The monoclonal antibody nBT062 conjugated to cytotoxic Maytansinoids has selective cytotoxicity against CD138-positive multiple myeloma

cells in vitro and in vivo". *Clinical cancer research : an official journal of the American Association for Cancer Research,* **15**(12), 4028-4037.

Ilangumaran, S., He, H.T. and Hoessli, D.C., (2000). "Microdomains in lymphocyte signalling: beyond GPI-anchored proteins". *Immunology today,* **21**(1), 2-7.

Illert, B., Otto, C., Vollmers, H.P., Hensel, F., Thiede, A. and Timmermann, W., (2005). "Human antibody SC-1 reduces disseminated tumour cells in nude mice with human gastric cancer". *Oncology reports,* **13**(4), 765-770.

Immunoportal
www.immunoportal.com

Iozzo RV, Cohen I., (1994). "Altered proteoglycan gene expression and the tumor stroma". *EXS*. **70**, 199–214.

Irie, R.F., Ollila, D.W., O'Day, S. and Morton, D.L., (2004). "Phase I pilot clinical trial of human IgM monoclonal antibody to ganglioside GM3 in patients with metastatic melanoma". *Cancer immunology, immunotherapy : CII,* **53**(2), 110-117.

Ishikawa, N., Daigo, Y., Yasui, W., Inai, K., Nishimura, H., Tsuchiya, E., Kohno, N. and Nakamura, Y., (2004). "ADAM8 as a novel serological and histochemical marker for lung cancer". *Clinical cancer research : an official journal of the American Association for Cancer Research,* **10**(24), 8363-8370.

Isoai, A., Giga-Hama, Y., Shinkai, K., Mukai, M., Akedo, H. and Kumagai, H., (1990). "Purification and characterization of tumour invasion-inhibiting factors". *Japanese journal of cancer research : Gann,* **81**(9), 909-914.

Isoai, A., Goto-Tsukamoto, H., Yamori, T., Oh-hara, T., Tsuruo, T., Silletti, S., Raz, A., Watanabe, H., Akedo, H. and Kumagai, H., (1994). "Inhibitory effects of tumour invasion-inhibiting factor 2 and its conjugate on disseminating tumour cells". *Cancer research,* **54**(5), 1264-1270.

Israeli, R.S., Powell, C.T., Fair, W.R. and Heston, W.D., (1993). "Molecular cloning of a complementary DNA encoding a prostate-specific membrane antigen". *Cancer research,* **53**(2), 227-230.

Ivashkiv, L.B., (2009). "Cross-regulation of signaling by ITAM-associated receptors". *Nature immunology,* **10**(4), 340-347.

Jacobs, E.J., Rodriguez, C., Brady, K.A., Connell, C.J., Thun, M.J. and Calle, E.E., (2006). "Cholesterol-lowering drugs and colorectal cancer incidence in a large United States cohort". *Journal of the National Cancer Institute,* **98**(1), 69-72.

Jaffers, G.J., Fuller, T.C., Cosimi, A.B., Russell, P.S., Winn, H.J. and Colvin, R.B., (1986). "Monoclonal antibody therapy. Anti-idiotypic and non-anti-idiotypic antibodies to OKT3 arising despite intense immunosuppression". *Transplantation,* **41**(5), 572-578.

Jakobovits, A., Amado, R.G., Yang, X., Roskos, L. and Schwab, G., (2007). "From XenoMouse technology to panitumumab, the first fully human antibody product from transgenic mice". *Nature biotechnology,* **25**(10), 1134-1143.

Jang, H.I. and Lee, H., (2003). "A decrease in the expression of CD63 tetraspanin protein elevates invasive potential of human melanoma cells". *Experimental & molecular medicine,* **35**(4), 317-323.

Janssen, J.W., Schulz, A.S., Steenvoorden, A.C., Schmidberger, M., Strehl, S., Ambros, P.F. and Bartram, C.R., (1991). "A novel putative tyrosine kinase receptor with oncogenic potential". *Oncogene,* **6**(11), 2113-2120.

Jung, S.H., Lee, T., Kim, K. and George, S.L., (2004). "Admissible two-stage designs for phase II cancer clinical trials". *Statistics in medicine,* **23**(4), 561-569.

Kamal, A., Ying, Y. and Anderson, R.G., (1998). "Annexin VI-mediated loss of spectrin during coated pit budding is coupled to delivery of LDL to lysosomes". *The Journal of cell biology,* **142**(4), 937-947.

Karmakar, S. and Mukherjee, R., (2003). "Integrin receptors and ECM proteins involved in preferential adhesion of colon carcinoma cells to lung cells". *Cancer letters,* **196**(2), 217-227.

Kato, K., Hida, Y., Miyamoto, M., Hashida, H., Shinohara, T., Itoh, T., Okushiba, S., Kondo, S. and Katoh, H., (2002). "Overexpression of caveolin-1 in esophageal squamous cell carcinoma correlates with lymph node metastasis and pathologic stage". *Cancer,* **94**(4), 929-933.

Kelley, L.C., Shahab, S. and Weed, S.A., (2008). "Actin cytoskeletal mediators of motility and invasion amplified and overexpressed in head and neck cancer". *Clinical & experimental metastasis,* **25**(4), 289-304.

Kerrigan, J.J., McGill, J.T., Davies, J.A., Andrews, L. and Sandy, J.R., (1998). "The role of cell adhesion molecules in craniofacial development". *Journal of the Royal College of Surgeons of Edinburgh,* **43**(4), 223-229.

Khurana, V., Bejjanki, H.R., Caldito, G. and Owens, M.W., (2007). "Statins reduce the risk of lung cancer in humans: a large case-control study of US veterans". *Chest,* **131**(5), 1282-1288.

Kim, D.H., Jung, H.D., Kim, J.G., Lee, J.J., Yang, D.H., Park, Y.H., Do, Y.R., Shin, H.J., Kim, M.K., Hyun, M.S. and Sohn, S.K., (2006). "FCGR3A gene polymorphisms may correlate with response to frontline R-CHOP therapy for diffuse large B-cell lymphoma". *Blood,* **108**(8), 2720-2725.

Kim, S., Takahashi, H., Lin, W.W., Descargues, P., Grivennikov, S., Kim, Y., Luo, J.L. and Karin, M., (2009). "Carcinoma-produced factors activate myeloid cells through TLR2 to stimulate metastasis". *Nature,* **457**(7225), 102-106.

Kjoller, L., (2002). "The urokinase plasminogen activator receptor in the regulation of the actin cytoskeleton and cell motility". *Biological chemistry,* **383**(1), 5-19.

Klatka, J., (2002). "Syndecan-1 expression in laryngeal cancer". *European archives of oto-rhino-laryngology : official journal of the European Federation of Oto-Rhino-Laryngological Societies (EUFOS) : affiliated with the German Society for Oto-Rhino-Laryngology - Head and Neck Surgery,* **259**(3), 115-118.

Kleeff, J., Ishiwata, T., Kumbasar, A., Friess, H., Buchler, M.W., Lander, A.D. and Korc, M., (1998). "The cell-surface heparan sulfate proteoglycan glypican-1 regulates growth factor action in pancreatic carcinoma cells and is overexpressed in human pancreatic cancer". *The Journal of clinical investigation,* **102**(9), 1662-1673.

Kleeff, J., Wildi, S., Kumbasar, A., Friess, H., Lander, A.D. and Korc, M., (1999). "Stable transfection of a glypican-1 antisense construct decreases tumorigenicity in PANC-1 pancreatic carcinoma cells". *Pancreas,* **19**(3), 281-288.

Kohler, G. and Milstein, C., (1975). "Continuous cultures of fused cells secreting antibody of predefined specificity". *Nature,* **256**(5517), 495-497.

Koike, M. and Koike, A., (2008). "Accumulation of Ku80 proteins at DNA double-strand breaks in living cells". *Experimental cell research,* **314**(5), 1061-1070.

Koorstra, J.B., Karikari, C.A., Feldmann, G., Bisht, S., Rojas, P.L., Offerhaus, G.J., Alvarez, H. and Maitra, A., (2009). "The Axl receptor tyrosine kinase confers an adverse prognostic influence in pancreatic cancer and represents a new therapeutic target". *Cancer biology & therapy,* **8**(7), 618-626.

Kopper, L. and Timar, J., (2005). "Genomics of prostate cancer: is there anything to "translate"?". *Pathology oncology research : POR,* **11**(4), 197-203.

Kufe, D., Pollock, R., Weichselbaum, R., Bast, R., Gansler, T., Holland, J., Frei III, E., (2003). "Cancer Medicine". Editors; Hamilton (Canada): BC Decker Inc.; 6th Edition.

Kumar-Singh, S., Jacobs, W., Dhaene, K., Weyn, B., Bogers, J., Weyler, J. and Van Marck, E., (1998). "Syndecan-1 expression in malignant mesothelioma: correlation with cell differentiation, WT1 expression, and clinical outcome". *The Journal of pathology,* **186**(3), 300–305.

Kusano, Y., Yoshitomi, Y., Munesue, S., Okayama, M. and Oguri, K., (2004). "Cooperation of syndecan-2 and syndecan-4 among cell surface heparan sulfate proteoglycans in the actin cytoskeletal organization of Lewis lung carcinoma cells". *Journal of Biochemistry,* **135**(1), 129-137.

Lafleur, M.A., Xu, D. and Hemler, M.E., (2009). "Tetraspanin proteins regulate membrane type-1 matrix metalloproteinase-dependent pericellular proteolysis". *Molecular biology of the cell,* **20**(7), 2030-2040.

Lagadec, C., Meignan, S., Adriaenssens, E., Foveau, B., Vanhecke, E., Romon, R., Toillon, R.A., Oxombre, B., Hondermarck, H. and Le Bourhis, X., (2009). "TrkA overexpression enhances growth and metastasis of breast cancer cells". *Oncogene,* **28**(18), 1960-1970.

Lagadec, C., Romon, R., Tastet, C., eignan, S., Com, E., Page, A., Bidaux, G., Hondermarck, H. and Le Bourhis, X., (2010). *"Ku86 is important for TrkA overexpression-induced breast cancer cell invasion".* WILEY-VCH Verlag. **4**(6-7), 580-590

Lai, C. and Lemke, G., (1991). "An extended family of protein-tyrosine kinase genes differentially expressed in the vertebrate nervous system". *Neuron,* **6**(5), 691-704.

Lakhan, S.E., Sabharanjak, S. and De, A., (2009). "Endocytosis of glycosylphosphatidylinositol-anchored proteins". *Journal of Biomedical Science,* **16**, 93.

Landen, C.N., Kim, T.J., Lin, Y.G., Merritt, W.M., Kamat, A.A., Han, L.Y., Spannuth, W.A., Nick, A.M., Jennnings, N.B., Kinch, M.S., Tice, D. and Sood, A.K., (2008). "Tumour-selective response to antibody-mediated targeting of alphavbeta3 integrin in ovarian cancer". *Neoplasia (New York, N.Y.),* **10**(11), 1259-1267.

Larkin, A., Moran, E., Kennedy, S.M. and Clynes, M., (2005). "Monoclonal antibody 5C3 raised against formalin fixed paraffin-embedded invasive breast tumour tissue: characterisation of its reactive antigen via immunoprecipitation and internal sequencing". *Journal of immunological methods,* **303**(1-2), 53-65.

Lazo, P.A., (2007). "Functional implications of tetraspanin proteins in cancer biology". *Cancer science,* **98**(11), 1666-1677.

Le Tourneau, C., Lee, J.J. and Siu, L.L., (2009). "Dose escalation methods in phase I cancer clinical trials". *Journal of the National Cancer Institute,* **101**(10), 708-720.

Leonard, J.P., Coleman, M., Kostakoglu, L., Chadburn, A., Cesarman, E., Furman, R.R., Schuster, M.W., Niesvizky, R., Muss, D., Fiore, J., Kroll, S., Tidmarsh, G., Vallabhajosula, S. and Goldsmith, S.J., (2005). "Abbreviated chemotherapy with fludarabine followed by tositumomab and iodine I 131 tositumomab for untreated follicular lymphoma". *Journal of clinical oncology : official journal of the American Society of Clinical Oncology,* **23**(24), 5696-5704.

Levy, P., Munier, A., Baron-Delage, S., Di Gioia, Y., Gespach, C., Capeau, J. and Cherqui, G., (1996). "Syndecan-1 alterations during the tumorigenic progression of human colonic Caco-2 cells induced by human Ha-ras or polyoma middle T oncogenes". *British Journal of Cancer,* **74**(3), 423–431.

Li, G., Miles, A., Line, A. and Rees, R.C., (2004). "Identification of tumour antigens by serological analysis of cDNA expression cloning". *Cancer immunology, immunotherapy : CII,* **53**(3), 139-143.

Li, G., Nelsen, C. and Hendrickson, E.A., (2002). "Ku86 is essential in human somatic cells". *Proceedings of the National Academy of Sciences of the United States of America,* **99**(2), 832-837.

Li, S., Schmitz, K.R., Jeffrey, P.D., Wiltzius, J.J., Kussie, P. and Ferguson, K.M., (2005). "Structural basis for inhibition of the epidermal growth factor receptor by cetuximab". *Cancer cell,* **7**(4), 301-311.

Li, Y., Ye, X., Tan, C., Hongo, J.A., Zha, J., Liu, J., Kallop, D., Ludlam, M.J. and Pei, L., (2009). "Axl as a potential therapeutic target in cancer: role of Axl in tumour growth, metastasis and angiogenesis". *Oncogene,* **28**(39), 3442-3455.

Lim, J.W., Kim, H. and Kim, K.H., (2002). "Expression of Ku70 and Ku80 mediated by NF-kappa B and cyclooxygenase-2 is related to proliferation of human gastric cancer cells". *The Journal of biological chemistry,* **277**(48), 46093-46100.

Lin, H.C., Sudhof, T.C. and Anderson, R.G., (1992). "Annexin VI is required for budding of clathrin-coated pits". *Cell,* **70**(2), 283-291.

Lin, M., DiVito, M.M., Merajver, S.D., Boyanapalli, M. and van Golen, K.L., (2005). "Regulation of pancreatic cancer cell migration and invasion by RhoC GTPase and caveolin-1". *Molecular cancer,* **4**(1), 21.

Lin, M.Z., Teitell, M.A. and Schiller, G.J., (2005). "The evolution of antibodies into versatile tumor-targeting agents". *Clinical cancer research : an official journal of the American Association for Cancer Research,* **11**(1), 129-138.

Linenberger, M.L., (2005). "CD33-directed therapy with gemtuzumab ozogamicin in acute myeloid leukemia: progress in understanding cytotoxicity and potential mechanisms of drug resistance". *Leukemia : official journal of the Leukemia Society of America, Leukemia Research Fund, U.K,* **19**(2), 176-182.

Linke, R., Klein, A. and Seimetz, D., (2010). "Catumaxomab: Clinical development and future directions". *mAbs,* **2**(2),.

Liotta, L.A., (1986). "Tumour invasion and metastases--role of the extracellular matrix: Rhoads Memorial Award lecture". *Cancer research,* **46**(1), 1-7.

Liotta, L.A., Tryggvason, K., Garbisa, S., Hart, I., Foltz, C.M. and Shafie, S., (1980). "Metastatic potential correlates with enzymatic degradation of basement membrane collagen". *Nature,* **284**(5751), 67-68.

Liu, S.H., Lin, C.Y., Peng, S.Y., Jeng, Y.M., Pan, H.W., Lai, P.L., Liu, C.L. and Hsu, H.C., (2002). "Down-regulation of annexin A10 in hepatocellular carcinoma is associated with vascular invasion, early recurrence, and poor prognosis in synergy with p53 mutation". *The American journal of pathology,* **160**(5), 1831-1837.

Luo, M. and Guan, J.L., (2009). "Focal adhesion kinase: A prominent determinant in breast cancer initiation, progression and metastasis". *Cancer letters,* .

Liu, J.W., Shen, J.J., Tanzillo-Swarts, A., Bhatia, B., Maldonado, C.M., Person, M.D., Lau, S.S. and Tang, D.G., (2003). "Annexin II expression is reduced or lost in prostate cancer cells and its re-expression inhibits prostate cancer cell migration". *Oncogene,* **22**(10), 1475-1485.

Lynch, E.M., Moreland, R.B., Ginis, I., Perrine, S.P. and Faller, D.V., (2001). "Hypoxia-activated ligand HAL-1/13 is lupus autoantigen Ku80 and mediates lymphoid cell adhesion in vitro". *American journal of physiology.Cell physiology,* **280**(4), C897-911.

Mack, G.S. and Marshall, A., (2010). "Lost in migration". *Nature biotechnology,* **28**(3), 214-229.

Maehara, H., Kaname, T., Yanagi, K., Hanzawa, H., Owan, I., Kinjou, T., Kadomatsu, K., Ikematsu, S., Iwamasa, T., Kanaya, F. and Naritomi, K., (2007). "Midkine as a novel target for antibody therapy in osteosarcoma". *Biochemical and biophysical research communications,* **358**(3), 757-762.

Mantovani, A., (2009). "Cancer: Inflaming metastasis". *Nature,* **457**(7225), 36-37.

Marvin, J.S. and Zhu, Z., (2005). "Recombinant approaches to IgG-like bispecific antibodies". *Acta Pharmacologica Sinica,* **26**(6), 649-658.

Masters, J.R., (2002). "HeLa cells 50 years on: the good, the bad and the ugly". *Nature reviews.Cancer,* **2**(4), 315-319.

Matsumoto A, Ono M, Fujimoto Y, Gallo RL, Bernfield M, Kohgo Y., (1997). "Reduced expression of syndecan-1 in human hepatocellular carcinoma with high metastatic potential". *International Journal of Cancer*; **74**(5), 482–91.

Mayeur, G.L., Kung, W.J., Martinez, A., Izumiya, C., Chen, D.J. and Kung, H.J., (2005). "Ku is a novel transcriptional recycling coactivator of the androgen receptor in prostate cancer cells". *The Journal of biological chemistry,* **280**(11), 10827-10833.

Mayor, S. and Riezman, H., (2004). "Sorting GPI-anchored proteins". *Nature reviews.Molecular cell biology,* **5**(2), 110-120.

Mazzocca, A., Coppari, R., De Franco, R., Cho, J.Y., Libermann, T.A., Pinzani, M. and Toker, A., (2005). "A secreted form of ADAM9 promotes carcinoma invasion through tumour-stromal interactions". *Cancer research,* **65**(11), 4728-4738.

McBride, S., Meleady, P., Baird, A., Dinsdale, D. and Clynes, M., (1998). "Human lung carcinoma cell line DLKP contains 3 distinct subpopulations with different growth and attachment properties". *Tumour biology : the journal of the International Society for Oncodevelopmental Biology and Medicine,* **19**(2), 88-103.

McCarron, P.A., Olwill, S.A., Marouf, W.M., Buick, R.J., Walker, B. and Scott, C.J., (2005). "Antibody conjugates and therapeutic strategies". *Molecular interventions,* **5**(6), 368-380.

McGraw-Hill Higher Education
www.mhhe.com

Mendoza, A., Hong, S.H., Osborne, T., Khan, M.A., Campbell, K., Briggs, J., Eleswarapu, A., Buquo, L., Ren, L., Hewitt, S.M., Dakir el, H., Garfield, S., Walker, R., Merlino, G., Green, J.E., Hunter, K.W., Wakefield, L.M. and Khanna, C., (2010). "Modeling metastasis biology and therapy in real time in the mouse lung". *The Journal of clinical investigation,* **120**(8), 2979-2988.

Mennerich, D., Vogel, A., Klaman, I., Dahl, E., Lichtner, R.B., Rosenthal, A., Pohlenz, H.D., Thierauch, K.H. and Sommer, A., (2004). "Shift of syndecan-1 expression from epithelial to stromal cells during progression of solid tumours". *European journal of cancer (Oxford, England : 1990),* **40**(9), 1373-1382.

Mochizuki, S. and Okada, Y., (2007). "ADAMs in cancer cell proliferation and progression". *Cancer science,* **98**(5), 621-628.

Monastyrskaya, K., Babiychuk, E.B. and Draeger, A., (2009). "The annexins: spatial and temporal coordination of signaling events during cellular stress". *Cellular and molecular life sciences : CMLS,* **66**(16), 2623-2642.

Monferran, S., Paupert, J., Dauvillier, S., Salles, B. and Muller, C., (2004). "The membrane form of the DNA repair protein Ku interacts at the cell surface with metalloproteinase 9". *The EMBO journal,* **23**(19), 3758-3768.

Mosesson, Y., Mills, G.B. and Yarden, Y., (2008). "Derailed endocytosis: an emerging feature of cancer". *Nature reviews.Cancer,* **8**(11), 835-850.

Mussunoor, S. and Murray, G.I., (2008). "The role of annexins in tumour development and progression". *The Journal of pathology,* **216**(2), 131-140.

Najib, N.M., Idkaidek, N., Adel, A., Admour, I., Astigarraga, R.E., Nucci, G.D., Alam, S.M., Dham, R. and Qumaruzaman, (2003). "Pharmacokinetics and bioequivalence evaluation of two simvastatin 40 mg tablets (Simvast and Zocor) in healthy human volunteers". *Biopharmaceutics & drug disposition,* **24**(5), 183-189.

Nakajima, M., Welch, D.R., Wynn, D.M., Tsuruo, T. and Nicolson, G.L., (1993). "Serum and plasma M(r) 92,000 progelatinase levels correlate with spontaneous metastasis of rat 13762NF mammary adenocarcinoma". *Cancer research,* **53**(23), 5802-5807.

Nakato, H., Futch, T.A. and Selleck, S.B., (1995). "The division abnormally delayed (dally) gene: a putative integral membrane proteoglycan required for cell division patterning during postembryonic development of the nervous system in Drosophila". *Development (Cambridge, England),* **121**(11), 3687-3702.

Nelson, A.L., Dhimolea, E. and Reichert, J.M., (2010). "Development trends for human monoclonal antibody therapeutics". *Nature reviews.Drug discovery,* 9(10), 767-774.

Newton, R., Bradley, E., Levy, R., Doval, D., Bondarde, S., Sahoo, T., Lokanatha, D., Julka, P., Nagarkar R. and Friedman, S., (2010). "Clinical benefit of INCB7839, a potent and selective ADAM inhibitor, in combination with trastuzumab in patients with metastatic HER2+ breast cancer". *Journal of Clinical Oncology*, ASCO Annual Meeting Proceedings (Post-Meeting Edition). **28**(15) (May 20 Supplement), 2010: 3025

Nikitovic, D., Katonis, P., Tsatsakis, A., Karamanos, N.K. and Tzanakakis, G.N., (2008). "Lumican, a small leucine-rich proteoglycan". *IUBMB life,* **60**(12), 818-823.

Nikkola, J., Vihinen, P., Vuoristo, M.S., Kellokumpu-Lehtinen, P., Kahari, V.M. and Pyrhonen, S., (2005). "High serum levels of matrix metalloproteinase-9 and matrix metalloproteinase-1 are associated with rapid progression in patients with metastatic melanoma". *Clinical cancer research : an official journal of the American Association for Cancer Research,* **11**(14), 5158-5166.

Nilson, B.H., Logdberg, L., Kastern, W., Bjorck, L. and Akerstrom, B., (1993). "Purification of antibodies using Protein-L-binding framework structures in the light chain variable domain". *Journal of immunological methods,* **164**(1), 33-40.

Nimmerjahn, F. and Ravetch, J.V., (2005). "Divergent immunoglobulin g subclass activity through selective Fc receptor binding". *Science (New York, N.Y.),* **310**(5753), 1510-1512.

Ning, S., Tian, J., Marshall, D.J. and Knox, S.J., (2010). "Anti-alphav integrin monoclonal antibody intetumumab enhances the efficacy of radiation therapy and reduces metastasis of human cancer xenografts in nude rats". *Cancer research,* **70**(19), 7591-7599.

Nolens, G., Pignon, J.C., Koopmansch, B., Elmoualij, B., Zorzi, W., De Pauw, E. and Winkler, R., (2009). "Ku proteins interact with activator protein-2 transcription factors and contribute to ERBB2 overexpression in breast cancer cell lines". *Breast cancer research : BCR,* **11**(6), R83.

O'Bryan, J.P., Frye, R.A., Cogswell, P.C., Neubauer, A., Kitch, B., Prokop, C., Espinosa, R.,3rd, Le Beau, M.M., Earp, H.S. and Liu, E.T., (1991). "Axl, a Transforming Gene Isolated from Primary Human Myeloid Leukemia Cells, Encodes a Novel Receptor Tyrosine Kinase". *Molecular and cellular biology,* **11**(10), 5016-5031.

Orlichenko, L.S. and Radisky, D.C., (2008). "Matrix metalloproteinases stimulate epithelial-mesenchymal transition during tumour development". *Clinical & experimental metastasis,* **25**(6), 593-600.

Orth, J.D., Krueger, E.W., Weller, S.G. and McNiven, M.A., (2006). "A novel endocytic mechanism of epidermal growth factor receptor sequestration and internalization". *Cancer research,* **66**(7), 3603-3610.

Ohshima, M., Tadakuma, T., Hayashi, H., Inoue, K. and Itoh, K., (2010). "Generation of a recombinant single-chain variable fragment (scFv) targeting 5-methyl-2'-deoxycytidine". *Journal of Biochemistry,* **147**(1), 135-141.

Ovalle, S., Gutierrez-Lopez, M.D., Olmo, N., Turnay, J., Lizarbe, M.A., Majano, P., Molina-Jimenez, F., Lopez-Cabrera, M., Yanez-Mo, M., Sanchez-Madrid, F. and Cabanas, C., (2007). "The tetraspanin CD9 inhibits the proliferation and tumorigenicity of human colon carcinoma cells". *International journal of cancer.Journal international du cancer,* **121**(10), 2140-2152.

Pastuskovas, C.V., Mallet, W., Clark, S., Kenrick, M., Majidy, M., Schweiger, M., Van Hoy, M., Tsai, S.P., Bennett, G., Shen, B.Q., Ross, S., Fielder, P., Khawli, L. and Tibbitts, J., (2010). "The effect of immune-complex formation on the distribution of a novel antibody to the ovarian tumor antigen CA125". *Drug metabolism and disposition: the biological fate of chemicals,* .

Penas, P.F., Garcia-Diez, A., Sanchez-Madrid, F. and Yanez-Mo, M., (2000). "Tetraspanins are localized at motility-related structures and involved in normal

human keratinocyte wound healing migration". *The Journal of investigative dermatology,* **114**(6), 1126-1135.

Perez, E.A., (2008). "Cardiac toxicity of ErbB2-targeted therapies: what do we know?". *Clinical breast cancer,* **8 Suppl 3**, S114-20.

Plevy, S., Salzberg, B., Van Assche, G., Regueiro, M., Hommes, D., Sandborn, W., Hanauer, S., Targan, S., Mayer, L., Mahadevan, U., Frankel, M. and Lowder, J., (2007). "A phase I study of visilizumab, a humanized anti-CD3 monoclonal antibody, in severe steroid-refractory ulcerative colitis". *Gastroenterology,* **133**(5), 1414-1422.

Pols, M.S. and Klumperman, J., (2009). "Trafficking and function of the tetraspanin CD63". *Experimental cell research,* **315**(9), 1584-1592.

Pons, M., Tebar, F., Kirchhoff, M., Peiro, S., de Diego, I., Grewal, T. and Enrich, C., (2001). "Activation of Raf-1 is defective in annexin 6 overexpressing Chinese hamster ovary cells". *FEBS letters,* **501**(1), 69-73.

Poynter, J.N., Gruber, S.B., Higgins, P.D., Almog, R., Bonner, J.D., Rennert, H.S., Low, M., Greenson, J.K. and Rennert, G., (2005). "Statins and the risk of colorectal cancer". *The New England journal of medicine,* **352**(21), 2184-2192.

Pucci, S., Mazzarelli, P., Rabitti, C., Giai, M., Gallucci, M., Flammia, G., Alcini, A., Altomare, V. and Fazio, V.M., (2001). "Tumor specific modulation of KU70/80 DNA binding activity in breast and bladder human tumor biopsies". *Oncogene,* **20**(6), 739-747.

Qu, Z., Griffiths, G.L., Wegener, W.A., Chang, C., Govindan, S.V., Horak, I.D., Hansen, H.J. and Goldenberg, D.M., (2005). "Development of humanized antibodies as cancer therapeutics". *Methods,* **36**(1), 84-95.

Rabbani, S.A., Ateeq, B., Arakelian, A., Valentino, M.L., Shaw, D.E., Dauffenbach, L.M., Kerfoot, C.A. and Mazar, A.P., (2010). "An anti-urokinase plasminogen activator receptor antibody (ATN-658) blocks prostate cancer invasion, migration, growth, and experimental skeletal metastasis in vitro and in vivo". *Neoplasia (New York, N.Y.),* **12**(10), 778-788.

Raymond, E., Faivre, S. and Armand, J.P., (2000). "Epidermal growth factor receptor tyrosine kinase as a target for anticancer therapy". *Drugs,* **60 Suppl 1**, 15-23; discussion 41-2.

Reardon, D. A., Cloughsey, T. F., Raizer, J. J., Laterra, J. , Schiff, D., Yang, X., Loh E., and Wen. P.I., (2008). "Phase II study of AMG 102, a fully human neutralizing antibody against hepatocyte growth factor/scatter factor, in patients with recurrent glioblastoma multiforme" Journal of Clinical Oncology, ASCO Annual Meeting Proceedings (Post-Meeting Edition). **26**(15S), 2051

Reichert, J.M. and Dewitz, M.C., (2006). "Anti-infective monoclonal antibodies: perils and promise of development". *Nature reviews.Drug discovery,* **5**(3), 191-195.

Reiland, J., Sanderson, R.D., Waguespack, M., Barker, S.A., Long, R., Carson, D.D. and Marchetti, D., (2004). "Heparanase degrades syndecan-1 and perlecan heparan sulfate: functional implications for tumour cell invasion". *The Journal of biological chemistry,* **279**(9), 8047-8055.

Rentero, C., Evans, R., Wood, P., Tebar, F., Vila de Muga, S., Cubells, L., de Diego, I., Hayes, T.E., Hughes, W.E., Pol, A., Rye, K.A., Enrich, C. and Grewal, T., (2006). "Inhibition of H-Ras and MAPK is compensated by PKC-dependent pathways in annexin A6 expressing cells". *Cellular signalling,* **18**(7), 1006-1016.

Revets, H., De Baetselier, P. and Muyldermans, S., (2005). "Nanobodies as novel agents for cancer therapy". *Expert opinion on biological therapy,* **5**(1), 111-124.

Ricart, A.D. and Tolcher, A.W., (2007). "Technology insight: cytotoxic drug immunoconjugates for cancer therapy". *Nature clinical practice.Oncology,* **4**(4), 245-255.

Ricart, A.D., Tolcher, A.W., Liu, G., Holen, K., Schwartz, G., Albertini, M., Weiss, G., Yazji, S., Ng, C. and Wilding, G., (2008). "Volociximab, a chimeric monoclonal antibody that specifically binds alpha5beta1 integrin: a phase I, pharmacokinetic, and biological correlative study". *Clinical cancer research : an official journal of the American Association for Cancer Research,* **14**(23), 7924-7929.

Ricciardelli, C., Russell, D.L., Ween, M.P., Mayne, K., Suwiwat, S., Byers, S., Marshall, V.R., Tilley, W.D. and Horsfall, D.J., (2007). "Formation of hyaluronan- and versican-rich pericellular matrix by prostate cancer cells promotes cell motility". *The Journal of biological chemistry,* **282**(14), 10814-10825.

Ricciardelli, C., Sakko, A.J., Ween, M.P., Russell, D.L. and Horsfall, D.J., (2009). "The biological role and regulation of versican levels in cancer". *Cancer metastasis reviews,* **28**(1-2), 233-245.

Rody, A., Holtrich, U., Gaetje, R., Gehrmann, M., Engels, K., von Minckwitz, G., Loibl, S., Diallo-Danebrock, R., Ruckhaberle, E., Metzler, D., Ahr, A., Solbach, C., Karn, T. and Kaufmann, M., (2007). "Poor outcome in estrogen receptor-positive breast cancers predicted by loss of plexin B1". *Clinical cancer research : an official journal of the American Association for Cancer Research,* **13**(4), 1115-1122.

Roodink, I., Franssen, M., Zuidscherwoude, M., Verrijp, K., van der Donk, T., Raats, J. and Leenders, W.P., (2010). "Isolation of targeting nanobodies against co-opted tumor vasculature". *Laboratory investigation; a journal of technical methods and pathology,* **90**(1), 61-67.

Rosen, P.J., Sweeney, C.J., Park, D.J., Beaupre, D.M., Deng, H., Leitch, I.M., Shubhakar, P., Zhu, M., Oliner, K.S., Anderson, A. and Yee, L.K., (2010). "A phase Ib study of AMG 102 in combination with bevacizumab or motesanib in patients with advanced solid tumors". *Clinical cancer research : an official journal of the American Association for Cancer Research,* **16**(9), 2677-2687.

Rosenthal, N. and Brown, S., (2007). "The mouse ascending: perspectives for human-disease models". *Nature cell biology,* **9**(9), 993-999.

Ross, D.T., Scherf, U., Eisen, M.B., Perou, C.M., Rees, C., Spellman, P., Iyer, V., Jeffrey, S.S., Van de Rijn, M., Waltham, M., Pergamenschikov, A., Lee, J.C., Lashkari, D., Shalon, D., Myers, T.G., Weinstein, J.N., Botstein, D. and Brown, P.O., (2000). "Systematic variation in gene expression patterns in human cancer cell lines". *Nature genetics,* **24**(3), 227-235.

Ross, D.T., Scherf, U., Eisen, M.B., Perou, C.M., Rees, C., Spellman, P., Iyer, V., Jeffrey, S.S., Van de Rijn, M., Waltham, M., Pergamenschikov, A., Lee, J.C., Lashkari, D., Shalon, D., Myers, T.G., Weinstein, J.N., Botstein, D. and Brown, P.O., (2000). "Systematic variation in gene expression patterns in human cancer cell lines". *Nature genetics,* **24**(3), 227-235.

Rossi, S. (2009), "Defining the cell surface proteoglycan metastatic signature of cancer cells: role of Glypican-5 in the control of cell motility", *Biologia Evolutiva e Funzionale, Tesi di dottorato*.
http://hdl.handle.net/1889/1062

Sainaghi, P.P., Castello, L., Bergamasco, L., Galletti, M., Bellosta, P. and Avanzi, G.C., (2005). "Gas6 induces proliferation in prostate carcinoma cell lines expressing the Axl receptor". *Journal of cellular physiology,* **204**(1), 36-44.

Sakwe, A.M., Koumangoye, R., Goodwin, S.J. and Ochieng, J., (2010). "Fetuin-A (ahsg) is a major serum adhesive protein that mediates growth signaling in breast tumor cells". *The Journal of biological chemistry,* **Epub ahead of print**.

Sallmyr, A., Du, L. and Bredberg, A., (2002). "An inducible Ku86-degrading serine protease in human cells". *Biochimica et biophysica acta,* **1593**(1), 57-68.

Sanderson, R.D., (2001). "Heparan sulfate proteoglycans in invasion and metastasis". *Seminars in cell & developmental biology,* **12**(2), 89-98.

Santin, A.D., Diamandis, E.P., Bellone, S., Soosaipillai, A., Cane, S., Palmieri, M., Burnett, A., Roman, J.J. and Pecorelli, S., (2005). "Human kallikrein 6: a new potential serum biomarker for uterine serous papillary cancer". *Clinical cancer research : an official journal of the American Association for Cancer Research,* **11**(9), 3320-3325.

Satoh, M., Wang, J. and Reeves, W.H., (1995). "Role of free p70 (Ku) subunit in posttranslational stabilization of newly synthesized p80 during DNA-dependent protein kinase assembly". *European journal of cell biology,* **66**(2), 127-135.

Savore, C., Zhang, C., Muir, C., Liu, R., Wyrwa, J., Shu, J., Zhau, H.E., Chung, L.W., Carson, D.D. and Farach-Carson, M.C., (2005). "Perlecan knockdown in metastatic prostate cancer cells reduces heparin-binding growth factor responses in vitro and tumour growth in vivo". *Clinical & experimental metastasis,* **22**(5), 377-390.

Sawada, M., Hayes, P. and Matsuyama, S., (2003). "Cytoprotective membrane-permeable peptides designed from the Bax-binding domain of Ku70". *Nature cell biology,* **5**(4), 352-357.

Sawada, M., Sun, W., Hayes, P., Leskov, K., Boothman, D.A. and Matsuyama, S., (2003). "Ku70 suppresses the apoptotic translocation of Bax to mitochondria". *Nature cell biology,* **5**(4), 320-329.

Sawaki, M., Iwata, H., Sato, Y., Wada, M., Toyama, T., Sasaki, E., Yatabe, Y., Imai, T. and Ohashi, Y., (2010). "Phase II study of preoperative systemic treatment with the combination of docetaxel and trastuzumab in patients with locally advanced HER-2-overexpressing breast cancer". *Breast (Edinburgh, Scotland),* **19**(5), 370-376.

Schirle, M., Keilholz, W., Weber, B., Gouttefangeas, C., Dumrese, T., Becker, H.D., Stevanovic, S. and Rammensee, H.G., (2000). "Identification of tumour-associated MHC class I ligands by a novel T cell-independent approach". *European journal of immunology,* **30**(8), 2216-2225.

Schmitz-Esser, S., Linka, N., Collingro, A., Beier, C.L., Neuhaus, H.E., Wagner, M. and Horn, M., (2004). "ATP/ADP translocases: a common feature of obligate intracellular amoebal symbionts related to Chlamydiae and Rickettsiae". *Journal of Bacteriology,* **186**(3), 683-691.

Scott, A.M., Wiseman, G., Welt, S., Adjei, A., Lee, F.T., Hopkins, W., Divgi, C.R., Hanson, L.H., Mitchell, P., Gansen, D.N., Larson, S.M., Ingle, J.N., Hoffman, E.W., Tanswell, P., Ritter, G., Cohen, L.S., Bette, P., Arvay, L., Amelsberg, A., Vlock, D., Rettig, W.J. and Old, L.J., (2003). "A Phase I dose-escalation study of sibrotuzumab in patients with advanced or metastatic fibroblast activation protein-positive cancer". *Clinical cancer research : an official journal of the American Association for Cancer Research,* **9**(5), 1639-1647.

Sears, H.F., Herlyn, D., Steplewski, Z. and Koprowski, H., (1984). "Effects of monoclonal antibody immunotherapy on patients with gastrointestinal adenocarcinoma". *Journal of Biological Response Modifiers,* **3**(2), 138-150.

Senter, P.D. and Springer, C.J., (2001). "Selective activation of anticancer prodrugs by monoclonal antibody–enzyme conjugates". *Advanced Drug Delivery Reviews,* **53**(3), 247-264.

Seraphin, B., (2002). "Identification of transiently interacting proteins and of stable protein complexes". *Advances in Protein Chemistry,* **61**, 99-117.

Shanbhogue, A.K., Karnad, A.B. and Prasad, S.R., (2010). "Tumour response evaluation in oncology: current update". *Journal of computer assisted tomography,* **34**(4), 479-484.

Sharma B, Handler M, Eichstetter I, Whitelock JM, Nugent MA, Iozzo RV., (1998). "Antisense targeting of perlecan blocks tumor growth and angiogenesis in vivo". *The Journal of clinical investigation*. **102**(8), 1599–608.

Shaw, L.M., Chao, C., Wewer, U.M. and Mercurio, A.M., (1996). "Function of the integrin alpha 6 beta 1 in metastatic breast carcinoma cells assessed by expression of a dominant-negative receptor". *Cancer research,* **56**(5), 959-963.

Shellman, Y.G., Ribble, D., Miller, L., Gendall, J., Vanbuskirk, K., Kelly, D., Norris, D.A. and Dellavalle, R.P., (2005). "Lovastatin-induced apoptosis in human melanoma cell lines". *Melanoma research,* **15**(2), 83-89.

Shen, J., Vil, M.D., Jimenez, X., Iacolina, M., Zhang, H. and Zhu, Z., (2006). "Single variable domain-IgG fusion. A novel recombinant approach to Fc domain-containing bispecific antibodies". *The Journal of biological chemistry,* **281**(16), 10706-10714.

Shields, J.M., Pruitt, K., McFall, A., Shaub, A. and Der, C.J., (2000). "Understanding Ras: 'it ain't over 'til it's over'". *Trends in cell biology,* **10**(4), 147-154.

Shieh, Y.S., Lai, C.Y., Kao, Y.R., Shiah, S.G., Chu, Y.W., Lee, H.S. and Wu, C.W., (2005). "Expression of axl in lung adenocarcinoma and correlation with tumour progression". *Neoplasia (New York, N.Y.),* **7**(12), 1058-1064.

Shigeta, M., Sanzen, N., Ozawa, M., Gu, J., Hasegawa, H. and Sekiguchi, K., (2003). "CD151 regulates epithelial cell-cell adhesion through PKC- and Cdc42-dependent actin cytoskeletal reorganization". *The Journal of cell biology,* **163**(1), 165-176.

Shikano, S., Coblitz, B., Wu, M. and Li, M., (2006). "14-3-3 Proteins: Regulation of Endoplasmic Reticulum Localization and Surface Expression of Membrane Proteins". *Trends in cell biology,* **16**(7), 370-375.

Shinkawa, T., Nakamura, K., Yamane, N., Shoji-Hosaka, E., Kanda, Y., Sakurada, M., Uchida, K., Anazawa, H., Satoh, M., Yamasaki, M., Hanai, N. and Shitara, K., (2003). "The absence of fucose but not the presence of galactose or bisecting N-acetylglucosamine of human IgG1 complex-type oligosaccharides shows the critical role of enhancing antibody-dependent cellular cytotoxicity". *The Journal of biological chemistry,* **278**(5), 3466-3473.

Shintani, Y., Higashiyama, S., Ohta, M., Hirabayashi, H., Yamamoto, S., Yoshimasu, T., Matsuda, H. and Matsuura, N., (2004). "Overexpression of ADAM9 in non-small cell lung cancer correlates with brain metastasis". *Cancer research,* **64**(12), 4190-4196.

Shiomi, T., Inoki, I., Kataoka, F., Ohtsuka, T., Hashimoto, G., Nemori, R. and Okada, Y., (2005). "Pericellular activation of proMMP-7 (promatrilysin-1) through interaction with CD151". *Laboratory investigation; a journal of technical methods and pathology,* **85**(12), 1489-1506.

Shulman, M., Wilde, C.D. and Kohler, G., (1978). "A better cell line for making hybridomas secreting specific antibodies". *Nature,* **276**(5685), 269-270.

Simizu, S., Takagi, S., Tamura, Y. and Osada, H., (2005). "RECK-mediated suppression of tumour cell invasion is regulated by glycosylation in human tumour cell lines". *Cancer research,* **65**(16), 7455-7461.

Simmons, K. "The Extracellular Matrix"
http://kentsimmons.uwinnipeg.ca/cm1504/cellwall.htm

Simons, K. and Toomre, D., (2000). "Lipid rafts and signal transduction". *Nature reviews.Molecular cell biology,* **1**(1), 31-39.

Sleijfer, S., van der Gaast, A., Planting, A.S., Stoter, G. and Verweij, J., (2005). "The potential of statins as part of anti-cancer treatment". *European journal of cancer (Oxford, England : 1990),* **41**(4), 516-522.

Sloan, E.K., Stanley, K.L. and Anderson, R.L., (2004). "Caveolin-1 inhibits breast cancer growth and metastasis". *Oncogene,* **23**(47), 7893-7897.

Small, J.V., Stradal, T., Vignal, E. and Rottner, K., (2002). "The lamellipodium: where motility begins". *Trends in cell biology,* **12**(3), 112-120.

Soiffer, R.J., Freedman, A.S., Neuberg, D., Fisher, D.C., Alyea, E.P., Gribben, J., Schlossman, R.L., Bartlett-Pandite, L., Kuhlman, C., Murray, C., Freeman, A., Mauch, P., Anderson, K.C., Nadler, L.M. and Ritz, J., (1998). "CD6+ T cell-depleted allogeneic bone marrow transplantation for non-Hodgkin's lymphoma". *Bone marrow transplantation,* **21**(12), 1177-1181.

Srivastava, M., Bubendorf, L., Srikantan, V., Fossom, L., Nolan, L., Glasman, M., Leighton, X., Fehrle, W., Pittaluga, S., Raffeld, M., Koivisto, P., Willi, N., Gasser, T.C., Kononen, J., Sauter, G., Kallioniemi, O.P., Srivastava, S. and Pollard, H.B., (2001). "ANX7, a candidate tumour suppressor gene for prostate cancer". *Proceedings of the National Academy of Sciences of the United States of America,* **98**(8), 4575-4580.

Stamenkovic, I., (2003). "Extracellular matrix remodelling: the role of matrix metalloproteinases". *The Journal of pathology,* **200**(4), 448-464.

Stanley MJ, Stanley MW, Sanderson RD, Zera R., (1999). "Syndecan- 1 expression is induced in the stroma of infiltrating breast carcinoma". *American Journal of Clinical Pathology*, **112**(3), 377–83.

Stellas, D., Karameris, A. and Patsavoudi, E., (2007). "Monoclonal antibody 4C5 immunostains human melanomas and inhibits melanoma cell invasion and metastasis". *Clinical cancer research : an official journal of the American Association for Cancer Research,* **13**(6), 1831-1838.

Stevanovic, S., (2002). "Identification of tumour-associated T-cell epitopes for vaccine development". *Nature reviews.Cancer,* **2**(7), 514-520.

Stipp, C.S., Kolesnikova, T.V. and Hemler, M.E., (2003). "Functional domains in tetraspanin proteins". *Trends in biochemical sciences,* **28**(2), 106-112.

Strandh, M., Ohlin, M., Borrebaeck, C.A. and Ohlson, S., (1998). "New approach to steroid separation based on a low affinity IgM antibody". *Journal of immunological methods,* **214**(1-2), 73-79.

Strathdee, G., (2002). "Epigenetic versus genetic alterations in the inactivation of E-cadherin". *Seminars in cancer biology,* **12**(5), 373-379.

Sun, W., Fujimoto, J. and Tamaya, T., (2004). "Coexpression of Gas6/Axl in human ovarian cancers". *Oncology,* **66**(6), 450-457.

Suntharalingam, G., Perry, M.R., Ward, S., Brett, S.J., Castello-Cortes, A., Brunner, M.D. and Panoskaltsis, N., (2006). "Cytokine storm in a phase 1 trial of the anti-CD28 monoclonal antibody TGN1412". *The New England journal of medicine,* **355**(10), 1018-1028.

Sylvester, R., Van Glabbeke, M., Collette, L., Suciu, S., Baron, B., Legrand, C., Gorlia, T., Collins, G., Coens, C., Declerck, L. and Therasse, P., (2002). "Statistical methodology of phase III cancer clinical trials: advances and future perspectives". *European journal of cancer (Oxford, England : 1990),* **38 Suppl 4**, S162-8.

Swiercz, J.M., Worzfeld, T. and Offermanns, S., (2008). "ErbB-2 and met reciprocally regulate cellular signaling via plexin-B1". *The Journal of biological chemistry,* **283**(4), 1893-1901.

Tahir, S.A., Yang, G., Ebara, S., Timme, T.L., Satoh, T., Li, L., Goltsov, A., Ittmann, M., Morrisett, J.D. and Thompson, T.C., (2001). "Secreted caveolin-1 stimulates cell survival/clonal growth and contributes to metastasis in androgen-insensitive prostate cancer". *Cancer research,* **61**(10), 3882-3885.

Takeda, S., Igarashi, T., Mori, H. and Araki, S., (2006). "Crystal structures of VAP1 reveal ADAMs' MDC domain architecture and its unique C-shaped scaffold". *The EMBO journal,* **25**(11), 2388-2396.

Takenawa, T. and Suetsugu, S., (2007). "The WASP-WAVE protein network: connecting the membrane to the cytoskeleton". *Nature reviews.Molecular cell biology,* **8**(1), 37-48.

Tan, H.T., Low, J., Lim, S.G. and Chung, M.C., (2009). "Serum autoantibodies as biomarkers for early cancer detection". *The FEBS journal,* **276**(23), 6880-6904.

Teoh, G., Urashima, M., Greenfield, E.A., Nguyen, K.A., Lee, J.F., Chauhan, D., Ogata, A., Treon, S.P. and Anderson, K.C., (1998). "The 86-kD subunit of Ku autoantigen mediates homotypic and heterotypic adhesion of multiple myeloma cells". *The Journal of clinical investigation,* **101**(6), 1379-1388.

Testa, J.E., Brooks, P.C., Lin, J.M. and Quigley, J.P., (1999). "Eukaryotic expression cloning with an antimetastatic monoclonal antibody identifies a tetraspanin (PETA-3/CD151) as an effector of human tumour cell migration and metastasis". *Cancer research,* **59**(15), 3812-3820.

Theobald, J., Hanby, A., Patel, K. and Moss, S.E., (1995). "Annexin VI has tumour-suppressor activity in human A431 squamous epithelial carcinoma cells". *British journal of cancer,* **71**(4), 786-788.

Thermon Scientific: Pierce Protein Research Products
www.piercenet.com

Thornthwaite, J.T., McDuffee, E.C., Harris, R.B., Secor McVoy, J.R. and Lane, I.W., (2004). "The cancer recognition (CARE) antibody test". *Cancer letters,* **216**(2), 227-241.

Tiacci, E., Orvietani, P.L., Bigerna, B., Pucciarini, A., Corthals, G.L., Pettirossi, V., Martelli, M.P., Liso, A., Benedetti, R., Pacini, R., Bolli, N., Pileri, S., Pulford, K., Gambacorta, M., Carbone, A., Pasquarello, C., Scherl, A., Robertson, H., Sciurpi, M.T., Alunni-Bistocchi, G., Binaglia, L., Byrne, J.A. and Falini, B., (2005). "Tumor protein D52 (TPD52): a novel B-cell/plasma-cell molecule with unique expression pattern and Ca(2+)-dependent association with annexin VI". *Blood,* **105**(7), 2812-2820.

Tkachenko, E., Rhodes, J.M. and Simons, M., (2005). "Syndecans: new kids on the signaling block". *Circulation research,* **96**(5), 488-500.

Tonoli, H. and Barrett, J.C., (2005). "CD82 metastasis suppressor gene: a potential target for new therapeutics?". *Trends in molecular medicine,* **11**(12), 563-570.

Torimura, T., Ueno, T., Kin, M., Ogata, R., Inuzuka, S., Sugawara, H., Kurotatsu, R., Shimada, M., Yano, H., Kojiro, M., Tanikawa, K. and Sata, M., (1999). "Integrin alpha6beta1 plays a significant role in the attachment of hepatoma cells to laminin". *Journal of hepatology,* **31**(4), 734-740.

Tsujita, K., Kaikita, K., Hayasaki, T., Honda, T., Kobayashi, H., Sakashita, N., Suzuki, H., Kodama, T., Ogawa, H. and Takeya, M., (2007). "Targeted deletion of class A macrophage scavenger receptor increases the risk of cardiac rupture after experimental myocardial infarction". *Circulation,* **115**(14), 1904-1911.

Uegaki, K., Adachi, N., So, S., Iiizumi, S. and Koyama, H., (2006). "Heterozygous inactivation of human Ku70/Ku86 heterodimer does not affect cell growth, double-strand break repair, or genome integrity". *DNA repair,* **5**(3), 303-311.

University of Colorado at Colorado Springs
www.uccs.edu

Valentijn, A.J., Zouq, N. and Gilmore, A.P., (2004). "Anoikis". *Biochemical Society transactions,* **32**(Pt3), 421-425.

Van Ginkel, P.R., Gee, R.L., Walker, T.M., Hu, D., Heizmann, C.W. and Polans, A.S., (1998). "The identification and differential expression of calcium-binding proteins associated with ocular melanoma". *Biochimica et Biophysica Acta (BBA) - Molecular Cell Research,* **1448**(2), 290-298.

Verkman, A.S., Hara-Chikuma, M. and Papadopoulos, M.C., (2008). "Aquaporins--new players in cancer biology". *Journal of Molecular Medicine (Berlin, Germany),* **86**(5), 523-529.

Vernon, A.E. and LaBonne, C., (2004). "Tumour metastasis: a new twist on epithelial-mesenchymal transitions". *Current biology : CB,* **14**(17), R719-21.

Vidal, C.I., Mintz, P.J., Lu, K., Ellis, L.M., Manenti, L., Giavazzi, R., Gershenson, D.M., Broaddus, R., Liu, J., Arap, W. and Pasqualini, R., (2004). "An HSP90-mimic peptide revealed by fingerprinting the pool of antibodies from ovarian cancer patients". *Oncogene,* **23**(55), 8859-8867.

Vila de Muga, S., Timpson, P., Cubells, L., Evans, R., Hayes, T.E., Rentero, C., Hegemann, A., Reverter, M., Leschner, J., Pol, A., Tebar, F., Daly, R.J., Enrich, C. and Grewal, T., (2009). "Annexin A6 inhibits Ras signalling in breast cancer cells". *Oncogene,* **28**(3), 363-377.

Visiongain. (2010). "Monoclonal Antibodies in Cancer Therapy: World Market Prospects 2010-2025". PRLog (Press Release)

Vogel, S.N., Fitzgerald, K.A. and Fenton, M.J., (2003). "TLRs: differential adapter utilization by toll-like receptors mediates TLR-specific patterns of gene expression". *Molecular interventions,* **3**(8), 466-477.

Volpi, N., Schiller, J., Stern, R. and Soltes, L., (2009). "Role, metabolism, chemical modifications and applications of hyaluronan". *Current medicinal chemistry,* **16**(14), 1718-1745.

Vuoriluoto, K., Jokinen, J., Kallio, K., Salmivirta, M., Heino, J. and Ivaska, J., (2008). "Syndecan-1 supports integrin alpha2beta1-mediated adhesion to collagen". *Experimental cell research,* **314**(18), 3369-3381.

Walsh, N., Clynes, M., Crown, J. and O'Donovan, N., (2009). "Alterations in integrin expression modulates invasion of pancreatic cancer cells". *Journal of experimental & clinical cancer research : CR,* **28**, 140.

Walsh, N., O'Donovan, N., Kennedy, S., Henry, M., Meleady, P., Clynes, M. and Dowling, P., (2009). "Identification of pancreatic cancer invasion-related proteins by proteomic analysis". *Proteome science,* **7**, 3.

Wang, D., Hincapie, M., Guergova-Kuras, M., Kadas, J., Takacs, L. and Karger, B.L., (2010). "Antigen identification and characterization of lung cancer specific monoclonal antibodies produced by MAb proteomics". *Journal of proteome research,* **9**(4), 1834-1842.

Ward, E.S., Gussow, D., Griffiths, A.D., Jones, P.T. and Winter, G., (1989). "Binding activities of a repertoire of single immunoglobulin variable domains secreted from Escherichia coli". *Nature,* **341**(6242), 544-546.

Wang, J., Satoh, M., Pierani, A., Schmitt, J., Chou, C.H., Stunnenberg, H.G., Roeder, R.G. and Reeves, W.H., (1994). "Assembly and DNA binding of recombinant Ku (p70/p80) autoantigen defined by a novel monoclonal antibody specific for p70/p80 heterodimers". *Journal of cell science,* **107 (Pt 11)**(Pt 11), 3223-3233.

Weed, S.A. and Parsons, J.T., (2001). "Cortactin: coupling membrane dynamics to cortical actin assembly". *Oncogene,* **20**(44), 6418-6434.

Weil, D., Garcon, L., Harper, M., Dumenil, D., Dautry, F. and Kress, M., (2002). "Targeting the kinesin Eg5 to monitor siRNA transfection in mammalian cells". *BioTechniques,* **33**(6), 1244-1248.

Weiner, L.M., Surana, R. and Wang, S., (2010). "Monoclonal antibodies: versatile platforms for cancer immunotherapy". *Nature reviews.Immunology,* **10**(5), 317-327.

Werb, Z., Tremble, P.M., Behrendtsen, O., Crowley, E. and Damsky, C.H., (1989). "Signal transduction through the fibronectin receptor induces collagenase and stromelysin gene expression". *The Journal of cell biology,* **109**(2), 877-889.

Wesolowski, J., Alzogaray, V., Reyelt, J., Unger, M., Juarez, K., Urrutia, M., Cauerhff, A., Danquah, W., Rissiek, B., Scheuplein, F., Schwarz, N., Adriouch, S., Boyer, O., Seman, M., Licea, A., Serreze, D.V., Goldbaum, F.A., Haag, F. and Koch-Nolte, F., (2009). "Single domain antibodies: promising experimental and therapeutic tools in infection and immunity". *Medical microbiology and immunology,* **198**(3), 157-174.

Wildeboer, D., Naus, S., Amy Sang, Q.X., Bartsch, J.W. and Pagenstecher, A., (2006). "Metalloproteinase disintegrins ADAM8 and ADAM19 are highly regulated in

human primary brain tumors and their expression levels and activities are associated with invasiveness". *Journal of neuropathology and experimental neurology,* **65**(5), 516-527.

Wilex
http://www.wilex.de/R&D/uPA_Target.htm

Wilker, E. and Yaffe, M.B., (2004). "14-3-3 Proteins--a focus on cancer and human disease". *Journal of Molecular and Cellular Cardiology,* **37**(3), 633-642.

Willems, A., Schoonooghe, S., Eeckhout, D., De Jaeger, G., Grooten, J. and Mertens, N., (2005). "CD3 x CD28 cross-interacting bispecific antibodies improve tumor cell dependent T-cell activation". *Cancer immunology, immunotherapy : CII,* **54**(11), 1059-1071.

Winkler, U., Jensen, M., Manzke, O., Schulz, H., Diehl, V. and Engert, A., (1999). "Cytokine-release syndrome in patients with B-cell chronic lymphocytic leukemia and high lymphocyte counts after treatment with an anti-CD20 monoclonal antibody (rituximab, IDEC-C2B8)". *Blood,* **94**(7), 2217-2224.

Wulfing, P., Diallo, R., Kersting, C., Wulfing, C., Poremba, C., Rody, A., Greb, R.R., Bocker, W. and Kiesel, L., (2003). "Expression of endothelin-1, endothelin-A, and endothelin-B receptor in human breast cancer and correlation with long-term follow-up". *Clinical cancer research : an official journal of the American Association for Cancer Research,* **9**(11), 4125-4131.

Wulfing, P., Tio, J., Kersting, C., Sonntag, B., Buerger, H., Wulfing, C., Euler, U., Boecker, W., Tulusan, A.H. and Kiesel, L., (2004). "Expression of endothelin-A-receptor predicts unfavourable response to neoadjuvant chemotherapy in locally advanced breast cancer". *British journal of cancer,* **91**(3), 434-440.

Wong, J.H., Aguero, B., Gupta, R.K. and Morton, D.L., (1988). "Recovery of a cell surface fetal antigen from circulating immune complexes of melanoma patients". *Cancer immunology, immunotherapy : CII,* **27**(2), 142-146.

Wong, O.G., Nitkunan, T., Oinuma, I., Zhou, C., Blanc, V., Brown, R.S., Bott, S.R., Nariculam, J., Box, G., Munson, P., Constantinou, J., Feneley, M.R., Klocker, H., Eccles, S.A., Negishi, M., Freeman, A., Masters, J.R. and Williamson, M., (2007). "Plexin-B1 mutations in prostate cancer". *Proceedings of the National Academy of Sciences of the United States of America,* **104**(48), 19040-19045.

Woof, J.M. and Burton, D.R., (2004). "Human antibody-Fc receptor interactions illuminated by crystal structures". *Nature reviews.Immunology,* **4**(2), 89-99.

Wright, M.D., Moseley, G.W. and van Spriel, A.B., (2004). "Tetraspanin microdomains in immune cell signalling and malignant disease". *Tissue antigens,* **64**(5), 533-542.

Wu, C.W., Li, A.F., Chi, C.W., Lai, C.H., Huang, C.L., Lo, S.S., Lui, W.Y. and Lin, W.C., (2002). "Clinical significance of AXL kinase family in gastric cancer". *Anticancer Research,* **22**(2B), 1071-1078.

Wu, X., Suetsugu, S., Cooper, L.A., Takenawa, T. and Guan, J.L., (2004). "Focal adhesion kinase regulation of N-WASP subcellular localization and function". *The Journal of biological chemistry,* **279**(10), 9565-9576.

Yamaguchi, H. and Condeelis, J., (2007). "Regulation of the actin cytoskeleton in cancer cell migration and invasion". *Biochimica et biophysica acta,* **1773**(5), 642-652.

Yan, L., Hsu, K. and Beckman, R.A., (2008). "Antibody-based therapy for solid tumors". *Cancer journal (Sudbury, Mass.),* **14**(3), 178-183.

Yang, X.H., Richardson, A.L., Torres-Arzayus, M.I., Zhou, P., Sharma, C., Kazarov, A.R., Andzelm, M.M., Strominger, J.L., Brown, M. and Hemler, M.E., (2008). "CD151 accelerates breast cancer by regulating alpha 6 integrin function, signaling, and molecular organization". *Cancer research,* **68**(9), 3204-3213.

Yang, Y., MacLeod, V., Dai, Y., Khotskaya-Sample, Y., Shriver, Z., Venkataraman, G., Sasisekharan, R., Naggi, A., Torri, G., Casu, B., Vlodavsky, I., Suva, L.J., Epstein, J., Yaccoby, S., Shaughnessy, J.D.,Jr, Barlogie, B. and Sanderson, R.D., (2007). "The syndecan-1 heparan sulfate proteoglycan is a viable target for myeloma therapy". *Blood,* **110**(6), 2041-2048.

Ye, X., Li, Y., Stawicki, S., Couto, S., Eastham-Anderson, J., Kallop, D., Weimer, R., Wu, Y. and Pei, L., (2010). "An anti-Axl monoclonal antibody attenuates xenograft tumour growth and enhances the effect of multiple anticancer therapies". *Oncogene,* **29**(38), 5254-5264.

Yilmaz, M. and Christofori, G., (2009). "EMT, the cytoskeleton, and cancer cell invasion". *Cancer metastasis reviews,* **28**(1-2), 15-33.

Yilmaz, M., Christofori, G., Lehembre, F., (2007). "Distinct mechanisms of tumor invasion and metastasis". *Trends in Molecular Medicine*, **13**(12), 535-41.

Yu, E., Song, K., Moon, H., Maul, G.G. and Lee, I., (1998). "Characteristic immunolocalization of Ku protein as nuclear matrix". *Hybridoma,* **17**(5), 413-420.

Zafir-Lavie, I., Michaeli, Y. and Reiter, Y., (2007). "Novel antibodies as anticancer agents". *Oncogene,* **26**(25), 3714-3733.

Zambuzzi, W.F., Yano, C.L., Cavagis, A.D., Peppelenbosch, M.P., Granjeiro, J.M. and Ferreira, C.V., (2009). "Ascorbate-induced osteoblast differentiation recruits distinct MMP-inhibitors: RECK and TIMP-2". *Molecular and cellular biochemistry,* **322**(1-2), 143-150.

Zhang, Y.X., Knyazev, P.G., Cheburkin, Y.V., Sharma, K., Knyazev, Y.P., Orfi, L., Szabadkai, I., Daub, H., Keri, G. and Ullrich, A., (2008). "AXL is a potential target for therapeutic intervention in breast cancer progression". *Cancer research,* **68**(6), 1905-1915.

Zhang, Z., Zhu, L., Lin, D., Chen, F., Chen, D.J. and Chen, Y., (2001). "The three-dimensional structure of the C-terminal DNA-binding domain of human Ku70". *The Journal of biological chemistry,* **276**(41), 38231-38236.

Zhao, Q., Barclay, M., Hilkens, J., Guo, X., Barrow, H., Rhodes, J.M. and Yu, L.G., (2010). "Interaction between circulating galectin-3 and cancer-associated MUC1 enhances tumour cell homotypic aggregation and prevents anoikis". *Molecular cancer,* **9**, 154.

Zijlstra, A., Lewis, J., Degryse, B., Stuhlmann, H. and Quigley, J.P., (2008). "The inhibition of tumour cell intravasation and subsequent metastasis via regulation of in vivo tumour cell motility by the tetraspanin CD151". *Cancer cell,* **13**(3), 221-234.

Zoller, M., (2009). "Tetraspanins: push and pull in suppressing and promoting metastasis". *Nature reviews.Cancer,* **9**(1), 40-55.

APPENDICES

Appendix I

1. Ultrapure water

Ultrapure water (UHP) was used in the preparation of all media and solutions. This water was purified to a standard of 12-18 MΩ/cm resistance by a reverse osmosis system (Millipore Mill-RO 10 Plus, Elastat UHP).

2. Glassware

The solutions used in the various stages of cell culture were stored in sterile glass bottles. All sterile bottles and other glassware required for cell culture related applications were prepared as follows: glassware and lids were soaked in a 2% RBS- 25 (AGB Scientific) for 1 hour. After this time, they were cleansed and washed in an industrial dishwasher, using Neodisher detergent and rinsed twice with UHP. The resulting materials were sterilised by autoclaving.

3. Sterilisation procedures

All thermostable solutions, water and glassware were sterilised by autoclaving at 121°C for 20 minutes at 15 p.s.i. Thermolabile solutions were filtered through 0.22 μm sterile filters (Millipore, Millex-GV SLGV025BS). Larger volumes (up to 10 litres) of thermolabile solutions were filter sterilised through a micro-culture bell filter (Gelman, 12158).

4. Preparation of cell culture media

Basal media used during cell culture was prepared as followed: 10X media (DMEM (Sigma, D5648) was added to sterile UHP water, buffered with HEPES and $NaHCO_3$ as required and adjusted to a pH of 7.45-7.55 using sterile 1.5M HCl. The medium was then filtered through a sterile 0.22μm bell filters (Gelman, 12158) and stored in sterile 500ml bottles at 4°C. Basal media were stored at 4°C for up to three months. The HEPES buffer was prepared by dissolving 23.8g of

HEPES in 80ml UHP water and this solution was then sterilised by autoclaving. Then 5ml sterile 5M NaOH was added to give a final volume autoclaving. Complete media was then prepared as described in Materials & Methods, Table 2.2: supplements of 2mM l-glutamine (Gibco, 11140-0350) and 100mM sodium pyruvate (Gibco, 11360-035) were added as required. Complete media was stored for a maximum of one month.

Sources of other types of media:

- DMEM/Ham's F12 1:1 = represented by ATCC in this project and produced in house
- RPMI-1640 (made in house)
- McCoy5A (Lonza; 12-688F)
- Keratinocyte (Gibco, 17005) and supplements:
    - EGF (Epidermal Growth Factor supplement supplied as 25 µg stock (Gibco, 10450-013)
    - BPE (Bovine Pituitary Extract) supplement supplied as 25mg stock (Gibco, 13028-014)

Hybridoma and SP2/O-Ag14 myeloma cells were grown in a basic basal medium of commercially available DMEM, DMEM with Glutamax I (Glutamax is L-Amyl-L-Glutamine, high glucose concentration – 4.5mg (Gibco, 61965-026) supplemented with 10% heat inactivated FCS (Myoclone, Gibco, 10082-147). This was further supplemented for hybridoma growth and hybridoma cloning with 1% penicillin streptomycin and 5% briclone (Archport Ltd.). Briclone is a conditioned medium collected from a human cell line, for use in post fusion stages of hybridoma production and cloning, replacing the function of feeder cells. Sterility checks were performed on all bottles of media by inoculation of media samples on to Colombia blood agar (Oxoid, CM217), Sabauraud dextrose (Oxoid, CM217) and Thioglycolate broth (Oxoid, CM173). All sterility checks were then incubated at both 25°C and 37°C. These tests facilitated the detection of bacterial, yeast and fungal contamination.

5. Monitoring of sterility of cell culture solutions

Sterility testing was performed on all cell culture media and related culturing solutions. Samples of prepared basal media were incubated at 37°C for a period of seven days. This ensured that no bacterial or fungal contamination was present in the media.

6. Indirect staining procedure for Mycoplasma analysis.

Mycoplasma-negative NRK (Normal rat kidney fibroblast) cells were used as indicator cells for this analysis. The cells were incubated with a sample volume of supernatant from the cell lines in question and the examined for *mycoplasma* contamination. A fluorescent Hoechst stain was used in the analysis. The stain binds specifically to DNA and so stains the nucleus of the cells in addition to any *mycoplasma* present. *Mycoplasma* infection was indicated by fluorescent bodies in the cytoplasm of the NRK cells.

Table 1: - NP/40 Lysis Buffer for immunopecipitation studies (Total Volume, 500mls; pH 8.5):

Components	Final Conc.
425ml UHP	-
0.5% NP/40	2.5ml NP-40
150mM NaCl	15ml 5M NaCl
50mM Tris-HCl	25ml 1M Tris-HCL

Table 2: - Lysis Buffer C for immunoprecipitation studies (Total Volume, 40mls; pH 8.5):

Components	Quantity
7M Urea	16.8ml
2M Thiourea	6g
4% CHAPS	1.6g
30mM Tris	0.1g

Table 3: - Buffers used for Silver Staining Procedure

Buffer	Component	Volume
Fixer (100ml)	MeOH	50ml
	24ml Glacial Acetic Acid	12ml
	Formalin	50µl
	UHP	38ml
Wash (100ml)	EtOH	36ml
	UHP	64ml
Sensitising (100ml)	$Na_2S_2O_3$	0.02g
	UHP	100ml
Silver Nitrate (100ml)	$AgNO_3$	0.2g
	Formalin	76µl
	UHP	100ml
Developer (200ml)	Na_2CO_3	12g
	Formalin	100µl
	Sensitising Buffer	4ml
	UHP	196ml
Stop Solution	MeOH	50ml
	Glacial Acetic Acid	12ml
	UHP	38ml

Table 4.: - Antibodies used during the course of this work

Primary Antibody	Dilution	
β-actin (Monoclonal)	1:10,000	A5441, Sigma
α-Tubulin (Monoclonal)	1/1000	T6199, Sigma
Annexin A6 (Polyclonal)	1/5000	ab52221, Abcam
Ku70 (Polyclonal)	1/5000	ab10878, Abcam
Ku80 (Monoclonal)	1/12,000	ab80592, Abcam
Prohibitin (Monoclonal)	1/400 - 1/800	CP34, Calbiochem
Protein 14-3-3 ε (Polyclonal)		NBP1-32695, Novis Biologicals
Secondary Antibody	**Dilution**	
Swine Anti-Rabbit HRP	1/2000	P0399, Dako
Goat Anti-Mouse HRP	1/2000	P0447, Dako
Goat Anti-Rabbit HRP	1/2000	P0448, Dako
Swine Anti-Rabbit FITC	1/40	F0054, Dako
Rabbit Anti-Mouse FITC	1/40	F0261, Dako

Table 5: - List of siRNAs used during the course of this work

Target Name	Ambion Product I.D.
Scrambled	4390843
Kinesin	AM4639
Annexin A6 #1	s1397
Annexin A6 #2	s1396
Annexin A6 #3	s1395
ATP dependent DNA Helicase 2 subunit 2 #1	s5455
ATP dependent DNA Helicase 2 subunit 2 #2	s52594
ATP dependent DNA Helicase 2 subunit 1 #1	s14952
ATP dependent DNA Helicase 2 subunit 1 #2	s14953
ATP dependent DNA Helicase 2 subunit 1 #3	s14954

Appendix II

Protein Identification Results obtained with MAb 7B7 G5 (2)

						P (pro)	Score	Peptide (Hits)	MW
Scan(s)	Peptide	MH+	DeltaM	z	Type	P (pep)	XC	Ions	Sp
KU70_HUMAN RecName: Full=ATP-dependent DNA helicase 2 subunit 1; AltName: Full=ATP-dependent DNA helicase II 70 kDa subunit; AltName: Full=Lupus Ku autoantigen protein p70; Short=Ku70; AltName: Full=70 kDa subunit of Ku antigen; AltName: Full=Thyroid-lupu						**1.23526E-09**	**50.23**	**5 (50000)**	**69799.2**
976	R.QIILEKEETEELKR.F	1757.964355	0.002733136	2	CID	4.75974E-07	3.80	20/26	438.5
1017	R.IM*LFTNEDNPHGNDSAK.A	1918.859967	0.001774869	2	CID	1.23526E-09	4.77	23/32	886.2
1244	R.TFNTSTGGLLLPSDTKR.S	1807.954834	0.001512432	2	CID	4.40144E-08	3.71	18/32	620.9
1540	K.KPGGFDISLFYR.D	1399.736816	4.75888E-05	2	CID	1.98974E-06	3.38	17/22	767.7
1650	R.DSLIFLVDASK.A	1207.65686	-0.000318622	2	CID	3.27486E-05	3.02	17/20	1130.4

						P (pro)	Score	Peptide (Hits)	MW
Scan(s)	Peptide	MH+	DeltaM	z	Type	P (pep)	XC	Ions	Sp
KU70_HUMAN RecName: Full=ATP-dependent DNA helicase 2 subunit 1; AltName: Full=ATP-dependent DNA helicase II 70 kDa subunit; AltName: Full=Lupus Ku autoantigen protein p70; Short=Ku70; AltName: Full=70 kDa subunit of Ku antigen; AltName: Full=Thyroid-lupu						**2.33E-14**	**200.26**	**20 (20 0 0 0 0)**	**69799.2**
893	K.VEYSEEELKTHISK.G	1691.84863	0.00139	2	CID	3.00E-05	3.43	18/26	874.0
1005	K.TEGDEEAEEEQEENLEASGDYK.Y	2500.99585	0.00273	2	CID	5.27E-12	4.10	23/42	473.2
1011	R.QIILEKEETEELKR.F	1757.96436	-0.00192	3	CID	7.71E-09	3.11	23/52	704.4
1038	R.IM*LFTNEDNPHGNDSAK.A	1918.85997	-0.00018	2	CID	1.37E-11	4.87	24/32	1119.8
1249	R.TFNTSTGGLLLPSDTKR.S	1807.95483	-0.00020	2	CID	3.37E-09	4.14	18/32	651.6
1282	R.SDSFENPVLQQHFR.N	1703.81360	0.00017	2	CID	1.23E-06	3.78	17/26	940.8
1385	R.TFNTSTGGLLLPSDTK.R	1651.85376	-0.00081	2	CID	2.16E-07	4.06	24/30	1533.6
1551	K.NIYVLQELDNPGAK.R	1573.82202	-0.00068	2	CID	1.22E-07	4.24	20/26	2294.1
1576	R.DIISIAEDEDLR.V	1388.69031	-0.00142	2	CID	3.14E-07	3.36	19/22	1381.8
1627	K.KPGGFDISLFYR.D	1399.73682	-0.00032	2	CID	3.01E-07	3.46	20/22	1649.4
1651	R.DTGIFLDLM*HLK.K	1418.73481	-0.00039	2	CID	4.04E-06	3.25	18/22	1133.2
1783	K.IISSDRDLLAVVFYGTEKDK.N	2269.20752	-0.00033	3	CID	5.96E-09	5.26	33/76	1804.4
1836	R.NIPPYFVALVPQEEELDDQK.I	2344.17065	0.00151	2	CID	8.98E-07	2.77	20/38	339.4
1844	R.DLLAVVFYGTEKDK.N	1597.84717	-0.00007	2	CID	1.02E-09	3.62	18/26	926.8
1858	R.FDDPGLM*LM*GFKPLVLLK.K	2066.10647	0.00124	2	CID	1.53E-06	2.95	17/34	301.1
1880	K.IISSDRDLLAVVFYGTEK.D	2026.08557	0.00078	2	CID	1.03E-09	4.43	24/34	2031.6
1990	R.DLLAVVFYGTEK.D	1354.72534	-0.00056	2	CID	1.85E-07	3.09	18/22	1392.7
1998	K.IQVTPPGFQLVFLPFADDKR.K	2288.24365	0.00273	2	CID	2.33E-14	4.55	23/38	919.0
2003	R.NLEALALDLM*EPEQAVDLTLPK.V	2439.26872	0.00428	2	CID	2.01E-12	4.92	27/42	1185.2
2133	K.IQVTPPGFQLVFLPFADDK.R	2132.14258	0.00249	2	CID	1.27E-13	4.71	28/36	1997.8

						P (pro)	Score	Peptide (Hits)	MW
Scan(s)	Peptide	MH+	DeltaM	z	Type	P (pep)	XC	Ions	Sp
KU70_HUMAN RecName: Full=ATP-dependent DNA helicase 2 subunit 1; AltName: Full=ATP-dependent DNA helicase II 70 kDa subunit; AltName: Full=Lupus Ku autoantigen protein p70; Short=Ku70; AltName: Full=70 kDa subunit of Ku antigen; AltName: Full=Thyroid-lupu						**3.33E-10**	**130.21**	**13 (13 0 0 0 0)**	**69799.2**
275	K.IM*ATPEQVGK.M	1089.56087	-0.00016	2	CID	1.70E-04	2.64	14/18	698.9
452	K.VEYSEEELKTHISK.G	1691.84863	0.00127	2	CID	6.30E-07	3.90	19/26	1433.5
518	R.QIILEKEETEELKR.F	1757.96436	0.00151	2	CID	6.87E-08	3.69	16/26	394.4
607	R.IM*LFTNEDNPHGNDSAK.A	1918.85997	-0.00019	3	CID	4.87E-05	3.83	27/64	607.5
700	R.ILELDQFKGQQGQK.R	1631.87512	0.00249	2	CID	2.84E-06	3.54	19/26	1141.8
738	K.KQELLEALTK.H	1172.68848	-0.00020	2	CID	3.82E-03	2.58	14/18	931.2
772	R.TFNTSTGGLLLPSDTKR.S	1807.95483	0.00188	2	CID	2.71E-08	4.20	19/32	752.4
783	R.SDSFENPVLQQHFR.N	1703.81360	0.00078	2	CID	3.33E-10	3.96	17/26	875.1
961	R.ILELDQFK.G	1005.56152	-0.00056	2	CID	4.55E-04	2.47	12/14	502.7
1039	K.NIYVLQELDNPGAK.R	1573.82202	0.00139	2	CID	1.33E-03	2.74	17/26	712.0
1085	K.KPGGFDISLFYR.D	1399.73682	0.00066	2	CID	5.20E-06	3.01	17/22	744.6
1120	R.DTGIFLDLM*HLK.K	1418.73481	0.00144	2	CID	8.57E-05	2.84	15/22	713.0
1213	R.DSLIFLVDASK.A	1207.65686	0.00029	2	CID	8.85E-08	3.13	16/20	812.6
527	R.YGSDIVPFSK.V	1112.56226	0.00005	2	CID	1.30E-05	2.27	15/18	781.7
543	-.LTIGSNLSIR.-	1073.63135	-0.00020	2	CID	6.99E-05	2.18	13/18	357.0
553	R.HIEIFTDLSSR.F	1317.67969	0.00078	2	CID	9.96E-05	3.56	17/20	980.2
561	K.KDEKTDTLEDLFPTTK.I	1880.94873	0.00162	3	CID	2.07E-05	4.73	29/60	1671.5
703	K.CFSVLGFCK.S	1117.51697	-0.00081	2	CID	2.10E-04	2.13	12/16	565.9

						P (pro)	Score	Peptide (Hits)	MW
Scan(s)	Peptide	MH+	DeltaM	z	Type	P (pep)	XC	Ions	Sp
KU86_HUMAN RecName: Full=ATP-dependent DNA helicase 2 subunit 2; AltName: Full=ATP-dependent DNA helicase II 80 kDa subunit; AltName: Full=Lupus Ku autoantigen protein p86; AltName: Full=86 kDa subunit of Ku antigen; AltName: Full=Ku86; AltName: Full=Ku80						**2.08E-07**	**30.21**	**3 (3 0 0 0 0)**	**82652.4**
1257	R.YGSDIVPFSK.V	1112.56226	0.00017	2	CID	9.87E-07	3.03	15/18	995.1
1390	R.HIEIFTDLSSR.F	1317.67969	0.00066	2	CID	2.08E-07	3.16	17/20	1220.9
1605	K.SQLDIIIHSLK.K	1266.74158	0.00066	2	CID	5.48E-06	3.11	16/20	1158.0

						P (pro)	Score	Peptide (Hits)	MW
Scan(s)	Peptide	MH+	DeltaM	z	Type	P (pep)	XC	Ions	Sp
KU86_HUMAN RecName: Full=ATP-dependent DNA helicase 2 subunit 2; AltName: Full=ATP-dependent DNA helicase II 80 kDa subunit; AltName: Full=Lupus Ku autoantigen protein p86; AltName: Full=86 kDa subunit of Ku antigen; AltName: Full=Ku86; AltName: Full=Ku80						**4.31E-12**	**90.25**	**9 (9 0 0 0 0)**	**125731**
445	K.EEASGSSVTAEEAKK.F	1522.72314	0.00102	2	CID	2.75E-08	3.84	19/28	1
504	K.EEASGSSVTAEEAK.K	1394.62817	0.00041	2	CID	3.10E-08	3.53	23/26	1
992	K.KKDQVTAQEIFQDNHEDGPTAK.K	2499.21094	0.00107	3	CID	4.31E-12	4.39	35/84	1
1155	K.DQVTAQEIFQDNHEDGPTAK.K	2243.02100	0.00151	2	CID	5.76E-09	4.93	22/38	1
1394	R.HIEIFTDLSSR.F	1317.67969	-0.00142	2	CID	3.13E-08	3.27	18/20	1
1596	K.SQLDIIIHSLK.K	1266.74158	-0.00105	2	CID	1.14E-05	3.43	17/20	1
1604	K.TDTLEDLFPTTK.I	1380.68933	-0.00044	2	CID	8.20E-07	3.37	18/22	1
1694	K.KYAPTEAQLNAVDALIDSM*SLAK.K	2465.25922	-0.00265	3	CID	3.78E-07	4.04	30/88	1
1816	K.YAPTEAQLNAVDALIDSM*SLAK.K	2337.16425	0.00132	2	CID	3.30E-11	4.54	25/42	1

						P (pro)	Score	MW	Peptide (Hits)
Scan(s)	Peptide	MH+	DeltaM	z	Type	P (pep)	XC	Sp	Ions
KU86_HUMAN ATP-dependent DNA helicase 2 subunit 2 (ATP-dependent DNA helicase II 80 kDa subunit) (Lupus Ku autoantigen protein p86) (86 kDa subunit of Ku antigen) (Ku86) (Ku80) (Thyroid-lupus autoantigen) (TLAA) (CTC box-binding factor 85 kDa subunit) (CT						**1.11E-15**	**180.26**	**82652.4**	**18 (18 0 0 0 0)**
215	-.AFREEAIK.-	963.52582	-0.00014	2	CID	7.19E-03	2.60	617.6	12/14
249	K.ALQEKVEIK.Q	1057.62524	-0.00068	2	CID	3.42E-03	2.89	780.5	13/16
250	-.SQIPLSK.-	772.45636	0.00079	1	CID	9.09E-03	1.87	342.2	9/12
263	R.HSIHWPCR.L	1092.51563	0.00005	2	CID	8.50E-06	2.55	606.5	13/14
313	K.KVITM@FVQR.Q	1137.64488	0.00129	2	CID	9.30E-05	2.72	786.2	14/16
318	K.KKDQVTAQEIFQDNHEDGPTAK.K	2499.21094	0.00455	3	CID	1.11E-15	5.20	1824.1	37/84
324	-.KKDQVTAQEIFQDNHEDGPTAK.-	2499.21094	0.00112	4	CID	3.20E-05	4.10	750.2	41/126
379	K.GITEQQKEGLEIVK.M	1571.86389	0.00188	2	CID	9.71E-07	3.96	1311.0	18/26
396	R.LGGHGPSFPLK.G	1109.61023	-0.00020	2	CID	4.08E-05	2.85	693.7	15/20
403	-.VITM@FVQR.-	1009.54991	-0.00061	2	CID	7.65E-04	2.23	468.1	12/14
440	-.TWTVVDAK.-	919.48834	0.00092	1	CID	9.36E-03	1.91	337.6	10/14
477	R.ANPQVGVAFPHIK.H	1377.76379	-0.00056	2	CID	8.46E-07	3.33	583.3	15/24
523	R.LFQCLLHR.A	1086.58777	0.00005	2	CID	4.62E-03	2.45	911.8	12/14
527	R.YGSDIVPFSK.V	1112.56226	0.00005	2	CID	1.30E-05	2.27	781.7	15/18
543	-.LTIGSNLSIR.-	1073.63135	-0.00020	2	CID	6.99E-05	2.18	357.0	13/18
553	R.HIEIFTDLSSR.F	1317.67969	0.00078	2	CID	9.96E-05	3.56	980.2	17/20
561	K.KDEKTDTLEDLFPTTK.I	1880.94873	0.00162	3	CID	2.07E-05	4.73	1671.5	29/60
703	K.CFSVLGFCK.S	1117.51697	-0.00081	2	CID	2.10E-04	2.13	565.9	12/16

Appendix III

Protein Identification Results obtained with MAb 9E1 24 (6)

						P (pro)	Score	MW	Peptide (Hits)
Scan(s)	Peptide	MH+	DeltaM	z	Type	P (pep)	XC	Sp	Ions
ANXA6_HUMAN Annexin A6 (Annexin-6) (Annexin VI) (Lipocortin VI) (P68) (P70) (Protein III) (Chromobindin-20) (67 kDa calelectrin) (Calphobindin-II) (CPB-II) [MA						**3.41E-12**	**70.26**	**75825.7**	**7 (7 0 0 0 0)**
807	R.TNEQMHQLVAAYK.D	1532.75256	0.26384	2	CID	1.52E-08	4.11	1520.8	20/24
1283	K.SLEDALSSDTSGHFR.R	1621.74524	1.40398	2	CID	4.16E-10	3.87	1413.0	21/28
1623	-.SEIDLLNIR.-	1072.59973	-0.16138	1	CID	5.73E-04	1.83	230.5	9/16
1627	R.DAFVAIVQSVK.N	1176.66235	1.24712	2	CID	3.50E-05	4.15	1849.3	17/20
1667	R.DLEADIIGDTSGHFQK.M	1745.83411	0.36785	2	CID	3.41E-12	4.41	1629.3	23/30
1874 - 1875	R.EDAQVAAEILEIADTPSGDK.T	2072.00293	0.49822	2	CID	1.28E-11	5.16	1648.1	23/38
2055	K.WGTDEAQFIYILGNR.S	1782.88098	1.11882	2	CID	9.23E-10	4.66	2842.8	24/28

						P (pro)	Score	MW	Peptide (Hits)
Scan(s)	Peptide	MH+	DeltaM	z	Type	P (pep)	XC	Sp	Ions
ANXA6_HUMAN RecName: Full=Annexin A6; AltName: Full=Annexin-6; AltName: Full=Annexin VI; AltName: Full=Lipocortin VI; AltName: Full=p68; AltName: Full=p70; AltName: Full=Protein III; AltName: Full=Chromobindin-20; AltName: Full=67 kDa calelectrin; AltName						**4.79E-06**	**40.17**	**75825.7**	**4 (4 0 0 0 0)**
319	K.GAGTDEKTLTR.I	1148.59058	0.00066	2	CID	4.97E-05	3.40	755.1	16/20
408	R.AINEAYKEDYHK.S	1480.70667	0.00176	2	CID	4.22E-05	3.01	499.6	14/22
523	K.GTVRPANDFNPDADAK.A	1687.80347	0.00237	2	CID	6.12E-03	3.46	1099.6	19/30
1289	K.ALLALCGGED.-	1018.48743	0.00079	1	CID	4.79E-06	2.06	386.0	10/18

						P (pro)	Score	MW	Peptide (Hits)
Scan(s)	Peptide	MH+	DeltaM	z	Type	P (pep)	XC	Sp	Ions
ANXA6_HUMAN RecName: Full=Annexin A6; AltName: Full=Annexin-6; AltName: Full=Annexin VI; AltName: Full=Lipocortin VI; AltName: Full=p68; AltName: Full=p70; AltName: Full=Protein III; AltName: Full=Chromobindin-20; AltName: Full=67 kDa calelectrin; AltName						**1.10E-09**	**200.22**	**75825.7**	**20 (20 0 0 0 0)**
344	R.QRQEVCQSYK.S	1325.62671	0.00005	2	CID	6.62E-06	3.07	353.0	15/18
358	K.GAGTDEKTLTR.I	1148.59058	0.00005	2	CID	6.28E-03	2.86	520.4	15/20
495	R.AINEAYKEDYHK.S	1480.70667	0.00115	2	CID	1.04E-04	3.04	861.0	16/22
544	K.M*TNYDVEHTIKK.E	1494.72571	0.00115	2	CID	1.76E-04	3.46	919.1	18/22
579	K.TTGKPIEASIR.G	1172.66333	-0.00044	2	CID	6.05E-04	2.37	377.2	15/20
629	K.MTNYDVEHTIKK.E	1478.73083	0.00090	2	CID	7.91E-04	3.39	1264.9	18/22
669	K.M*TNYDVEHTIK.K	1366.63074	0.00090	2	CID	1.87E-05	3.32	561.2	15/20
672	R.TNEQM*HQLVAAYK.D	1548.74750	0.00071	2	CID	9.82E-05	3.39	741.0	18/24
676	K.GTVRPANDFNPDADAK.A	1687.80347	0.00115	2	CID	4.25E-07	3.95	1199.9	20/30
889	K.EIKDAISGIGTDEK.C	1475.75879	0.00090	2	CID	2.14E-06	2.64	378.2	16/26
1141	R.LIVGLM*RPPAYCDAK.E	1719.89210	0.00175	2	CID	3.91E-04	2.66	163.8	13/28
1196	K.SLHQAIEGDTSGDFLK.A	1717.83911	0.00078	2	CID	5.52E-07	4.44	1614.1	21/30
1213	K.SLEDALSSDTSGHFR.R	1621.74524	0.00090	2	CID	1.10E-09	3.72	1378.0	21/28
1282	R.SELDM*LDIR.E	1107.53505	-0.00034	2	CID	4.81E-03	3.23	1173.3	14/16
1409	K.DLIADLK.Y	787.45599	0.00031	1	CID	2.30E-03	2.42	584.9	10/12
1559	K.ALLALCGGED.-	1018.48743	0.00079	1	CID	5.33E-07	3.09	550.0	12/18
1605	-.LVFDEYLK.-	1026.55066	0.00110	1	CID	2.44E-03	2.10	803.8	10/14
1629	-.SEIDLLNIR.-	1072.59973	-0.00068	2	CID	9.03E-03	2.58	514.2	13/16
1670	R.DAFVAIVQSVK.N	1176.66235	0.00017	2	CID	9.89E-06	3.48	1540.5	16/20
1698	K.ALIEILATR.T	999.61969	-0.00081	2	CID	1.96E-03	2.75	850.5	14/16

						P (pro)	Score	Peptide (Hits)	MW
Scan(s)	Peptide	MH+	DeltaM	z	Type	P (pep)	XC	Ions	Sp
1433E_HUMAN RecName: Full=14-3-3 protein epsilon; Short=14-3-3E						**3.80E-07**	**20.17**	**2 (2 0 0 0 0)**	**29155.4**
1198	R.YLAEFATGNDRK.E	1384.68555	-0.00020	2	CID	3.80E-07	3.13	17/22	1095.8
1300	K.VAGM*DVELTVEER.N	1463.70464	0.00073	2	CID	1.67E-05	3.39	19/24	1194.0

						P (pro)	Score	Peptide (Hits)	MW
Scan(s)	Peptide	MH+	DeltaM	z	Type	P (pep)	XC	Ions	Sp
1433B_PONAB 14-3-3 protein beta/alpha						1.14E-08	28.21	3 (2 1 0 0 0)	28064.8
450	K.AVTEQGHELSNEER.N	1598.74048	-0.00020	2	CID	1.14E-08	4.24	19/26	1464.2
517	-.VISSIEQK.-	903.51459	-0.00024	1	CID	2.48E-04	1.74	10/14	423.0
621	R.YLSEVASGDNK.Q	1182.56372	-0.00166	2	CID	3.19E-04	2.93	16/20	770.8

						P (pro)	Score	Peptide (Hits)	MW
Scan(s)	Peptide	MH+	DeltaM	z	Type	P (pep)	XC	Ions	Sp
gi|52000883|sp|P63102.1|1433Z_RAT RecName: Full=14-3-3 protein zeta/delta; AltName: Full=Protein kinase C inhibitor protein 1; Short=KCIP-1; AltName: Full=Mitochondrial import stimulation factor S1 subunit						**3.68E-06**	**20.17**	**2 (2 0 0 0 0)**	**27753.7**
984	R.YLAEVAAGDDKK.G	1279.65283	-0.00068	2	CID	8.11E-06	3.33	18/22	1408.6
1006	K.SVTEQGAELSNEER.N	1548.71362	0.00041	2	CID	3.68E-06	3.22	18/26	1104.1

						P (pro)	Score	Peptide (Hits)	MW
Scan(s)	Peptide	MH+	DeltaM	z	Type	P (pep)	XC	Ions	Sp
1433E_HUMAN RecName: Full=14-3-3 protein epsilon; Short=14-3-3E						**1.27E-09**	**30.21**	**3 (3 0 0 0 0)**	**29155.4**
774	R.IISSIEQKEENK.G	1417.75330	0.00054	2	CID	5.05E-05	3.44	18/22	1146.8
1138	K.VAGM*DVELTVEER.N	1463.70464	-0.00085	2	CID	1.27E-09	4.11	18/24	1397.6
1219	R.YLAEFATGNDR.K	1256.59058	-0.00081	2	CID	1.38E-05	2.75	15/20	896.4

						P (pro)	Score	Peptide (Hits)	MW
Scan(s)	Peptide	MH+	DeltaM	z	Type	P (pep)	XC	Ions	Sp
1433E_HUMAN 14-3-3 protein epsilon (14-3-3E)						**1.15E-06**	**10.19**	**1 (1 0 0 0 0)**	**29155.4**
1390	K.VAGM*DVELTVEER.N	1463.70464	0.00147	2	CID	1.15E-06	3.87	20/24	1797.9

						P (pro)	Score	Peptide (Hits)	MW
Scan(s)	Peptide	MH+	DeltaM	z	Type	P (pep)	XC	Ions	Sp
ADT1_HUMAN ADP/ATP translocase 1 (Adenine nucleotide translocator 1) (ANT 1) (ADP,ATP carrier protein 1) (Solute carrier family 25 member 4) (ADP,ATP carrier protein, heart/skeletal muscle isoform T1)						**4.21E-07**	**20.14**	**2 (2 0 0 0 0)**	**33043.2**
1246	K.LLLQVQHASK.Q	1136.67859	-0.00032	2	CID	9.33E-04	2.80	15/18	1134.7
1597	R.AAYFGVYDTAK.G	1205.58374	-0.00154	2	CID	4.21E-07	2.63	16/20	1040.1
ADT2_HUMAN RecName: Full=ADP/ATP translocase 2; AltName: Full=Adenine nucleotide translocator 2; Short=ANT 2; AltName: Full=ADP,ATP carrier protein 2; AltName: Full=Solute carrier family 25 member 5; AltName: Full=ADP,ATP carrier protein, fibroblast isofo						**8.53E-07**	**30.21**	**3 (3 0 0 0 0)**	**32874.2**
1246	K.LLLQVQHASK.Q	1136.67859	-0.00032	2	CID	9.33E-04	2.80	15/18	1134.7
1691	R.AAYFGIYDTAK.G	1219.59937	-0.00056	2	CID	1.55E-04	2.66	16/20	1124.9
1897	K.DFLAGGVAAAISK.T	1219.66809	-0.00032	2	CID	8.53E-07	4.14	21/24	2681.7
ADT3_HUMAN RecName: Full=ADP/ATP translocase 3; AltName: Full=Adenine nucleotide translocator 2; AltName: Full=ANT 3; AltName: Full=ADP,ATP carrier protein 3; AltName: Full=Solute carrier family 25 member 6; AltName: Full=ADP,ATP carrier protein, isoform						**4.21E-07**	**20.14**	**2 (2 0 0 0 0)**	**32845.2**
1246	K.LLLQVQHASK.Q	1136.67859	-0.00032	2	CID	9.33E-04	2.80	15/18	1134.7
1597	R.AAYFGVYDTAK.G	1205.58374	-0.00154	2	CID	4.21E-07	2.63	16/20	1040.1

						P (pro)	Score	Peptide (Hits)	MW
Scan(s)	Peptide	MH+	DeltaM	z	Type	P (pep)	XC	Ions	Sp
ADT1_HUMAN ADP/ATP translocase 1 (Adenine nucleotide translocator 1) (ANT 1) (ADP,ATP carrier protein 1) (Solute carrier family 25 member 4) (ADP,ATP carrier protein, heart/skeletal muscle isoform T1)						**6.20E-09**	**20.16**	**2 (2 0 0 0 0)**	**33043.2**
868	K.LLLQVQHASK.Q	1136.67859	-0.00068	2	CID	1.79E-04	2.66	13/18	695.0
1769	R.YFPTQALNFAFK.D	1446.74158	0.00005	2	CID	6.20E-09	3.29	19/22	842.7
ADT2_HUMAN RecName: Full=ADP/ATP translocase 2; AltName: Full=Adenine nucleotide translocator 2; Short=ANT 2; AltName: Full=ADP,ATP carrier protein 2; AltName: Full=Solute carrier family 25 member 5; AltName: Full=ADP,ATP carrier protein, fibroblast isofo						**6.20E-09**	**20.16**	**2 (2 0 0 0 0)**	**32874.2**
868	K.LLLQVQHASK.Q	1136.67859	-0.00068	2	CID	1.79E-04	2.66	13/18	695.0
1769	R.YFPTQALNFAFK.D	1446.74158	0.00005	2	CID	6.20E-09	3.29	19/22	842.7
ADT3_HUMAN RecName: Full=ADP/ATP translocase 3; AltName: Full=Adenine nucleotide translocator 2; AltName: Full=ANT 3; AltName: Full=ADP,ATP carrier protein 3; AltName: Full=Solute carrier family 25 member 6; AltName: Full=ADP,ATP carrier protein, isoform						**6.20E-09**	**20.16**	**2 (2 0 0 0 0)**	**32845.2**
868	K.LLLQVQHASK.Q	1136.67859	-0.00068	2	CID	1.79E-04	2.66	13/18	695.0
1769	R.YFPTQALNFAFK.D	1446.74158	0.00005	2	CID	6.20E-09	3.29	19/22	842.7

						P (pro)	Score	Peptide (Hits)	MW
Scan(s)	Peptide	MH+	DeltaM	z	Type	P (pep)	XC	Ions	Sp
gi|113459|sp|P05141.6|ADT2_HUMAN RecName: Full=ADP/ATP translocase 2; AltName: Full=Adenine nucleotide translocator 2						**8.53E-07**	**30.21**	**3 (3 0 0 0 0)**	**32874.2**
1246	K.LLLQVQHASK.Q	1136.67859	-0.00032	2	CID	9.33E-04	2.80	15/18	1134.7
1691	R.AAYFGIYDTAK.G	1219.59937	-0.00056	2	CID	1.55E-04	2.66	16/20	1124.9
1897	K.DFLAGGVAAAISK.T	1219.66809	-0.00032	2	CID	8.53E-07	4.14	21/24	2681.7

						P (pro)	Score	Peptide (Hits)	MW
Scan(s)	Peptide	MH+	DeltaM	z	Type	P (pep)	XC	Ions	Sp
ADT1_HUMAN RecName: Full=ADP/ATP translocase 1; AltName: Full=Adenine nucleotide translocator 1; Short=ANT 1; AltName: Full=ADP,ATP carrier protein 1; AltName: Full=Solute carrier family 25 member 4; AltName: Full=ADP,ATP carrier protein, heart/skeletal m						**4.74E-09**	**28.19**	**3 (2 1 0 0 0)**	**33043.2**
1467	R.AAYFGVYDTAK.G	1205.58374	-0.00178	2	CID	2.64E-06	2.58	16/20	1155.2
2017	R.YFPTQALNFAFK.D	1446.74158	-0.00056	2	CID	4.74E-09	2.93	18/22	740.2
2111	-.GM*GGAFVLVLYDEIKK.-	1755.93497	0.00001	2	CID	3.64E-07	3.74	18/30	855.5
ADT3_HUMAN RecName: Full=ADP/ATP translocase 3; AltName: Full=Adenine nucleotide translocator 2; AltName: Full=ANT 3; AltName: Full=ADP,ATP carrier protein 3; AltName: Full=Solute carrier family 25 member 6; AltName: Full=ADP,ATP carrier protein, isoform						**3.64E-07**	**20.19**	**2 (2 0 0 0 0)**	**32845.2**
1932	K.DFLAGGIAAAISK.T	1233.68372	-0.00056	2	CID	1.41E-05	3.45	20/24	2304.9
2111	R.GM*GGAFVLVLYDELKK.V	1755.93497	0.00001	2	CID	3.64E-07	3.74	18/30	855.5

						P (pro)	Score	Peptide (Hits)	MW
Scan(s)	Peptide	MH+	DeltaM	z	Type	P (pep)	XC	Ions	Sp
gi|464371|sp|P35232|PHB_HUMAN Prohibitin						**5.12E-10**	**70.25**	**7 (7 0 0 0 0)**	**29785.9**
1053	R.NVPVITGSK.D	914.53058	0.00067	1	CID	5.35E-04	1.82	11/16	401.6
1601	R.IFTSIGEDYDER.V	1444.65906	-0.00020	2	CID	2.72E-08	3.11	19/22	1095.5
1609	K.DLQNVNITLR.I	1185.65857	-0.00081	2	CID	6.93E-05	3.31	16/18	1429.0
1662	R.FDAGELITQR.E	1149.58984	-0.00239	2	CID	1.44E-06	3.36	17/18	1993.8
1704	R.ILFRPVASQLPR.I	1396.84229	-0.00100	3	CID	5.41E-04	3.11	21/44	382.3
1785	R.KLEAAEDIAYQLSR.S	1606.84351	-0.00166	2	CID	5.12E-10	5.10	23/26	3017.1
2349	K.FGLALAVAGGVVNSALYN VDAGHR.A	2371.25171	0.00107	3	CID	9.54E-08	4.84	34/92	982.0

						P (pro)	Score	Peptide (Hits)	MW
Scan(s)	Peptide	MH+	DeltaM	z	Type	P (pep)	XC	Ions	Sp
gi|464371|sp|P35232.1|PHB_HUMAN RecName: Full=Prohibitin						**3.01E-11**	**60.28**	**6 (6 0 0 0 0)**	**29785.9**
944	K.AAIISAEGDSK.A	1061.54736	0.95806	2	CID	1.29E-06	2.73	15/20	661.4
1027	R.NVPVITGSK.D	914.53058	0.00061	1	CID	4.92E-04	2.10	12/16	472.6
1581	K.DLQNVNITLR.I	1185.65857	-0.00081	2	CID	1.22E-04	3.11	15/18	1113.5
1614	R.FDAGELITQR.E	1149.58984	-0.00252	2	CID	4.16E-07	3.30	16/18	1550.6
1752	R.KLEAAEDIAYQLSR.S	1606.84351	0.00054	2	CID	5.86E-08	5.56	24/26	3424.7
2191	K.FGLALAVAGGVVNSALYN VDAGHR.A	2371.25171	0.00016	3	CID	3.01E-11	4.68	35/92	1251.8

						P (pro)	Score	Peptide (Hits)	MW
Scan(s)	Peptide	MH+	DeltaM	z	Type	P (pep)	XC	Ions	Sp
PHB_HUMAN RecName: Full=Prohibitin						**2.27E-07**	**20.18**	**2 (2 0 0 0 0)**	**29785.9**
846	K.AAIISAEGDSK.A	1061.54736	-0.00012	1	CID	2.27E-07	2.00	11/20	176.7
1551	R.FDAGELITQR.E	1149.58984	-0.00130	2	CID	4.59E-06	3.51	17/18	1764.5

						P (pro)	Score	Peptide (Hits)	MW
Scan(s)	Peptide	MH+	DeltaM	z	Type	P (pep)	XC	Ions	Sp
PHB_HUMAN Prohibitin						**5.12E-10**	**70.25**	**7 (7 0 0 0 0)**	**29785.9**
1053,	R.NVPVITGSK.D	914.53058	0.00067	1	CID	5.35E-04	1.82	11/16	401.6
1601,	R.IFTSIGEDYDER.V	1444.65906	-0.00020	2	CID	2.72E-08	3.11	19/22	1095.5
1609,	K.DLQNVNITLR.I	1185.65857	-0.00081	2	CID	6.93E-05	3.31	16/18	1429.0
1662,	R.FDAGELITQR.E	1149.58984	-0.00239	2	CID	1.44E-06	3.36	17/18	1993.8
1704,	R.ILFRPVASQLPR.I	1396.84229	-0.00100	3	CID	5.41E-04	3.11	21/44	382.3
1785,	R.KLEAAEDIAYQLSR.S	1606.84351	-0.00166	2	CID	5.12E-10	5.10	23/26	3017.1
2349,	K.FGLALAVAGGVVNSALYNV DAGHR.A	2371.25171	0.00107	3	CID	9.54E-08	4.84	34/92	982.0

						P (pro)	Score	Peptide (Hits)	MW
Scan(s)	Peptide	MH+	DeltaM	z	Type	P (pep)	XC	Ions	Sp
PHB_HUMAN RecName: Full=Prohibitin						**1.27E-10**	**60.26**	**6 (6 0 0 0 0)**	**29785.9**
892	R.NVPVITGSK.D	914.53058	0.00012	1	CID	8.56E-05	2.22	12/16	522.2
1466	R.IFTSIGEDYDER.V	1444.65906	-0.00191	2	CID	6.82E-09	3.14	19/22	1123.3
1525	R.FDAGELITQR.E	1149.58984	-0.00154	2	CID	8.86E-06	3.21	16/18	1634.3
1659	R.KLEAAEDIAYQLSR.S	1606.84351	-0.00252	2	CID	1.27E-10	5.10	23/26	3066.7
2089	K.AAELIANSLATAGDGLIELR.K	1998.08655	0.00054	2	CID	7.58E-09	5.03	27/38	2354.4
2149	R.NITYLPAGQSVLLQLPQ.-	1855.03235	0.00041	2	CID	9.63E-05	3.33	17/32	688.4

						P (pro)	Score	Peptide (Hits)	MW
Scan(s)	Peptide	MH+	DeltaM	z	Type	P (pep)	XC	Ions	Sp
gi|50401474|sp|Q76MY1|RS4X_MACFU 40S ribosomal protein S4, X isoform						**1.29E-12**	**70.20**	**7 (7 0 0 0 0)**	**29579.1**
827	K.DANGNSFATR.L	1052.47559	0.98406	2	CID	2.80E-05	2.21	15/18	853.7
968	K.YALTGDEVKK.I	1123.59937	-0.00130	2	CID	1.03E-05	2.69	15/18	1086.0
1130	K.GIPHLVTHDAR.T	1215.65930	-0.00032	2	CID	8.27E-07	2.51	15/20	648.4
1203	R.ERHPGSFDVVHVK.D	1506.78113	0.00139	2	CID	3.73E-06	2.95	15/24	377.7
1620	K.VNDTIQIDLETGK.I	1445.74817	-0.00056	2	CID	2.85E-06	4.00	19/24	1638.1
1838	R.LSNIFVIGK.G	990.59827	-0.00026	2	CID	2.15E-05	3.36	14/16	1340.0
1974	R.TDITYPAGFM*DVISIDK.T	1901.92011	0.00133	2	CID	1.29E-12	3.63	22/32	740.8
gi|133948|sp|P22090|RS4Y1_HUMAN 40S ribosomal protein S4, Y isoform 1						**8.27E-07**	**40.20**	**4 (4 0 0 0 0)**	**29437.0**
827	K.DANGNSFATR.L	1052.47559	0.98406	2	CID	2.80E-05	2.21	15/18	853.7
968	K.YALTGDEVKK.I	1123.59937	-0.00130	2	CID	1.03E-05	2.69	15/18	1086.0
1130	K.GIPHLVTHDAR.T	1215.65930	-0.00032	2	CID	8.27E-07	2.51	15/20	648.4
1203	R.ERHPGSFDVVHVK.D	1506.78113	0.00139	2	CID	3.73E-06	2.95	15/24	377.7
gi|27805713|sp|Q8TD47|RS4Y2_HUMAN 40S ribosomal protein S4, Y isoform 2						**8.27E-07**	**30.13**	**3 (3 0 0 0 0)**	**29276.9**
827	K.DANGNSFATR.L	1052.47559	0.98406	2	CID	2.80E-05	2.21	15/18	853.7
968	K.YALTGDEVKK.I	1123.59937	-0.00130	2	CID	1.03E-05	2.69	15/18	1086.0
1130	K.GIPHLVTHDAR.T	1215.65930	-0.00032	2	CID	8.27E-07	2.51	15/20	648.4

						P (pro)	Score	Peptide (Hits)	MW
Scan(s)	Peptide	MH+	DeltaM	z	Type	P (pep)	XC	Ions	Sp
gi|417719|sp|P23396.2|RS3_HUMAN RecName: Full=40S ribosomal protein S3						**1.75E-07**	**30.16**	**3 (3 0 0 0 0)**	**26671.4**
1062	K.GGKPEPPAM*PQPVPTA.-	1589.79920	0.00004	2	CID	7.45E-04	3.09	15/30	358.4
1231	K.KPLPDHVSIVEPK.D	1458.83154	0.00005	2	CID	6.03E-06	3.19	19/24	1101.0
1518	K.DEILPTTPISEQK.G	1470.76868	-0.00044	2	CID	1.75E-07	2.75	19/24	684.8

						P (pro)	Score	Peptide (Hits)	MW
Scan(s)	Peptide	MH+	DeltaM	z	Type	P (pep)	XC	Ions	Sp
RS4Y1_HUMAN 40S ribosomal protein S4, Y isoform 1						**8.27E-07**	**40.20**	**4 (4 0 0 0 0)**	**29437.0**
827,	K.DANGNSFATR.L	1052.47559	0.98406	2	CID	2.80E-05	2.21	15/18	853.7
968,	K.YALTGDEVKK.I	1123.59937	-0.00130	2	CID	1.03E-05	2.69	15/18	1086.0
1130,	K.GIPHLVTHDAR.T	1215.65930	-0.00032	2	CID	8.27E-07	2.51	15/20	648.4
1203,	R.ERHPGSFDVVHVK.D	1506.78113	0.00139	2	CID	3.73E-06	2.95	15/24	377.7
RS4Y2_HUMAN 40S ribosomal protein S4, Y isoform 2						**8.27E-07**	**30.13**	**3 (3 0 0 0 0)**	**29276.9**
827,	K.DANGNSFATR.L	1052.47559	0.98406	2	CID	2.80E-05	2.21	15/18	853.7
968,	K.YALTGDEVKK.I	1123.59937	-0.00130	2	CID	1.03E-05	2.69	15/18	1086.0
1130,	K.GIPHLVTHDAR.T	1215.65930	-0.00032	2	CID	8.27E-07	2.51	15/20	648.4

						P (pro)	Score	Peptide (Hits)	MW
Scan(s)	Peptide	MH+	DeltaM	z	Type	P (pep)	XC	Ions	Sp
RS3_HUMAN RecName: Full=40S ribosomal protein S3						**4.96E-13**	**60.26**	**6 (6 0 0 0 0)**	**26671.4**
1077	K.KPLPDHVSIVEPK.D	1458.83154	-0.00178	2	CID	3.03E-07	3.40	19/24	1029.1
1215	R.ELAEDGYSGVEVR.V	1423.66992	0.00005	2	CID	1.24E-08	3.41	20/24	2014.6
1396	K.DEILPTTPISEQK.G	1470.76868	-0.00203	2	CID	6.85E-06	2.73	20/24	839.3
1495	K.KPLPDHVSIVEPKDEILPTTPISEQK.G	2910.58228	-0.00076	3	CID	2.41E-11	4.84	30/100	786.2
1790	K.FVDGLM*IHSGDPVNYYVDTAVR.H	2484.18639	-0.00093	3	CID	4.96E-13	5.13	36/84	1552.0
1799	R.FGFPEGSVELYAEK.V	1572.75806	-0.00142	2	CID	6.32E-12	3.07	20/26	860.0
RS4X_MACFU RecName: Full=40S ribosomal protein S4, X isoform						**3.16E-12**	**20.18**	**2 (2 0 0 0 0)**	**29579.1**
1041	R.ERHPGSFDVVHVK.D	1506.78113	-0.00093	2	CID	1.58E-07	3.13	16/24	435.0
1862	R.TDITYPAGFM*DVISIDK.T	1901.92011	0.00157	2	CID	3.16E-12	3.67	24/32	947.5

						P (pro)	Score	Peptide (Hits)	MW
Scan(s)	Peptide	MH+	DeltaM	z	Type	P (pep)	XC	Ions	Sp
RS4X_MACFU RecName: Full=40S ribosomal protein S4, X isoform						4.56E-05	20.14	2 (2 0 0 0 0)	29579.1
800	K.YALTGDEVKK.I	1123.59937	-0.00130	2	CID	3.12E-04	2.19	16/18	1098.4
1691	R.TDITYPAGFM*DVISIDK.T	1901.92011	0.00084	2	CID	4.56E-05	2.87	17/32	385.2

Protein Name	Gene Symbol	Protein AC Number	MW (kDa)
Myosin 10	MYH10	gi| 215274129|	228.9
Myosin 11	MYH11	gi| 13432177|	228
Myosin 9	MYH9	gi| 6166599|	226.5
Heat Shock 90, Beta	HSP90AB1	gi| 39644662|	83.26
Lamin A/C	LMNA	gi| 55957499|	79.39
Heat Shock 70, Protein 5	HSPA5	gi| 86577744|	72.33
Heat Shock 70, Protein 8	HSPA8	gi| 48257068|	70.89
Annexin A1	ANXA1	gi| 197692503|	69.97
HnRP Q	SYNCRIP	gi| 56204904|	69.63
Elongation factor 1-alpha 1	EF1A1	gi| 55584035|	50.1
Annexin A2	ANXA2	gi| 62202495|	50.1
HnRP G	RBMX	gi| 14279350|	42.33
Actin - α	ACTA1	gi| 49456549|	42
B - Actin	ACTB	gi| 4501885|	41.73
HnRP A1	HNRPA1L3	gi| 190360152|	38.74
HnRP A2/B1	HNRPA2B1	gi| 14043072|	37.43
60S Ribosomal Protein-L7	RPL7	gi|133021|	29.22
Filaggrin-2	FLG2	gi| 62122917|	24.8
Histone H1.5	HIST1H1B	gi| 19856407|	22.58
Histone H1.3	HIST1H1D	gi| 121925|	22.35
Histone H1.1	HIST1H1A	gi| 18202479|	21.84
S100-A9	S100A9	gi| 49457442|	13.24

Table 6: - Proteins identified from excised bands immunoprecipitated with MAb 7B7 G5 (2), MAb 9E1 24 (6), and the IgG and IgM negative controls, through mass spectrometry. The above proteins were as such disregarded for further characterisation.

Appendix IV

Densitometry Histograms of Western Blot Analysis of siRNA transfected Cells

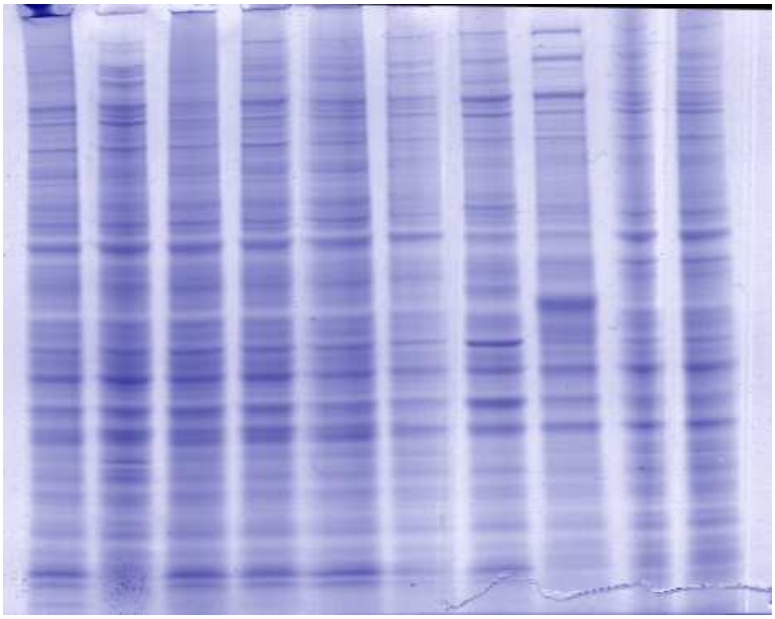

A B C D E F G H I J

Figure 1: **-** A representative SDS-PAGE gel showing equal loading of cell lysates (10µg loaded per lane).

A. MiaPaCa-2 clone 3;

B. MiaPaCa-2 clone 3 Matrigel;

C. MiaPaCa-2 clone 3 Membrane;

D. MiaPaCa-2 clone 8;

E. MiaPaCa-2 clone 8 Membrane;

F. Lox IMVI;

G. MDA-MB-435 Membrane;

H. SK-Mel 28 Membrane;

I. WM-115;

J. WM-266-4;

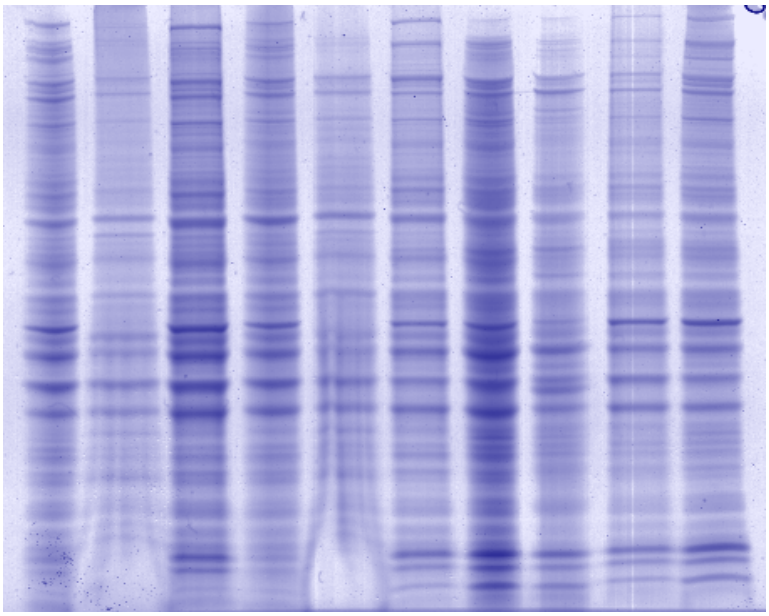

K L M N O P Q R S T

Figure 2: - A representative SDS-PAGE gel showing equal loading of cell lysates (10µg loaded per lane).

K. DLKP;
L. DLKP-A;
M. DLKP-SQ;
N. DLKP-I;
O. DLKP-M;
P. H1299;
Q. SNB-19;
R. C/68;
S. HCT-116;
T. HCT-116 (20ug)

Appendix V

Densitometry Histograms of Western Blot Analysis of siRNA transfected Cells

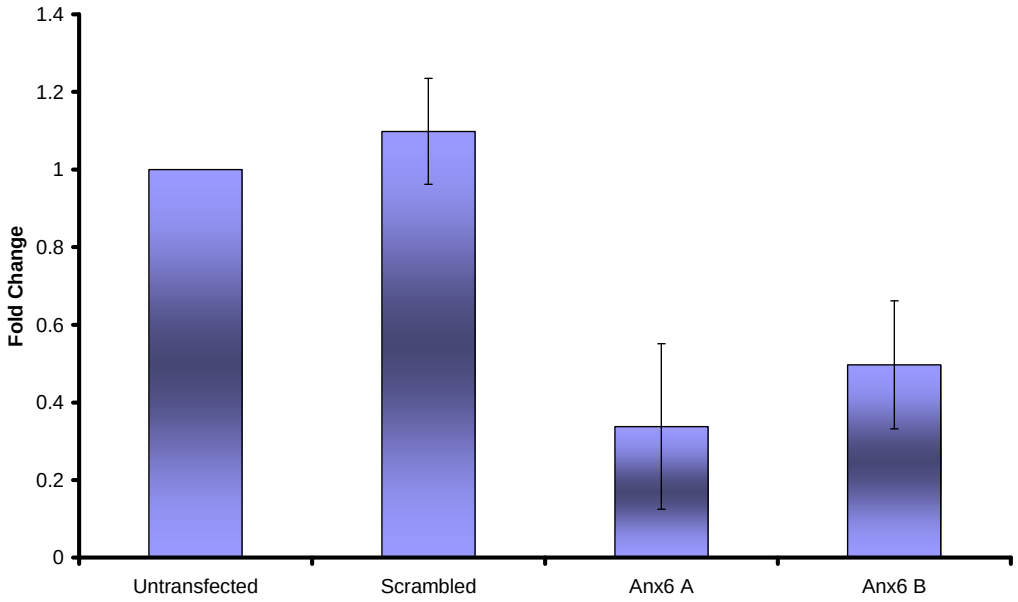

Figure 3: - Representative histogram showing the level of Annexin A6 knockdown in MiaPaCa-2 clone 3 cells following transfection by a nonsense control siRNA (Scrambled), and 2 siRNAs targeting the Annexin A6 protein (Anx6 A & Anx6 B). Expression levels were normalised with α-tubulin (not shown). Data shown is mean ± standard deviation (n = 3).

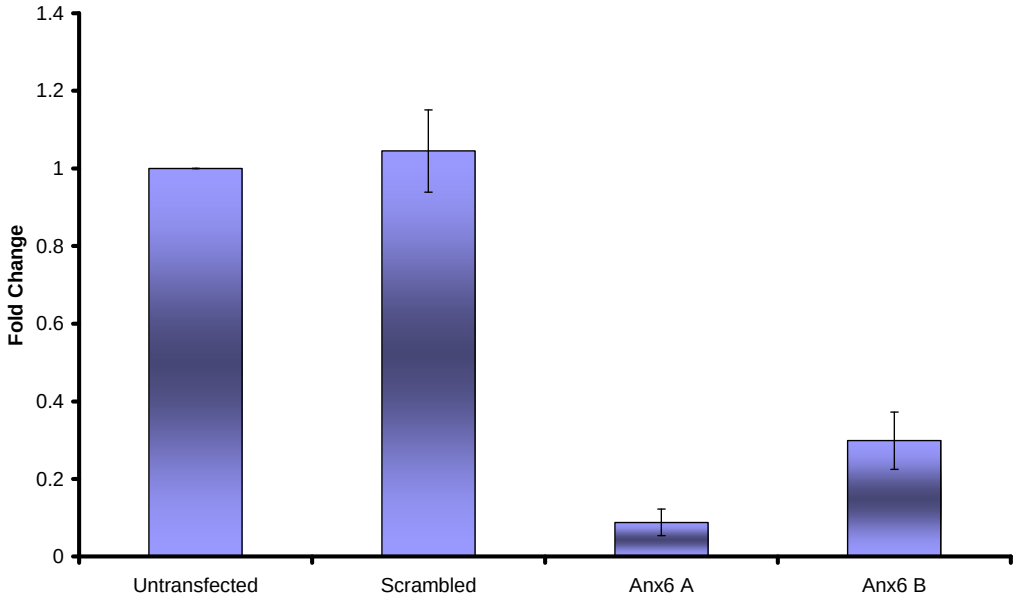

Figure 4: - Representative histogram showing the level of Annexin A6 knockdown in DLKP-M cells following transfection by a nonsense control siRNA (Scrambled), and 2 siRNAs targeting the Annexin A6 protein (Anx6 A & Anx6 B). Expression levels were normalised with α-tubulin (not shown). Data shown is mean ± standard deviation (n = 3).

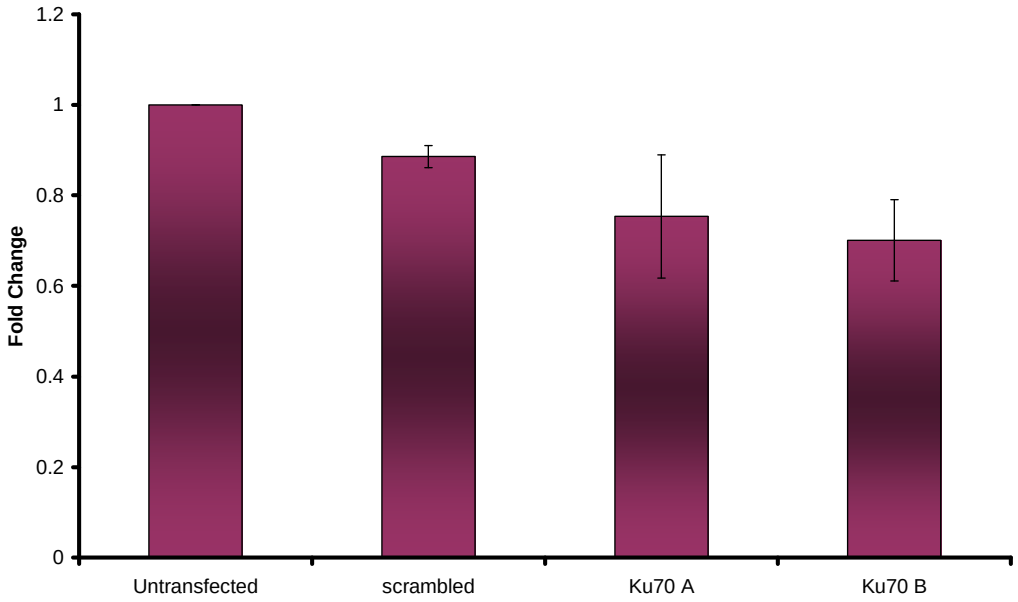

Figure 5: - Representative histogram showing the level of Ku70 knockdown in MiaPaCa-2 clone 3 cells following transfection by a nonsense control siRNA (Scrambled), and 2 siRNAs targeting the Ku70 protein (Ku70 A & Ku70 B). Expression levels were normalised with α-tubulin (not shown). Data shown is mean ± standard deviation (n = 3).

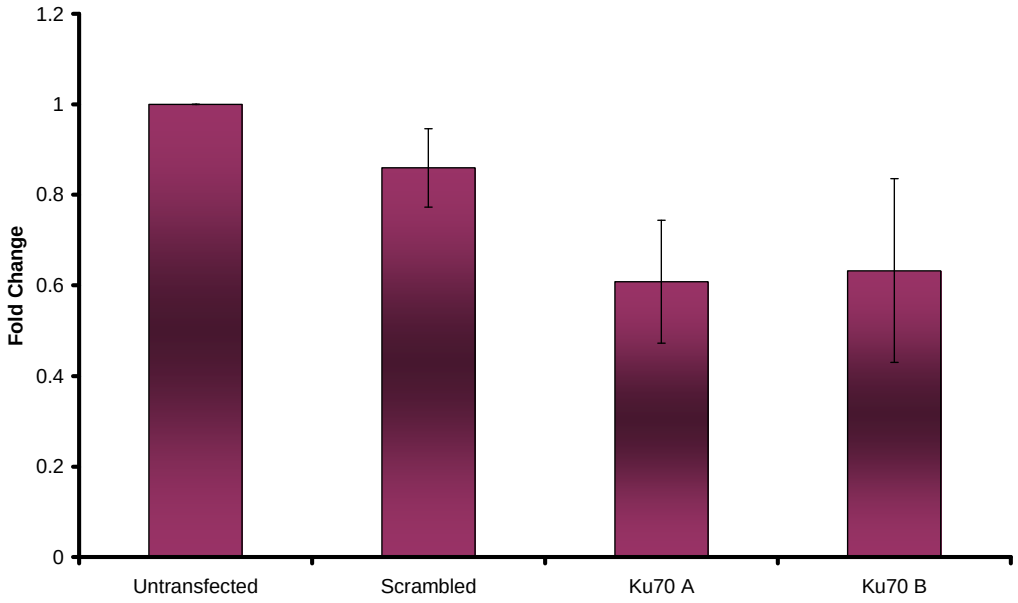

Figure 6: - Representative histogram showing the level of Ku70 knockdown in DLKP-M cells following transfection by a nonsense control siRNA (Scrambled), and 2 siRNAs targeting the Ku70 protein (Ku70 A & Ku70 B). Expression levels were normalised with α-tubulin (not shown). Data shown is mean ± standard deviation (n = 3).

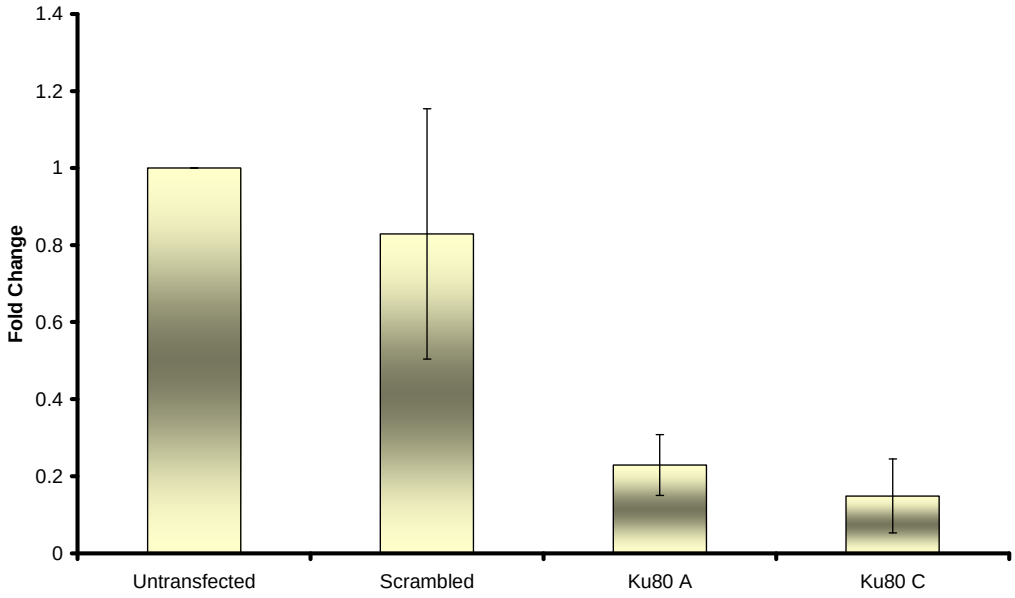

Figure 7: - Representative histogram showing the level of Ku80 knockdown in MiaPaCa-2 clone 3 cells following transfection by a nonsense control siRNA (Scrambled), and 2 siRNAs targeting the Ku80 protein (Ku80 A & Ku80 C). Expression levels were normalised with α-tubulin (not shown). Data shown is mean ± standard deviation (n = 3).

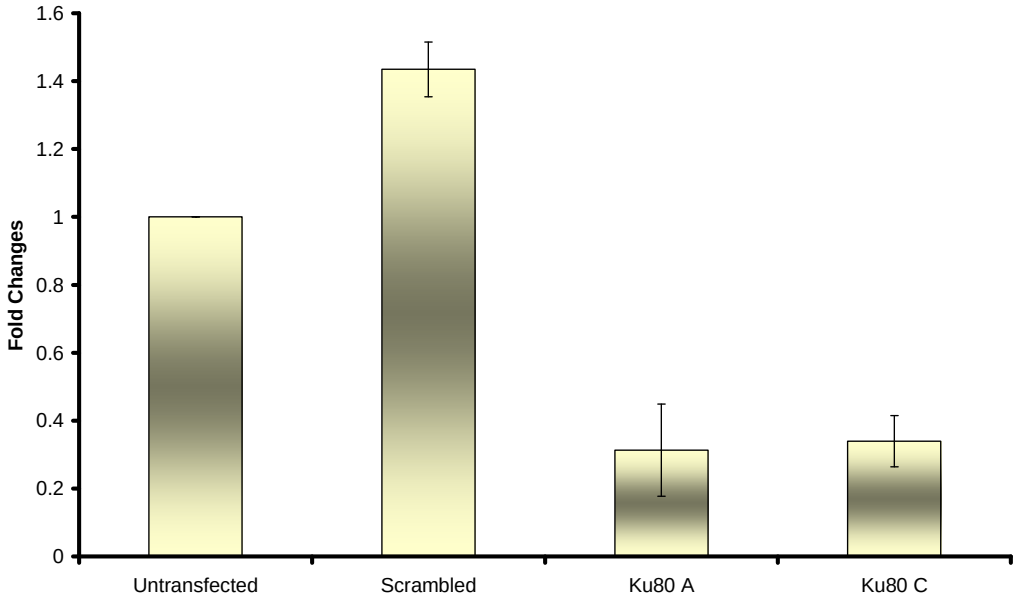

Figure 8: - Representative histogram showing the level of Ku80 knockdown in DLKP-M cells following transfection by a nonsense control siRNA (Scrambled), and 2 siRNAs targeting the Ku80 protein (Ku80 A & Ku80 C). Expression levels were normalised with α-tubulin (not shown). Data shown is mean ± standard deviation (n = 3).

Appendix VI

Complete Zymograpgy Gel showing effect of MAbs on MMP-9 activity in the MDA-MB-231 breast cell line.

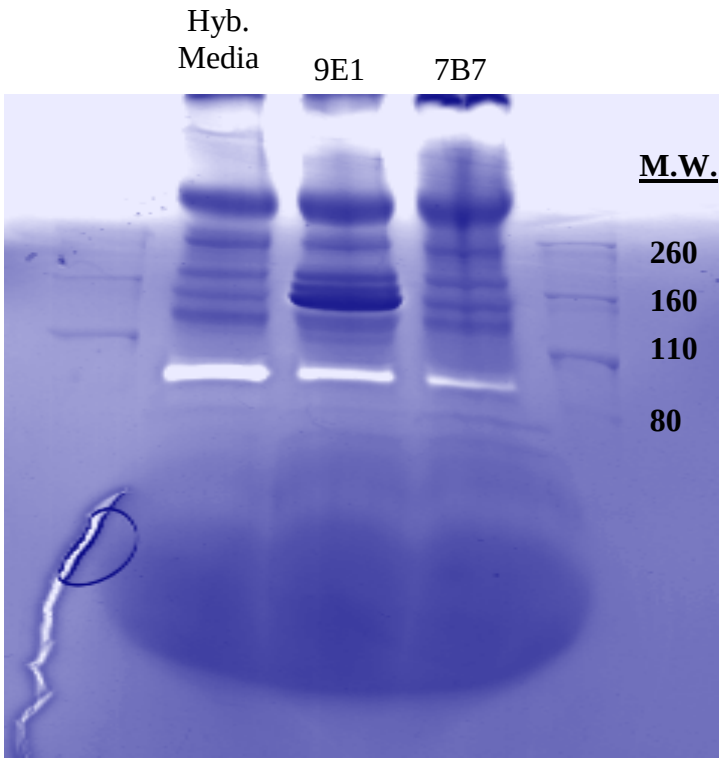

Figure 9: - Graph and zymography gel showing effect of MAb 7B7 G5 (2) and MAb 9E1 24 (6) on MMP-9 activity in the MDA-MB-231 breast cell line. Cells incubated with both MAbs show a decrease in the activity of MMP-9 when compared to control hybridoma medium (no MAb) representing normal MMP-9 activity.